Analysis of novel cysteine-rich peptides during reproductive processes in *Zea mays*

DISSERTATION

ZUR ERLANGUNG DES DOKTORGRADES DER NATURWISSENSCHAFTEN
(DR. RER. NAT.) DER FAKULTÄT FÜR BIOLOGIE UND VORKLINISCHE MEDIZIN

UNIVERSITÄT REGENSBURG

vorgelegt von

Lele Wang

aus Hebei, China

im November 2020

Das Promotionsgesuch wurde eingereicht am 13.11.2020.

Die Arbeit wurde angeleitet von Prof. Dr. Thomas Dresselhaus und Dr. Liangzi Zhou.

Unterschrift: _____

Lele Wang

Meinen Eltern.

Meinen Liebsten.

„Dance like no one is watching.

Sing like no one is listening.

Love like you've never been hurt.

And live like it's heaven on Earth."

Mark Twain

This thesis contains data of the following manuscript that was submitted for publication:

CHAPTER 2 and CHAPTER 3

Wang, L., Zhou, L., Ge, Z., Mergner, J., Küster, B, Längst, G., Qu, L., and Dresselhaus, T. The RALF signaling pathway regulating cell wall integrity during pollen tube growth is conserved in maize. (submitted)

I conducted bioinformatical analysis and performed all experiments except the phosphoproteomic analysis of samples generated from pollen tubes of wild type and RNAi-*RALFs* lines. The manuscript was written by me and T. Dresselhaus. The paragraphs in Chapter 2 and Chapter 3 about generation and analysis of CRISPR-Cas9 transgenic maize lines and promoter analysis are excluded from the publication.

Additionally, I contributed to the following manuscripts:

Ge, Z., Zhao, Y., Liu, M., Zhou, L., Wang, L., Zhong, S., Hou, S., Jiang, J., Liu, T., Huang, Q., Xiao, J., Gu, H., Wu, H., Dong, J., Dresselhaus, T., Cheung, A., and Qu, L. (2019). LLG2/3 are co-receptors in BUPS/ANX-RALF signaling to regulate *Arabidopsis* pollen tube integrity. *Current Biology* **29**, 3256-3265.

I performed recombinant protein purification for the paper.

Flores-Tornero, M., Wang, L., Potěšil, D., Hafidh, S., Vogler, F., Zdráhal, Z., Honys, D., Sprunck, S., and Dresselhaus, T. (2020). Comparative analyses of angiosperm secretomes identify apoplastic pollen tube functions and novel secreted peptides. *Plant Reproduction* DOI: 10.1007/s00497-020-00399-5.

I performed maize secretome samples preparation and part of bioinformatic maize secretome data analyses.

CONTENTS

SUMMARY

To successfully complete double fertilization, flowering plants require a battery of signaling peptides to precise regulate the various processes from pollen germination towards sperm cell release and gamete fusion. Small secreted cysteine-rich peptides or proteins (CRPs) play key roles for cell-cell communication during the various reproductive processes.

In this work, **Chapter 1** shortly introduces gametophyte development in angiosperms (flowering plants) and the reproduction process. **Chapter 2** describes the identification and functional exploration maize Rapid Alkalinization Factor (RALF) peptides belong to the most strongly expressed *CRP* genes in pollen. The focus of **Chapter 3** is the interactions between RALF peptides and receptor-like kinases, co-receptors and cell wall proteins. **Chapter 4** describes the investigation of maize Pollen Ole e 1-like (POE) proteins and a defensin-like (DEFL) protein belonging to CRP groups whose genes are specifically expressed in pollen and pollen tubes. Finally, **Chapter 5** discusses the results from this work in a broader context and provides an outlook for further studies.

The major focuses of the thesis were on RALF signaling peptides and their functions during the process of pollen tube growth control in maize (*Zea mays* L.). The function of RALF peptides in maintaining pollen tube integrity during reproduction was previously described in *Arabidopsis thaliana*, but how RALF peptides distribute in the maize genome, to which extent functions are conserved and whether there are specific functions in maize were still unknown. To explore the distribution and features of maize RALF peptides, whole genome blast searchers were carried out. Beside the 20 *ZmRALF* genes identified previously, additional four *ZmRALF* genes were founded. Phylogenetic analysis was done to compare the 24 ZmRALF and 37 AtRALF peptides. Based on sequence similarity and structure features, RALF peptides form the two species could be classified into four clades. Clade I and II are typical RALF peptides containing a propeptide and YISY as well as YY interaction domains. Clade III contains only RALF peptides from *Arabidopsis* containing a YISY but lacking an YY interaction domain. Clade IV RALF peptides are short and lack all typical features described above. Their function(s) are unknown. This thesis therefore investigated two types of RALF peptides: ZmRALF2/3 from Clade II and ZmRALF1/5 from Clade IV. They are the most abundant *RALF* genes in maize as their transcript occupied about

97% of all pollen tube expressed *RALF* genes. To explore subcellular localization of ZmRALF peptides, eGFP-fusion proteins driven by the pollen-specific AtRALF4 promoter were transformed into *Arabidopsis thaliana*. According to microscopic analysis of *in vitro* germinated pollen tube, ZmRALF2/3 were mainly detected to the cell wall while ZmRALF1/5 localized in vesicles/granules to the cytoplasm, but were not secreted *in vitro*. To further investigate the function of ZmRALF peptides, RNA interference mutants (RNAi-*RALFs*) were generated to downregulate *ZmRALF1/2/3*. In RNAi-*RALFs* mutant lines, expression level of *ZmRALFs* were downregulated to about half compared with wild type pollen. Phenotypic analysis of RNAi-*RALFs* mutants showed that *in vitro* germinated pollen tubes were unstable and tend to burst in the subapical region of the tube; male gametophyte transmission, but not female transmission efficiency were significantly decreased. *Catharanthus roseus* receptor like kinase 1-like proteins (CrRLK1Ls), LORELEI-like-GPI-anchored proteins (LLGs), and Leucine-riche repeat extensins (LRXs) were reported to interact with typical RALF peptides in *Arabidopsis thaliana* and Tomato. To investigate the function of these interactors in RALF signaling pathway, genome blasts were carried out. 17 CrRLK1L protein genes, four for LLGs and 17 for LRXs were found. Putative maize homologues of *Arabidopsis* FERONIA (FER), ANXURE 1/2 (ANX1/2), Buddha's Paper Seal 1/2 (BUPS1/2), LLGs and LRXs were named as ZmFERL1, ZmFERL4, ZmFERL7/9, ZmLLGs and ZmPEXs, respectively. Apart from *ZmFERL1* that is not expressed in male gametophytic cells, the other homologues genes are exclusively expressed in pollen and pollen tubes. Multiple pull-down assays confirmed the interaction between Clade II RALF peptides ZmRALF2/3 and their putative interactors, while Clade IV peptides ZmRALF1/5 did not show any interaction with these proteins. Binding affinities between ZmRALFs and ZmCrRLK1Ls and ZmPEX2 were tested with Microscale Thermophoresis (MST). According to the result, ZmRALF2/3 strongly bind with ZmPEX2, less tightly with ZmFERL4/7/9, and only weakly with ZmFERL1. Clade II RALF peptides ZmRALF2/3 interacted also with *Arabidopsis* ANXs/BUPSs/LRXs and *vice versa*, while Clade IV RALF peptides ZmRALF1/5 did not. Different CRISPR/sCas9 mutants were generated and genotyped to investigate the functions of ZmFERLs in future studies.

Beside RALFs, POE and DEFL, two further CRPs were investigated. In maize, there are 27 *POE* genes, which could be classified into three groups. This work focused on Clade I-A *POE* gene named as *ZmPOE1.1* and *ZmPOE1.2*, which are highly similar with each other regarding protein

sequences and expression pattern. To investigate the functions of *ZmPOEs*, RNA interference and CRISPR/Cas9 mutants were generated. In RNAi-*POEs*, *ZmPOE1.1/1.2* were downregulated to about 20% compared with wild type levels, but no obvious phenotypic defects could be observed using *in vitro* germinated pollen tubes. Fragment deletions were found in Cas9-*POEs* lines. Pollen tubes from Cas9-*POEs* mutants were unstable around 90 minutes after germination *in vitro*.

ZmDEFL1 is highly and exclusively expressed in pollen. An RNA interference mutant was generated to investigate the function *ZmDEFL1*. In RNAi-*DEFL1*, expression level of *ZmDEFL1* was downregulated to 5% compared with wild type levels. However, I could not detect an effect on pollen germination and growth *in vitro* nor a male gametophyte transmission defect.

Taken together, the RALF signaling pathway, which regulates cell wall integrity during pollen tube growth is conserved between maize and *Arabidopsis*. *ZmPOEs* are required for *in vitro* pollen tube growth, but more tests are needed to the functional mechanism. *ZmDEFL1* was not found to be essential during maize double fertilization.

CHAPTER 1. DOUBLE FERTILIZATION IN PLANTS

Different from sperm cells of animals, mosses, ferns and some gymnosperms, sperm cells of angiosperms are non-motile. For double fertilization, sperm cells are transported as passive cargo by the male gametophyte (pollen/pollen tube) to the female gametophyte (embryo sac). To ensure successful double fertilization, batteries of signaling molecules are involved in this process. In this chapter, gametophyte development and following reproduction processes will be shortly introduced.

1.1 Angiosperm female gametophyte development

The female reproductive cells of seed plants are developed in ovules, which consist of an outer layer of integuments and an inner nucellus megasporangium. Female gametophyte development can be divided into two steps: megasporogenesis and megagametogenesis. There are over 15 types of megasporogenesis formations across plant families (Schmid *et al.*, 2015). However, about 70% of flowering plants follow a pattern called *Polygonum*-type development, including maize and *Arabidopsis* (Jones *et al.*, 2012).

Megasporogenesis starts from meiosis of megaspore mother cells (MMCs) that generate four megaspores (Figure 1.1). In *Polygonum*-type plants, the megaspore at the most chalazal region enlarges and the remaining three spores undergo degradation, producing a single functional megaspore. In megagametogenesis, the functional megaspore further goes through three mitotic nuclei divisions, producing an embryo sac including seven cells with eight nuclei. The first mitosis produces two nuclei which later move to the opposite direction. The two nuclei will perform two extra rounds of mitosis and generate eight nuclei. One of the four nuclei from each side migrates to the center to form polar nuclei. Meanwhile, cytoplasm and cell wall start to initiate around the three nuclei in each side. The cells closer to the chalazal region become three antipodal cells; the cells close to micropyle region differentiate into an egg cell and the synergid cells. Cell wall of synergid cells specify the micropyle region by a filiform apparatus that forms a highly thickened structure, consisting of numerous finger-like projections into the synergid cytoplasm. This structure significantly increases the surface area of the plasma membrane of synergid cells, which is thought to be required for pollen tube attraction (Márton *et al.*, 2005).

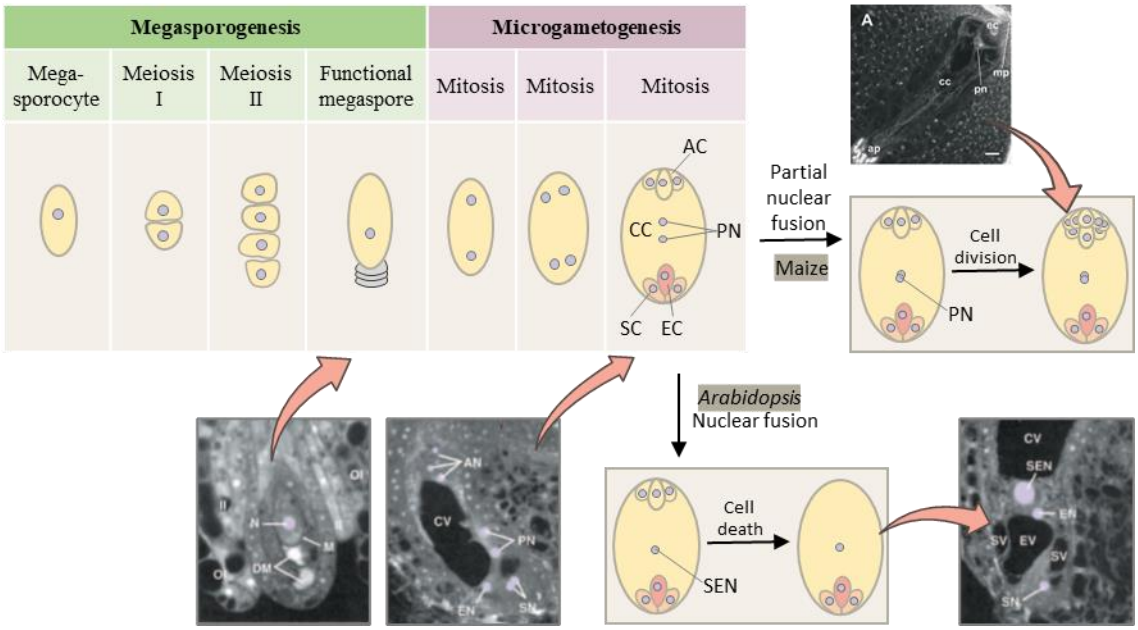

Figure 1.1 The *Polygonum* pattern of female gametophyte development. This pattern of cell division is typical of more than 70% of angiosperms. The process can be divided into two stages: megasporogenesis, during which meiosis occurs, and megagametogenesis, during which the surviving haploid megaspore divides mitotically to produce an embryo sac (female gametophyte). In *Arabidopsis* and some other species, the polar nuclei (PN) fuse to form a secondary endosperm nucleus (SEN). AC/AP, antipodal cell; AN, antipodal cell nucleus; CC, central cell; CV, central cell vacuole; DM, degenerate megaspore; EC, egg cell; EN, egg nucleus; EV, egg vacuole; II, inner integument; M, megaspore; N, nucleus; OI, outer integument; SC, synergid cell; SN, synergid nucleus; SV, synergid vacuole; MP, micropyle. Image was drawn based on description and images presented in Joes *et al.*, 2012; Lausser *et al.*, 2010.

1.2 Plant male gametophyte development

Male gametophyte development is highly conserved among all angiosperms and well described (Bedinger and Fowler, 2009; van der Linde and Walbot, 2019). At the molecular level, the understanding of male gametophyte development is far better compared with the formation of embryo sacs (Hater *et al.*, 2020; Jones *et al.*, 2012). Before pollen germination, male gametophyte development can be divided into three phases: pre-meiotic (development of microsporocytes and associated cells); microsporogenesis (development of microspore) and microgametogenesis (development of pollen grain).

Male gametophyte pre-meiotic development starts with the generation of a central set of archesporial cells and a surrounding layer of primary parietal cells (Figure 1.2.A). The archesporial cells develop into pollen mother cell (PMC); the primary parietal cells go through divisions and result in three cell layers (from outer epidermis to inner PMC): endothecium, middle layer, and tapetum (Figure 1.2.B). Endothecium function as an energy storage tissue to sustain and control anther development. The function of the middle layer is less understood: it will crush prior to the completion of meiosis (van der Linde and Walbot, 2019). In contrast, the function of tapetum cells is well described. They have two main functions: manufacture compounds that make up the pollen exine and produce callase, which is required to release the microspores from the tetrad at the end of meiosis (Jones *et al.*, 2012).

Microsporogenesis and microgametogenesis encompass the development events that from archesporial cell to mature pollen. Firstly, archesporial cells undergo mitosis and differentiate into pollen mother cells, which further undertake meiosis including two cell divisions. As a result a tetrad of haploid microspores is formed. Newly produced haploid microspores are held together by an exterior callose wall. Soon thereafter tapetum secreted callase release the microspores (Figure 1.2.C). The individual microspore owns a central nucleus and begin to acquire an outer cell wall (exine). It gets nutrients from the tapetum and keeps growing, multiple small vacuoles are generated and eventually fuse into a single large vacuole. Along with microspore enlargement, their nuclei move to a position near the cell wall (Figure 1.2.D).

Microgametogenesis starts from the first asymmetric cell division of pollen mitosis that produce bicellular pollen, which consist of a larger vegetative nucleus and a smaller generative nucleus that cellularized later (Figure 1.2.E). Following the first pollen mitosis, intine is formed between plasma membrane and exine. Intine is rich in cellulose, pectins and proteins. Subsequently, the generative cell undergoes a second pollen mitosis that yields two sperm cells (Figure 1.2.F). Following anther dehiscence, pollen is released and land on papilla cells or silk hairs in grasses, start hydration and germination after being recognized.

There are great advantages to study pollen development in the model and crop plant maize: (1) maize generates a huge number of pollen grains accounting to more than 25million in a single plant. (2) Compared with the well-studied model plant *Arabidopsis thaliana*, anther and pollen from maize are larger and easier to get (van der Linde and Walbot, 2019).

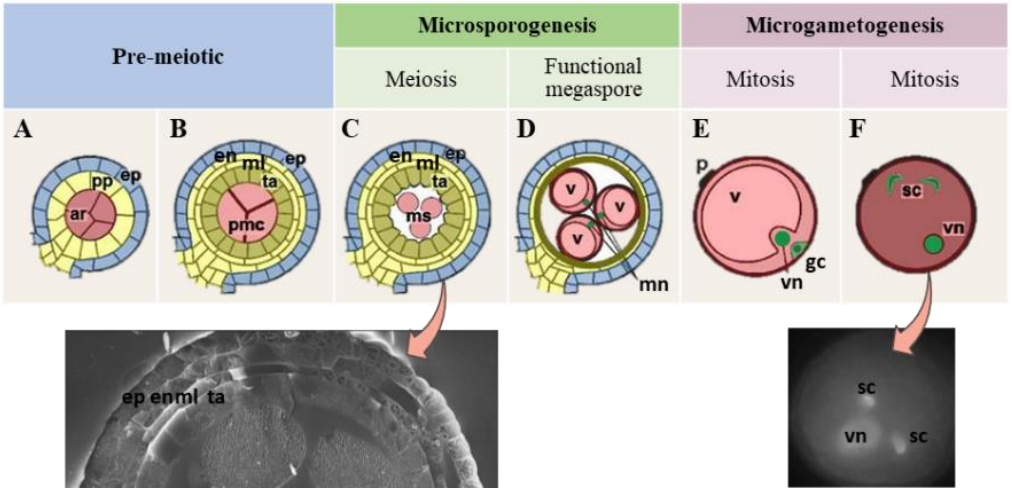

Figure 1.2 Development of the male gametophyte in maize. (A) Archesporial cells, embedded in a primary parietal cell layer, differentiate into (B) pollen mother cells, surrounded from the tapetum cells, middle layer cell and endothecium, which are derived from the primary parietal layer. (C, D) Pollen mother cells undergo meiosis to form enlarging microspores. (E) Microspores undergo mitosis to produce a vegetative and a generative nucleus and cellularization gives rise to the generative cell. (F) Two sperm cells located in the cytoplasm of the vegetative cell are formed by mitosis of the generative cell. Abbreviations: ar = archesporial cells, en = endothecium, ep = epidermis, gc = generative cell, ml = middle layer, mn = micro-spore nucleus, ms = microspores, pmc = pollen mother cells, pp = primary parietal layer, sc = sperm cells, ta = tapetum, v = vacuole, vn = vegetative nucleus. Image was drawn based on description and images presented in Bedinger and Fowler, 2009; Tsou *et al.*, 2015; Begcy and Dresselhaus, 2017.

1.3 Pollen tube growth: a very long journey

Pollen tube growth starts from the landing of pollen grain on the stigma, following by pollen hydration and germination, pollen tube penetration and growth through the transmitting tract toward ovules, ending in ceased growth in one synergid cell. The pollen tube journey was divided into five phases (Lausser and Dresselhaus, 2010) (Figure 1.3): in Phase I, pollen land on stigmata and start hydration after being recognized. In Phase II, pollen tubes penetrate the stigma (silk hair cells in maize) and reach the transmitting tract that links stigma, style, and ovaries in a pistil. In Phase III, pollen tubes growth along the transmitting tract till the ovule. In Phase IV, pollen tubes are guided to the micropylar region under the control of the ovule. This phase is further divided into funicular guidance and micropylar guidance in the Brassicaceae and other families, while funicular guidance does not exist in the Poaceae. At the end of journey, in Phase V, pollen tubes grow through and around the filiform apparatus, reach and stop in one synergid cell. Finally, pollen tube burst, sperm cells are released and fuse with either egg cell or central cell.

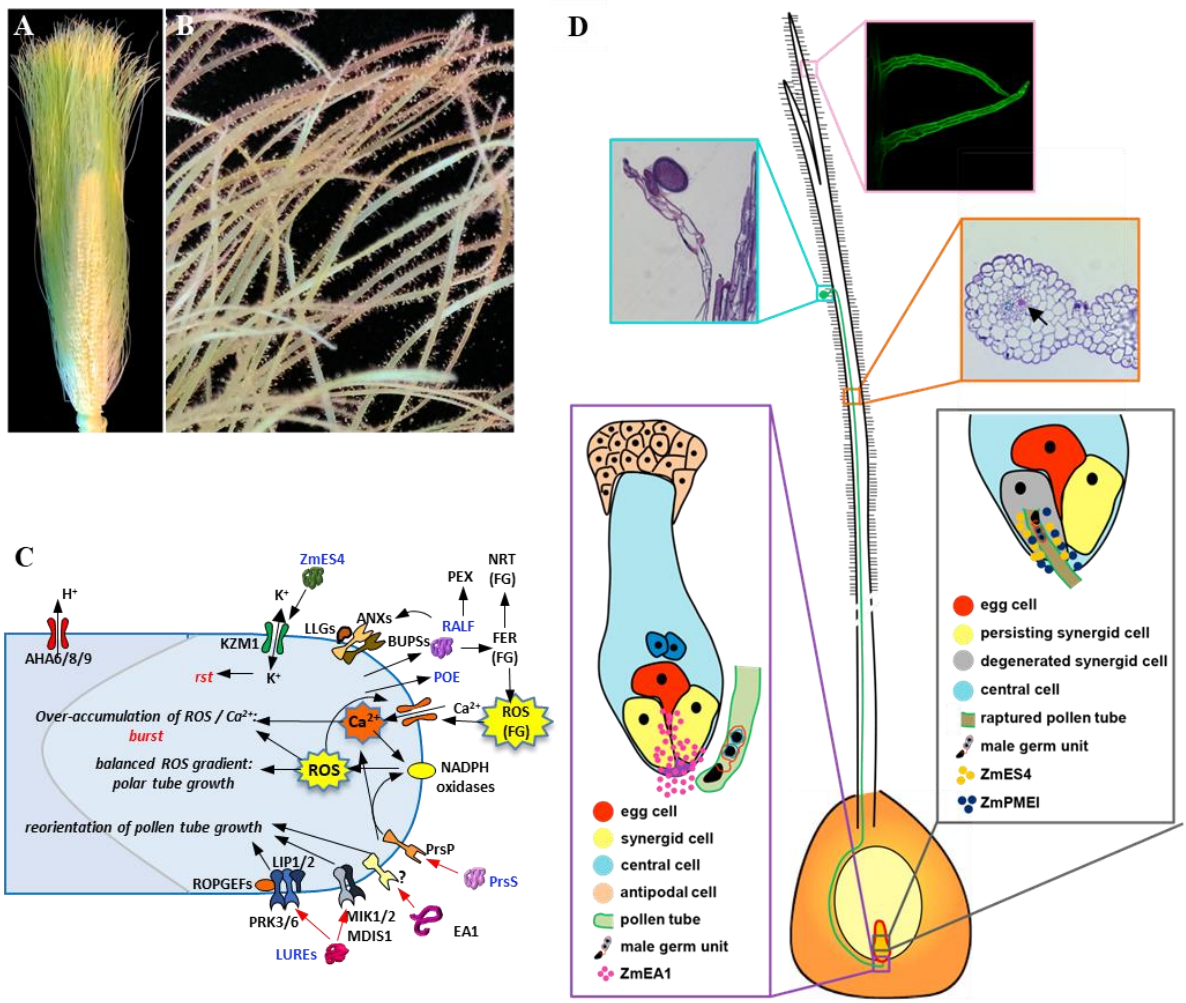

Figure 1.3 Progamic phase and fertilization process in maize. (A) Maize cob at silking stage. Husk leaves have been removed. Each silk fiber represents an elongated stigma attached to a single ovary. (B) Freshly pollinated maize silks. Numerous light-yellow pollen grains are adhered at papillae hairs of silk fibers. (C) Schematic representation of peptide signaling at the apex and sub-apex region of plant pollen tubes. Interactions during growth towards the female gametophyte (FG) is depicted, with a special emphasis on the role of ion and ROS downstream signaling events. Cellular responses in pollen tubes are indicated. Red arrows represent direct interaction of the signaling peptide with cell surface proteins. Black arrows represent ion flux and activation or blocking activity. Blue texts represent the cysteine rich peptides. (D) A schematic model showing the journey of one pollen tube from a papillae hair through the transmitting tract of stigma and style toward the female gametophyte is shown in the middle. Propidium iodide staining pseudocolored in green shows two papillae hairs in the pink box at the top right. Blue box at top left shows toluidine blue staining of a germinating pollen tube invaded in a silk hair. Orange box shows cross-section through the silk showing a pollen tube (arrow) in the transmitting tract. Bottom left: schematic of a mature female gametophyte consisting of the cells indicated. A pollen tube containing the male germ unit (two sperm cells associated to the vegetative tube nucleus) in its tip is attracted by secreted ZmEA1 peptides. Pollen tube burst occurs through the activity of secreted ZmES4 and ZmPMEI proteins as illustrated in the box at bottom right. Image was drawn based on description and images presented in Bircheneder and Dresselhaus, 2016; Zhou *et al.*, 2017.

1.3.1 Phase I: Pollen adhesion and hydration

Pollen surface is covered with pollen coat that play key role in adhesion and hydration (Kim *et al.*, 2019). There were 14 maize pollen coat proteins (PCPs) identified, which classified into three groups (Gong *et al.*, 2015). Group1: hydrolases synthesized in tapetum including cysteine protease, endoxylanase, β-glucanase, and putative subtilase. Group 2: allergens synthesized from pollen including Zea m 1 (β-expansin 1/10), Zea m 2, Zea m 12 (profilin), and Zea m 13 (exopolygalacturonase). Group3: other PCPs including ABA-induced caleosin, RhoGDI 1, RAB2A. Among those PCPs, only xylanse, β-glucanase, and β-expansin 1 were functionally characterized. Xylanase helps to provide sufficient water for pollen germination (Suen and Huang, 2007); β-glucanase promote hydrolyzes the stigma wall during pollen germination (Suen *et al.*, 2003); β-expansin can loosen stigmatic cell walls and promote pollen tube penetration (Cosgrove *et al.*, 1997).

In most Brassicaceae plants, self-incompatibility (SI) is wildly distributed to prevent self-fertilization (Nasrallah, 2019). The SI system in Brassicaceae is mainly controlled by *S* locus that contains two linked genes from male and female reproduction tissues: the *S*-locus cysteine-rich protein (SCR) ligand in pollen coat and the *S*-locus receptor kinase (SRK) in stigma epidermis. In maize, the initiation of pollen germination is more like to be mechanical controlled instead of precise recognition system: the alien pollen requires dry stigma from other species could germinate on maize stigma, while those require wet stigma cannot (Lausser *et al.*, 2010). Therefor the physical character could be the first barrier of inter-species cross in maize.

1.3.2 Phase II: Penetration in silk hairs and growth towards the transmitting tract

After germination, pollen tube try to penetrate the stigma and find the transmitting tract, which initiated the second recognition system (Lausser and Dresselhaus, 2010). When maize stigma was applied with pollen from different species, most of alien pollen could germinate, but only maize and its sister genus *Tripsacum dactyloids* could penetrate the silk hair cells and find the transmitting tract (Lausser *et al.*, 2010). Until now, there are to my knowledge no molecular studies about the interaction between pollen and silk hairs in maize. The differential gene expression comparison of silk hairs before/after pollen tube penetration would greatly promote the understanding of this second recognition system.

1.3.3 Phase III: Growth in the transmitting tract

Only a limited number of signaling molecules were identified during pollen tube growth in the transmitting tract. In tomato, pollen-specific leucine-rich repeat receptor kinases LePRK1/2 interact with STIGMA-SPECIFIC PROTEIN 1 (STIG1) from female tissue (Tang *et al.*, 2004). It was presumed that STIG1-LePRK2 promotes pollen tube growth by affecting reactive oxygen species (ROS) production (Huang *et al.*, 2014). LEUCINE-RICH REPEAT EXTENSIN (LRX) proteins, another pollen-specific proteins contain leucine-rich repeat structure, are involved in maintaining pollen tube integrity via interaction with RAPID ALKALINIZATON FACTOR 4/19 (RALF4/19) (Mecchia *et al.*, 2017) (see also Chapter 3).

Beside the leucine-rich repeat structure containing proteins, *Catharanthus roseus* receptor 1 like kinases (CrRLK1L) and their corresponding interactors are also involved in pollen tube guidance in maize (Zhou and Dresselhaus, 2019) (Chapter 3). The CrRLK1L-RALF-LLG autocrine signaling pathway maintains pollen tube integrity during pollen tube growth (Ge *et al.*, 2019a). Double mutation of *ANXUR1/2* (*ANX1/2*) or *Buddha's Paper Seal 1/2* (*BUPS1/2*) genes in *Arabidopsis* resulted in ceased pollen tube growth *in vivo*, similar to the mutations from their co-receptor LORELEI-like-GPI-anchored protein 2/3 (LLG2/3) or ligands RALF4/19 (Ge *et al.*, 2019b). The CrRLK1L-RALF-LLG signaling network includes downstream components such as NADPH oxidase *RbohH* and *RbohJ* (Boisson-Dernier *et al.*, 2013), receptor-like cytoplasmic kinase *MARIS* (*MRI*) (Boisson-Dernier *et al.*, 2015), Type One Protein Phosphatase (TOPP) and *ATUNIS1/2* (*AUN1/2*) (Franck *et al.*, 2018).

Arabinogalactan proteins (AGPs) are encoded by another gene family participating in communication between pollen tube and transmitting tract (Pereira *et al.*, 2016b). AGPs is a big family of highly hydroxyproline-rich glycoproteins that distribute throughout the plant kingdom (Showalter, 2001). These glycoproteins mainly localize at the plasma membrane by a glycosylphosphatidylinositol (GPI) anchor and are suggested to play important functions in plants including reproduction process (Pereira *et al.*, 2016b). In tobacco, transmitting tissue-specific AGPs promote pollen tube growth in a semi-*in vivo* culture system (Wu *et al.*, 2001).

In the un-pollinated silk of maize, 1427 genes showed specifically or preferentially expression (Xu *et al.*, 2012). After pollination, 172 genes were induced, most of which are involved in RNA transcription, signaling transduction, and lipid metabolism processes (Xu *et al.*, 2013). Some of

those genes might be involved in the communication between pollen tube and transmitting tract. For example, in maize dent-sterile popcorn, gametophyte factors (Ga) *S*-haplotype (Ga-*S*) exerts a female unilateral cross-incompatibility (UCI) by producing a barrier to non-self pollen (Wang *et al.*, 2018a). MicroRNAs (miRNAs) are also involved in the pollen-pistil interactions (Li *et al.*, 2013). After pollination, 38 miRNAs were found to be differentially expressed.

1.3.4 Phase IV: Pollen tube guidance by the ovule

In maize, pollen tube growth in the ovarial cavity from the end of the transmitting tract towards the micropylar region is mainly mechanically controlled by the shape of the ovule surface cells (Lausser and Dresselhaus, 2010). When the pollen tube reaches the area about 100-200 nm distance from the micropyle/egg apparatus, micropylar guidance directs the pollen tube through a few cell layers of nucellar cells inside the embryo sac. The first signal molecule discovered to attract pollen tubes in maize is ZmEA1 (Márton *et al.*, 2005), which is produced in the egg apparatus that included egg cell and two synergid cells. It accumulated in granules at the chalazal pole of the female gametophyte (Uebler *et al.*, 2015). However, *ZmEA1* is only present in the Poaceae. In eudicots, micropylar pollen tube is mediated with the help of defensin-like cysteine rich peptides named LURE (Okuda *et al.*, 2009; Takeuchi and Higashiyama, 2012). In *Arabidopsis*, the LURE signaling network includes the upstream synergid-expressed transcription factor MYB98, the pollen tube tip-localized interactors POLLEN RECEPTOR-LIKE KINASE6 (PRK6) (Takeuchi and Higashiyama, 2016), MALE-DISCOVERER1(MDIS1)-MDIS1-INTERACTING RECEPTOR-LIKE KINASE (MIK) heteromer (Wang *et al.*, 2016), and LOST IN POLLEN TUBE GUIDANCE (LIP1/2) (Liu *et al.*, 2013). Exclusively in *Torenia fournieri*, pollen tube chemotropic response to LURE peptide needs the ovular AGPs-derived Activation Molecule for Response Capability (AMOR) (Mizukami *et al.*, 2016). However, the AtLURE1-PRK6 signaling network is not indispensable in *Arabidopsis*, as the knockout of *AtLURE1* gene family did not affect fertility (Zhong *et al.*, 2019). Compared with the conspecific AtLUREs signal, XIUQIU1-4, another CRPs secreted by synergid cells, attract pollen tubes in a species-independent but family-specific manner (Zhong *et al.*, 2019).

Beside these well-studied genes in the micropylar guidance, many other components contribute to the tube attraction. These include, for example, a calcium gradient and nitric oxide (NO) as general components (for review see Zhou and Dresselhaus, 2019) and believed to be significantly

important.

1.3.5 Phase V: Gametophyte interactions

Once arrived at the micropyle, pollen tubes aim to enter the embryo sac. Pollen tube needs to go through or around the filiform apparatus to penetrate and stop growth in the receptive synergid cell (Márton *et al.*, 2005). The accurate stop in a synergid cell is necessary for sperm cells release. In maize, egg apparatus secreted ZmES4 controls the opening of pollen tube localized potassium channel KZM1, which correlates to pollen tube burst (Amien *et al.*, 2010). Similarly, *in vitro* application of ZmPMEI1 was capable to induce pollen tube burst in a concentration-dependent manner (Woriedh *et al.*, 2013).

In *Arabidopsis*, CrRLK1L family member FERONIA (FER) controls pollen tube growth arrest inside the embryo sac. *FER* mutation resulted in overgrowth of pollen tubes in synergid cell (Huck *et al.*, 2003), which is also presented in the mutation of FER related genes: FER co-receptor *LORELEI* (Liu *et al.*, 2016b); FER involved localization of *NORTIA* (NTA) (Kessler *et al.*, 2010); FER interactor Early Nodulin-like proteins (ENDOLs) (Hou *et al.*, 2016); FER paralogues HERCULES RECEPTOR KINASE 1 (HERK1) and ANJEA (ANJ) (Galindo‐Trigo *et al.*, 2020). Moreover, FER regulates the esterification state of pectin and nitric oxide at the filiform apparatus to prevent multiple pollen tube entrance (Duan *et al.*, 2020). Besides, vacuolar acidification mediated by AP1G and V-ATPases is involved in pollen tube reception (Wang *et al.*, 2017). Pollen tubes itself also control the growth in synergid cell as the mutation of pollen-specific genes *MYB97/101/120* (Liang *et al.*, 2013), *TRUN*, or *EVAN* (Lindner *et al.*, 2015) caused also overgrowth of pollen tubes in synergid cells. After pollen tube burst, sperm cells are released and fuse with two female gametes, egg and central cell, marking the end of the double fertilization process.

1.4 Aims of this work

Extracellular signaling peptides/proteins are intensively used during double fertilization across the plant kingdom. These include RALFs (Campbell and Turner, 2017), DEFENSINs (Sher Khan *et al.*, 2019), and Arabinogalactan proteins (AGPs) (Pereira *et al.*, 2016a). Some are species or family-specific like *EALs* in the Poaceae (Uebler *et al.*, 2015), or LURE1s in *Arabidopsis* and XIUQIUs in the Brassicaceae (Zhong *et al.*, 2019). In some cases, protein sequences within

peptide family members could be very diverse. For example, LUREs belong to the defensin-like protein family, but with the exception of the arrangement of cysteine residues, LURE protein sequences of *Torenia fournieri* and *Arabidopsis thaliana* show little homology among each other.

Maize is one of the most important cereals both for human and animal consumption. A better understanding of maize reproduction processes would ultimately benefit to the maize breeding technology improvement.

During plant reproduction processes, it was reported that CRPs are overrepresented in angiosperms (Bircheneder and Dresselhaus, 2016). According to unpublished RNA-seq data in the lab on various reproductive tissues of maize (e.g. pollen tube, silk, silk hairs, pollinated-silk) many *CRP* genes are expressed in these tissues. Some *CRPs* even show a pollen-specific expression pattern and belong to the most strongly expressed genes in the male gametophyte. This study should focus on three types of them: *RALF*, *Pollen Ole e1 (POE),* and *DEFL* genes. The goal was to explore the distribution of these genes in the maize genome, to identify interactors and possible functions. Functions of various RALF members in plant development and reproduction have been elucidated in *Arabidopsis*. However, the function of RALF peptides in maize have not investigated. The distribution of *RALF* genes in the maize genome should be studied, the subcellular localization of various RALF members, and function(s) in pollen tube growth via generation of RNA interference gene knockdown mutants. Putative interaction partners like ZmCrRLK1Ls, ZmLLGs, and ZmLRX/ZmPEXs should be identified based on available knowledge in *Arabidopsis* and the interactions tested. In addition, the conservation of RALF interactions should be studied using maize and *Arabidopsis* as models. Although maize *Pollen Ole e1-like* genes were first described many years ago (Hanson *et al.*, 1989), their function(s) are still unclear. Two of the most strongly expressed *POE1* genes should be investigated via RNAi and CRISPR/Cas9 mutant construction. *DEFL* genes represent another highly polymorphic family expressed in pollen tubes (Parisi *et al.*, 2019). A member representing one of the 10 most strongly expressed genes in pollen tubes should be studied in maize.

CHAPTER 2. IDENTIFICATION AND FUNCTIONAL ANALYSIS OF MAIZE RALF PEPTIDES

2.1 Introduction

Rapid alkalinization factors (RALF) peptides, a group of cysteine rich peptide hormone, have been investigated for 20 years. More than 70 papers focused on RALF peptides research have been published. Why RALF peptides attracted so much attention? Here will be a summary on how people understand the function of RALF peptides step by step in the last 20 years, and the remaining mysterious which needs to explore in the future.

2.1.1 Distribution of RALF peptides across the plant kingdom

RALF peptide was discovered accidentally. As byproduct of tobacco systemin purification, a RALF peptide was identified with the ability to cause rapid alkalinization within nanomolar concentration, that's why it was named as RALF afterwards (Pearce *et al.*, 2001b). Because of the alkalinization ability, RALF peptide was supposed to have similar defensive function as systemin. However, application of RALF peptide did not induce the synthesis of trypsin inhibitor as systemin did, which was the sign of wound signal transduction (Pearce *et al.*, 2001a). RALF peptides were distributed in more than 16 plant species, suggesting their multiple functions during plant development (Pearce *et al.*, 2001b). Therefore, as a novel peptide hormone, functional analysis of RALF peptides was initiated.

Nine *RALF* genes were identified in *Arabidopsis thaliana* genome (Pearce *et al.*, 2001b), while the real number of *RALF* genes was more than this. Just one year later, 34 *AtRALF* genes were identified (Olsen *et al.*, 2002). Until now, a total number of 37 *RALF* genes were reported in *Arabidopsis* (Abarca *et al.*, 2020). Later, *RALF* genes were identified in more and more plant species. for example, there are 5 *RALF* genes in *Solanum chacoense* (Germain *et al.*, 2005); 16 *RALF* genes in *Oryza sativa* (Cao and Shi, 2012); 38 *RALF* genes in *Chinese cabbage* (Shi *et al.*, 2017). With wide-ranging phylogenetic analysis of the RALF family across plant kingdom, 795 RALF peptides were identified in 51 species, even in the early-diverging angiosperm *Amborella trichopoda* (Campbell and Turner, 2017). RALF peptides were not only being found in plants, but

was also discovered in Fungi (Masachis *et al.*, 2016). More than 26 phytopathogenic fungi contain *RALF* genes, and their protein sequences were well conserved with plant RALF peptides (Thynne *et al.*, 2017).

2.1.2 Overall expression of *RALF* genes in various plant species

Within plant, *RALF* genes were distributed across varies tissues. RALF peptide was initially isolated from tobacco leaves (Pearce *et al.*, 2001b), following research revealed it's ubiquitously expression pattern. For instance, *ScRALF1/3* were predominantly expressed in ovaries and large fruits of *Solanum chacoense* (Germain *et al.*, 2005); *NaRALF* was highly expressed in roots and petioles of *Nicotiana attenuata* (Wu *et al.*, 2007); *SlPRALF* was identified as a pollen-specific peptide from *Solanum lycopersicum* (Covey *et al.*, 2010). In *Arabidopsis*, *RALF* genes could be found in almost all tested tissues (Cao and Shi, 2012).

Fused with an N-terminal GFP-tag, subcellular localization of RALF peptide was investigated in *Nicotiana benthamiana* (Escobar *et al.*, 2003). The RALF-GFP signal was first detected within ER, and later gradually migrated to apoplast/cell wall. Synthesized *LeRALF* peptide could be totally dissociated from suspension cell culture by acid washes, indicating their apoplast localization (Scheer *et al.*, 2005). After germination, pollen-specific SlPRALF peptide can be detected in pollen germination medium, demonstrating the SlPRALF was secreted out from pollen tube (Covey *et al.*, 2010).

2.1.3 Four basic features of RALF peptides

There were four features that distinguish RALF peptides from other peptide hormones. First, as a cysteine rich peptide hormone, the fundamental feature of RALF relies on its cysteine residues arrangement pattern, which divides RALF peptides into three types with two or four cysteine residues (Silverstein *et al.*, 2007).

The second feature of RALF peptides is the existence of propeptide. NaRALF was found as a short peptide with 49 amino acids, while the full length of its coding sequence can be translated into a preproprotein of 115 amino acids which harbored mature RALF peptide sequence at C terminus (Pearce *et al.*, 2001b). The double arginine residues which positioned two amino acids upstream of the mature peptide was proposed to be the processing site for proteolytic enzyme.

This was proved by the treatment of Sphingosine-1-Phosphate (S1P), a Golgi-localized subtilisin-like serine protease (Srivastava *et al.*, 2009). *Arabidopsis* S1P recognize canonical (RXXL or RXLX, X represent any amino acids) cleavage site was widely spread in RALF peptides (Campbell and Turner, 2017; Liu *et al.*, 2007). The substitution of RR residues to GG blocked the processing and resulted in the absent of mature RALF peptide (Srivastava *et al.*, 2009).

The third feature of RALF peptides is the interaction motif YI/LSY in the N-terminus of mature RALF peptides. In tomato (*Solanum lycopersicum*), YISY motif was necessary for the activity of SlRALF (Pearce *et al.*, 2010). Substitution of alanine with isoleucine in YISY caused activity reduction, while the substitution of other three amino acids showed no effect on activity, indicating the isoleucine residue was critical for the peptide activity. Besides, the mature peptide of ScRALF5 and PtdRALF1/2 with YLSY motif were also functional, indicating the interaction with corresponding receptor relied on a hydrophobic R-group at this position. By analyzing the crystal structure of RALF23-LLG2-ectoFER complex from *Arabidopsis*, the conserved YISY motif was proved to be the core region of inducing the complex between FERONIA and LLG (Xiao *et al.*, 2019).

The fourth feature of RALF peptides is the double tyrosine (YY) interaction motif between the first and second cysteine residues following YI/LSY motif. Complex of AtRALF4-AtLRX8 was formed directly on double tyrosine residues of RALF peptides, so this motif was identified as the core of interaction between RALF peptide and leucine-rich repeat extensins (LRXs) (Moussu *et al.*, 2020).

2.1.4 Diverse functions of RALF peptides

As a ubiquitously expressed peptide hormone, RALF peptides play different roles in various tissues at different time of plant development. In root, knock out of tobacco *NaRALF* gene resulted in longer roots and abnormal root hairs (Wu *et al.*, 2007). Similar phenotypes were observed in *ralf1* mutant in *Arabidopsis* (Bergonci *et al.*, 2014) and *ralf1* mutant in Russian dandelion (Wieghaus *et al.*, 2019). AtRALF34 played an important role in orchestrating formative cell division in the pericycle of lateral root (Murphy *et al.*, 2016). In leaf, AtRALF23 peptide treatment or gene overexpression led to the inhibition of *elf18*-induced ROS production (Stegmann *et al.*, 2017), while the effect dismissed in *feronia* (receptor of RALF, discussed in Chapter 3) mutant. Application of AtRALF1 peptide promotes stomatal closure and inhibits its opening (Yu and

Assmann, 2018).

RALF peptides play important roles during reproduction process. In *Solanum lycopersicum*, *in vitro* application of pollen-specific SlPRALF peptide inhibited the early phase of pollen tube elongation (Covey *et al.*, 2010). In *Arabidopsis thaliana, Atralf4/19* double mutants disrupted pollen tube integrity and induced pollen tube burst (Ge *et al.*, 2017; Mecchia *et al.*, 2017). Ovule-derived *AtRALF34* was proposed to be a paracrine signal enabling pollen tube to respond to the ovular environment (Ge *et al.*, 2017). In *Solanum chacoense*, ScRALF3 is involved in male and female gametophyte development, and downregulation of *ScRALF3* gene resulted in the decreased pollen viability and starch (Loubert‐Hudon *et al.*, 2020).

RALF peptides also have effect on responding to abiotic and biotic stress in plant. Wounding induced *ScRALF2* expression (Germain *et al.*, 2005); salt stress promoted mature AtRALF22 release which induced the internalization of FERONIA, by which regulating salt stress tolerance (Zhao *et al.*, 2018); immune response to hypovirulent bacterium *Pseudomonas syringae* pv. *tomato* (Pto) DC3000 could be strengthen by AtRALF17 peptide pretreatment, while AtRALF23 peptide treatment showed opposite function (Stegmann *et al.*, 2017).

2.1.5 The linkage of RALF peptides with other signaling molecules

To perform multiple functions in plants, RALF peptides need to cooperate with different interactors. Since the first RALF peptide cell membrane receptor FERONIA was found in *Arabidopsis* (Haruta *et al.*, 2014), many interactors were discovered. They work together with RALF peptides to regulate various signaling pathways (Chapter 3). Here, we only focus on the traditional plant hormones signaling molecules.

Plant hormones control all aspects of plant growth and responding to biotic/abiotic stresses. Classical plant hormones include abscisic acid (ABA), auxins (AUX), ethylene (ETH), brassinosteroids (BRs), cytokinins (CKs), gibberellins (GAs), jasmonate (JAs), salicylic acid (SA), and so on. In hybrid poplar suspension cells, transcription of *PtdRALF2* was completely suppressed by addition of methyl jasmonate (MeJa), while was not changed by addition of cytokinin or auxin (Haruta and Constabel, 2003). In contrast, expression level of *AtRALF34* was downregulated by auxin treatment in *Arabidopsis* lateral roots (Murphy *et al.*, 2016). Suppression of *AtRALF1* rendered plants hypersensitive to ABA treatment (Chen *et al.*, 2016) and caused less

affection by BRs treatment on root growth (Bergonci *et al.*, 2014). Over expression of *AtRALF22* showed higher levels of JA and SA compared with wild type (Zhao *et al.*, 2020). It is therefore likely that RALF peptides collaborate with various plant hormones to achieve fine-tuned of plant growth.

2.1.6 RALF peptides functional mechanism

Alkalinization ability of RALF peptides was commonly presented in different plant species. Isolated PtRALF1 peptide elicited stronger and faster alkalinization activity than other tested elicitors in hybrid poplar culture medium (Haruta and Constabel, 2003). *NaRALF* knock out resulted in slower apoplastic pH oscillation and increased pH at the tips of trichoblasts in *Nicotiana attenuata* (Wu *et al.*, 2007). It was proposed that fungal pathogens used RALF peptides functional homologues in their host plants to induce an upshift in extracellular pH, which promoted their infection and suppress host plant immunity (Masachis *et al.*, 2016). Application of RALF peptide could increase cytoplasmic Ca^{2+} level (Haruta *et al.*, 2008), which was treated as the reason for alkalinization ability (Gjetting *et al.*, 2020).

However, the function of RALF peptides was not always linked with its alkalinization activity. For example, there was no significant pH change by *in vitro* application of synthetic pollen-specific SlPRALF peptide to pollen germination medium (Covey *et al.*, 2010). Recombinant pollen-specific AtRALF4 peptide was not able to induce the alkalinization of cell suspension medium as the other AtRALF peptides (do Canto *et al.*, 2014). In pollen, RALF peptides were mainly function in maintaining the cell wall integrity by cooperating with various related interactors (Ge *et al.*, 2017; Ge *et al.*, 2019a; Mecchia *et al.*, 2017).

2.1.7 Limitation on RALF knowledge so far

Up to now, most RALF studies focused on different tissues from *Arabidopsis*. Beside *Arabidopsis*, only several RALF peptides were investigated, including tomato (Covey *et al.*, 2010), tobacco (Pearce *et al.*, 2001b). Furthermore, among the limited number of investigated plants, only grass sugarcane (*Saccharum spp.*) belongs to monocots, so the function of RALF peptides in monocots is still unclear. Here, a comprehensive study about maize RALF peptides was carried out, which could greatly contribute to the understanding of the function of RALF peptides in monocots.

2.2 Experimental procedures

There are many commonly used methods were depicted in detail. If experiments were performed strictly according to the introduction of manufacture from commercial kits or published paper, they will not be introduced in detail. Only those with modification will be described.

2.2.1 Bioinformatic analysis

2.2.1.1 Genome blast of maize RALF genes

According to mRNA expression data derived from different maize tissues, three *RALF* genes which were highly and exclusively expressed in pollen were found. In terms of the mRNA expression level (TPM, Transcripts Per Kilobase Million), three *RALF* genes were named as *ZmRALF1*, *ZmRALF2* and *ZmRALF3* (*Zea mays RALF 1/2/3*). Putative open reading frame (ORF) was identified and translated into protein using the online tool ExPASY (https://web.expasy.org/translate/). The predicted proteins were named as ZmRALF1, ZmRALF2 and ZmRALF3.

To identify potential members of *Zea mays RALF* genes (*ZmRALFs*), two databases were used for searching. ZmRALF1/2/3 mature peptides were used as queries to run BLASTP (protein-protein BLAST) in the non-redundant protein sequences (nr) of *Zea mays* (taxi:4577) in NCBI database (https://blast.ncbi.nlm.nih.gov/). To avoid the missing of any possible homologue, the same queries were used to run TBLASTN in protein database Gramene (http://ensembl.gramene.org/). BLOSUM62 matrix was used in both blasts. The output protein sequences were manually selected, only the ones with high query cover (>50%) and E-score (< 0.05) were taken into consideration. The selected peptides were further confirmed according to the cysteine residues arrange model (Silverstein *et al.*, 2007). After RALF peptides were identified, the correspond locus tag (B73 RefGen_v4) or gene symbol were extracted from NCBI.

2.2.1.2 Gene information and expression pattern

Gene information of *ZmRALF* genes was extracted from Gramene. *Arabidopsis* RALF (AtRALF) protein sequences were extracted form protein database UniProt (Consortium, 2019), in which the manually annotated ones were chosen. The signal peptides were predicted by SignalP-5.0 server

(http://www.cbs.dtu.dk/services/SignalP/**,** (Almagro Armenteros *et al.*, 2019)), and the prepropeptide sequences were identified according to RALF protein features (section 2.1.3).

Expression data of maize *RALF* genes (TPM, transcriptions per kilobase million) were extracted from unpublished date from Dresslhaus' group. *Arabidopsis RALFs* mRNA expression data (FPKM, fragments per kilobase million) were download from GENEVESITGATOR database mRNA-seq Gene level (www.genevestigator.com). It should be noted that the expression pattern of genes in pollen is absent in the database. In the investigation of *Arabidopsis* pollen transcriptome, RNA-seq of *Arabidopsis* pollen and seedling were performed (Loraine *et al.*, 2013). To integrate the expression data from two databases, the commonly performed seedling genes' expression level was used for normalization. As the seedling expression data from Loraine *et al.*, 2013 is coincide with those in GENEVESTOR, the pollen expression data was directly integrated to this work.

2.2.1.3 Ideogram construction

Maize chromosome information and localization of *ZmRALF* genes on chromosomes were extracted from Graneme. Localization of *ZmRALF* genes were manually marked on the bar that represent the chromosome. Chromosomes were drawn according to the real length.

2.2.1.4 Protein motif search

In order to search conserved motifs in maize RALF peptides, online tool MEME5.1.1 (Motif EM for Motif Elicitation, http://meme-suite.org/tools/meme, (Bailey *et al.*, 2009)) was used with the following parameters: number of repetitions = any, maximum number of motifs = 5, and with optimum motif widths constrained to between 4 and 50 residues. Only motifs with expected value lower than 1×10^{-8} were taken into consideration.

2.2.1.5 Protein alignment

RALF peptides were aligned using MEGA_X software (Kumar *et al.*, 2018). There are two alignment methods installed: MUSCLE and CLUSTALW. It was reported that MUSCLE perform similar accuracy with CLUSTALW but faster (Edgar, 2004). Thus, MUSCLE align method was used for multiple protein sequences alignment.

To better present the similarity of protein sequences, GeneDoc version 2.7 (Nicholas and Nicholas, 1997) and Jalview 2.0 (Waterhouse *et al.*, 2009) were used. GeneDoc version 2.7 display the amino acids in black and white, with conserved shading mode that highlight the similarity. Jalview 2.0 display the alignments in color, which exhibit the specific mode of sequences.

2.2.1.6 Generation of phylogenetic tree and visualization of protein sequence conservation

Protein sequence alignment result was used for phylogenetic tree construction. Phylogenetic relationships of 24 RALF mature peptides from *Zea mays* and 37 from *Arabidopsis thaliana* were used. The evolutionary history was inferred using the Neighbor-Joining method (Saitou and Nei, 1987). The bootstrap consensus tree inferred from 1000 replicates was taken to represent the evolutionary history of the taxa analyzed (Felsenstein, 1985). Branches corresponding to partitions reproduced in less than 50% bootstrap replicates were collapsed. The percentage of replicate trees in which the associated taxa clustered together in the bootstrap test (1000 replicates) were shown next to the branches. The evolutionary distances were computed using the Dayhoff matrix-based method (Dayhoff *et al.*, 1979) and were in the units of the number of amino acid substitutions per site. This analysis included 61 amino acid sequences. All positions with less than 40% site coverage were eliminated, i.e., fewer than 60% alignment gaps, missing data, and ambiguous bases were tolerated at any position (partial deletion option). Evolutionary analysis was conducted in MEGA_X (Kumar *et al.*, 2018). The phylogenetic tree was further optimized by online tool Evolview_v3 (https://www.evolgenius.info/evolview/, (Subramanian *et al.*, 2019)).

Gene ID of numbered *RALF* genes were present in the branches, while the *RALF* genes from *Arabidopsis* were highlight in brown. Four RALF clades were distinguished with different background colors.

The mRNA expression data from five given tissues were represented by dots. They are pollen (red), stigma (green), root (blue), leaf (yellow), and seed (red). The dot size represents the mRNA expression intensity. Accordingly, four expression levels were divided: the biggest dot represent TPM/FPKM value of gene higher than 1000; the big dot represent that between 100 to 1000; the small dot represent that between 10 to 100; the smallest dot represent that between 0-10.

To check the amino acids varieties in each group, amino acid sequence logo was generated. A

sequence logo is a graphical representation of an amino acid multiple sequence alignment. Each logo made up by stacks of symbols, on stack for each position in the sequence. Sequence conservation were indicated by the overall height of the stack, while the relative frequency of each amino acid is indicated by the height of symbols within the stick. In general, a sequence logo provides a richer and more precise description of compared sequences. Online tool WebLog 3 (http://weblogo.threeplusone.com/**,** (Crooks *et al.*, 2004)) was used.

2.2.2 Plant material

2.2.2.1 Plant growth condition and pollination

Maize seeds were soaked in water overnight and then transferred into small pots (10 cm diameter, 1 seed per pot). After genotyping, seedlings were transferred into 10 L pots. The plants were grown in greenhouse under controlled condition of 16 hour of light at 25 ± 2 °C and 8 hours of darkness at 21 ± 2 °C. The air humidity is maintained around 60-65%. To ensure enough light, additional 24,000 LUX light was provided. Plants were watered by an automated temperature-water-based irrigation system, which based on plant consumption in a time-based pre-programmed schedule. Fertilizer were applied with 2% Hakaphos (Compo Expert) twice a week and monitored throughout their entire vegetative and reproductive development.

Maize ears were covered with paper bags before silk emerging to avoid any pollen contamination. For crossing, the old pollen on tassel was removed in the morning. Two to three hours later, fresh pollens were used to pollinate the covered ear, afterwards the bags were marked and kept on the ear. Thirty days later after pollination, the plants were transferred into dry chamber with lower humidity and ceased watering. Around three weeks later, the corns were harvested.

Arabidopsis thaliana seeds were sown on soil and kept for 2-3 d at 4°C in the dark for stratification. Seedling were then grown at long-day conditions at 21°C for 16 hours of light under illumination of 150 μm s^{-1} m^{-2} and 8 hours of darkness at 18°C at 60% air humidity.

2.2.2.2 Pollen germination

To collect the pollen samples for *in vitro/in vivo* germination, old pollen was removed in the early morning and newly released pollen was collected, which ensured the good condition of pollen samples.

In vitro pollen germination was carried out (Schreiber and Dresselhaus, 2003). The solid pollen germination medium (PGM) ensured more than 90% of the wild type pollens germination. Pollen germination medium was made by mixing of 2x PGM (20% Sucrose; 0.005% H_3BO_3; 20mM CaCl2; 0.1 mM KH_2PO_4; 12% PEG4000, pH=5) liquid components and equal volume of autoclaved 0.6% NuSieveTM GTGTM agarose (Lonza) to a final concentration of 0.3%. 1.2 mL of PGM medium was applied into 35 mm petri dish and left at room temperature (RT) for 10 min. A relative thin and even layer of PGM was got by softly shaking the unconsolidated medium. Fresh pollens were directly collected by softly shaking the tassel, which were then evenly spread on the surface of pollen germination medium. Pollen was germinated at room temperature (22-23°C) in a wet chamber. The pollen tube germination status was checked with Nikon Eclipse 1500 with a 4x objective (Plan Fluor DL 4x/0.13, PHL).

In vivo pollen germination was carried out in greenhouse. Fresh pollens were collected with a paper bag and an excess of them were applied on silk. To avoid any pollen contamination, the covered bag on silk only shortly took off during pollination, afterwards it was immediately put back again. One hour later, 5 cm pollinated silk from top were cut off and fixed in 9:1 v/v ethanol: acetic acid at 4°C overnight. *In vivo* pollen tube visualization via aniline blue staining was achieved according to the method in Marten,1959 with adjustment. Fixed samples were rehydrated by water series. Then they were treated in 8 M sodium hydroxide for 2~4 hours to clear and soften the tissue. The softened silks were washed by water for 2~4 times. Staining was carried out in aniline blue stain solution (0.1% aniline blue; 0.1 M $K_2HPO_4 \cdot 3H_2O$, pH=11) overnight at 4°C. Specimens were washed and mounted with fresh staining solution on a slide with a cover slip and being analyzed under fluorescence microscope ZEISS Axio Imager 2 with a 20x objective (Plan-Apochromat 20x/0.8 M27) at 350~400nm (UVA) excitation.

2.2.2.3 Isolation of genomic DNA from maize plants

Genome DNA of maize was prepared from leaves of two weeks old seedling. Around 0.5 g from the tip of the youngest leaf were cut and collected in a 2 mL microcentrifuge tube with two metal balls (2 mm in diameter) inside. Samples were immediately frozen in liquid nitrogen. To beak the tissue, samples were grinded using a mill (MM200 Mixer Mill, Retsch) with 30K rpm for 2 min. 800 µL DNA extraction buffer (1% N-Lauryl-sarcosine, 100 mM Tris-HCl pH=8, 10 mM EDTA pH=8, 100 mM NaCl) and 800 µL PCI (Phenol/Chloroform/Isoamyl alcohol, 25:24:1, ROTH)

were added and mixed by oscillating for 10~20 seconds. After centrifuging for 7 min at 7000 rpm, the supernatant (around 700 µL) was collected in a new microcentrifuge tube to mix with 80 µL sodium acetate (3 N). Then 800 µL isopropanol was added and mixed by inverting the tube. The mixture was again centrifuged for 10 min at 13,000 rpm and the supernatant was discarded. The pellets were washed with 70% ethanol and dried at room temperature. Then the pellets were dissolved in 200 µL TE buffer (10 mM Tris/HCl pH=7, 1 mM EDTA) and stored at 4°C. For quantification and quality control, the gDNA was analyzed on 1% agarose (GeneOn) gel stained with 0.005% Roti-Safe GelStain (Car-Roth) and photometrically analyzed using the Nanodrop ND 100 (Thermo Fisher Scientific)

2.2.2.4 Isolation of total RNA and reverse transcriptase-PCR (RT-PCR)

For total RNA extraction from pollen, Invitrogen™ TRIzol™ Plus RNA Purification Kit (Thermo Fisher Scientific) was used. The tubes and tips used in RNA extraction process were RNase-free. The metal balls were autoclaved overnight at 180°C. Working bench and pipettes were cleaned with RNase *Zap* ® RNase Decontamination Solution (Thermo Fisher Scientific).

Total RNA was extracted according to the following protocol. Approximately 0.2 g pollen or pistil samples were collected in a 2 mL microcentrifuge tube with two metal balls inside. Samples were frozen in liquid nitrogen and ground to powder using a mill. 1 mL of TRIzol™ Reagent was added directly to the sample and oscillated to homogenize and lyse the cells. After 5 min incubation, 200 mL chloroform were added. Samples were homogenized by inverted several times and incubated for 2~3 min. After centrifuging 15 min at 12,000 x g at 4°C, the mixture separates into a lower red phenol-chloroform phase, interphase, and a colorless upper aqueous phase. Around 600 µL colorless supernatant containing RNA was transferred to a new tube and mixed with equal volume of 70% ethanol by hand shanking. To bind total RNA on column, the mixture was transferred into spin cartridge provided by the kit. Total RNA should bind to membrane by centrifuging at 12,000 g for 15 seconds. To remove any possible DNA contamination, RNase free DNase solution (QIAGEN) were added to spin and centrifuged. RNA on the membrane were washed by sequentially washing buffers supplied with the kit. Total RNA would be eluted out from membrane by adding 50 µL RNase-free water and centrifugation. For quantification and quality control, isolated RNA was photometrically analyzed using the Nanodrop ND 100 (Thermo Fisher Scientific) and stored at -80°C. 1 µg of total RNA was used for first strand cDNA synthesis using

Oligo (dT) 18 primer (Thermo Fisher Scientific) and Reverse Transcriptase (RevertAid™ reverse transcriptase, Thermo Fisher Scientific) according to the instruction.

2.2.2.5 Quantitative PCR (RT-qPCR)

ZmRALFs gene-specific quantitative PCR (qPCR) primers (Supplemental Table 2) were designed and tested. In a total volume of 20 µL, 50 ng cDNA were used as template, 200 nM gene-specific forward and reversed primers were added, 10 µl KAPA SYBR FAST qPCR Master Mix (2x) (Peqlab) were used to bind cDNA for fluorescence detection by a Master Cycler realplex2 (Eppendorf). qPCR was carried out in a two steps reaction: 95°C hold for three minutes to activate the enzyme, following by 40 cycles including each three seconds at 95°C denaturation and 20 seconds at 60°C for annealing and extension. The assay involved two biological replicates, each represented by two cDNA pools that were used as templates for three technical replicate reactions. Normalization was based on two internal maize reference genes, the maize membrane protein PB1A10.07c (reference gene 1, Zm00001d018359) and cullin (reference gene 2, Zm00001d024855) that were previously reported to be equally expressed in different tissues at different time points (Manoli *et al.*, 2012). Final data analysis was calculated with Excel sheets using the ΔΔCT method (Livak and Schmittgen, 2001).

2.2.3 Gene cloning and plasmids construction

To investigate the function and localization of RALFs, various constructs were made. The destination vectors various for the purpose, while the operations such as amplification, agarose gel running, gel recovery, and sequencing are the same. For each step, cloning products were transformed into *E.coli (DH5α or DB3.1* if CCDB included*)*. PCR test was applied to select the candidates, afterwards several single colonies were used for amplification and plasmid extraction (Bacterial Plasmid Miniprep Kit, Biocompare). Successfully cloning were finally confirmed by sequencing (Macrogen).

2.2.3.1 ZmRALFs protein expression plasmids construction

According to the S1P splicing feature of ZmRALF protein, the correspond mature peptide was identified and correspond DNA region was used for cloning. Gene specific primers (Supplemental Table 2) were designed and used for amplification with the template cDNA from maize pollen of

inbred line B73. To amplify the destination fragment, Phusion® High-Fidelity DNA Polymerase (New England BioLabs) was used. After polymerase chain reaction (PCR), samples were separated by 1% agarose gel and visualized by GEL iX20 Imager (iNTAS). The bands fit with the expected sizes were cut out and DNA was recovered from gel with QIAquick Gel Extraction Kit (QIAGEN). To ensure the quality of recovered DNA, the concentration was checked with Nanodrop ND 100, samples were finally stored at -20°C.

There are two types of plasmids with 6xHis tag were used in this research: pET53-DEST from NovaPro and pET-32b(+) from Novagen. For destination vector pET53-DEST, gateway cloning method was used. ZmRALF fragments were firstly cloned into pENTR-D-TOPO with Gateway ™ pENTR ™ / D-TOPO ™ cloning kit (Thermo Fisher Scientific). Then, the constructs were transferred to pET53-DEST individually by LR reaction using Gateway LR Clonase II Enzyme Mix (Thermo Fisher Scientific). For destination vector pET-32b(+), restriction cloning method was used. Amplified ZmRALF fragments and backbone pET-32b(+) were digested with corresponding restriction enzymes (New England BioLabs), purified by agarose gel and recovered with QIAquick Gel Extraction Kit. Then the backbone and fragments were ligated by T4 ligation (T4 DNA Ligase, New England BioLabs).

2.2.3.2 RNA interfering mutant construction

Considering that nine *RALF* genes are expressed in pollen of maize, an RNAi construct was generated to downregulate the whole gene family. Gene-specific transcribed regions of *ZmRALF1/2/3* generating together about 90% RALF transcripts in maize pollen were cloned after DNA amplification from genomic DNA in one vector and the RALF RNAi vector thereafter generated as follows: 604 bp (Supplemental Table 3) fragment from *ZmRALF1/2/3* (*ZmRALF1*: 190 bp, *ZmRALF2*: 212 bp, *ZmRALF3*: 202 bp) was cloned into the corresponding splicing sites of the pUbi-iF2 vector (DNA Cloning Service) that contains a maize Ubi promoter. The constructed plasmid was further amplified in *E.coli* to obtain higher amount for transformation. Middle scale plasmid extraction was performed by Invitrogen™ PureLink™ HiPure Plasmid Filter Midiprep Kit (Thermo Fisher Scientific) according to the manufacture.

2.2.3.3 CRISPR/Cas9 mutant construction

Guide RNA sequences were designed from online tool Breaking-Cas (Oliveros *et al.*, 2016) and

CRIPSPR-P v2.0 (Lei *et al.*, 2014) with the following parameters: *Zea mays* (4577) genome; NGG as PAM; the other were remained as default. Only the commonly output guide RNA fragments from two websites were considered. Among those fragments, the one with less off-targets and high score were chosen. The integration of guide RNA to pGW-Cas9 were carried out according to the description in Char *et al.*, 2017. The final constructs were further verified by restriction enzyme digestion.

2.2.3.4 ZmRALFs subcellular localization

For *ZmRALFs* subcellular localization studies in *Arabidopsis*, 2286 bps upstream of the ATG start codon of the *Arabidopsis AtRALF4* gene was used as promoter, followed by ORFs of *ZmRALF* genes cloned from maize pollen cDNA. First, the *AtRALF4* promoter region was cloned from *Arabidopsis* genomic DNA and the promoter was integrated into pB7FWG2.0 by restriction enzyme digestion and T4 DNA ligation. Then, the *ZmRALF* fragments were transferred individually by LR reaction using Gateway LR Clonase II Enzyme Mix (Thermo Fisher Scientific). The constructs contain a C-terminal fused eGFP sequence. Finally, gene constructs were transformed into *Arabidopsis thaliana ralf4ralf4/RALF19ralf19* double mutant line.

2.2.3.5 Transformation of maize and Arabidopsis

Maize mutants were created by Iowa State University Plant Transformation Facility (https://ptf.biotech.iastate.edu/). In brief, maize mutant constructs including RNAi-*RALFs* and Cas9-*RLAFs* were transferred to *Agrobacterium* strain EHA101 which was used for infecting immature Hi-II maize embryos. After identification of bialaphos-resistant callus lines by molecular analysis, the positive transformed callus was transferred to regeneration medium. Multiple plantlets per line were generated from callus. The plantlets in petri dish were recovered in incubator at 28 °C for several days after shipment, afterwards they were transferred into soil and being kept in greenhouse. *Arabidopsis* transformation was carried out with *Agrobacterium tumefaciens strains GV3101* (pMP90RK). The destination vectors were delivered to GV3101 *Agrobacterium* chemically competent cell. Floral dip method was applied to transform the constructs to the *Arabidopsis thaliana ralf4ralf4/RALF19ralf19* double mutant line as described (Clough and Bent, 1998). Mature seeds from transformed plants were vernalized and planted in soil. Three days after germination, BASTA-resistant seedlings were selected by spraying three

times with 200 mg/L BASTA (Bayer Crop Science) supplemented with 0.1% Tween 20. Those BASTA resistance seedling were selected and analyzed for the presence of transgene constructs by PCR using corresponding specific primer (Supplemental Table 2).

2.2.4 Protein purification

Protein related tests were carried out according to the protein purification protocol of The QIAexpressionist (QIAGEN) with modification. The destination constructs were transformed to BL21 (DE3) that normally used for heterologous protein expression in *E.coli*.

2.2.4.1 Protein solubility test

500 µL overnight *E. coli* culture containing the corresponding protein expression plasmid was added to 20 mL LB-medium (Yeast extract, 5 g/L; Tryptone, 10 g/L; Sodium chloride 10 g/L) with corresponding antibiotic and incubated in a 37°C shaker at 200 rpm for two hours (OD600~0.6). For comparison, 1 mL sample were taken as before induction (BI, noninduced control) and pelleted, resuspended in 50 µL 1x SDS-PAGE sample buffer (0.075 M Tris-HCl pH=8; 0.6 % SDS; 15% Glycerol; 7.5% β-mercaptoethanol; 0.0009% bromophenol blue). Afterwards, Isopropyl β-D-1-thiogalactopyranoside (IPTG, SERVA) was added (1 mM IPTG) for protein expression induction. After two hours incubation in a 37°C shaker at 200 rpm, 1 mL sample was taken as after induction (AI). Cells in the remaining 18 mL sample were collected by centrifugation and being resuspended in 2 mL His Lysis buffer (50 mM NaH_2PO_4; 300 mM NaCl; 10 mM Imidazole, pH=8) containing protease inhibitor, 0.5 mg/ml lysozyme and 1 mM phenylmethylsulfonyl fluoride (PMSF). Cell wall was broken by sonication (5 min, 6 cycle, 40% power) with BANDELIN SONOPULS HD 2070 homogenizer (BANDELIN). 100 µL of the sonicated lysate was centrifuged to separate soluble fraction (SF) and insoluble fraction (IF), which was added to new tubes with equal volume of 2x SDS-PAGE sample buffer. All four samples were boiled at 95°C for 5 min to denature, and stored at -20°C

2.2.4.2 Protein purification under native conditions

2 mL overnight *E. coli* culture containing the corresponding protein expression plasmid was added to 1-liter LB medium with corresponding antibiotic and incubated in a 37°C shaker at 200 rpm. Once an OD600 of 0.5-0.7 was reached, 1 mM IPTG (SERVA) was added and further incubated

in a 30°C shaker at 200 rpm for another 3~4 hours. Afterwards, *E.coli* cells were pelleted by centrifugation. The pellet was resuspended in 40 ml chilled His lysis buffer containing protease inhibitor, 0.5 mg/ml lysozyme and 1 mM PMSF. Cells were broken by repeated sonication until samples became transparent. Lysates were collected by centrifugation at 4°C for 20 minutes at 16,000 g. Supernatants were separated from lysates and incubated with affinity beads at 4°C overnight (His beads: Ni-NTA, QIAGEN). Protein-binding beads were collected by centrifugation and being washed several times with washing buffer (50 mM NaH_2PO_4; 300 mM NaCl; 20 mM imidazole, pH=8) to remove unspecific binding proteins. Proteins were eluted from beads by incubating with elution buffer (50 mM NaH_2PO_4; 300 mM NaCl; 250 mM imidazole, pH=8) containing protease inhibitor, 0.5 mg/ml lysozyme and 1 mM PMSF at 4°C for 2~4 hours. Proteins were further desalted with PD 10 desalting columns (GE-Healthcare) according to manufacture.

2.2.4.3 Protein purification under denaturing conditions

Those 6xHis tagged insoluble proteins could be purified under denaturing condition. Protein induction and expression procedures are similar between native condition and denaturing condition. The difference between two methods lies on the way to lyses the cell. Under native condition, the cells were broken by sonication. If the expressed protein is not soluble, it will remain in inclusion bodies that cannot be used for further experiment. While in denaturing condition, the cells were digest by strong detergents like 8 M urea or 6 M guanidine-HCl (Gu-HCl) that can easily solubilize the expressed protein. Protein got in this way is under denaturing condition that cannot directly be used for protein interaction test. Protein renaturation and refolding can be carried out on the Ni-NTA column itself prior to elution (Holzinger *et al.*, 1996) or in solution (Wingfield, 1995). In this research, the protein denaturing condition purification and renaturation were carried out according to the description (Goto *et al.*, 2011).

2.2.4.4 SDS-PAGE Coomassie Brilliant Blue staining and immunoblot analysis

There are two types of protein running gel: proteins bigger than 10 kilodalton (kDa) were separated by SDS-PAGE using Tris/Glycine buffer system (Laemmli, 1970); proteins smaller than 10 kDa were separated by Tris/Tricine buffer system (Schägger and Von Jagow, 1987). After SDS-PAGE running finished, proteins were stained with Coomassie Brilliant Blue (CBB, 0.2%

Coomassie brilliant blue; 45% methanol; 10% acetic acid) or transferred onto nitrocellulose membrane (Amersham™ Protran®, GE Healthcare) for 45 min at 260 mA. The membrane was blocked in blocking solution (5% milk powder in TBST) and washed three times with TBST buffer (50 mM Tris-HCl pH 7.5; 150 mM NaCl; 0.1% Tween-20), incubating with 6xHis tag monoclonal antibody (diluted 1:5000 in 1% milk TBST, Thermo Fisher Scientific) and second antibody against mouse (diluted 1:5000 in 1% milk TBST, Thermo Fisher Scientific), two times washing with TBST for 10 min were applied between incubations. Finally, the protein signals were detected on membrane with application of HRP juice (PJK Biotech) by ChemiDOC™MP Imaging System (Bio-RAD).

2.2.5 Pollen germination status calculation and analysis

For pollen germination status, Image J (Schneider *et al.*, 2012) was used to count and classify the record pictures made by microscope. The records were then manually transferred to Excel and analysis was done. R (https://CRAN.R-project.org/package=ggpubr) was used to draw paired germination status calculation.

2.3 Results

2.3.1 *RALF* genes in maize genome

Based on previous studies, there are 37 *RALF* genes in the *Arabidopsis thaliana* genome (do Canto *et al.*, 2014), 5 *RALF* genes in *Solanum chacoense* (Germain *et al.*, 2005), and *19 RALF genes* in *Zea mays* (Cao and Shi, 2012). In a more comprehensive analysis, 795 *RALF* genes were identified in 51 plant species including 20 *RALF* genes in *Zea mays* (Campbell and Turner, 2017).

Using maize ZmRALF1/ZmRALF2/ZmRALF3 protein sequences as queries, 24 *ZmRALF* genes were detected (Supplemental Table 1). Besides the 20 *ZmRALF* genes which were found in previous studies (Campbell and Turner, 2017; Cao and Shi, 2012), *Zm00001d004232, Zm00001d044677, Zm00001d004242, LOC103634741* were found in addition. Maize *RALF* genes were named as *ZmRALF1-23* and *ZmRALF33* according to their mRNA expression levels (rank by descending) in pollen tube. *ZmRALF33* (*Zm00001d049233*) was named in the Gramene database already, so this name was kept. To visualize the genome organization of 24 *ZmRALF* gene members, a chromosome localization map was drawn (Figure 2.1). Except for chromosome

5 and 9 which harboring no *ZmRALF* members, *ZmRALF* genes were distributed over all rest chromosomes. Chromosome 3 and 8 contain more *ZmRALF* genes than other chromosomes, but a closer clustering of *ZmRALF* genes pointing towards recent gene duplications was not observed. Except for *ZmRALF4*, *ZmRALF18*, and *ZmRALF23,* other *ZmRALF* genes do not possess intron.

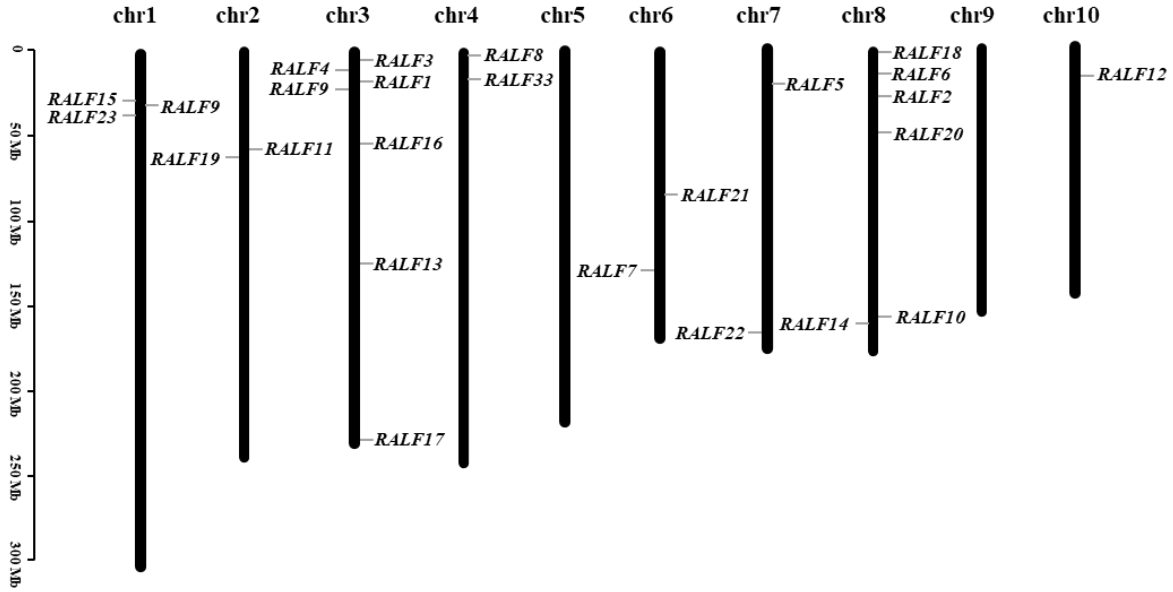

Figure 2.1 Chromosomal distribution of maize *RALF* genes. Chromosome numbers are shown at the top of each chromosome, and the approximate size in megabases (MB) is provided at the left side. The names of each *ZmRALF* gene showed is labelled at the sides of each chromosome.

2.3.2 ZmRALF peptides can be subdivided into four clades

Based on cysteine residues arrangement, RALF peptides can be subdivided into different clades. Three peptide types were distinguished based on genome-wide cysteine-pattern analysis of cysteine-rich peptide (CRP) including putative *RALF* genes (Silverstein *et al.*, 2007). The cysteine residues patterns were as follows: Type 1, CX{4,14}CX{22,51}CX{6,12}CX{5,14}CX{5,6}C; Type 2, CX{3,12}CX{5,21}CX{5,6}C, and Type 3, CX{5,6}C. Among 24 ZmRALF peptides, 12 ZmRALF peptides belong to Type 1 (2,3,7,8,9,12,13,14,15,18,23,33), 10 ZmRALF peptides belong to Type 2 (1,4,6,10,11,16,17,19,20,22) and only ZmRALF5 peptide belongs to Type 3. ZmRALF21 peptide cannot be placed into any of these three types, but due to the existing feature of S1P splicing site RRLL and interaction motif FISY, it was recognized as RALF peptide (Table 2.1).

Table 2.1 Peptide features of ZmRALFs. ZmRALF peptides were divided into three types according to their cysteine residues arrangement. Signal peptide region were extracted from UniProt. Subtilisin-like serine protease (S1P) motif, variation sequences in YI/LSY motif and YY motif were listed. The propeptide include amino acids before S1P motif.

RAFL protein	Signal peptide	Propeptide	Mature peptide	S1P	YI/LSY	YY	Cysteines arrange model	Type
ZmRALF1	1-25	-	49-74	-	-	-	C5C21C5C2	2
ZmRALF2	1-29	30-56	56-142	RRTL	YISY	YY	C6C46C10C12C5C5	1
ZmRALF3	1-29	30-59	59-145	RRTL	YISY	YY	C6C47C10C12C5C5	1
ZmRALF4	1-28	-	29-74	-	-	-	C5C21C5C3	2
ZmRALF5	1-28	-	29-78	-	-	-	C5C4	3
ZmRALF6	1-36	-	37-89	-	-	-	C5C21C5C2	2
ZmRALF7	1-22	23-50	50-129	RRAL	YISY	YY	C6C42C10C12C5C5	1
ZmRALF8	1-25	26-59	59-124	RRVQ		YY	C6C37C9C12C5C2	1
ZmRALF9	1-20	21-68	68-138	RRVL	YIGY	YY	C8C45C9C12C5C2	1
ZmRALF10	1-37	38-38	38-124	RREL	YISY	YY	C6C28C9C12C5C2	2
ZmRALF11	1-26	27-46	46-113	RRVL	-	-	C3C11C5C2	2
ZmRALF12	1-20	21-49	49-118	RRAL	YISY	YY	C6C37C9C12C5C2	1
ZmRALF13	1-20	21-53	53-124	RRAL	YISY	YY	C6C42C9C12C5C2	1
ZmRALF14	1-30	31-49	49-128	RREL	NIGY	YY	C8C29C9C12C5C2	1
ZmRALF15	1-25	26-58	58-145	RMRL	YISY	YY	C6C50C9C12C5C2	1
ZmRALF16	1-25	26-39	39-113	RRVL	YLSY	YY	C9C12C5C2	2
ZmRALF17	1-23	24-38	38-104	RRAL	SISY		C3C10C5C4	2
ZmRALF18	1-24	25-59	59-133	RRVL	YIGY	YY	C7C47C9C12C5C2	1
ZmRALF19	1-19	20-48	48-106	RRVL	-	-	C3C11C5C2	2
ZmRALF20	1-23	24-37	37-108	RVLQ	YLSY	YY	C20C9C12C5C2	2
ZmRALF21	1-30	31-22	22-125	RRLL	YISY	-	C40C7C43	-
ZmRALF22	1-22	23-35	35-128	RRRL	FISY	YY	C9C12C5C2	2
ZmRALF23	1-22	23-64	64-146	RLLL	-	YY	C22C35C9C12C5C2	1
ZmRALF33	1-31	32-22	22-109	RRLL	YISY	YY	C40C9C12C5C5	1

Apart from the arrangement pattern of cysteine residues, specific motifs were also reported to be important for RALF peptides function (Moussu *et al.*, 2020; Xiao *et al.*, 2019). Except for ZmRALF1/4/5/6 peptides, all other ZmRALF peptides contain a propeptide. A YISY motif is very common in RALF peptides and the substitution of isoleucine (I) with leucine (L) in this motif or substitution of other 3 residues with alanine (YISY to AISY/YIAY/YISA) did not reduce RALF peptide activity (Pearce *et al.*, 2010). In ZmRALF peptides, YIGY, NIGY, YLSY, SISY, FISY were therefore recognized as variants of YI/LSY, which plays a role as an interaction motif (Xiao *et al.*, 2019). The YY motif was found to be responsible for interacting with LRX proteins (Moussu *et al.*, 2020) and was being found in ZmRALF2 and ZmRALF3 peptides. Propeptide was missing in ZmRALF1/4/5/6 peptides, and also they do not possess YI/LSY or YY motifs (Figure 2.2).

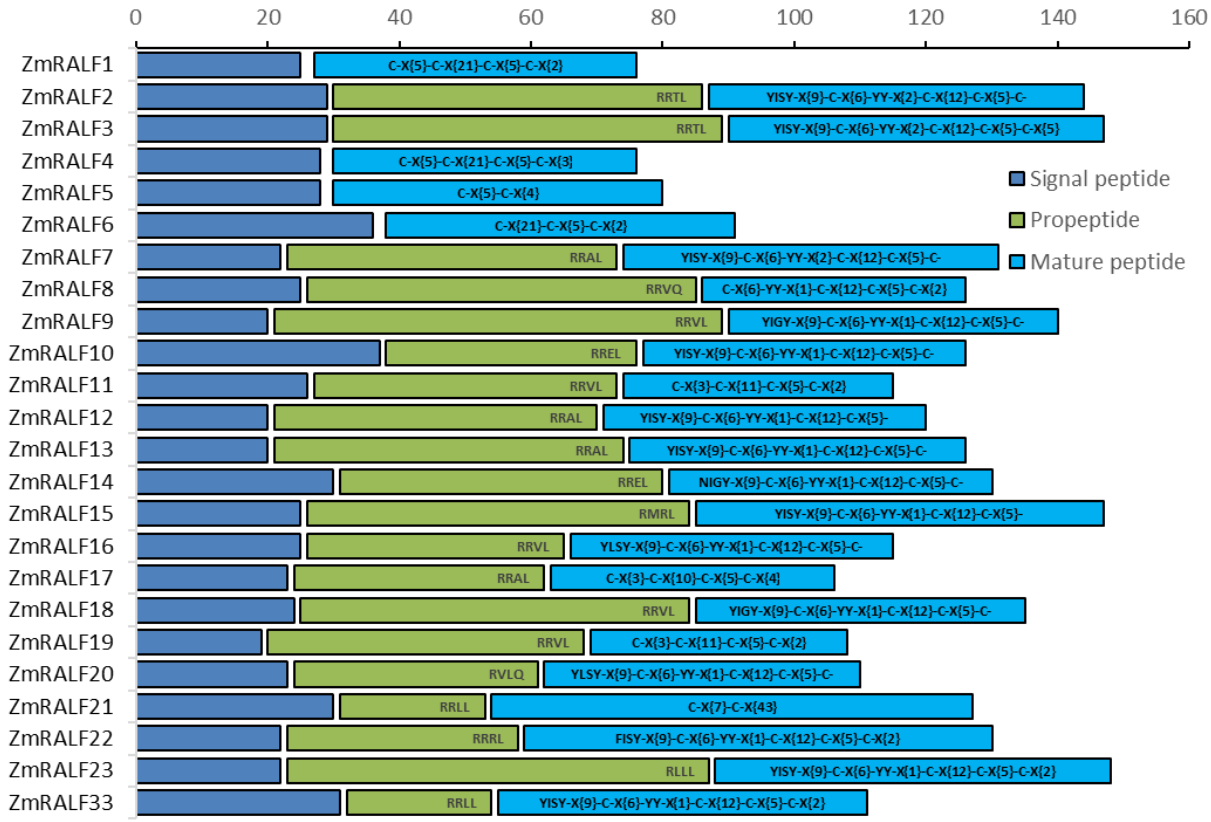

Figure 2.2 Structure schematic of ZmRALF peptides. RALF peptides were separated into 3 parts: signal peptide, propeptide, and mature peptide. In 24 ZmRALF peptides, ZmRALF1/4/5/6 peptides were short of propeptide. S1P motif (RXXL/RXLX) in the propeptide were marked. The cysteine residues, YI/LSY motif, YY motif were indicated. X represents any amino acid; numbers in curly braces indicate the range of variable residues.

Multiple sequence alignment was carried out to study the similarity of ZmRALF peptides (Figure 2.3). Hydrophobic alanine and leucine residues were enriched in signaling peptide region. More conserved sites were found in C-terminal region including YI/LSY, YY and S1P motif. To further recognize smaller individual motifs and discover more divergent patterns, motif searching was applied using MEME program (Bailey *et al.*, 2009). In combination with phylogenetic analysis, ZmRALF peptide sequences variation was clearly detected (Figure 2.4.A). ZmRALF peptides could be clustered into two major groups either containing or lacking the typical structure mentioned above. Motif 1 contains three cysteine residues and is commonly distributed in most ZmRALF peptides. ZmRALF11/17/19 peptides are short of this motif but possess the most conserved RGC residues typical for motif 1 (Figure 2.3). Motif 2 represents the most conserved RALF structure features: RRXL/RXLX-YISY-C-YY (X represents any amino acid), it is missing in ZmRALF1/4/5/6/11/17/19 peptides (Figure 2.4.B).

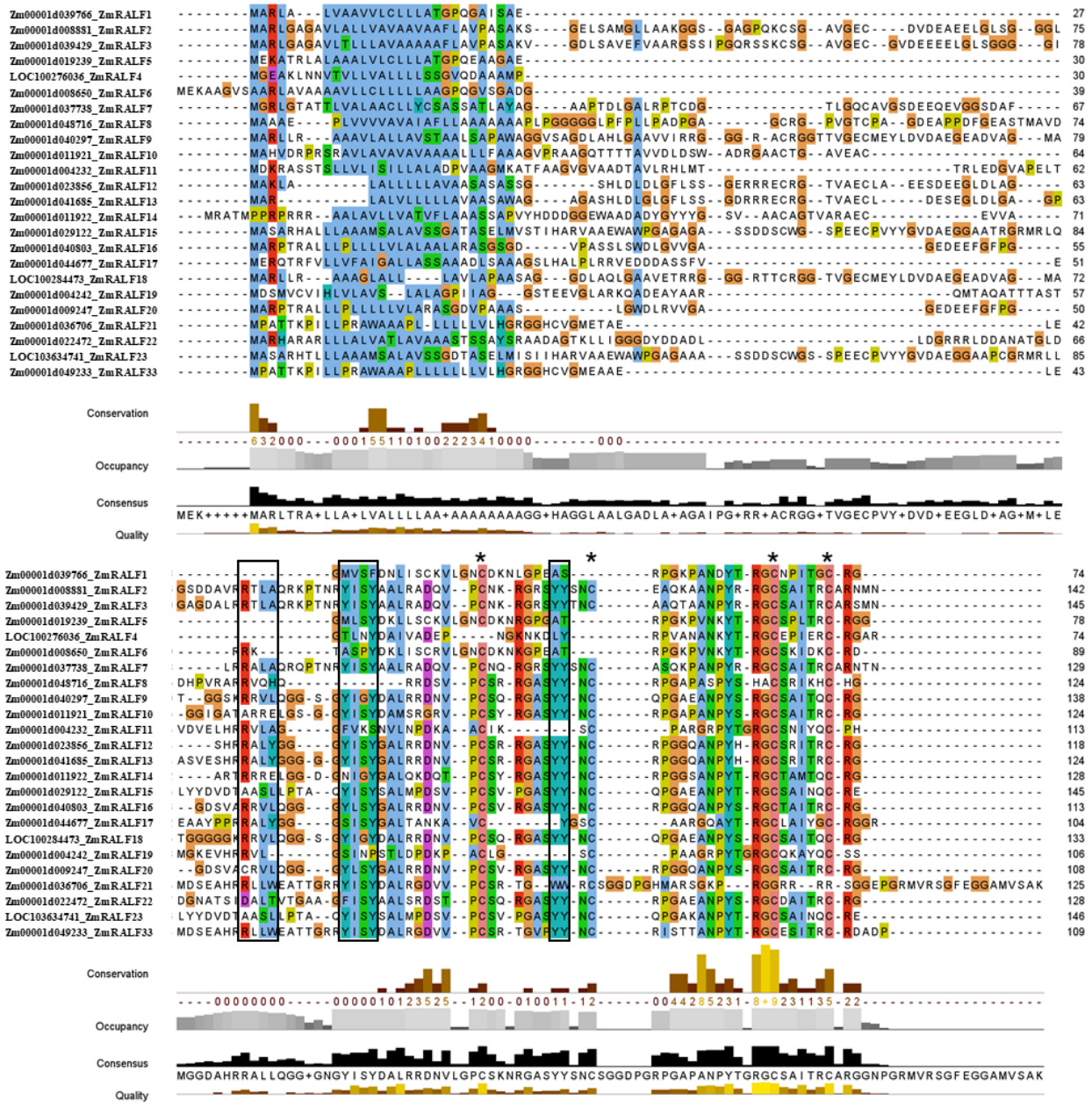

Figure 2.3 Multiple sequence alignment of ZmRALF peptides. Full length of ZmRALF peptides proteins were used. Alignment of 24 ZmRALF peptides was done using MUSCLE method in MEGAX, visualizing with Jalview (Waterhouse et al., 2009). Alignment of sequences was displayed in Clustal color code. Conserved motifs as RXXL/RXLX, YI/LSY, YY are highlight in black rectangle and cysteine residues are marked by asterisk on top. Conservation is measured as a numerical index reflecting the conservation of physico-chemical properties in the alignment. Occupancy annotation row shows number of un-gapped positions in each column of the alignment. Consensus displayed below the alignment is the percentage of the modal residue per column. Quality is a measure of the likelihood of observing the mutations (if any) in a particular column of the alignment.

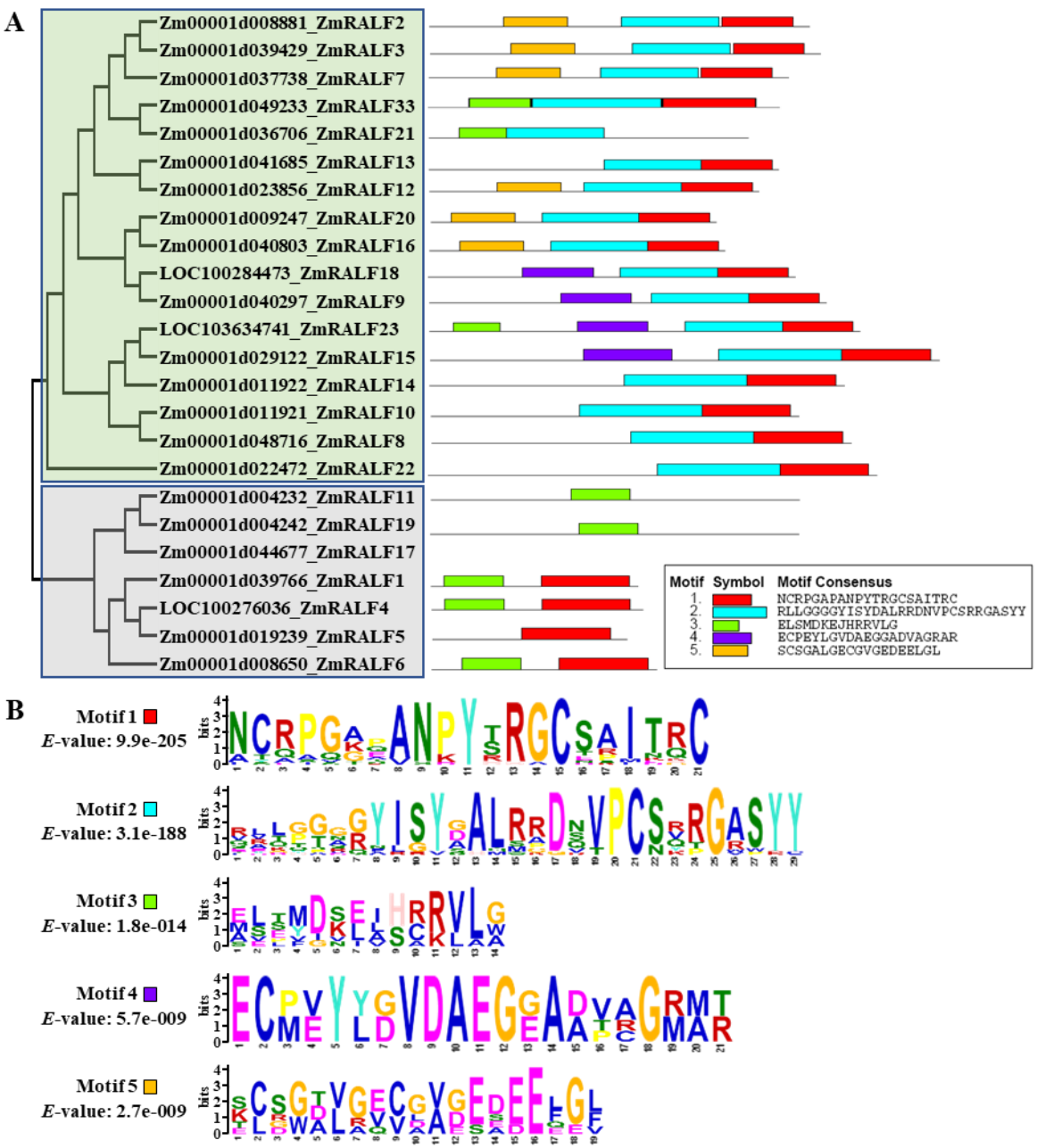

Figure 2.4. Phylogenetic analysis and motif identification of ZmRALF peptides. The program MEME5.1.1 was used to identify motifs present in maize RALF peptide sequences. Five motifs were found in ZmRALF peptides. ZmRALF17 peptide contain no motifs but a similar structure which mimic motif 3. (A) Phylogenetic analysis and motif composition of ZmRALF peptides. 24 ZmRALF peptides can be clustered into two groups which are highlighted with green and gray boxes. Motif 1 is commonly distributed across 24 ZmRALF peptides. Motif 2 is commonly shared only in upper group but not in lower group. Motif 3-5 only distrusted in several ZmRALF peptides. (B) Sequence logo and *E*-value of different motifs identified in ZmRALF peptides. The total height of a logo position depends on the degree of conservation in the corresponding multiple sequence alignment column. The height of each letter in the logo position is proportional to the observed frequency of the corresponding amino acid in the alignment column. *E*-value represents the statistical significance of the motif.

37 *Arabidopsis* RALF peptides were used to calculate their evolutionary relationship with maize RALF peptides. Mature RALF peptides were used to carry out multiple sequence alignment and phylogenetic analysis. According to the alignment (Supplemental Figure 1), the YISY motif and S1P motif were conserved in both species. However, different with ZmRALF peptides, only 8 out of 37 AtRALF peptides (1,4,19,22,23,24,31,33) contain YY residues, indicating the difference

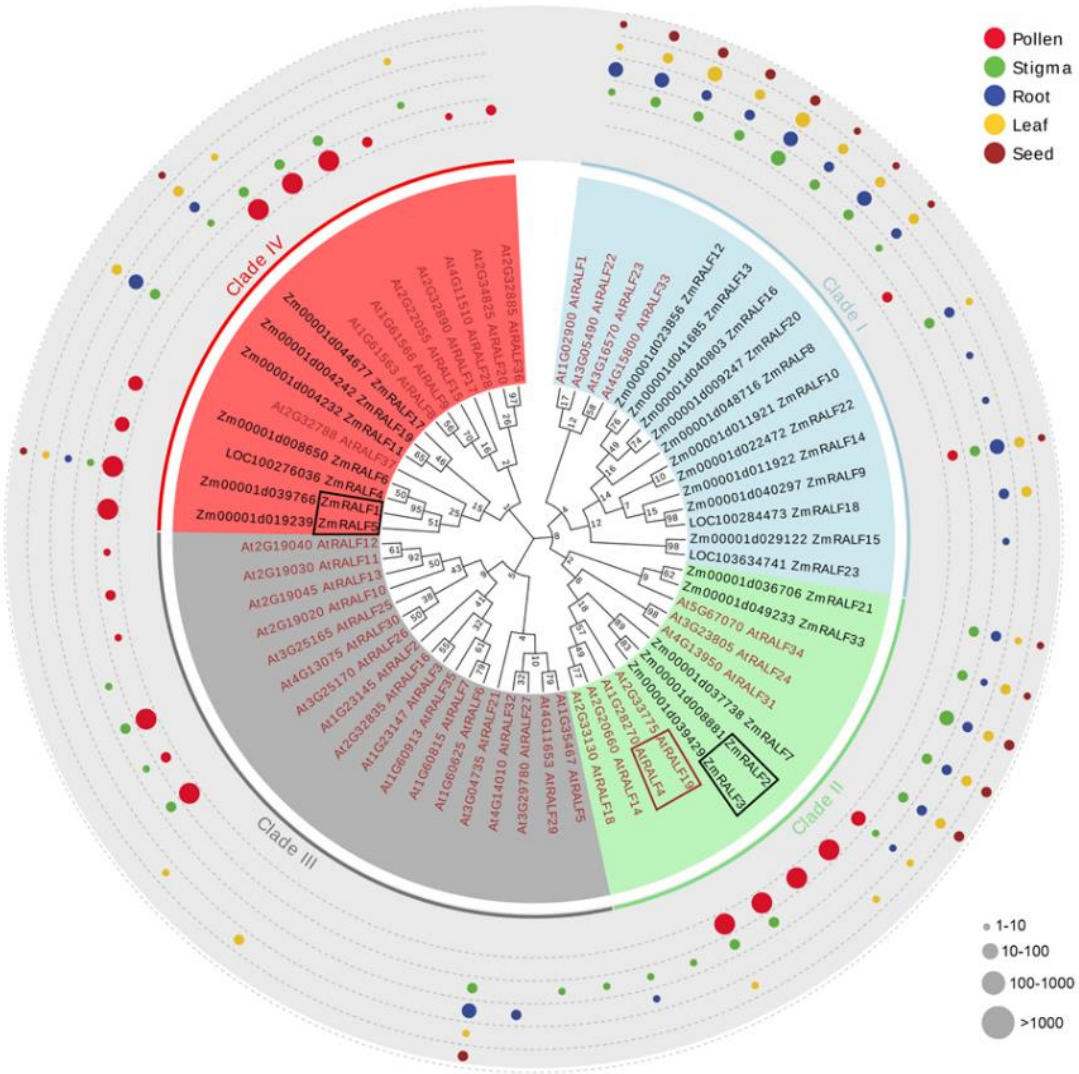

Figure 2.5. Phylogenetic and expression pattern analysis of maize and *Arabidopsis* RALF peptide families. Phylogram using all predicted mature maize (24 peptides) and *Arabidopsis* (37 peptides) peptide sequences. *Arabidopsis* AtRALF peptides are indicated in red and maize ZmRALF peptides in black. RALF peptides which will be investigated in more detail in this study were highlighted using rectangles. Clade I and II indicate RALF peptides with conserved RXXL/RXLX S1P protease cleavage site, YISY and YY domains, which are missing in Clade III and Clade IV RALFs. Colored dots show expression pattern of *RALF* genes in the five selected tissues indicated. Dot size correlates to expression level according to TPM values as indicated.

between these two species. Taking all observations above into consideration, RALF peptides in these two species were finally clustered into four clades (Figure 2.5). Clade I and II contain more typical RALF peptides that possess the conserved domains (Figure 2.6). Clade I RALF peptides were more divergent in the N-terminal region of mature peptide, while Clade II RALF peptides were comparable short and conserved in N-terminal, but variable in the C-terminal domain.

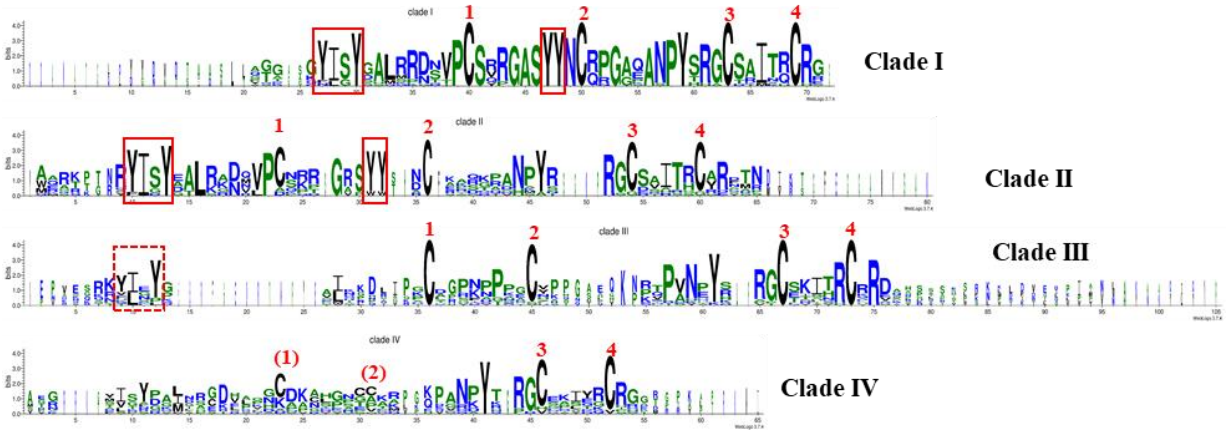

Figure 2.6 Divergence of RALF peptides across four major phylogenetic clades. WebLog3 plots showed residue conservation within mature RALF peptides from four clades. RALF peptides from Clade I and Clade II both showed typical structures including YISY and YY interaction domains (boxed in red) and four conserved cysteine residues. Clade I RALF peptides showed strong N-terminal variation, while Clade II RALF peptides are less conserved at the C-terminus. The YISY (botted red box), but not the YY motif can still be found in Clade III RALF peptides but both motifs are disappeared in Clade IV RALF peptides together with conserved cysteine residues.

Clade III contains only RALF peptides from *Arabidopsis* without the YY motif and they are variable in length at the C-terminal region. Clade IV RALF peptides are more different from each other and this clade contains even RALF peptides only have two cysteine residues (Figure 2.6). Notably, Clade II contains AtRALF4/19 peptides, which were previously reported to be involved in pollen tube growth (Ge *et al.*, 2017; Mecchia *et al.*, 2017).

To discover putative orthologs of *Arabidopsis RALF* genes in maize, expression level of *ZmRALF* genes were extracted from unpublished maize transcriptomics data from Dresselhaus group. Similar to *RALF* genes in *Arabidopsis*, *ZmRALF* genes are expressed in all analyzed tissues (Table 2.2). Notably, some *ZmRALF* genes are especially abundant in pollen: *ZmRALF1-8* genes are pollen-specific while *ZmRALF1/2/3/5* genes showing significantly high expression levels, as TPM (transcripts per million) value for each of them is more than 2500, meaning that they are the most strongly expressed genes in pollen (Table 2.2). *ZmRALF9-13* and *ZmRALF16* genes expressed

broadly in silk, seed, and root, but not in pollen. *ZmRALF12* was the only gene highly expressed in leaf. Pathogen infection studies of silks showed that expression patterns of *ZmRALF* genes was not affected by *Fusarium gaminearum* or *Ustilago maydis* hyphae, indicating that *ZmRALF* genes are not associated with immunity and abiotic stress. Importantly, *ZmRALF2/3* genes are the only pollen-specific *RALF* genes from Clade II with high expression level and thus likely putative orthologs of *Arabidopsis AtRALF4/19* genes (Figure 2.5).

Table 2.2 Expression level of maize *RALF* genes. mRNA expression level of genes was extracted from RNA-seq data, TPM value was shown.

Gene	Pollen_Tube	Pollinated_Silk	Silk	Seed	Leaf	Root	Fusarium_Silk	Ustilago_Silk
ZmRALF1	14791.2	1571.8	2.0	2.1	2.2	1.6	1.9	0.8
ZmRALF2	8029.0	766.2	0.9	1.0	0.9	0.8	1.1	0.3
ZmRALF3	7250.7	671.1	0.9	1.0	0.8	0.7	0.8	0.3
ZmRALF5	2866.3	237.3	0.4	0.4	0.3	0.3	0.3	0.1
ZmRALF4	395.8	39.8	0.2	0.1	0.0	0.1	0.0	0.0
ZmRALF6	156.8	21.3	0.3	0.1	0.1	0.1	0.1	0.2
ZmRALF7	113.3	17.4	3.9	3.5	1.0	5.5	1.2	6.2
ZmRALF8	51.9	24.5	0.1	0.1	0.2	0.0	0.0	0.0
ZmRALF9	32.6	11.8	14.3	65.0	1.8	241.5	6.0	4.1
ZmRALF10	0.7	9.5	21.6	4.0	0.4	10.9	0.1	1.1
ZmRALF11	0.3	22.7	44.1	12.0	0.6	136.2	5.0	14.6
ZmRALF12	0.2	417.8	511.8	346.9	97.1	257.9	92.9	407.0
ZmRALF13	0.1	26.9	46.8	82.5	4.6	43.4	3.0	14.3
ZmRALF14	0.1	0.0	0.0	0.1	0.0	2.4	0.0	0.0
ZmRALF15	0.0	0.0	0.0	0.5	0.0	1.4	0.0	0.0
ZmRALF16	0.0	49.0	92.2	68.3	8.6	304.5	80.9	42.0
ZmRALF17	0.0	3.0	6.0	27.4	1.1	66.3	0.0	0.0
ZmRALF18	0.0	0.1	0.1	14.0	0.6	12.1	0.0	0.0
ZmRALF19	0.0	0.0	0.0	0.0	0.0	0.0	0.0	0.0
ZmRALF20	0.0	3.2	3.4	12.5	7.5	20.0	16.3	11.1
ZmRALF21	0.0	14.9	27.2	9.3	5.2	11.4	1.7	9.9
ZmRALF22	0.0	0.0	0.0	0.2	0.0	7.5	0.2	0.0
ZmRALF23	-	-	-	-	-	-	-	-
ZmRALF33	0.0	15.5	49.3	29.7	7.3	6.3	0.1	0.6

Low Middle High

2.3.3 RNAi-*RALFs* caused pre-burst of pollen tube *in vitro*

To study the function of ZmRALF peptides during reproduction process, *ZmRALF* genes' RNA interference mutant (RNAi-*RALFs*) was generated. Among 24 *ZmRALF* genes, *ZmRALF1*, *ZmRALF2*, and *ZmRALF3* are the most abundant ones expressed only in pollen (Figure 2.7.B). Their peptides product represents two types of RALF: ZmRALF1 peptide belong to Clade IV which the S1P splicing site and YISY/YY interaction domain are missing (Figure 2.7.A).

ZmRALF2/3 peptides belong to Clade II with typical RALF peptide structures and are highly similar with each other in amino acid sequence. ZmRALF5 peptide, another Clade IV RALF protein, was also included in this study because of the strong pollen-specific expression pattern and specific amino acid feature.

RNAi mutant was generated to downregulate the highest expressed genes *ZmRALF1*, *ZmRALF2*, and *ZmRALF3*. C-terminal gene specific regions were chosen as target sequences. After transformation, eight independent RNAi-*RALFs* mutant lines were obtained. For transgenic mutant plants, self-pollination or crossing with Hi-II maize line were carried out to generate enough seeds. RNAi-*RALFs* mutant plants from the first generation (T1) were used for phenotype analysis.

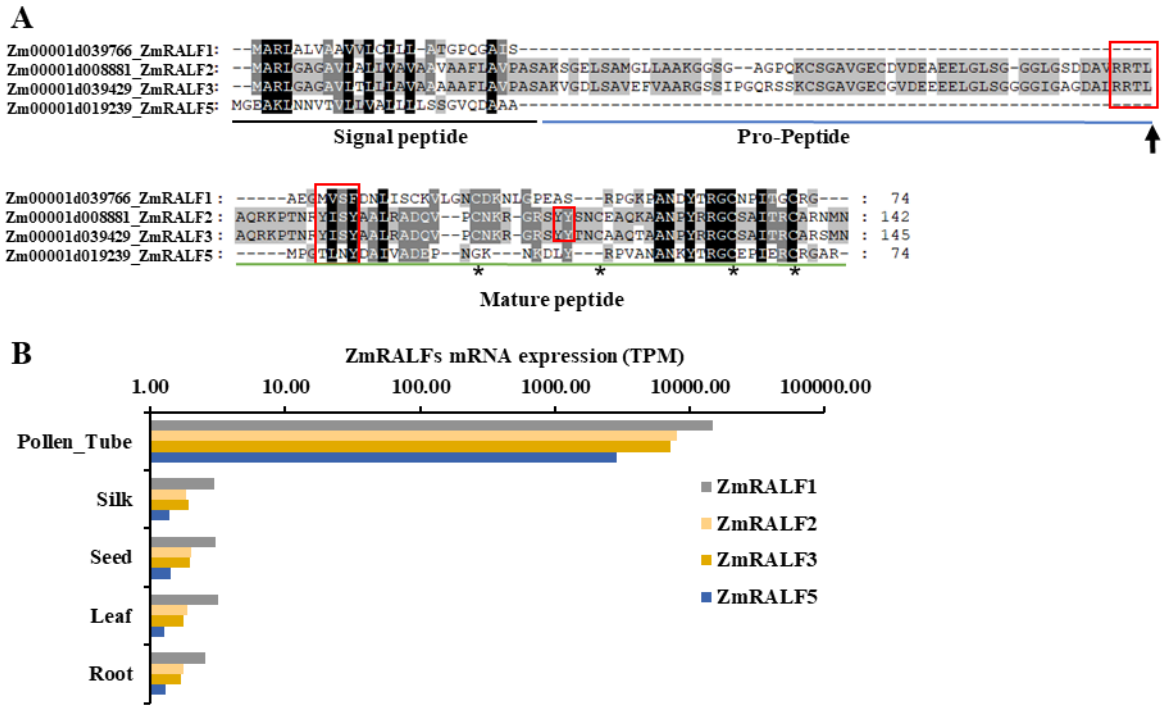

Figure 2.7 Sequence alignment and gene expression level of *ZmRALF1/2/3/5*. (A) Amino acid alignment of ZmRALF1/2/3/5. The RRTL S1P splicing site, functional domain YISY, and interaction domain YY were highlight in red rectangle, the cysteine residues were marked with asterisks. (B) mRNA expression levels (TPM) of the 4 most highly expressed maize *RALF* genes within different tissues.

The first step to study the RNAi-*RALFs* mutant was to quantify expression level of *RALF* genes in RNAi-*RALFs* mutant. Mature pollen from RNAi-*RALFs* mutant lines were collected. After total RNA extraction and cDNA synthesis, RT-qPCR was done to check the extent of *ZmRALF1/2/3* gene downregulation in six mutant lines (Figure 2.8). To make a proper

comparison, wild type sibling plants without RNAi-*RALFs* construct were used as control. RNAi-*RLAFs* mutants from Line2 and Line11 showed similar expression pattern as those in the wild type. In Line3, expression level of *ZmRALF1/2/3* genes were decreased to 65% of that in wild type. Line1, Line5 and Line7 displayed the genes down-regulation to half compared with wild type. Taking Line1 and Line5 into comparison, *ZmRALF1* gene down-regulation were similar in Line1 (54%) and Line5 (54%), but *ZmRALF2* gene expression was lower in Line5 (52%).

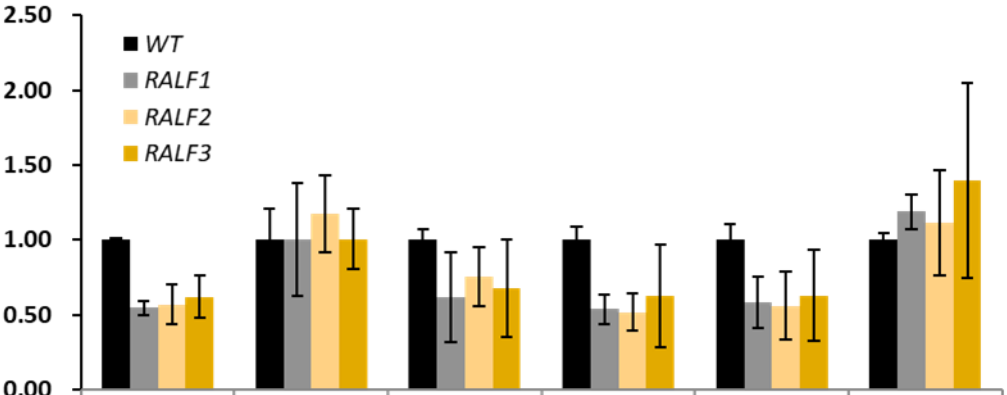

	line1	line2	line3	line5	line7	line11
RALF1	54.43%	100.17%	61.46%	53.58%	57.79%	118.76%
RALF2	56.76%	117.06%	75.20%	51.72%	55.67%	111.33%
RALF3	61.99%	100.61%	67.73%	62.29%	62.81%	139.62%

Figure 2.8 Expression level of *ZmRALF* genes in RNAi-*RALFs* mutant lines and corresponding wild type. The expression level of RNAi-*RALFs* was measured by RT-qPCR and normalized with two reference genes (PB1A10.07c and Cullin).

To check the pollen viability and activity, *in vitro* pollen germination test was carried out. Fresh pollen from RNAi-*RALFs* mutants and Hi-II (wild type) were spread on solid pollen germination medium and incubated. After 45 minutes germination *in vitro*, pollen germination status was recorded under microscope and calculated by ImageJ and R (Figure 2.9).

Normal pollen from Hi-II was used as comparison, with 79% pollen germinated and seldom burst (1%, pollen burst and pollen tube burst). In consist with the alteration on expression level, RNAi-*RALFs* mutant Line2 and Line11 showed similar pollen germination status as Hi-II did. RNAi-*RALFs* mutant Line3 and Line7 showed the lowest pollen germination ratio. There were more pollen tubes burst in Line3, while in Line7 there were more pollen burst. Line1 and Line5 showed normal pollen germination (71.63% and 81.11%), but much higher ratio of burst pollen tubes (20.45% and 22.78%). Half of the un-germinated pollen in Line1 and Line5 tend to burst (Figure

2.9.A). In summary, among eight RNAi-*RALFs* mutant lines, pollen from Line1 and Line5 were more unstable, epically the germinated pollen tube.

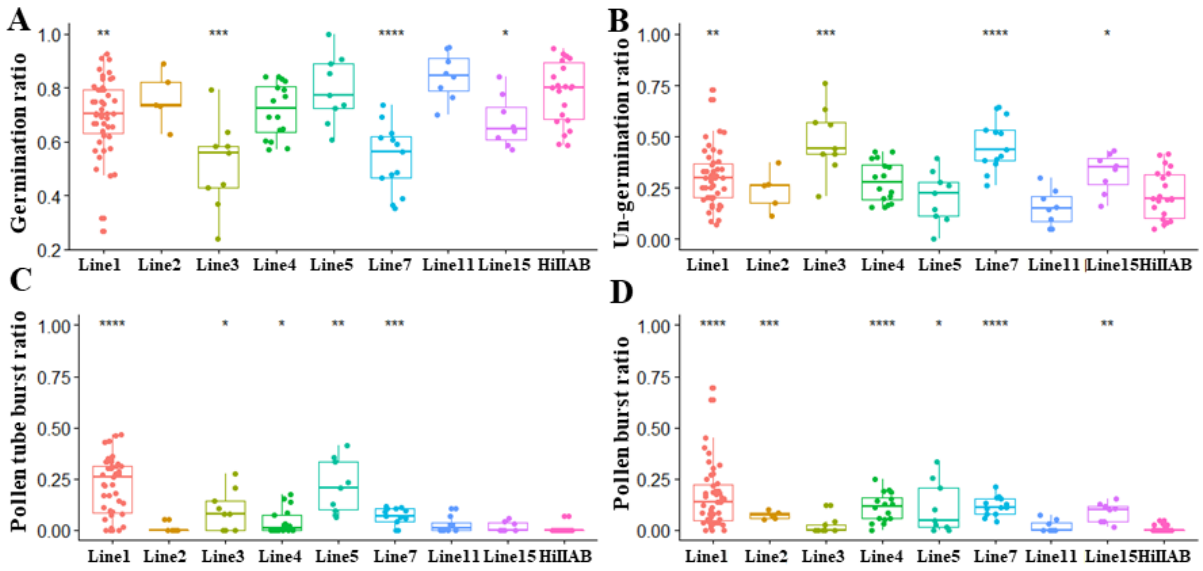

Figure 2.9 *In vitro* pollen germination status of RNAi-*RALFs* (45 minutes after germination). (A) Germinated ratio (B) Un-germinated ratio. (C) Pollen tube burst ratio. (D) Pollen burst ratio. The correspond values were compared with Hi-II (wild type). Significance: * p<0.05, ** p<0.01, *** p<0.001,**** p<0.0001.

To investigate the pollen status during germination in RNAi-*RALFs* mutant lines, pollen germination of Line1 and Line5 were recorded in time lapse (Figure 2.10). Since the pollen tube punched out, pollen tube status was recorded and calculated every five minutes. When it came to 115 minutes after germination, half of the pollen tubes were burst in Line1, while in Line5, almost all pollen tubes burst at that time point.

To further illustrate the pollen tube growth in RNAi-*RALFs* mutant Line5, a closer check and several longer time lapse records were performed (Figure 2.11). The germinated pollen tubes always burst at the shank but never at the apex region of pollen tube (Figure 2.11.A-B), indicating the down regulation of *ZmRALF* genes did not affect pollen tube growth but pollen tube wall integrity. In the continuously observation, pollen tube started to burst as early as 35 minutes after germination (Figure 2.11.C), and at this time pollen tube burst ratio was already significantly higher than that in wild type (Student T-test). When it came to 70 minutes after germination, a few pollen tubes from the corresponding wild type started to burst. Up to 95 minutes after germination, pollen tube burst ratio was similar between RNAi-*RALFs* mutants and wild type. Different with pollen tube burst after germination, some pollen from RNAi-*RALFs* immediately

burst once loaded on germination medium. In this test, the burst of pollen was kept in a low ratio. Even though, in the time frame from 40 to 100 minutes, the pollen burst ratio was higher in RNAi-*RALFs* mutant line.

In summary, the down regulation of *ZmRALF* genes in pollen decreased the pollen tube stability and caused a pre-burst phenotype during *in vitro* pollen germination.

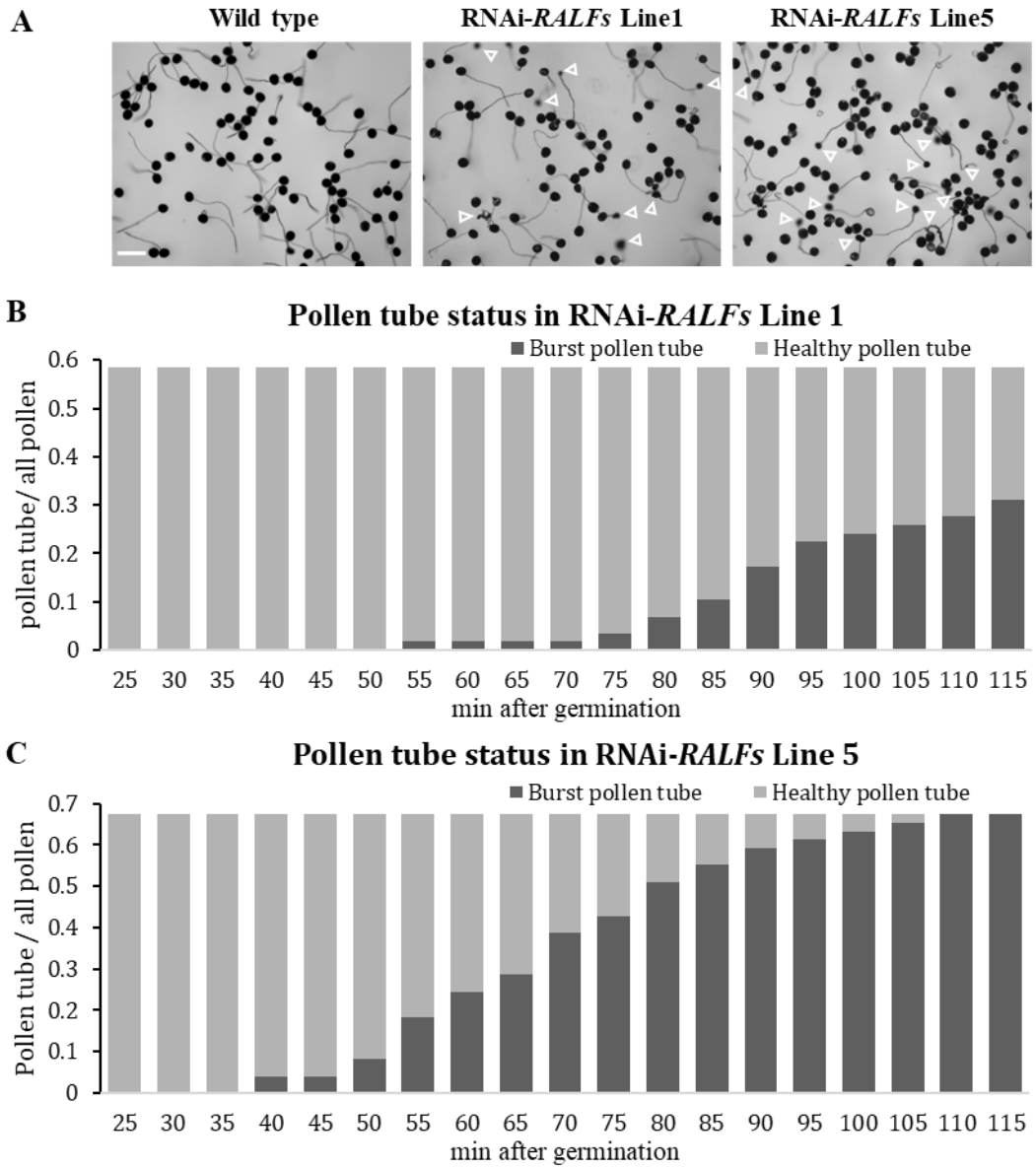

Figure 2.10 Pollen tube status of RNAi-*RALFs* mutant Line1 and Line5. Starting form 25 minutes after germination, pollen tube growth was recorded every 5 minutes. (A) Germination and growth of pollen from wild type and two RNAi-*RALFs* lines after 1 hour. Open arrowheads point towards burst pollen tubes. (B) Time-lapse record of pollen tube status in Line1. (C) Time-lapse record of pollen tube status in Line5.

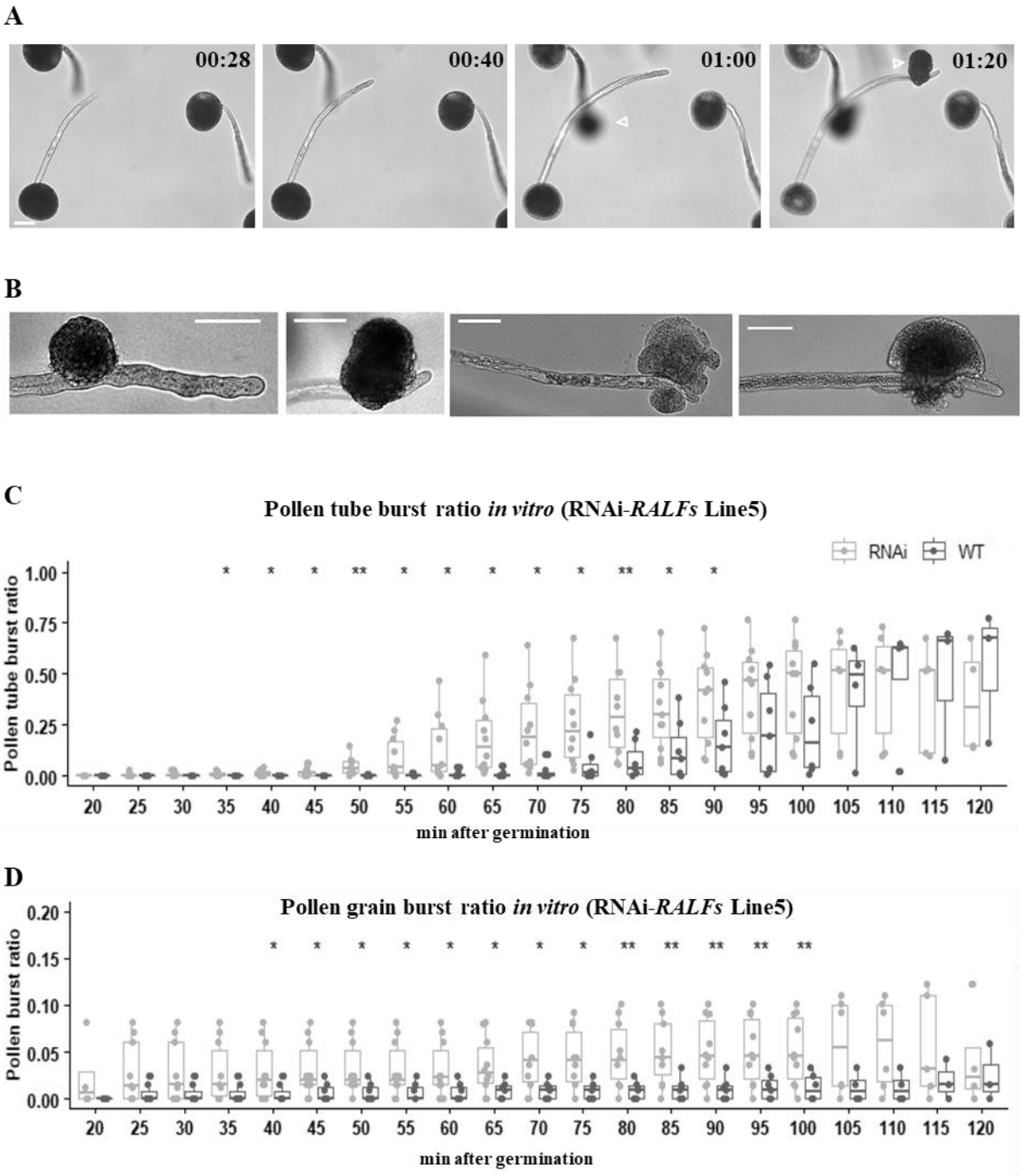

Figure 2.11 Pollen tubes from RNAi-*RALFs* mutants tend to burst during *in vitro* germination. (A) Time-lapse imaging of pollen tube from RNAi-*RALF*s mutant Line5 at indicated times. One pollen tube burst at 70 minutes and the second one at 90 minutes. Open arrowheads point towards burst pollen tubes. (B) Examples of burst pollen tubes. Note that all pollen tubes burst at the shank and never at the apex of the tube. (C) Burst ratio of pollen tube from RNAi-*RALFs* mutant Line5 was observed over time. Burst of un-germinated pollen grains (bottom) and germinated pollen tubes (top) were recorded. Scale bars is 200 μm in A and 50 μm in B and C. Significance: * $p<0.05$, ** $p<0.01$.

2.3.4 Downregulation of *ZmRALF* genes cause decreased male transmission efficiency

Once pollen landed on silk hair, the hydration and germination start (Zhou *et al.*, 2017). To check the growth of RNAi-*RALFs* mutants pollen tube in silk, *in vivo* germination test was carried out (Figure 2.12). One hour after pollination, the silks were cut out and stained with aniline blue to check the pollen tube growth condition *in vivo*. In contrast with the *in vitro* pollen tube burst which can be detected in RNAi-*RALFs* mutants, the *in vivo* pollen tube growth was normal at the beginning. Pollen from RNAi-*RALFs* mutants can successfully penetrate silk hair cells and enter

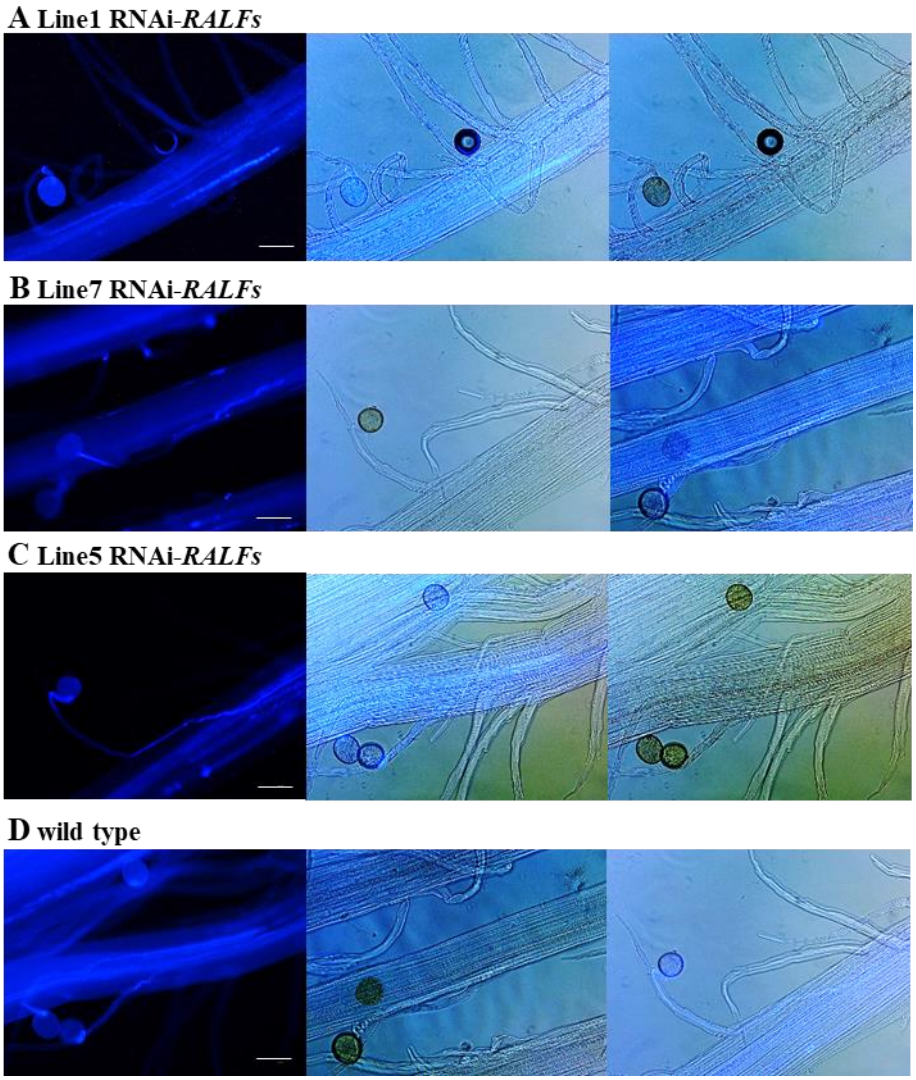

Figure 2.12 Pollen tube growth *in vivo* after one-hour germination. Pollen from RNAi-*RALFs* mutant lines and wild type growth normally in silk. Pollen from RNAi-*RLAFs* mutant Line1, Line5 and Line7 were germinated on silk for one hour and then fixed, followed by aniline blue staining. Corresponding wild type from Line5 was selected as control. After one-hour germination, there was no difference on pollen tube growth between RNAi-*RALFs* mutant lines and wild type. Bar:100μm.

the transmitting tract. After one-hour germination, pollen tubes already went through the silk hair cells and were growing along the transmitting tract (Figure 2.12). However, it does not mean the growth of pollen tube from RNAi-*RALFs* was not affected by *ZmRALFs* downregulation. It is noticeable that the maize silk could be 30 cm long and the growth of pollen tube in silk up to 24 hours. The pollen tube condition in the following growth process was unclear. Due to the thickness and long length of silk, it is hard to track the pollen tube growth *in vivo* for long time. Instead, the fertilization success could be checked to determine gametophyte transmission efficiency.

To check the function of *ZmRALF* genes, reciprocal crosses between wild type plants and RNAi-*RALFs* mutant lines were performed. RNAi-*RALFs* mutant plants from Line1 and Line5 were crossed with wild type (inbred line B73) or self-pollinated. As the copy number of RNAi-*RALFs* constructs in transgenic plants were not clear, the segregation ration in the self-pollination should be equal to (single copy) or higher (multiple copy) than 3:1. In a similar manner, the crossing with wild type should result in a segregation ratio equal to or higher than 1:1. When the RNAi-*RALFs* mutants were used as maternal and wild type paternal, the segregation ratio (Line1, 0.94:1; Line5, 1:1, Table 2.3) fits with the Mendel's genetic theorem. However, when RNAi-*RALFs* mutants were used as paternal, no matter whether the maternal was RNAi-*RALFs* mutants or wild type, the segregation ratios were significantly reduced (Table 2.3). In accordance with the pollen tube burst status *in vitro*, Line5 had the most severe reduction in male gametophyte transmission efficiency. It is apparent from this test that the RNAi-*RALFs* mutation decreased the male gametophyte transmission efficiency, while the female gametophyte transmission efficiency was not affected.

Table 2.3 Transmission efficiency of RNAi-*RALFs* mutant lines. RNAi-*RALFs* mutant lines were crossed with wild type (inbred lines B73) plants as indicated. A transmission efficiency of ≥1:1 and ≥3:1, respectively, is expected as lines may contain multiple transgene integrations. In RNAi-*RALFs* mutant lines, the transgene is fully transmitted via female gametophyte, but only partially by male gametophyte.

RNAi-*RALFs* mutant	Female	x	Male	Numbers of plants			Segregation expected	Segregation observed
				RNAi	WT	total		
Line1	RNAi-*RALF*s	×	RNAi-*RALF*s	59	85	144	≥3:1	0.69:1*
Line1	RNAi-*RALF*s	×	B73	31	33	64	≥1:1	0.94:1
Line1	B73	×	RNAi-*RALF*s	33	46	79	≥1:1	0.72:1*
Line5	RNAi-*RALF*s	×	RNAi-*RALF*s	54	123	177	≥3:1	0.44:1*
Line5	RNAi-*RALF*s	×	B73	39	39	78	≥1:1	1:1
Line5	B73	×	RNAi-*RALF*s	19	79	98	≥1:1	0.24:1*

2.3.5 ZmRALFs protein expression and purification form *E.coli*

To study the biochemical features and search putative partners, ZmRALF recombinant proteins need to be expressed and purified. Considering that the RALF propeptide was not functional (Srivastava *et al.*, 2009), so the predicted mature peptide coding sequences of *ZmRALF1/2/3/5* were cloned: ZmRALF1 and ZmRALF5 do not have propeptide, so the cloning started from the end of signal peptide region till the stop codon; ZmRALF2 and ZmRALF3 own propeptide, thus the cloning started from the end of propeptide till the stop codon.

E.coli is a well-established, and the most popular heterologous expression system used as a cell factory to produce recombinant proteins (Rosano and Ceccarelli, 2014). The heterologous production of AtRALF proteins in *E.coli* were reported to have the same activity as the synthetic RALF peptide (do Canto *et al.*, 2014), therefor the ZmRALF mature peptides were expressed in the same way. The coding sequences were cloned into pET-53-DEST Gateway destination vector with an N-terminal 6xHis-Tag. Resulting plasmids were used for heterologous expression in the *E.coli* strain BL21(DE3). The 6xHis-ZmRALF peptides were then tested for expression and solubility. 6xHis-ZmRALF5 peptide was not found after induction (Figure 2.13), it is possible that the protein was poorly expressed. 6xHis-ZmRALF1/2/3 peptides were detected after induction, while the peptides were found in the insoluble fraction.

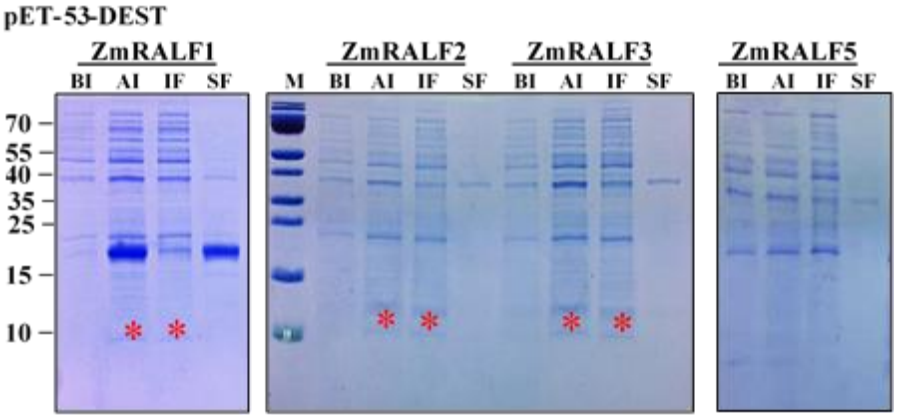

Figure 2.13 Production of 6xHis tagged ZmRALF proteins in BL21(DE3) (Coomassie stained gel). The production of recombinant ZmRALF proteins was induced in the *E.coli* strain BL21(DE3) at 37° for 3 hours. SDS-PAGE analysis revealed the proteins of appropriate size for 6xHis-ZmRALFs (expected molecular weight [MW]: ZmRALF1: 8.82 kDa, ZmRALF2: 10.41kDa, ZmRALF3: 10.54 kDa, ZmRALF5: 9.06 kDa, marked with red asterisks) in the bacterial lysate after induction (AI) and the insoluble fraction (IF), which was not present before induction (BI). There were not proper band in the test of ZmRALF5.

Moderate detergents in the lysis buffer could compromise the integrity of cell membranes, thereby improve lysis of cells and benefit to extraction of soluble protein (Johnson, 2013). To improve the solubility of ZmRALF proteins in *E.coli*, various nonionic detergents were applied in the cell lysis buffer (Figure 2.14). Triton X-100 and CA-630 belong to Triton family, which are slightly different in their average number of monomers per micelle (9.6 and 9.5) and their polyethylene glycol (PEG) based headgroup size. Tween-20 is a polysorbate-type nonionic surfactant formed by the ethoxylation of sorbitan before the addition of lauric acid. It could be applied as a solubilizing agent for membrane proteins (Alfalah *et al.*, 2005). Three detergents were added into the cell lysis buffer individually. However, the addition of detergents did not reduce the inclusion bodies formation, so 6xHis-tagged ZmRALF proteins cannot be purified under native condition.

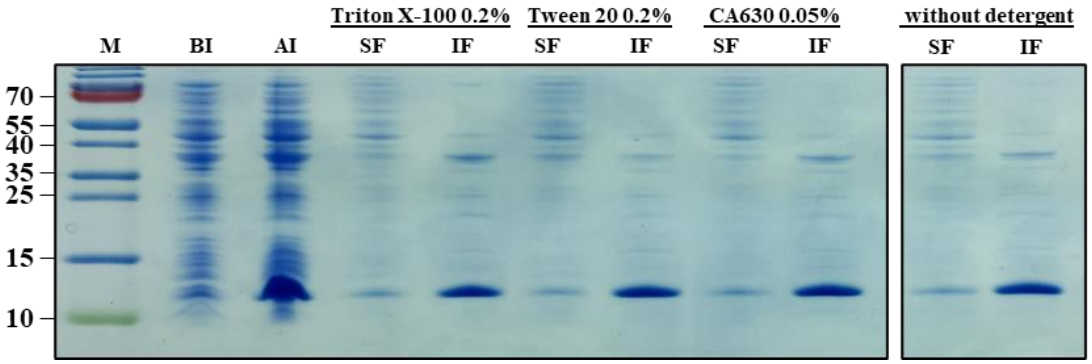

Figure 2.14 Cell lysis of ZmRALF2 expressed in BL21(DE3) with different detergents (Coomassie stained gel). The production of recombinant ZmRALF proteins was induced in the *E.coli* strain BL21(DE3) at 37° for 3 hours. SDS-PAGE analysis revealed the proteins of appropriate size for 6xHis-ZmRALFs (expected molecular weight [MW]: ZmRALF2: 10.41kDa, marked with red asterisks) in the bacterial lysate after induction (AI) and the insoluble fraction (IF), which was not present before induction (BI). Higher concentration of ZmRALF2 was found in insoluble fraction.

Recombinant proteins appeared in insoluble fraction result from the formation of inclusion bodies during protein expression in *E.coli*. There are many possible reasons for the formation of inclusion bodies, such as the expression conditions, the nature of protein, the host cell, and the expression level of destination vector . The standard procedures of protein purification under native condition would be badly limited in the presence of inclusion bodies. However, the purification of 6xHis-tagged proteins could also be performed under denaturing condition. Besides the nonionic detergents used in native condition, high concentration of strong detergents can also be used to lyse cell. 8 M urea or 6 M guanidinium chloride (Gu-HCl) were normally used in solubilizing the inclusion bodies (Rudolph and Lilie, 1996).

The purification of ZmRALF2/3 peptides in denaturing condition with 6M Gu-HCl were carried out (Figure 2.15). Different with the purification in native condition, there was a minimal amount of proteins in the insoluble fraction. The proteins obtained from denaturing condition were comparably pure and abundant. Using ÄKTA™ pure protein purification system (GE Healthcare), the soluble fraction contain ZmRALF2/3 mature peptides were purified by HisTrap™ Fast Flow column (GE Healthcare) with buffer contain linear gradient of 6 to 0 M urea. The ZmRALF2/3 eluted proteins without detergent were further refold and desalted with Amicon® Ultra-0.5 centrifugal filter (Merck) by buffer exchanging. The highly pure and abundant ZmRALF2/3 peptides were used in the following biochemical experiments and the antibody production.

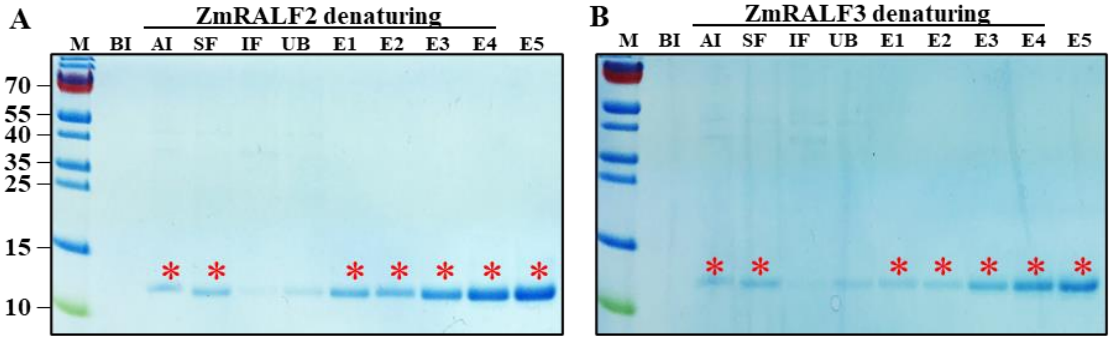

Figure 2.15 Denaturing purification of 6xHis-ZmRALF2/3 peptides (Coomassie stained gel). Production of 6xHis-ZmRALF2 was induced in the *E.coli* strain BL21 (DE3). On the gel, bands with molecular weight (MW) corresponding to the size of the recombinant protein were detected (ZmRALF2:10.41 kDa, ZmRALF3:10.54 kDa, marked with red asterisks). Detergent Gu-HCl-based lysis of the bacteria was followed by purification including refolding by ÄKTA™ pure protein purification system using buffers with decreasing urea concentration gradient. The enriched protein fractions were selected from linear dilution (E1-E5).

In parallel, coding sequences of mature ZmRALF peptides were cloned into the pET-32b(+) vector with N-terminal TrxA-Tag, 6xHis-Tag and S-Tag. Fused with the 109 aa thioredoxin (TrxA) partner, the inclusion bodies were turned to be soluble forms that are biologically active (LaVallie *et al.*, 1993). Expression of the TrxA-6xHis-S-ZmRALFs constructs were successful, as the proteins were mainly in the soluble fraction after sonication (Figure 2.16). Induction at 37° produced large amount ZmRALFs proteins. To avoid extra protein production under high temperature, the protein expression was also induced at 18° overnight. However, low temperature incubation caused an increased amount of inclusion bodies. ZmRALF peptides expression and purification were thus carried out at 37° (Figure 2.17) in native condition. The eluted ZmRALF peptides were further desalted with PD-10 column and used for the following biochemical tests.

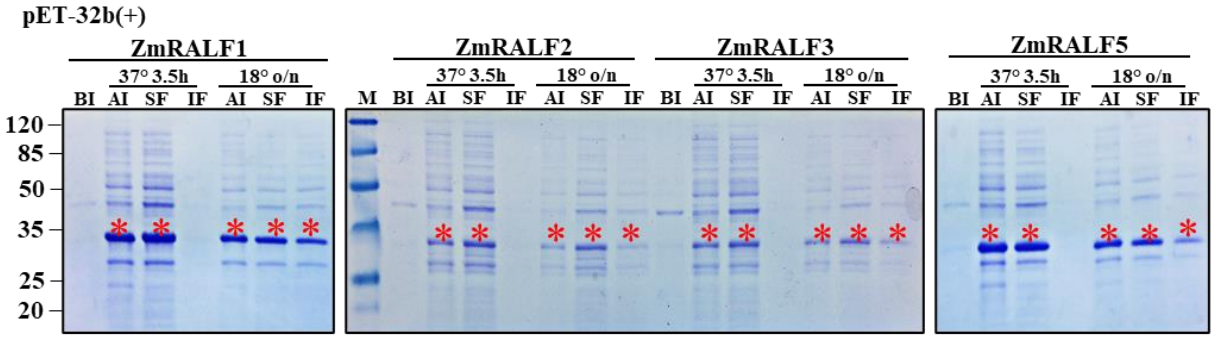

Figure 2.16 Production of ZmRALF peptides with pET-32(b+) in BL21(DE3) (Coomassie stained gel). The production of recombinant ZmRALF proteins was induced in the *E.coli* strain BL21(DE3) at 37° for 3.5 hours or 18° overnight. SDS-PAGE analysis revealed the proteins of appropriate size for TrxA-6xHis-S-ZmRALFs (expected molecular weight [MW]: ZmRALF1: 22.87 kDa, ZmRALF2: 24.26 kDa, ZmRALF3: 24.16 kDa, ZmRALF5: 22.88 kDa, marked with red asterisks) in the bacterial lysate after induction (AI) and the soluble fraction (SF), which was not present before induction (BI).

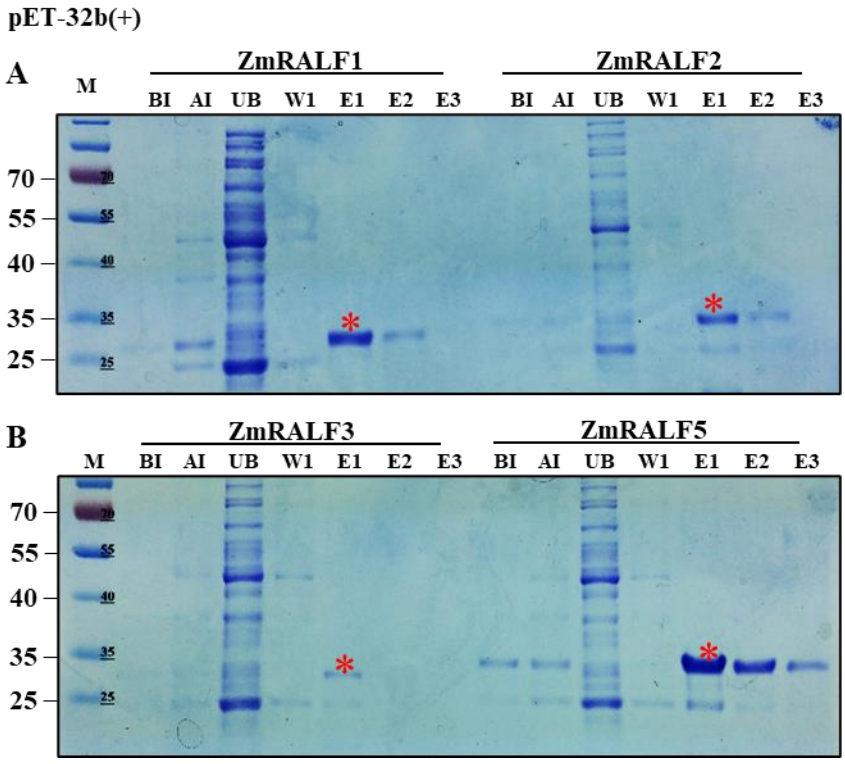

Figure 2.17 Native condition purification of TrxA-6xHis-S-ZmRALF1/2/3/5 from BL21(DE3) (Coomassie stained gel). Expression of TrxA-6xHis-S-ZmRALF2/3 proteins were induced in the *E.coli* strain BL21 (DE3) and checked with SDS-PAGE. Seldom protein bands are visible in the background of the eluted fractions, indicating the eluate was comparably pure. Abbreviations: BI = before induction, AI = after induction, UB = Unbound to beads fraction in the soluble fraction. W = wash fraction. E = protein elution.

2.3.6 Generation of new *ZmRALF* knockout mutant

Downregulation of Zm*RALF* genes induced unstable pollen tube *in vitro* and compromised male gametophyte transmission efficiency. In *Arabidopsis*, the knockout of *AtRALF4/19*, which are the orthologues of *ZmRALF2/3*, caused similar phenotype (Ge *et al.*, 2017; Mecchia *et al.*, 2017). It is reasonable to assume that the defects were caused by downregulation of *ZmRALF2/3* genes. The RNAi-*RALFs* mutants were constructed against *ZmRALF1/2/3* genes, in which the function of the most abundant maize *RALF* gene *ZmRALF1* is unclear. Different with ZmRALF2/3 peptides that own typical RALF peptide structures, ZmRALF1 is more like a RALF-related peptide (Campbell and Turner, 2017). Pollen-specific RALF peptide ZmRAFL5 is similar with ZmRALF1, but more specific as it is the only Type 3 RALF peptide in maize (Silverstein *et al.*, 2007). Therefore, these four highest pollen-expressed *RALF* genes belong to three different types.

To investigate the function of each gene, new mutant generation was necessary. As an efficient tool, clustered regularly interspaced short palindromic repeats/CRISPR-associated Cas9 (CRISPR/Cas9) were used to generate knockout mutants in different plant species. In maize, CRISPR/Cas9 was proved to be a sufficient tool to induce correspond mutation (Char *et al.*, 2017). The CRISPR/Cas9 system in this study consists of an *E.coli* cloning vector and an *Agrobacterium* binary vector (Char *et al.*, 2017). It can be used to clone up to four guide RNAs (Figure 2.18). In theory, the combination of two genes, each contain two guide RNAs, will result in three types of

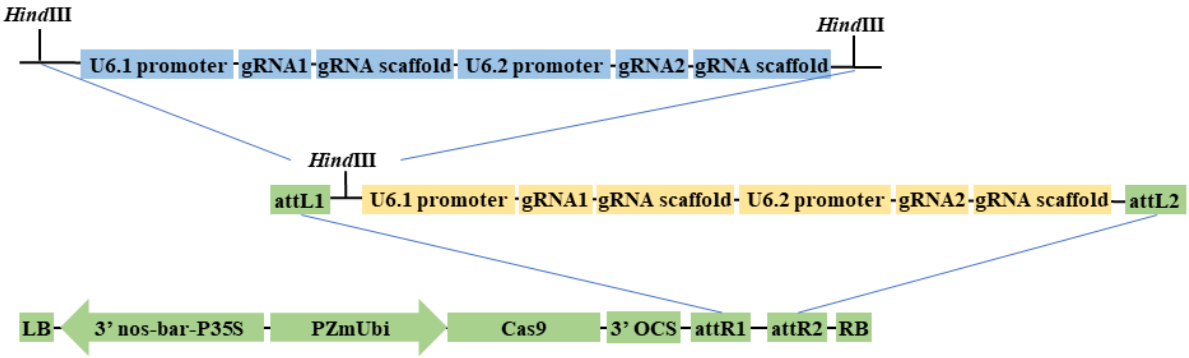

Figure 2.18 Schematic of CRISPR/Ca9 plasmid construction. Cloning vectors pENTR-gRNA1 (with two *Hind*III sites) or pENTR-gRNA2 (with one *Hind*III site) were sequentially digested with *Btg*ZI and *Bsa*I restriction enzymes for the insertions of two double-stranded oligonucleotides. The subcloning resulted in two intermediate constructs, pgRNA-IM1 and pgRNA-IM2, each carrying two gRNA expression cassettes. The cassettes flanked by the Gateway recombination sequences attL1 and attL2 were mobilized to the binary vector pGW-Cas9 through Gateway recombination, resulting in a single plasmid Cas9/gRNA binary construct for *Agrobacterium* mediated gene transfer.(Image was drawn based on description in Char et al., 2017)

editing: individually editing of each gene and the simultaneously editing of both genes.

The guide RNAs were designed based on the genome sequence of maize inbred line B73 (Jiao *et al.*, 2017). 20 base pair gene specific nucleotides followed by NGG (N represents any nucleotide) were selected as guide RNA (Figure 2.19.A). It is very important to note that the genome sequences of B73 and Hi-II are not exactly the same. To avoid any possible mismatch, the targets of designed guide RNAs in Hi-II plant were sequenced (Figure 2.19.B). Among the guide RNA fragments, sequence of *ZmRALF2* and *ZmRALF5* are the same in B73 and Hi-II. However, sequence of *ZmRALF1* is different in guide RNA2 and *ZmRALF3* is different in guide RNA1. So the sequences of guide RNAs were adjusted to match those in Hi-II.

Considering the DNA sequences similarity between *ZmRALF2* and *ZmRALF3* genes,

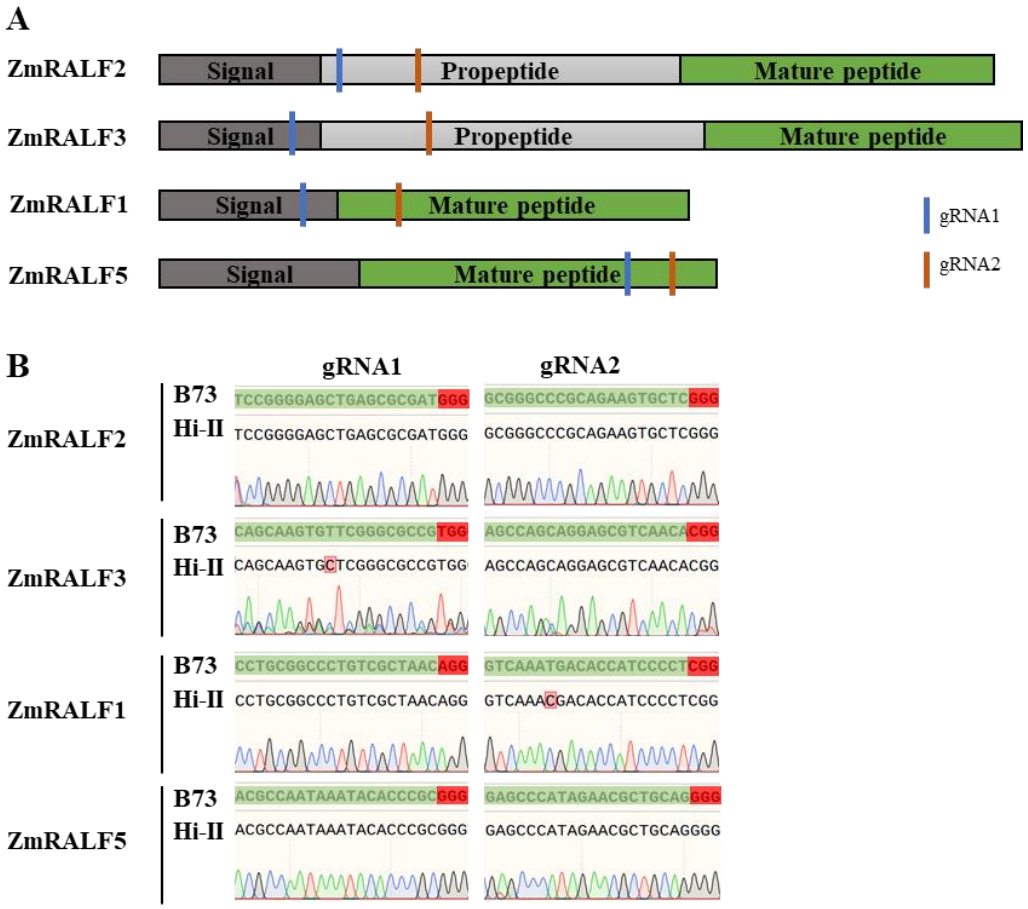

Figure 2.19 CRISPR/Cas9 guide RNA design and sequences. (A) Localization of guide RNAs in *ZmRALF* DNA sequences. (B) Sequencing of guide RNAs in B73 and Hi-II. The guide RNA sequences of *ZmRALF2/5* genes were same in two lines, while in *ZmRALF1* and *ZmRALF5* genes, there are single base pair difference (highlight in pink). The guide RNAs were stained in green, the correspond PAM domain (NGG) were stained in red.

CRISPR/Cas9 mutant was designed to target two genes at one time. Two guide RNAs from each gene were integrated into gRNA vector and further mobilized into destination vector pGW-Cas9 through Gateway recombination. There are both similarity and difference in peptide sequences between *ZmRALF1* and *ZmRALF5*, it would be useful to create all possible mutant combinations. Thus, the guide RNAs from *ZmRALF1* and *ZmRALF5* were cloned into a single construct.

Constructs sequences were confirmed by sequencing and restriction enzyme digestion (Table 2.4, Figure 2.20). The constructs were mobilized into *Agrobacterium* strain *EHA101* and transformed into maize Hi-II immature embryos. The T0 plants were self-pollinated or crossed with B73 for later phenotype analysis.

Table 2.4 ZmRALFs_pGW-Cas9 constructs identification. Two pGW-Cas9 destination vectors (*ZmRALF1/5* and *ZmRALF2/3*) were tested. The correspond exception bands size after digestion were listed in the table.

Constructs	Lane 1: *Bam*HI	Lane 2: *Eco*RV	Lane 3: *Xba*I	Lane 4: *Xho*I
ZmRALF1/5	**1. 12,124 bp**	**1. 14,364 bp**	**1. 11,104 bp**	**1. 10,377 bp**
pGW-Cas9	**2. 3516 bp**	**2. 4137 bp**	**2. 5708 bp**	**2. 4142 bp**
	3. 2239 bp	**3. 921 bp**	**3. 2638 bp**	**3. 2311 bp**
	4. 1571 bp	**4. 28 bp**		**4. 1399 bp**
				5. 921 bp
				6. 300 bp
ZmRALF2/3	**1. 12,125 bp**	**1. 14,364 bp**	**1. 11,104 bp**	**1. 10,377 bp**
pGW-Cas9	**2. 3516 bp**	**2. 4137 bp**	**2. 5708 bp**	**2. 4142 bp**
	3. 2239 bp	**3. 922 bp**	**3. 2639 bp**	**3. 2311 bp**
	4. 1571 bp	**4. 28 bp**		**4. 1399 bp**
				5. 922 bp
				6. 300 bp

MW: GeneRuler™ 1 kb DNA Ladder

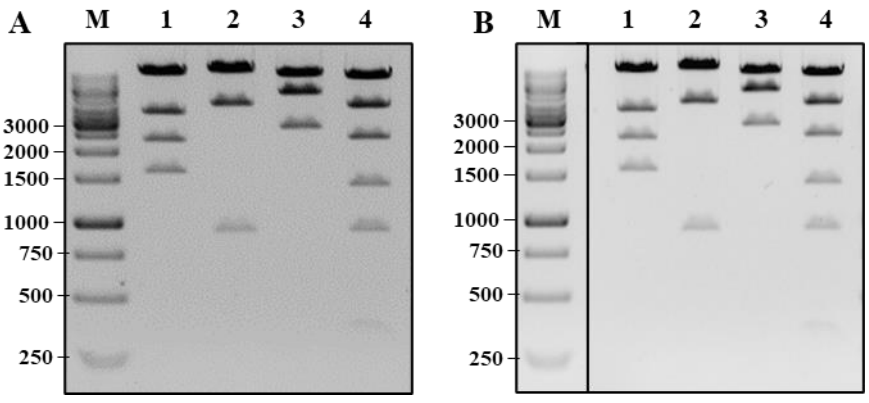

Figure 2.20 ZmRALFs_pGW-Cas9 constructs identification with restriction enzyme digestion. Four different restriction enzymes were used to ensure the correction of destination vector. M: gene ruler. 1: lane1, digested with *Bam*HI. 2: lane2, digested with *Eco*RV. 3: lane 3, digested with *Xba*I. 4: lane 4, digested with *Xho*I.

2.3.7 Subcellular localization of ZmRALF peptides in *Arabidopsis thaliana*

According to our RNA-seq data, *ZmRALF1/2/3/5* genes shown strong expression level in pollen tube. In another RNA-seq test against different reproduction organelles (Chen *et al.*, 2017), the expression patterns were different between *ZmRALF2/3* and *ZmRALF1/5* genes. *ZmRALF1/5* genes were more abundant in sperm cells, while *ZmRALF2/3* genes are not. GFP-tagged NtRALF was found to be expressed in cell wall (Escobar *et al.*, 2003). Pollen expressed AtRALF4/19 peptides were localized in the apoplast (Ge *et al.*, 2017). To explore the subcellular localization of ZmRALF peptides in the pollen tube, an enhanced green fluorescent protein (eGFP) at C-terminal was fused with *ZmRALF1/2/3/5* genes (including signal sequence). Around two kilobase pairs region of *AtRALF4* upstream was taken as promoter. The constructs were later transformed into model plant *Arabidopsis thaliana*.

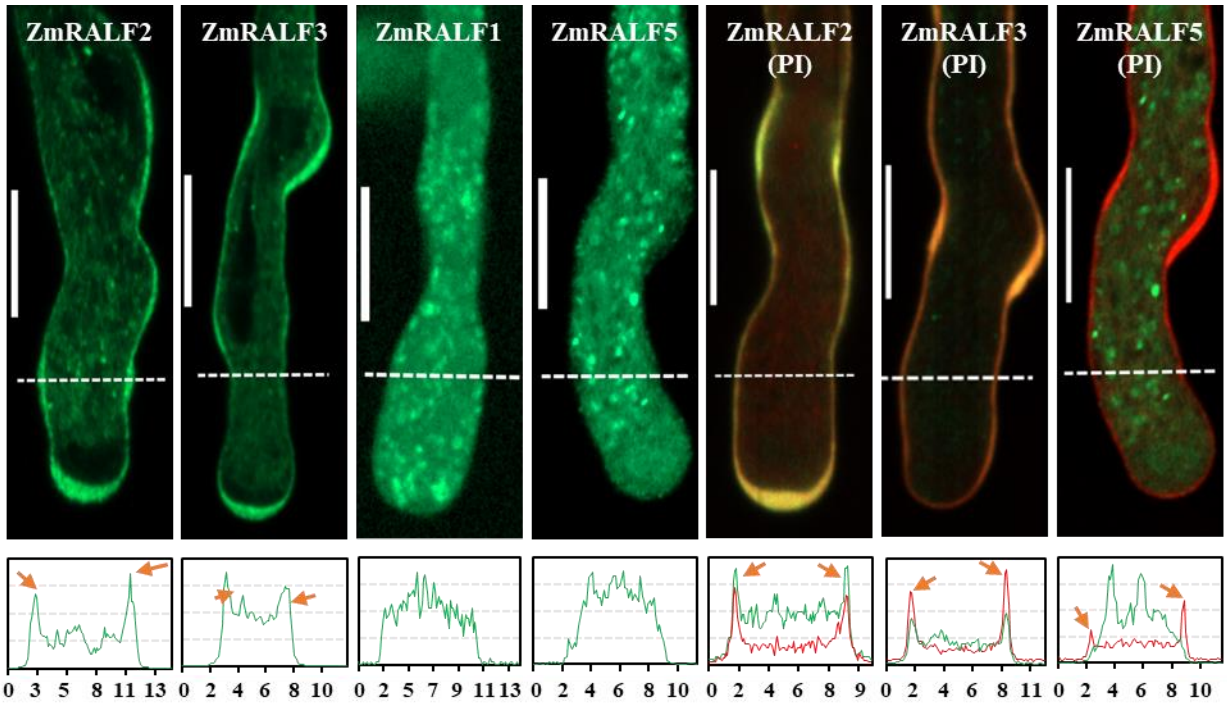

Figure 2.21 Maize Clade II RALF peptides locate to the cell wall and Clade III RALF peptides to cytosolic granules or vesicles of *Arabidopsis* pollen tubes. Around 2 kb upstream of the *AtRALF4* gene was used as promoter to express maize RALF peptides fused C-terminally to GFP in *Arabidopsis* pollen tubes. Top row showed images of indicated ZmRALF peptides with or without propidium iodide (PI) counter staining. Bottom row shows correlated relative green and/or red fluorescence intensity each 10 μm from the pollen tube apex (illustrated by white dashed lines). The x-axis values represent the distance in μm from the first dash at the left along the dashed line and the y-axis shows relative fluorescence intensity. Arrowheads indicate fluorescence signal enrichment in the cell wall. Scale bars are 10 μm.

Germinated *Arabidopsis* pollen tubes were checked under confocal microscope (Figure 2.21). Propidium iodide (PI) counter staining was added to differ the localization of cell membrane and apoplast. It was obvious that the subcellular localization of ZmRALF2/3 and ZmRALF1/5 peptides were different. ZmRALF2/3 peptides were localized at apoplast, especially at the tip of pollen tube. PI staining nicely co-localized with eGFP signal from ZmRALF2/3 peptides, further proved the apoplast localization. Meanwhile, the peptide fragments of ZmRALF2/3 were detected in the pollen germination medium when the maize pollen were germinated *in vitro* (Unpublished data from Dresselhaus group). ZmRALF1/5 peptides localized in the cytoplasm and was not detected on the membrane.

2.4 Discussion

Based on genome blast, 24 RALF peptides were detected in maize, 17 of which contain the conserved domains in Clade I and II as those in *Arabidopsis* (Figure 2.6). The untypical *RALF* genes such as *ZmRALF1* and *ZmRALF5* also exists in maize genome with unknown function. Mazie *RALF* genes identification was carried out before (Campbell and Turner, 2017; Cao and Shi, 2012; Sharma *et al.*, 2016), while the queries used for blast were taken from *Arabidopsis* RALF peptides. As indicated (Figure 2.6), Clade III and Clade IV RALF peptides were more divergent, which makes it hard to precisely target all maize RALF peptides from the query in *Arabidopsis*. Taking identified maize RALF peptides as query, the detected RALF peptides are more complete. By checking the fitness of RALF peptide features and cysteine residues arrangement (Silverstein *et al.*, 2007), RAFL peptides identification is also more reliable. Beside of the typical four features of RALF peptides, a commonly distributed motif (Motif 1) including also "untypical" RALF peptides was found (Figure 2.4).

According to the similarity of mature RALF peptide sequences, maize and *Arabidopsis* RALF peptides were classified into four groups, similar with the classification from Campbell and Turner, 2017. Functions of RALF peptides vary among different clades. Clade I and Clade II RALF peptides are more typical with all four RALF features. They also have similar function, such as AtRALF23/33 (Clade I) and AtRLAF34 (Clade II) were able to inhibit *elf18*-induced ROS production in leaf (Stegmann *et al.*, 2017). On the other hand, they are also different from each other. For example, in *Arabidopsis*, *theseus1* loss of function mutant didn’t response to AtRALF34 (Clade II) synthesis peptide treatment on root, but AtRALF1/22/23/33 (Clade I)

synthesis peptides treatment could inhibit root growth (Gonneau *et al.*, 2018); pollen expressed ANXs/BUPSs peptides could interact with AtRALF4/19/34 peptides (Clade II), but not with AtRALF23 peptide which is expressed in leaf (Ge *et al.*, 2017).

The function of RALF peptides in root were well studied, they are involved in root growth (Bergonci *et al.*, 2014; Campos *et al.*, 2018; Haruta *et al.*, 2014; Pearce *et al.*, 2001b), root hair growth (Du *et al.*, 2016; Murphy *et al.*, 2016), and nodules formation (Atkinson *et al.*, 2013; Combier *et al.*, 2008). There are 10 maize *RALF* genes expressed in root (Table 2.2), which may own similar functions. Among the 24 *ZmRALF* genes, nine of them are highly expressed in pollen, indicating their putative functions during reproduction. *ZmRALF1/2/3/5* genes are the most abundant ones, which occupy more than 97% of pollen *RALF* transcripts. Intriguingly, the correspond peptides of these four *RALF* genes belong to two clades: Clade II and Clade IV. In *Arabidopsis*, Clade II RALF peptides were well studied, including AtRALF 4/19 (Ge *et al.*, 2017; Mecchia *et al.*, 2017), AtRALF34 (Gonneau *et al.*, 2018; Murphy *et al.*, 2016), AtRALF24/31 (Zhao *et al.*, 2018). However, the function of Clade IV RALF peptide is poorly understood so far.

The studies on function of pollen-specific *RALF* genes are very limited. The first pollen-specific *RALF* gene was investigated in tomato (Covey *et al.*, 2010), which the correspond peptide could weakly inhibit pollen tube growth. Besides, ScRALF3 peptide is involved in microspore mitosis I (Loubert‐Hudon *et al.*, 2020), and BcMF14 downregulation resulted in curl/twist pollen tube (Li *et al.*, 2011). Only in *Arabidopsis*, the function of pollen-specific *RALF* genes *AtRLAF4/19* were well studied (Feng *et al.*, 2019; Ge *et al.*, 2017; Ge *et al.*, 2019a; Mecchia *et al.*, 2017). In fact, the distinctiveness of AtRALF4/19 peptides were discovered earlier. Among nine 6xHis-tagged AtRALF peptides (AtRALF1,4,19,22,23,24,31,33,34), AtRLAF4 peptide presented no activity in the alkalinization assay but AtRALF4/19 peptides showed strong inhibition on pollen tube growth (do Canto *et al.*, 2014). Thus, it was assumed that AtRALF4/19 peptides have different receptors and biological functions compared with other RALF peptides. The discoveries of ANXs/BUPSs/LRXs as interactors confirmed this hypothesis (Ge *et al.*, 2017; Mecchia *et al.*, 2017). Mature peptide sequences alignment revealed the similarity between ZmRALF2/3 and AtRALF4/19, which the knockout mutants showed defect on pollen tube growth both *in vitro* and *in vivo* (Ge *et al.*, 2017; Mecchia *et al.*, 2017). In a similar manner, the maize RNAi-*RALFs* mutants showed unstable pollen tube during *in vitro* pollen germination. One hour after pollination, the RNAi-*RALFs* mutant pollen tubes can be found in transmitting tract. However, it

does not mean there were no defect during later pollen tube growth. The knockout of *AtRALF4/19* genes result in the ceases of pollen tube in transmitting tract, but most of them could across style (Ge *et al.*, 2017). Considering the length of maize transmitting tract, it is speculated that the pollen tube from RNAi-*RALFs* cannot reach to the ovule, which was proved by the reduction on male gametophyte delivery efficiency.

ZmRALF2/3 peptides cell wall localization were proved by C-terminal eGFP fluorescence fusion protein coupled with PI staining. These results are also consist with the localization of *Nicotiana benthamiana* RALF peptide fused to GFP, *Solanum lycopersicum* pollen specific RALF peptide detected by immunolocalization (Covey *et al.*, 2010), and AtRALF4/19 peptides with C-terminal GFP tag (Ge *et al.*, 2017). The apoplast localization suggest that ZmRALF2/3 peptides are more likely performed their function on cell wall.

To our knowledge, cytoplasm localized ZmRALF1/5 peptides was the first identified localization of Clade IV RALF peptides. Their different localization with Clade I and Clade II RALF peptides suggest different functions. The only investigated Clade IV RALF peptide is AtRALF8 (Atkinson *et al.*, 2013), its gene overexpression induced longer and more root hairs compared with wild type. In contrast, overexpression of Clade I *RALF* gene *AtRALF1* or *AtRALF23* resulted in less and shorter root hairs (Matos *et al.*, 2008; Srivastava *et al.*, 2009). It seems that two types of RALF peptides function in different ways.

CHAPTER 3. DISCOVERY OF RALF INTERACTORS

3.1 Introduction

As a peptide hormone, function of RALF peptides relies on various interactors. There are two classes of receptors that underwent extensive studies: *Catharanthus roseus* receptor kinase 1 like (CrRLK1L) and leucine-rich repeat extensin (LRX).

FERONIA (FER), a prominent *Arabidopsis* CrRLK1L, was found to be the receptor of RALF peptides in root (Haruta *et al.*, 2014), and the RALF-CrRLK1L functions were widely studied. RALF-CrRLK1L interaction is present with various roles in almost all aspects of plants life: lateral root initiation (Gonneau *et al.*, 2018), stomata closure (Yu *et al.*, 2018), immune system reaction (Stegmann *et al.*, 2017), reproduction (Ge *et al.*, 2017; Mecchia *et al.*, 2017), abiotic stress response (Yu and Assmann, 2018), and so forth.

Even though the interaction of RALF-LRX was found decade ago (Covey *et al.*, 2010), it did not attract much attention until recently. For example, the strong binding of AtRLF4 to AtLRX8 in *Arabidopsis thaliana* provided interesting into LRX function regarding pollen tube growth (Moussu *et al.*, 2020).

3.1.1 RALF-CrRLK1L: a complex with multiple functions

FERONIA (FER) was discovered in 2003, N. Rotman from the Faure' group and N. Huck from the Grossniklaus' group simultaneously reported the overgrowth of pollen tubes in synergid cells of *feronia* mutants in *Arabidopsis thaliana* (Huck *et al.*, 2003; Rotman *et al.*, 2003). The finding provided the first evidence for female control over male gamete delivery. Further investigation revealed that FER was localized in the filiform apparatus, a cell wall region that attracts and captures pollen tubes to synergid cells (Escobar-Restrepo *et al.*, 2007). Once a pollen tube arrived at the ovule, FER-controlled nitric oxide (NO) accumulation mediated by pectin would be triggered, which blocks the entrance of further pollen tubes (Duan *et al.*, 2020). In case of the penetrated pollen tube, FER is involved in the induction of reactive oxygen species (ROS) and calcium signaling that mediate pollen tube rupture to release the sperm cells (Duan *et al.*, 2014; Ngo *et al.*, 2014). However, whether RALF is involved in the FER-controlled pollen tube

regulation is unclear, even though the accumulation of AtRALF34 peptide was found before fertilization (Ge *et al.*, 2017).

Different from the unclear role of RALF peptides in ovules, functions of the RALF-FER complex in vegetative tissues have been more well defined. In roots, AtRALF1 enhances the mutual phosphorylation of FER and the receptor-like cytoplasmic kinase RIPK to regulate cell growth (Du *et al.*, 2016); AtRALF1 activates FER by increasing its phosphorylation level, which activates ABI2 through the GEF-ROP pathway, leading to the feedback inhibition of ABA response (Chen *et al.*, 2016); AtRALF1-FER signaling also increases the abundance of ErbB3-binding protien1 (EBP1), accumulates in the nucleus and controls gene expression (Li *et al.*, 2018). In leaves, AtRALF23 binding to FER inhibits the immune response to fungi (Stegmann *et al.*, 2017). The binding of FER has been utilized by fungi, which secret RALF-like proteins that function via host plant FER to increase their infectious potential and suppress host immunity (Masachis *et al.*, 2016). In summary, the RALF-FER complex performs its function via various ways, including directly affecting cell growth by interacting with other receptors or plant hormone related proteins, or indirectly regulating gene expression by interacting with nuclear binding proteins as well as RNA binding proteins (Wang *et al.*, 2020).

FER belongs to the CrRLK1L family in *Arabidopsis*, which contain 17 members with similar structure (Figure 3.1): one or two malectin-like domain in the extracellular part, a transmembrane domain, and a kinase domain in the intercellular part (Li *et al.*, 2016). In CrRLK1L family, FER is not the only receptor of RALF. THESEUS1 (THE1) interacts with AtRALF34 to regulate lateral root initiation (Gonneau *et al.*, 2018); ANXURE (ANX)1/2 and Buddha's Paper Seal (BUPS)1/2 interact with AtRALF4/19 to maintain the pollen tube integrity (Ge *et al.*, 2017).

ANXs and BUPSs were special among CrRLK1Ls for their high expression in pollen (Ge *et al.*, 2017). ANX1 and ANX2 function redundantly to maintain cell wall integrity since *anx1anx2* double mutant pollen tubes cease growth and burst *in vitro* (Boisson-Dernier *et al.*, 2009; Miyazaki *et al.*, 2009). ANXs function via NADPH oxidase RbohH and RbohJ that are involved in the tip-focused calcium gradient during pollen tube growth (Boisson-Dernier *et al.*, 2013). RALF-FER complex interacts with RIPK, in a similar way, the receptor-like cytoplasmic kinase (RLCK) MARIS (MRI) functions downstream of ANXs as the phenotype of *anx1 anx2* double mutant could be rescued by a MRI^{R240C} mutant (Boisson-Dernier *et al.*, 2015). Furthermore, in a similar manner, it was deduced that RbohH and RbohJ function upstream of MRI. BUPSs double

mutants have similar pollen tube burst as *anx1anx2*, while the downstream interactors were not clear. It was speculated that ANXs and BUPSs form heterodimers, which share same downstream signaling pathway (Ge *et al.*, 2017).

CrRLK1L proteins are not limited to *Arabidopsis*, but they are also widely distributed across the plant kingdom (Figure 3.2). Orthologues of most characterized *Arabidopsis* CrRLK1L proteins could be found in the early divergent angiosperm lineage, *Amborella trichopoda* (Galindo-Trigo *et al.*, 2016). FERONIA function in reproduction is also ancient since the unicellular charophycean algae *Closterium peracerosum-strigosumlittorale* complex RLK1 (CpRLK1)

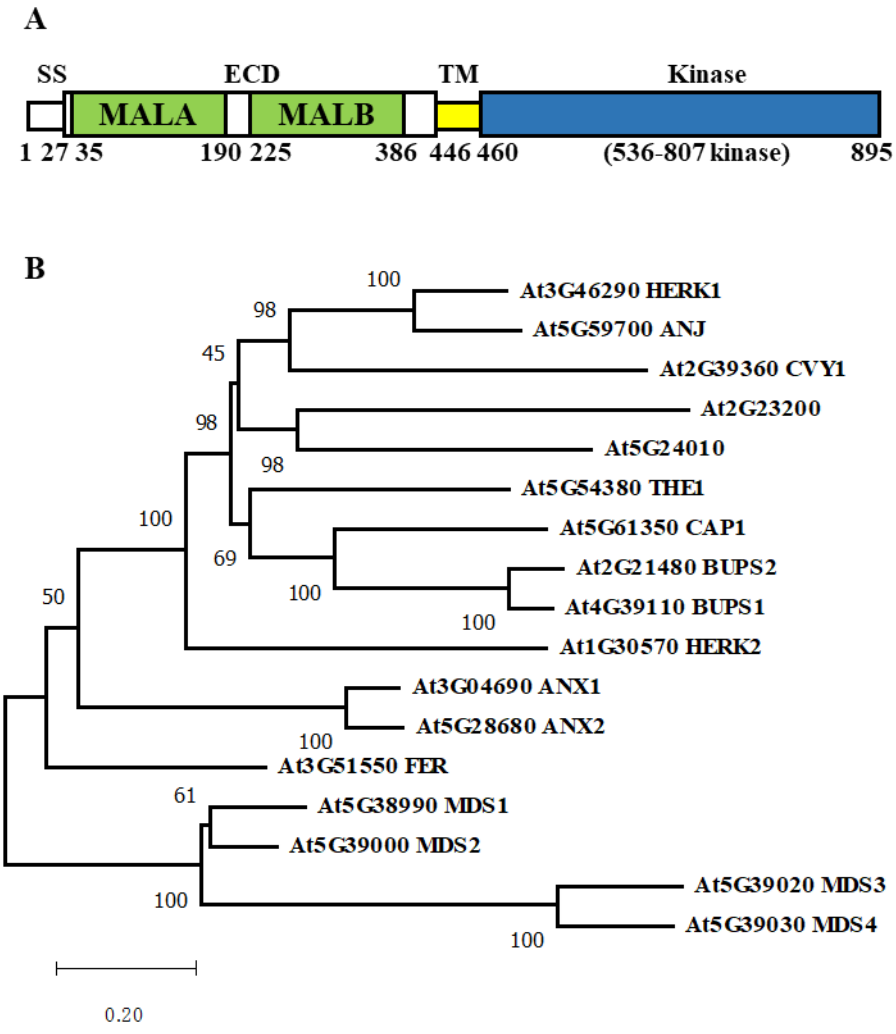

Figure 3.1 FERONIA protein domain structure and phylogenetic tree of the *Arabidopsis* CrRLK1L receptor kinase family. (A) Deduced FERONIA structural domains. SS, ECD, TM are, respectively, signal peptide, extracellular domain, transmembrane domain. MALA and MALB are tandem malectin-like domains. Numbers indicate amino acid residues. (B) The CrRLK1L protein family. Image was drawn based on description and images presented in Li *et al.*, 2016)

regulates osmotic pressure in the cell to allow proper gamete release (Hirano *et al.*, 2015). Besides *Arabidopsis*, CrRLK1L proteins were well characterized in rice. There are 16 *CrRLK1L* genes in rice (Nguyen *et al.*, 2015), five of which were studied in detail. FERONIA-like 1/2 (FLR1/2, also named DRUS1/2) were reported to be important for anther development by stimulating starch biosynthesis in pollen (Pu *et al.*, 2017). Together with FLR11 and FLR13, FLR1/2 involved in the fungi defense with contrasting functions (Huang *et al.*, 2020). BUPS-like *Ruptured Pollen tube* (*RUPO*) is specifically expressed in rice pollen and required for male gamete transmission (Liu *et al.*, 2016a). Except for these two plants, little is known about how CrRLK1Ls function in other species.

To perform their function, CrRLK1Ls need to cooperate with LORELEI (LRE) and LRE-like GPI-anchored proteins (LLGs) (Li *et al.*, 2015; Liu *et al.*, 2016b). The *LRE* gene encodes a glycosylphosphatidylinositol(GPI)-anchored protein (GAP) and co-localizes with FER in the

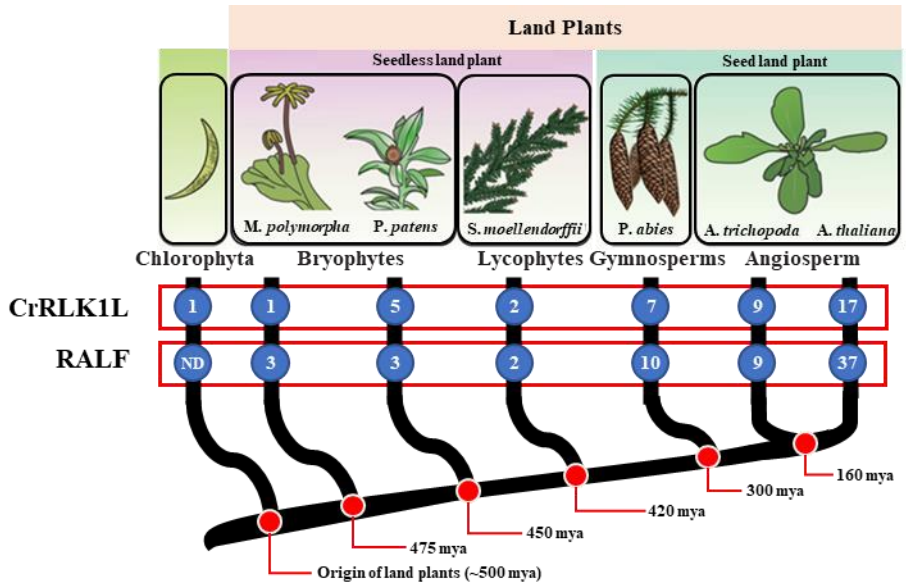

Figure 3.2 Occurrence of CrRLK1L and RALF across Streptophyta. Data is shown for the Chlorophyta species (*Ostreococcus lucimarinus*, *Chlamydomonas reinhardtii*, *Volvox carteri*, *Coccomyxa subellipsoidea*, *Micromonas pusilla*, and *Micromonas* sp; Charophyta *Closterium peracerosum-strigosum-littorale* complex); the liverwort *Marchantia polymorpha*; the model bryophyte *Physcomitrella patens*; the lycophyte *Selaginella moellendorffii*; the conifer *Picea abies*; the single living sister species to all other angiosperms *Amborella trichopoda*, and *Arabidopsis thaliana*. According to GenBank, Phytozome and ConGenIE databases, the CrRLK1L subfamily increases in number with developmental complexity. RALF is absent in Chlorophyta and present in land plants. Full genomic or transcriptomic records are not available for charophyte included in this figure (ND). Image was drawn based on description and images presented in Galindo-Trigo *et al*., 2016; Campbell and Turner, 2017.

filiform apparatus (Capron *et al.*, 2008). As a chaperon/co-receptor, LRE promotes the FER delivery from the endoplasmic reticulum to the cell membrane (Li *et al.*, 2015). The mutation of *LRE* caused similar defects as in *feronia* mutants where pollen tube failed to burst in synergid cell (Capron *et al.*, 2008). There are three other *LLGs* genes in *Arabidopsis*: vegetatively expressed *LLG1* and pollen specific expressed *LLG2/3*. In a similar way, LLG1 is a co-receptor of FER in root, involved in the FER-regulated RHO GTPase signaling complex regulation (Li *et al.*, 2015). LLG2/3 interact with ANXs/BUPSs to maintain pollen tube integrity, and the interactions require RALF as a glue to enhance complex formation (Ge *et al.*, 2019b; Xiao *et al.*, 2019). Similar to *CrRLK1L*, *LORELEI-like* genes have a plant-conserved distribution (Capron *et al.*, 2008), but are not widely investigated.

3.1.2 RALF-LRX complexes contribute to maintain cell wall integrity

Tomato Leucine-rich repeat extensin (LRX) protein is the first identified RALF interactor (Covey *et al.*, 2010). In a yeast two-hybrid screen for the interactor of tomato pollen-specific cell wall localized LRX protein, SlPRALF peptide was identified. However, they did not focus on the LRX-RALF interaction, instead discovering the function of pollen-specific SlPRALF peptide. This is the beginning of pollen-specific RALF peptide research. Although the LRX-RALF function did not attract much attention, the amino acid sequences similarity between SlPRALF and AtRALF4 was clearly shown, which might have inspired the investigation of AtRALF4-LRXs interaction (Mecchia *et al.*, 2017).

In *Arabidopsis thaliana*, several *RALF* genes (*RALF4,8,9,15,19,25,26*) were found to be expressed in pollen (Loraine *et al.*, 2013), among which AtRALF4 and AtRALF19 have typical RALF peptide structures (Chapter 2). Before the discovery of interaction between LRX8-11 with AtRALF4/19 (Mecchia *et al.*, 2017), the investigation on AtLRX proteins already started. *AtLRX* genes were divided into two groups according to their vegetative/reproductive expression preference (Baumberger *et al.*, 2003a). Vegetative AtLRXs are important to maintain the cell wall morphology, and *lrx* mutants show defects in tip-growing root hair cells (Baumberger *et al.*, 2003b). Other AtLRXs (8,9,10,11*)* may also contribute to maintain the integrity of pollen tube wall (Mecchia *et al.*, 2017; Moussu *et al.*, 2020).

In vitro AtRALF4 peptide application could inhibit pollen tube growth (do Canto *et al.*, 2014), while the effect disappeared in the pollen-specific *lrx* mutants (Mecchia *et al.*, 2017), indicating

LRXs were needed for the AtRALF function. Direct interaction of AtRALF4 with pollen-specific LRXs was also detected, which confirms the existence of LRX-RALF complexes. Furthermore, the binding affinity of LRX8 with AtRALF4 was as high as 3.5 nM (Moussu *et al.*, 2020), much higher than AtRALF4-ANX1 (310 nM, the strongest binding between AtRALF-CrRLK1L)(Ge *et al.*, 2017).

The high binding affinity resulted from the LRX protein structure (Figure 3.3). LRX protein consists of several parts: a signal peptide to direct the localization to the cell wall; a NT domain after the signal peptide is believed to be specific for individual LRX proteins (Herger *et al.*, 2020; Moussu *et al.*, 2020); a Leucine-rich repeats (LRR) domain protrude the cell wall interacting with ligands; a cysteine-rich region responsible for a disulfide-bound LRX dimer; a proline-rich extensin domain that anchors in the cell wall. Crystal structure analysis revealed that the LRR core of LRX provides a binding platform for AtRALF4 (Moussu *et al.*, 2020). The binding of AtRALF4-LRX8 occurred on Tyr83 and Tyr84 of AtRALF4, double disulfide bonds were also required for high-affinity binding.

Figure 3.3 Structure of LRX proteins. LRX proteins contain a signal peptide for protein export (SS), an N-terminal domain (NT-domain, brown), a leucine-rich domain with 11 full leucine-rich repeats (LRR, green), a cysteine-rich linker domain (CRD, yellow) and a C-terminal extensin domain (Extensin, blue).

Pollen specific AtLRXs redundantly regulate pollen tube wall integrity (Fabrice *et al.*, 2018; Sede *et al.*, 2018; Wang *et al.*, 2018b). In *lrx* triple or quadruple mutants, cell wall pectin and callose were significantly increased, pollen germination ratio and seed set were severely reduced. The MRI^{R240C} mutant could suppress the *anx1anx2* defect and partially rescue *rbohH rbohJ* male sterility, it could not relief the defect caused by *lrx8-11* quadruple mutants (Franck *et al.*, 2018). However, the mutation of ATUNIS1(AUN1^{D94N}), which functions downstream of AtRALF4/19, ANX1/2, and RbohH/J, could partially rescue the male sterility and pollen tube burst of *lrx8-11* quadruple mutants. In addition, even though the interaction of FERONIA and LRXs (1, 2, 3, 4, 5) were detected, the addition of AtRALF1 did not affect these interactions (Herger *et al.*, 2020). Moreover, in *Arabidopsis*, LRX4 (without extensin)-Citrine was detected in the membrane fraction of wild type and *fer-4* mutants, indicating LRX4 function was not relied on FERONIA

(Herger *et al.*, 2020). Taken together, the LRXs may not be directly involved in the RALF-CrRLK1L receptor complex but play an important role in RALF signaling pathway.

Besides tomato and *Arabidopsis*, LRXs were found in maize, rice, and other 13 species (Liu *et al.*, 2016c). ZmPEX1 and ZmPEX2 were the earliest pollen-specific LRX discovered (Rubinstein *et al.*, 1995a; Rubinstein *et al.*, 1995b). They were localized in the intine in mature pollen and to the callosic sheath of pollen tube, which are similar to pollen-specific LRXs in *Arabidopsis* (Fabrice *et al.*, 2018). However, the function of ZmPEX1 and ZmPEX2 are still unknown.

3.1.3 Other interactors

Although the RALF-LLG-CrRLK1L and RALF-LRX complexes are ubiquitously distributed across plant tissues, other possible interactors cannot be excluded. BRI1-associated receptor kinase 1 (*bak1*) mutants were insensitive to AtRALF1 in root (Dressano *et al.*, 2017). Co-immunoprecipitation (Co-IP) between BAK1 extracellular domain and AtRALF1 recombinant purified proteins revealed the interaction of BAK1 and AtRALF1 (Kd= 4.6 μM, weak binding). In a yeast two-hybrid system to search for AtRALF1 interactors, calmodulin-like protein 38 (CML38) was identified (Campos *et al.*, 2018) and found to mediate AtRALF1 root growth inhibition.

The receptors characterized until now are rather typical RALF peptides. However, in the RALF peptide family, there are RALF peptides are short of the typical structures, which are recognized to be RALF-related peptides (Campbell and Turner, 2017). For example, *AtRALF8* and *AtRALF9* show remarkably high gene expression level in pollen, even higher than *AtRALF4* (Loraine *et al.*, 2013), but the function is unknown. In maize, the most abundant RALF also belongs to RALF-related peptides (Chapter 2). It is meaningful to uncover the mysteries of RALF-related peptides in the future.

3.2 Experimental procedures

There are many overlaps on methods used in this chapter to those in Chapter 2, such as the gene expression database, sequence alignment and visualization. Only those experiments which use different or modified methods are introduced.

3.2.1 Genome blast of candidate RALF interact proteins

To uncover the CrRLK1L protein distribution in maize, protein blast was carried out. *Arabidopsis* FERONIA (At3g51550) was used as query to run BLASTP (protein-protein BLAST) in the non-redundant protein sequences (nr) of *Zea mays* (taxi:4577) at online tool NCBI (https://blast.ncbi.nlm.nih.gov/). The output sequences were manually selected, which take into consideration of query cover (>50%), E-score (< 0.05), and the presence of a malectin-like domain. 17 maize CrRLK1L proteins were found and the corresponding genes symbol (B73 RefGen_v4) were extracted from the protein introduction pages. As the most well-known gene in the *CrRLK1L* family is *FERONIA*, maize *CrRLK1L* genes were named as *FERONIA*-like genes. The *Arabidopsis* LORELEI (AT4G26466) protein was used to blast for maize LORELEI-like proteins (ZmLLGs) in a similar manner. *Arabidopsis* LORELEI-like proteins were extracted from UniProt.

To check the leucine-rich repeat extensin proteins (LRX) in maize, ZmPEX1 (LOC103648188) and ZmPEX2 (Zm00001d048715) were used to blast maize genome. According to the LRX protein features (Herger *et al.*, 2019), four pollen-specific PEXs and 15 LRXs were identified. Their corresponding gene symbols (B73 RefGen_v4) or locus tags were extracted from NCBI. *Arabidopsis* LRX protein sequences (Ringli, 2005) were extracted from UniProt.

3.2.2 Protein motif identification and phylogenetic tree

Full-length CrRLK1L proteins from maize and *Arabidopsis* were used to perform alignment and phylogenetic analysis in MEGA X. Typical CrRLK1L proteins contain a malectin-like domain, a transmembrane domain and a kinase domain. ZmCrRLK1L protein motifs were extracted form Pfam (https://pfam.xfam.org/) (El-Gebali *et al.*, 2019) and added to the phylogenetic tree. Phylogenetic analysis of LLGs was carried out in a similar manner. Ser-$Pro_{2\text{-}n}$ amino acid repeats are commonly possessed in LRX extensin domains, which the number are highly variable (Herger *et al.*, 2019). To obtain reliable alignment, LRX protein sequences' signal peptide and extensin domain were removed. The phylogenetic analysis was carried out in a similar manner as RALFs.

3.2.3 Protein expression plasmids construction.

All receptor-like kinases in this study were cloned into pMAL-p2p plasmid (provided by Kamila

Kalinowska) with an N-terminal MBP tag, including the ectodomain of ZmFERL1/4/7/9 and ZmPEX2/4, or whole protein without the signal peptide for ZmLLG1/2 and AtLRX9/10/11. Besides, ectodomains of ZmFERL1/4/7/9 were cloned into pGEX-6P1 (GE Healthcare) with an N-terminal GST tag. Constructs were transformed into *E. coli* strain BL21 for protein expression and purification.

3.2.4 Protein purification from *E.coli*

The target protein expression and purification procedures are similar to those for 6xHis-tagged RALFs, they only differ in the buffers and protein binding beads. For GST/MBP protein induction, 0.2-0.5 mM IPTG were used to avoid too fast growth resulting in the formation of inclusion body. The lysis buffer (50 mM Tris pH7.5, 150 mM NaCl, 0.05% CA630 from Sigma-Aldrich, protease inhibitor, 0.5 mg/ml lysozyme, 1 mM PMSF) as well as the wash buffer (100 mM Tris-HCl, 1 mM PMSF, pH 8) of GST/MBP tagged protein purification were identical. GST tagged protein binds to glutathione-agarose beads (ROTH), MBP tagged protein needs amylose beads (New England Biolabs). The elution buffers were also different, since GST tagged protein needs 15 mg/mL reduced glutathione in 100 mM Tris-HCl, MBP tagged protein needs 25 mg/mL maltose in 100 mM Tris-HCl. Proteins were further desalted in protein buffer (3.9 mM NaH_2PO_4, 6.1 mM Na_2HPO_4, 200 µl, 1 mM DTT, 1 mM EDTA, 1 mM PMSF, pH 7.5) with PD-10 columns. To improve the concentration of MBP tagged proteins for the MST test, purified proteins were further concentrated with Amicon® Ultra 50K device (Merck). FLAG-tagged ectodomains of *Arabidopsis* ANX1/2 and BUPS1/2 proteins were obtained from a previous study (Ge *et al.*, 2017). Protein concentrations were measured via Bradford protein assay as described (He, 2011).

3.2.5 Pull-down assay and MST test

The *in vitro* binding or pull-down assays were carried out as described (Ge *et al.*, 2017). ZmRALF and AtRALF proteins contained a 6xHis-tag and MBP/GST-tags were present in ZmFERLs, AtANXs, AtBUPSs, ZmLLGs, ZmPEXs, and AtLRXs. Briefly, samples were mixed in 500 µL binding buffer (20 mM Tris-HCl, pH=7.5, 1% CA630) and rotated at 4°C for 2 hours before addition of His-beads (Ni-NTA, QIAGEN). After continuous rotating for another 2 hours, beads were pelleted and washed for five times. Samples were boiled in SDS-loading buffer and analyzed by SDS-PAGE and western blot. As antibodies we used a His antibody (6xHis-Tag Monoclonal

Antibody, Thermo Fisher Scientific), an MBP antibody (Anti-MBP Monoclonal Antibody, HRP conjugated, NEB), a GST antibody (GST Tag Monoclonal Antibody, Thermo Fisher Scientific) and a FLAG antibody (anti-Flag-HRP, Sigma-Aldrich). For interaction studies of biotinylated AtRALF4/19 with GST-tagged ZmFERL7/9 and MBP-tagged ZmFERL1/4, the procedure was the same despite that His-beads were substituted by Streptavidin Magnetic Particles (Spherotech).

To test the binding affinity of maize RALF peptides with the correspond interactors, Microscale Thermophoresis (MST) assays were carried out by using a Monolish NT.1.115 (NanoTemper Technologies). 6xHis-tagged RALF proteins were labeled with red dyes according to the manufacturers' recommendation. 6x His-tagged RALF proteins were diluted to 200 nM in PBST buffer (137 mM NaCl, 2.5 mM KCl, 10 mM Na_2HPO_4, 2 mM KH_2PO_4, 0.05% Tween-20 at pH 7.4). A volume of 100 µL protein solution (200 nM) was mixed with 100 µL dye solution (100 nM) diluted from a labeling kit (Monolith His-Tag Labeling Kit RED-tris-NTA 2nd Generation) and incubated at room temperature for 30 min. After centrifugation, dye-labelled proteins were mixed using a gradient dilution of interactors (ZmFERL1/4/7/9, ZmPEX2/4). Samples were loaded into silica capillaries (NT.115 Standard Treated Capillaries) and measured at 40% MST power and 10% LED power. Recorded data were analyzed with MO.Affinity Analysis 2.3 (NanoTemper Technologies).

3.2.6 RNAi-*RALFs* phosphoproteomic analysis

To compare the phospho-proteome of wild type and RNAi-*RALF* mutant lines, fresh pollen was germinated *in vitro* for 20 minutes in liquid PGM as described in section 2.2.2.2. Successful pollen germination and tube formation was checked by using an inverted microscope (Nikon Eclipse TE2000-S) with a 4x objective (Plan Fluor DL 4x/0.13, PHL). Pollen tubes were filtered by PluriStrainer® 40 µm (pluriSelect) and washed twice with fresh liquid PGM. 50 mg of pollen tube samples were transferred from the surface of the strainer into a 1.5 mL collection tube and immediately frozen in liquid nitrogen for phospho-proteome analyses and stored at -80 ºC .

The phospho-proteome was generated as described (Mergner *et al.*, 2020). 100 µg precipitated, washed and in urea digestion buffer re-suspended total protein was digested with trypsin and TMT-labeled as described. Nano-flow LC-ESI-MS measurements were performed with labelled samples using a Dionex 3000 HPLC (Thermo Fisher Scientific) coupled to a Q Exactive HF or Fusion Lumos Tribrid mass spectrometer (Thermo Fisher Scientific). Finally, samples were

measured with a SPS-MS3 method on an Orbitrap Fusion LUMOS mass spectrometer. Full-scan MS1 spectra (m/z 360-1300) were acquired with 60,000 resolution, an automatic gain control (AGC) target value of 4e5 and 50 ms maximum injection time. For MS2 based peptide identification precursor ions were fragmented via CID (NCE of 35%, activation Q of 0.25) and recorded in the Orbitrap at 15,000 resolution (isolation window 0.7 m/z, AGC target value of 5e4, maxIT of 22 ms). The 10 most intense peptide fragments for each precursor were selected in the ion trap and further fragmented via HCD (NCE of 55%). An additional MS3 spectrum for TMT quantification was subsequently obtained in the Orbitrap at 50,000 resolution (scan range 100 – 1,000 m/z, charge dependent isolation window from 1.2 m/z (2+) to 0.7 (5-6+), AGC of 1.2e5, maxIT of 120 ms). Peptide and protein identification and quantification was performed with MaxQuant (Cox and Mann, 2008) using standard settings (version 1.5.8.3; 1.6.0.16). Raw files were searched against a maize database (*Zea mays*.AGPv4.pep.all.fasta; ensemblgenomes download 2016) and common contaminants.

3.3 Results

3.3.1 The maize genome contains conserved *CrRLK1L* family genes

CrRLK1L proteins were widely spread across species, even in the earliest divergent angiosperm lineage *Amborella trichopoda* (Galindo-Trigo *et al.*, 2016). In land plants, there are 17 members in *Arabidopsis thaliana* (Li *et al.*, 2017), 26 members in the Chinese white pear tree *Pyrus bretschneideri* (Kou *et al.*, 2017), and 67 members in the common apple tree *Malus domestica* (Zuo *et al.*, 2018). However, there was no report about CrRLK1L family members in *Zea mays*.

To explore CrRLK1L in maize, the amino acid sequence of FERONIA from *Arabidopsis* was used as a query to blast the maize genome. 17 *CrRLK1L* genes were found in maize and named as maize *FERONIA-like* (*ZmFERL*) genes due to their similarity with FERONIA (Supplemental Table 1). A chromosome localization map was drawn to illustrate the genomic origins of *ZmFERL* genes. They distribute across seven chromosomes of maize, except for chromosome 4, 5, and 10 (Figure 3.4) that do not harbor any *ZmFERL* members. Only *ZmFERL7*, *ZmFERL10*, and *ZmFERL17* contain introns.

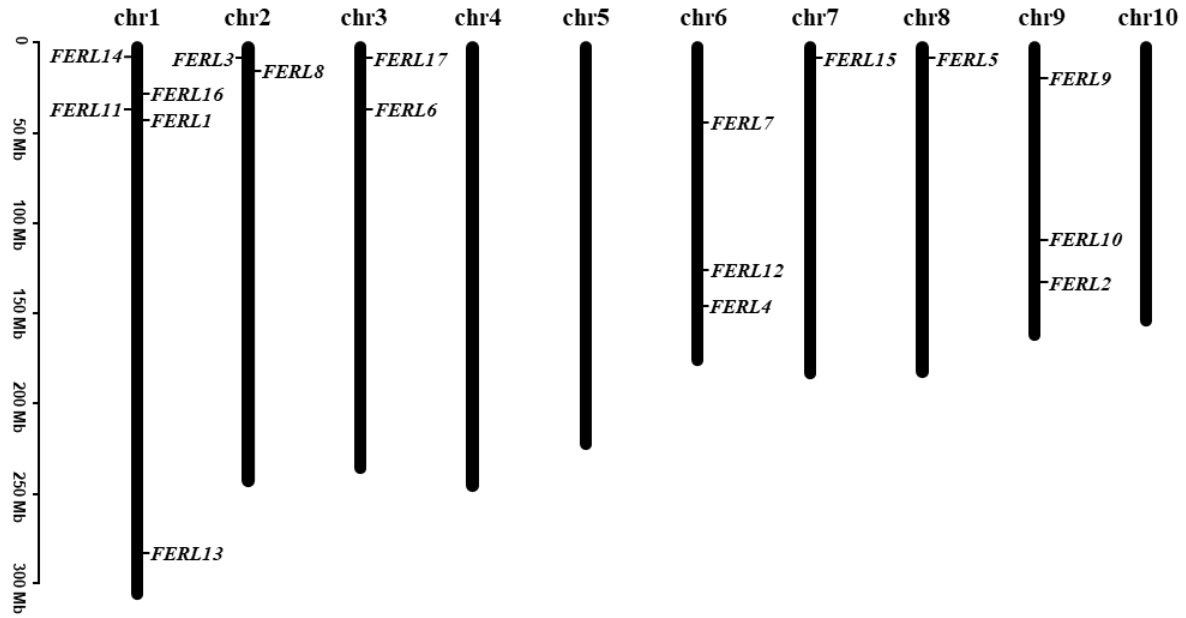

Figure 3.4 Chromosomal distribution of maize *FERONIA*-like genes. Chromosome numbers are shown at the top of each chromosome, and the approximate size in megabases (MB) is provided at the left side. The names of each *FERL* gene showed is labelled at the sides of each chromosome.

To investigate the conservation of CrRLK1L proteins, phylogenetic analysis was carried out between maize and *Arabidopsis* (Figure 3.5). Full-length CrRLK1L proteins were used to construct the evolutionary tree. According to the result, CrRLK1L proteins from the two species are highly conserved. *Arabidopsis* CrRLK1L proteins are around 850 amino acids long, maize FERONIA-like protein sequences ranged from 474 to 917 amino acids (Supplemental Table 1). Special features of CrRLK1L family proteins are an extracellular malectin-like domain and a cytoplasmic protein kinase domain (Boisson-Dernier *et al.*, 2011). According to the Pfam protein database (El-Gebali *et al.*, 2019), all *Arabidopsis* CrRLK1L proteins contain these two features, plus an N-terminal signal sequence and a transmembrane domain, so do all maize FERL proteins except ZmFERL16 and ZmFERL17 (Figure 3.5). Maize FERL proteins' tyrosine kinase domains are commonly around 270 amino acids, but shorter in ZmFERL7 with only 165 amino acids. Of note, ZmFERL9 is unique in its protein kinase domain, similar to MDS3 in *Arabidopsis*.

In *Arabidopsis*, *FERONIA* gene is expressed everywhere except in pollen, whereas *ANXUR1/2* and *BUPS1/2* preferentially expressed in pollen. Unpublished data from the Dresselhaus group was used to report the expression pattern of *ZmFERL* genes. Interestingly, expression patterns of *ZmFERL* genes are very similar to *CrRLK1L* genes in *Arabidopsis*. ZmFERL1 has the highest

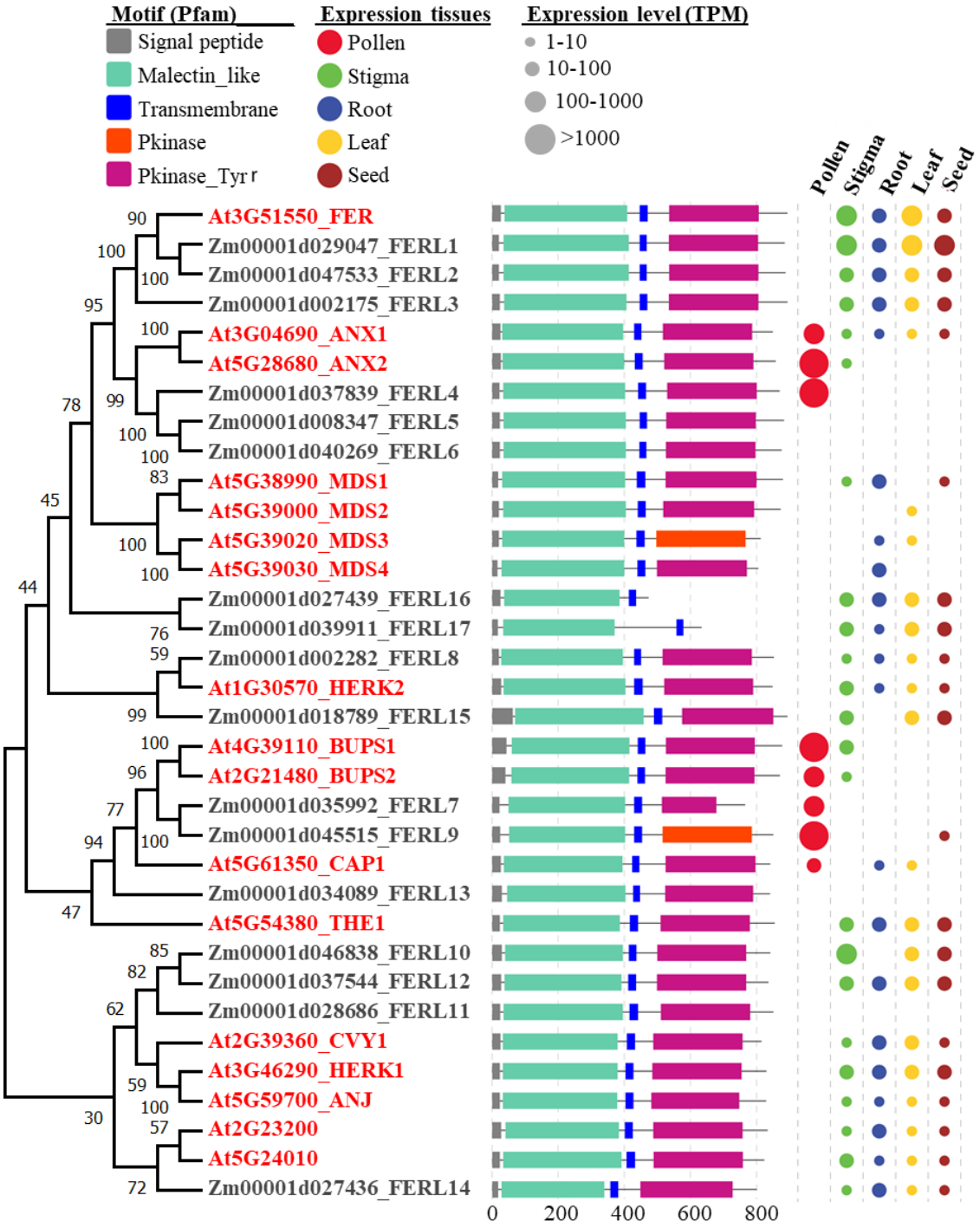

Figure 3.5 Phylogenetic tree of 34 CrRLK1L proteins from maize and *Arabidopsis* with their domain organization and expression pattern. Full-length proteins were used to generate the phylogram. *Arabidopsis* CrRLKs1Ls are indicated in red and maize ones in black letters. The domain organization for each CrRLK1L member was extracted from Pfam and drawn in the middle. Protein sequences were obtained from UniProt databases. Colored dots show expression pattern of *FERL* genes in the five selected tissues indicated. Dot size correlates to expression level determined by TPM (transcript per million) values as indicated.

similarity in protein sequence with FERONIA, and *ZmFERL1*, *ZmFERL2*, and *ZmFERL3* genes were expressed in four out of the five tissues but not in pollen (Figure 3.5). *ZmFERL4* is solely expressed in pollen and closely related to *ANXs*. *ZmFERL7* and *ZmFERL9* are pollen-specific genes that comparable with *BUPSs*. Expression of *ZmFERL5*, *ZmFERL6*, *ZmFERL11* and *ZmFERL13* genes were not detected in tissues selected. Besides those genes, the other maize *FERONIA-like* genes were widely expressed but not in pollen (Table 3.1).

It is obvious that there are orthologues of the well-studied *Arabidopsis CrRLK1L* genes in maize: *ZmFERL1/2/3* are orthologues of *FERONIA*; *ZmFERL4* is the orthologue of *ANXs*; *ZmFERL7/9* are orthologues of *BUPSs*. The functional investigation of these maize CrRLK1L proteins would expand the knowledge of the maize reproductive signaling network.

Table 3.1 Expression level of maize *FERONIA-like* genes. Genes' mRNA expression levels were extracted from RNA-seq data (Dresselhaus group). Values are in transcripts per million (TPM).

Gene	Pollen_Tube	Pollinated_Silk	Silk	Seed	Leaf	Root
ZmFERL1	0.2	131.1	239.8	164.9	50.4	197.7
ZmFERL2	0.1	75.5	98.7	39.2	12.4	56.3
ZmFERL3	0.1	39.9	43.8	25.6	61.8	37.9
ZmFERL4	1265.1	184.0	0.3	0.2	0.1	0.1
ZmFERL5	0.1	0.0	0.0	0.0	0.0	0.1
ZmFERL6	0.2	0.2	0.1	0.2	0.2	0.1
ZmFERL7	991.7	117.2	0.2	0.3	0.1	0.1
ZmFERL8	0.1	5.6	8.3	9.2	1.8	9.3
ZmFERL9	1651.2	201.2	0.8	1.4	0.2	0.2
ZmFERL10	0.0	97.2	193.1	54.2	0.6	82.9
ZmFERL11	0.0	0.0	0.0	0.0	0.0	0.0
ZmFERL12	0.1	24.9	39.6	41.1	15.2	43.4
ZmFERL13	0.0	0.0	0.1	0.0	0.0	0.6
ZmFERL14	0.0	10.4	4.2	7.4	21.1	6.8
ZmFERL15	0.0	20.0	26.9	46.7	0.6	22.7
ZmFERL16	0.8	48.0	63.7	25.7	24.1	67.6
ZmFERL17	0.0	6.6	12.4	24.1	1.3	14.3

Low Middle High

3.3.2 ZmFERLs protein purification

To investigate whether the ligand-receptor pattern of RALF-CrRLK1L also exists in maize, ZmFERL proteins were needed. The RALF-CrRLK1L interaction region lies on the malectin-like domain that is part of CrRLK1L protein's extracellular region (Xiao *et al.*, 2019). To produce ZmFERL proteins, the coding sequences of ZmFERL1/4/7/9 protein extracellular domains (ecto-

ZmFERLs) were cloned into the pGEX-6P-1 vector with an N-terminal glutathione-S-transferase-tag (GST-tag). The GST tag was frequently used to increase the solubility of the fused proteins of interested (Schäfer *et al.*, 2015). GST-bound protein can be expressed as soluble protein in the *E.coli* cytoplasm in high amounts and with full enzymatic activity. The resulting plasmids were used for heterologous expression in the *E.coli* strains BL21 (DE3). In the solubility test of GST-tag fusion proteins, ZmFERL7 and ZmFERL9 proteins were found in the soluble fractions (Figure 3.6). However, ZmFERL1 and ZmFERL4 proteins were not soluble, but more abundant in the insoluble fraction.

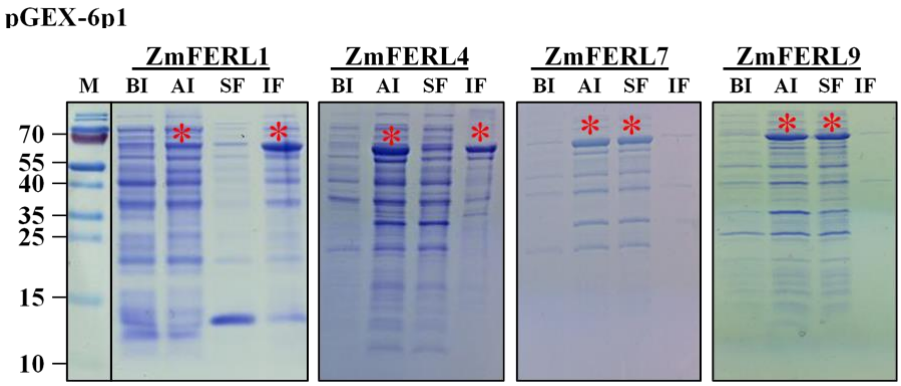

Figure 3.6 Production of GST-tagged ecto-ZmFERL proteins in BL21(DE3) (Coomassie stained gels). The production of recombinant ecto-ZmFERL proteins were induced in the *E.coli* strain BL21(DE3) at 37° for 3 hours. SDS-PAGE analysis revealed the proteins of appropriate size for GST-ecto-ZmFERLs (expected molecular weight [MW]: ZmFERL1: 73.03 kDa, ZmFERL4: 72.88 kDa, ZmFERL7: 71.29 kDa, ZmFERL9: 69.71 kDa, marked with red asterisks) in the bacterial lysate after induction (AI) that were not visible before induction (BI). ZmFERL7 and ZmFERL9 appeared in the soluble fractions (SF). ZmFERL1 and ZmFERL4 were in the insoluble fractions (IF).

In parallel, the ecto-ZmFERL1/4/7/9 coding sequence were cloned into the pMAL-p2p protein expression vector with an N-terminal maltose binding protein (MBP). MBP is a more effective solubilizing agent than GST. The fusion of MBP can promote the folding of the fused protein into its biologically active conformation properly (Kapust and Waugh, 1999). *E.coli* strain BL21 (DE3) was used for protein expression. The fusion with the N-terminal MBP-tag indeed promotes the solubility of ZmFERL1/4 proteins (Figure 3.7). In addition, the protein with MBP tags have fewer extra bands on Coomassie brilliant blue staining.

The GST-tagged ecto-ZmFERL7/9 and MBP-tagged ecto-ZmFERL1/4/7/9 proteins were purified, similar to the procedure of 6xHis-tagged protein purification under native condition. The purified proteins were used for the following RALF-CrRLK1L interaction test.

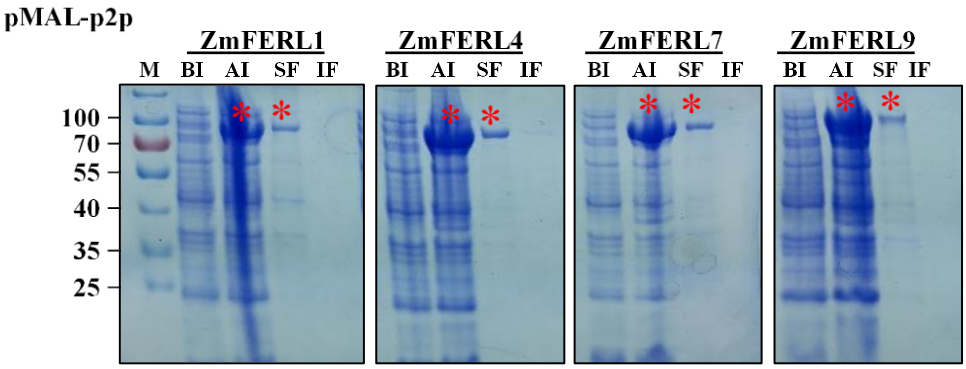

Figure 3.7 Production of MBP-tagged ecto-ZmFERL proteins in BL21(DE3) (Coomassie stained gels). The production of recombinant MBP-ecto-ZmFERL proteins were induced in the *E.coli* strain BL21(DE3) at 37° for 3 hours. SDS-PAGE analysis revealed the proteins of appropriate size for MBP-ecto-ZmRALFs (expected molecular weight [MW]: ZmFERL1: 92.46 kDa, ZmFERL4: 92.32 kDa, ZmFERL7: 97.42 kDa, ZmFERL9: 89.14 kDa, marked with red asterisks) in the bacterial lysate after induction (AI) and soluble fractions (SF), which were not visible before induction (BI) and absent from the insoluble fraction (IF).

3.3.3 RALF-CrRLK1L interaction in maize

Pull-down assays were carried out between the N-terminal MBP/GST-tagged ectodomain of ZmFERL1/4/7/9 proteins and the 6xHis-tagged ZmRALF1/2/3/5 mature peptides. 6xHis-binding Ni-NTA beads were used for the complex purification. The resulting solutions were checked with an 6xHis antibody firstly to verify the presence of ZmRALF peptides in the pull-down assays (Figure 3.8). The presence of ZmFERL proteins bound to ZmRALF peptides was visualized by detection with ecto-FERL proteins corresponding antibody (GST antibody for ecto-FERL7/9, MBP antibody for ecto-FERL1/4). ZmRALF2 and ZmRALF3 mature peptides were able to bind to ectodomains of all four ZmFERL proteins, whereas no binding could be seen for ZmRALF1 or ZmRALF5 peptides. ZmRALF1/5 and ZmRALF2/3 peptides differ in amino acid sequences and pollen tube subcellular localization (Chapter 2). The interaction results take it a step further, since the receptors of ZmRALF1/5 and ZmRALF2/3 peptides also seem to be different.

Although the interaction between mature ZmRALF2/3 peptides and ecto-ZmFERL1/4/7/9 proteins were detected, the preference of ZmRALF peptides binding to each receptor was unclear. Since *ZmFERL1* is expressed in the silk, the interaction of ZmRALF2/3 peptides with ZmFERL1 protein points out the communication of male and female tissue during reproduction. The interaction of mature ZmRALF2/3 peptides with ecto-ZmFERL4/7/9 proteins indicates a role in

the regulation for homeostasis of pollen tube since *ZmFERL4/7/9* genes are preferentially expressed in pollen.

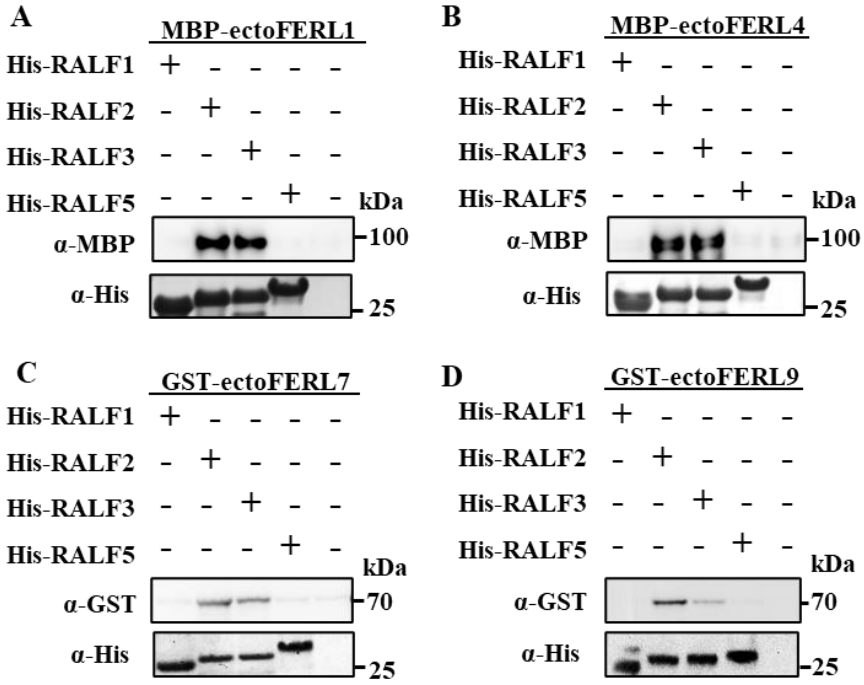

Figure 3.8 Clade II, but not Clade III/IV pollen tube expressed RALF peptides interact with ZmFERL receptor kinases. (A) Pull-down assays using MBP-tagged ectodomains of the FER homolog ZmFERL1 (B) the ANX1/2 homolog ZmFERL4 (C,D) as well as GST-tagged ectodomains of the BUPS1/2 homologs ZmFERL7/9 each in combination with 6xHis-tagged ZmRALF1/2/3/5 as indicated. Only ZmRALF2/3 interact significantly with ZmFERL proteins.

To further explore the binding preference for receptors, Microscale Thermophoresis (MST) assays were conducted with mature ZmRALF2/3 peptides and MBP-ecto-ZmFERL1/4/7/9 proteins. MST is a well-studied technology to quantify the affinities of protein-protein interactions. MST is based on the detection of a temperature gradient induced fluorescence change, which relies on the labeled protein's molecular properties such as size, charge, and hydration shell. At least one of these features' changes when the fluorescent labeled protein bind with non-fluorescent ligand (Mueller *et al.*, 2017). Thus, this technique is highly sensitive and allows for a precise quantification of molecular interaction.

The MST test measures the binding affinity between proteins, which is represented by the equilibrium dissociation constant (Kd). In principle, the smaller the Kd value, the stronger the

binding. Notably, according to the fitted curves (Figure 3.9), lowest binding affinity occurs in the case of the FER orthologue ZmFERL1, which is not expressed in pollen. ZmFERL1 Kd value was ~810 nM with ZmRALF2 (Figure 3.9.A) and ~1733 nM with ZmRALF3 (Figure 3.9.B). In contrast, ZmRALF2/3 preferred binding to ZmFERL9, as both Kds were ~105 nM. Interestingly, the ANXUR-like ZmRALF4 and BUPS-like ZmRALF7 show similar binding affinity to ZmRALF2/3 with moderate Kd values, between the high affinity of ZmFERL1 and the low affinity of ZmFERL9 (Figure 3.9).

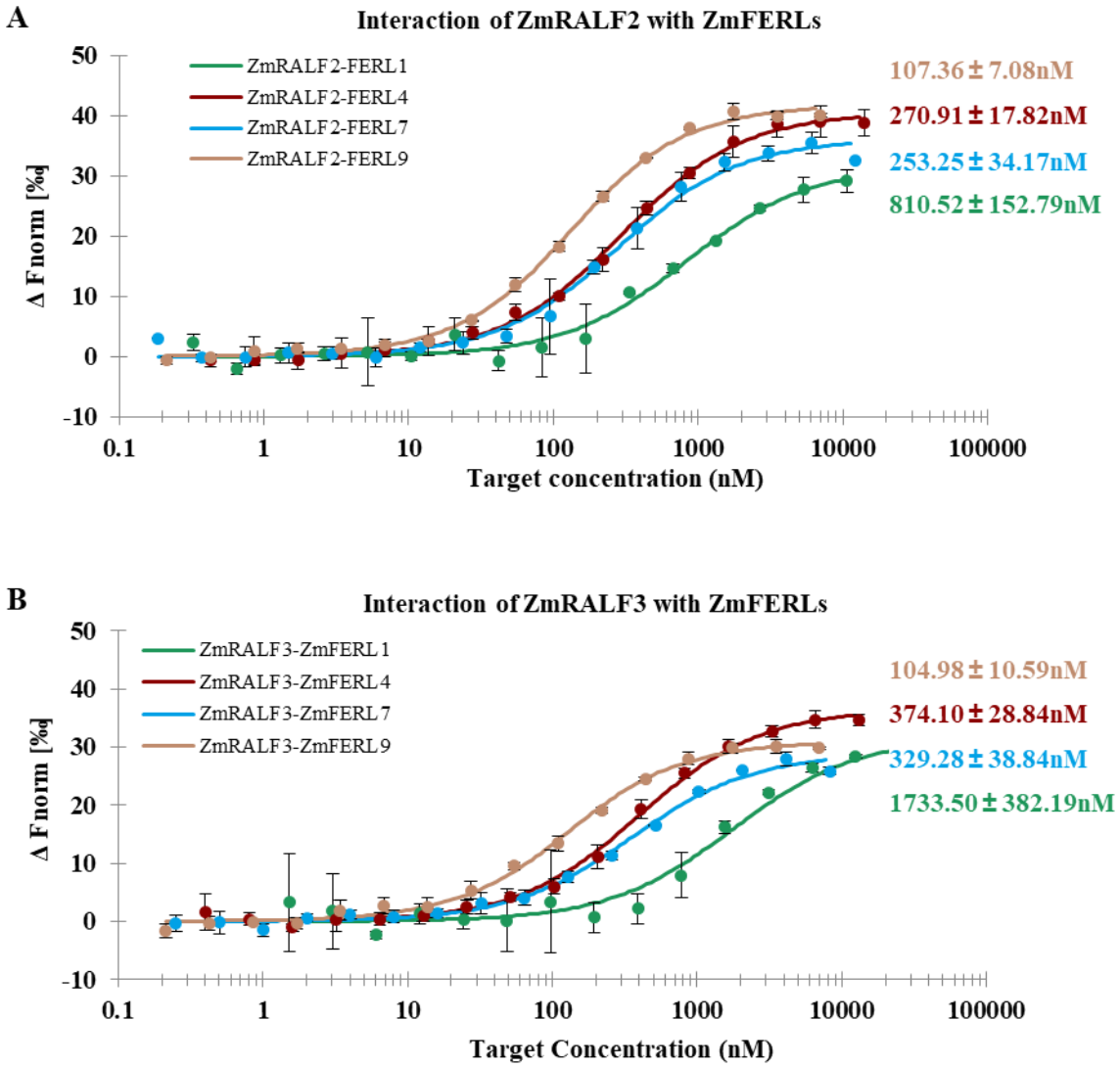

Figure 3.9 Microscale thermophoresis (MST) binding affinity assays using ZmRALF2/3 in combination with ecto-ZmFERL1/4/7/9. MST binding affinity (Kd) values are indicated. ZmFERL9 binds with ZmRALF2/3 most tightly, ZmFERL1 least. (A) MST assay curves of mature ZmRALF2 peptide with ectodomain of ZmFERL1/4/7/9 proteins. (B) MST assay curves of mature ZmRALF3 peptide with ectodomain of ZmFERL1/4/7/9 proteins.

3.3.4 RALF-CrRLK1L interaction is conserved in maize and *Arabidopsis*

Proteins interaction tests via the pull-down and the MST assay proved that RALF-CrRLK1L interactions are conserved in maize. The similar RALF-CrRLK1L interaction pattern in maize and *Arabidopsis* brought the question about the evolutional functional conservation. To explore this, *in vitro* pull-down assays of RALF-CrRLK1L were performed between two species. The biotin labeled AtRALF4/19 peptides were incubated with the ectodomain of MBP-tagged ZmFERL1/4 or GST-tagged ZmFERL7/9 proteins individually (Figure 3.10.A-B). As a result, AtRALF4 interacted with all four ecto-ZmFERL proteins, but AtRALF19 only interacted with ZmFERL1, and did not interact or only weakly with ZmFERL4/7/9 proteins. In the opposite experimental setup, 6xHis-tagged ZmRALF2/3, but not ZmRALF1/5, interacted with the ectodomains of Flag-tagged ANXs/BUPSs (Figure 3.10.C).

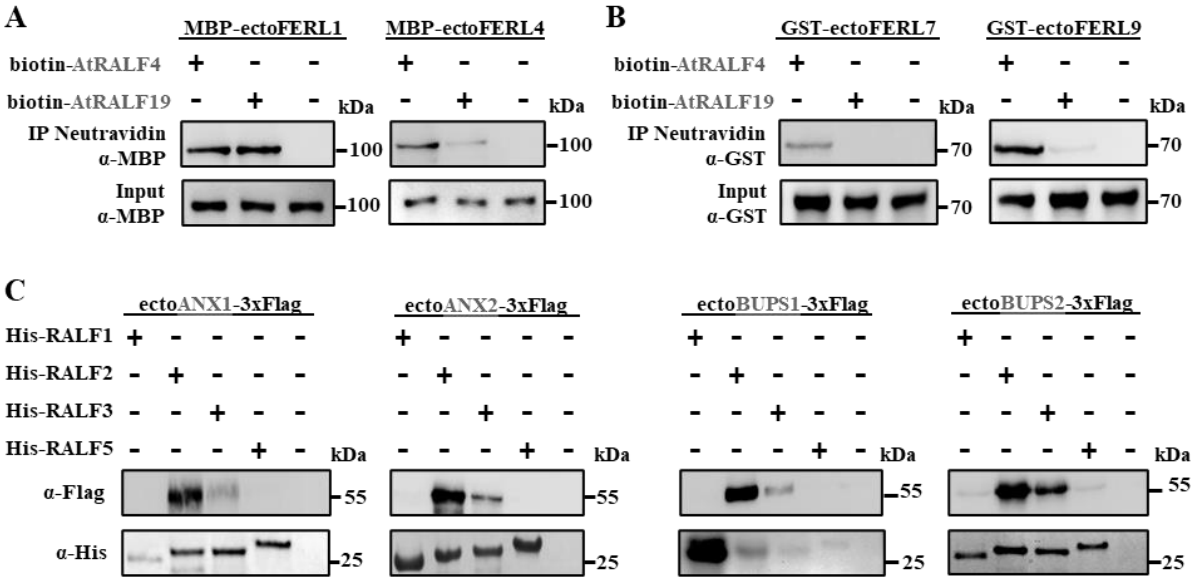

Figure 3.10 Maize ZmFERL receptor kinases are capable of interacting with Clade II *Arabidopsis* RALF peptides and *vice versa*. (A) Pull-down assay using MBP-tagged ectodomains of ZmFERL1 and ZmFERL4 in combination with biotin labelled pollen-expressed AtRALF4 and AtRALF19 peptides. (B) Pull-down assay using GST-tagged ectodomains of ZmFERL7 and ZmFERL9, and biotinylated AtRALF4 and AtRALF19 peptides. (C) Pull-down assay using Flag-tagged ectodomains of *Arabidopsis* ANX1, ANX2, BUPS1 and BUPS2 with 6xHis-tagged maize ZmRALF1/2/3/5 peptides, respectively.

3.3.5 ZmFERL mutant generation

To explore the function of *ZmFERL* genes in maize, CRISPR/Cas9 knockout mutations were generated. Candidate guide RNAs were designed with the online tool Breaking-Cas (Oliveros *et*

al., 2016) using the B73 reference genome, and their sequences were verified in the Hi-II genome to ensure their applicability in the transformable Hi-II lines (Supplemental Figure 2).Because *ZmFERL1/2/3* genes are redundantly expressed in the silk, the knockout of any single one of them may not be efficient to induce any defect. It would be more efficient to target three genes together in one construct. Thus, two common guide RNAs for *ZmFERL1* and *ZmFERL2* were selected (Figure 3.11) and cloned into pENTR-gRNA1. Another two guide RNAs for *ZmFERL3* were cloned into pENTR-gRNA2. For *ZmFERL4*, two guide RNAs close to the transmembrane domain were used and cloned into pENTR-gRNA1. As both *ZmFERL7* and *ZmFERL9* were orthologues of *BUPSs*, two common guide RNAs in the extracellular domain with a distance of 410 bp were selected. The plasmids including guide RNAs were integrated into the pGW-Cas9 vector. The constructs were transformed into *Agrobacterium* strain EHA101 and then transformed into immature maize Hi-II embryos. The T0 plants were self-pollinated or crossed with B73.

Through sequencing, a variety of mutations were identified (Figure 3.12). In the Cas9-*ZmFERL1/2/3* mutant Line7, 12 bp were deleted from *ZmFERL1* and 48 bp were deleted from *ZmFERL3*, no edit was found in *ZmFERL2*; in Line5, 1 bp insertion in *ZmFERL1* resulted in a shorter version of the protein. In the Cas9-*ZmFERL4* mutant lines, 294 bp including the transmembrane domain were deleted in Line1; single base pair insertions cause the early stop of protein in Line2 and Line3.

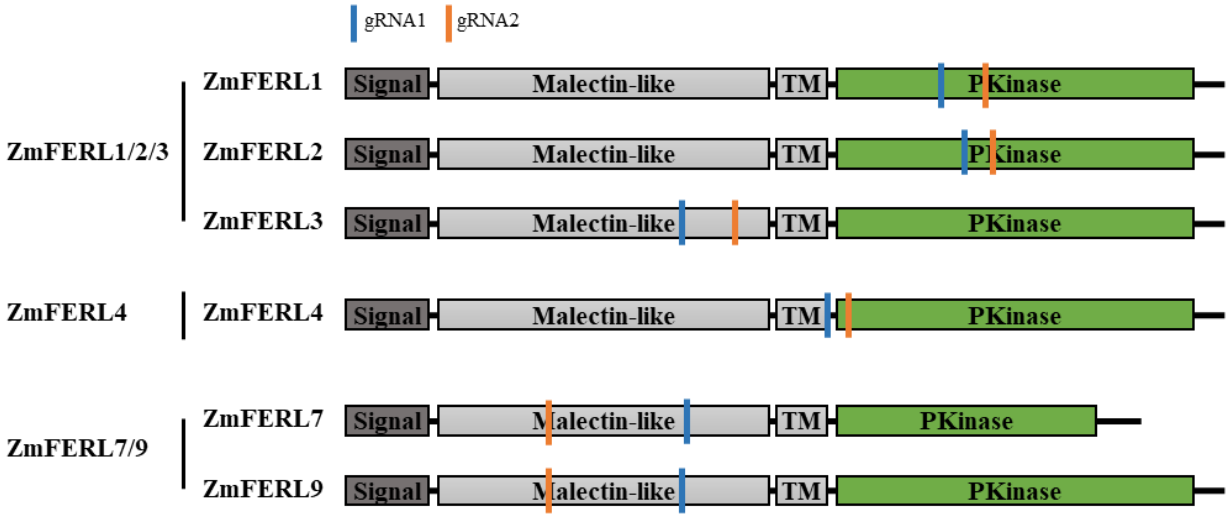

Figure 3.11 Structure of ZmFERL proteins and the gRNAs designed to generate double strand breaks in exons. ZmFERL proteins consist of signal sequence, malectin-like domain, transmembrane domain (TM) and protein kinase domain. Guide RNAs for *ZmFERL1/2/3* were combined, same with *ZmFERL7/9*. Location of the gRNAs were marked as indicated.

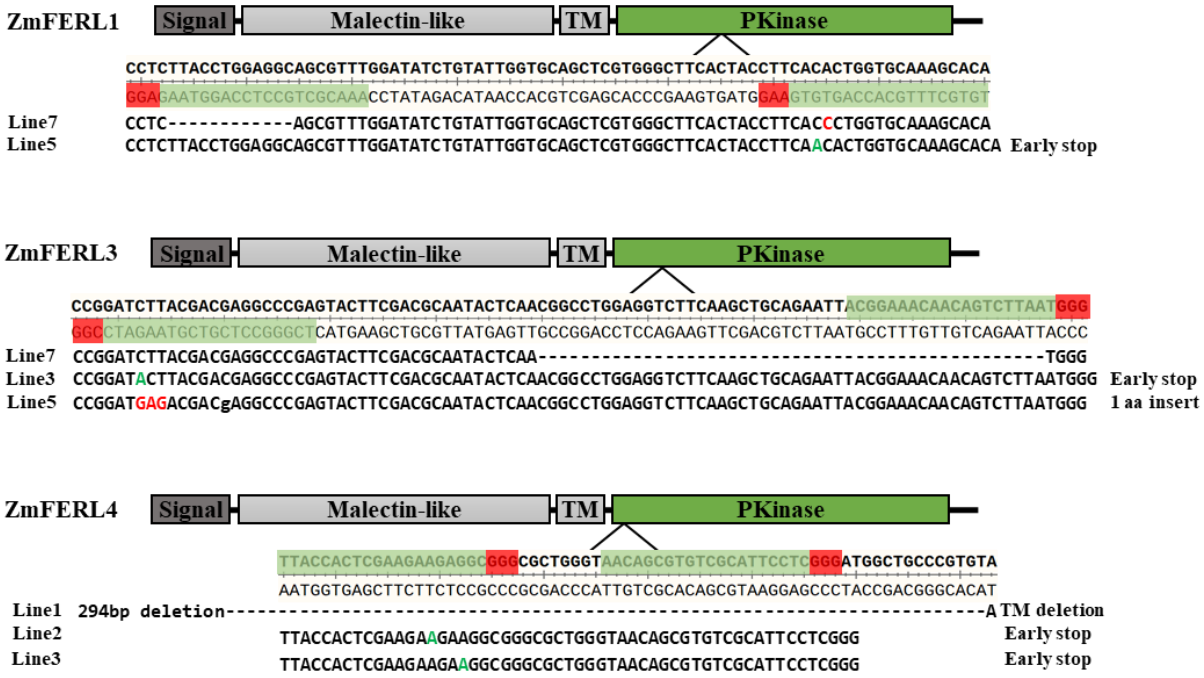

Figure 3.12 Sequences from selected T1 plants with site-specific mutations and the corresponding gene regions. The nucleotides changes are represented by dash for deletion, red for mutation, green for insertion. Wild type gRNA sequences and PAM domain are marked on the top.

3.3.6 LORELEI-like GPI-anchored proteins are involved in the ZmRALF signaling network

In maize, there are four LORELEI-like-GPI-anchored (ZmLLG) proteins that closely resemble orthologues of AtLLGs (Supplemental Table 1). *ZmLLG1* and *ZmLLG2* display a pollen-specific expression pattern (Figure 3.13.A), which is consistent with *LLG2* and *LLG3* in *Arabidopsis* (Ge *et al.*, 2019b). The composition of *LORELEI-like* genes was similar in maize and *Arabidopsis*, all contains three exons and two introns. *ZmLLG3* and *ZmLLG4* were slightly different in the length of the second intron, which extend up to 9521 bp. Except for this, the coding sequences of eight *LORELEI-like* genes were similar in length.

Sequence alignments revealed the conservation of eight LORELEI-like proteins (Figure 3.13.B), with all containing eight cysteine residues and the ND domain. Two glycine residues between the 7th and 8th cysteine residues were reported to be core responsible for RALF binding (Xiao *et al.*, 2019). All four maize LORELEI-like proteins contain these two glycine residues, which indicates that interaction of RALF-LLG also exists in maize.

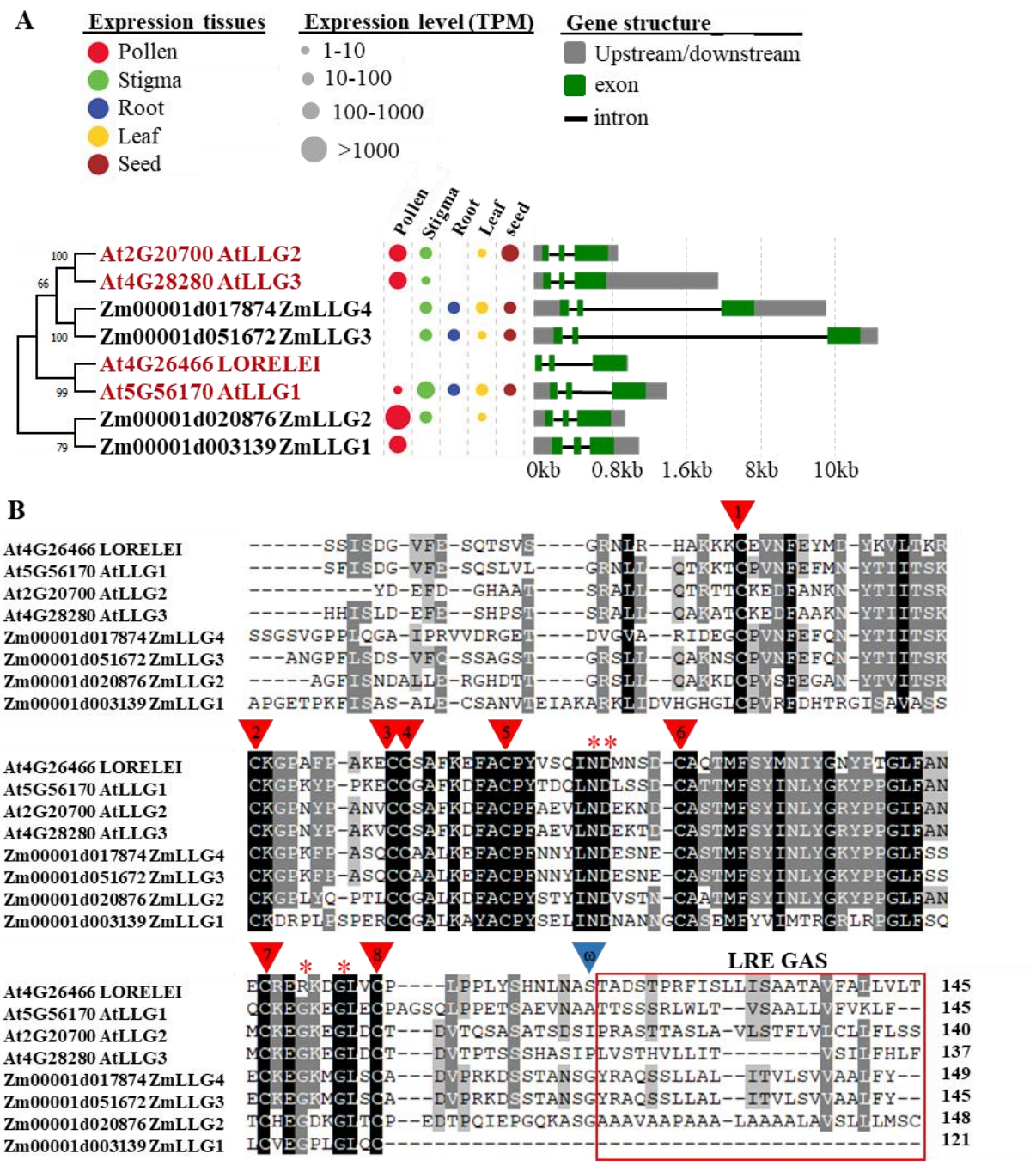

Figure 3.13 Phylogenetic tree of eight LLG proteins from maize and *Arabidopsis* with their expression patterns and conserved domain organization and amino acid residues. (A) Phylogenetic tree of LLG proteins from maize and *Arabidopsis*. Expression pattern and relative transcript levels are indicated by dots. Gene structures are indicated. (B) Alignment of maize and *Arabidopsis* LGGs (the numbers provide full-length sequences). Note that N-terminal signal peptide sequences were cut off for the alignment. Mature LGGs contain eight conserved cysteine residues (red arrowheads) and a conserved Asn-Asp (ND) domain and glycine residues (red asterisks). The region required for GPI-anchor addition (omega-side shown by a blue arrowhead, and GAS domain boxed in red) are indicated at the C-terminus. This region is lacking in ZmLLG1.

The interaction of ZmRALF peptides with ZmFERL proteins are in consist with the interaction of RALF-CrRLK1L in *Arabidopsis*. To investigate the conservation of LLG-RALF-FER complex, the interaction of ZmRALF peptides and ZmLLG proteins were tested. The MBP-tagged ZmLLG1 and ZmLLG2 were incubated with 6xHis-tagged mature ZmRALF1/2/3/5 peptides individually. The mixture was purified with Ni-NTA His beads and solutions were checked with His antibody and MBP antibody (Figure 3.14). It could be clearly seen that mature ZmRALF2/3 peptides interact with ZmLLG1 and ZmLLG2 proteins, in contrast to ZmRALF1/5 peptides.

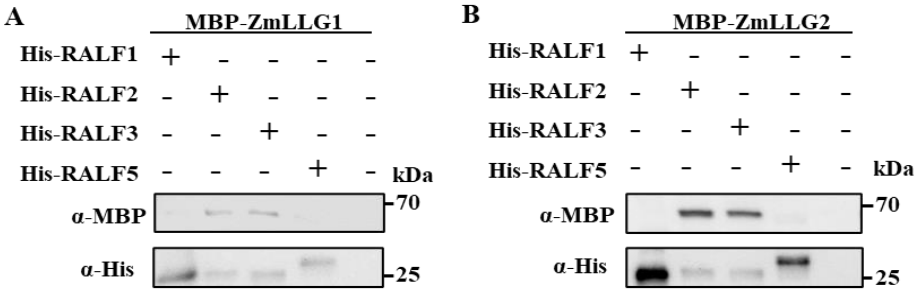

Figure 3.14 ZmRALF2/3 and ZmLLG1/2 interact with each other. (A) Pull-down assay between MBP-tagged ZmLLG1 protein and 6x His-tagged ZmRALF1/2/3/5 mature peptides. (B) Pull-down assay between MBP-tagged ZmLLG2 protein and 6x His-tagged mature ZmRALF1/2/3/5 mature peptides.

3.3.7 Leucine-rich repeat extensin (LRX) proteins in maize

Pollen extensin-like 2 (PEX2) is one of the earliest identified pollen-specific protein (Rubinstein *et al.*, 1995b). It consists of a signal peptide, a leucine-rich repeat domain and a proline-rich extensin domain. The homologues in *Arabidopsis* were named as leucin-rich repeat extensin proteins (LRX) (Baumberger *et al.*, 2003a). There are 11 *LRX* genes in *Arabidopsis thaliana*, while only *PEX1/2* genes in maize were reported. Taking the ZmPEX2 protein sequence as a query, 19 maize *LRX genes* were found (Supplemental Table 1), four of which possess the pollen specific high mRNA expression. Beside PEX1 and PEX2 (Rubinstein *et al.*, 1995a; Rubinstein *et al.*, 1995b), PEX3 and PEX4 were also found in pollen. All *LRX* genes distributed on maize chromosomes except chromosome 9 (Supplement Figure 3). Pollen specific LRX proteins PEX1/2/3/4 are distributed in four chromosomes.

LRX genes were grouped to be vegetative and reproductive (Ringli, 2005). To explore the possible role of maize *LRX* genes, phylogenetic analysis of LRXs in maize and *Arabidopsis* were carried

out (Figure 3.15). ZmPEX1-4 are close analogues of AtLRX8-11 which were reported to be receptors for AtRALF4/19 peptides and maintain the cell wall stability (Mecchia *et al.*, 2017; Moussu *et al.*, 2020). Alignment of ZmPEX1-4 and AtLRX8-11 revealed high similarity of the protein sequences (Figure 3.16). All of eight proteins have conserved NT domain, leucine-rich repeats, and cysteines rich domains (Herger *et al.*, 2019). Besides, another conserved domain was found in C-terminal. There were more Serine-Proline$_{2\text{-}n}$ repeats in maize PEXs compared with AtLRXs. The conserved structure suggests similar function.

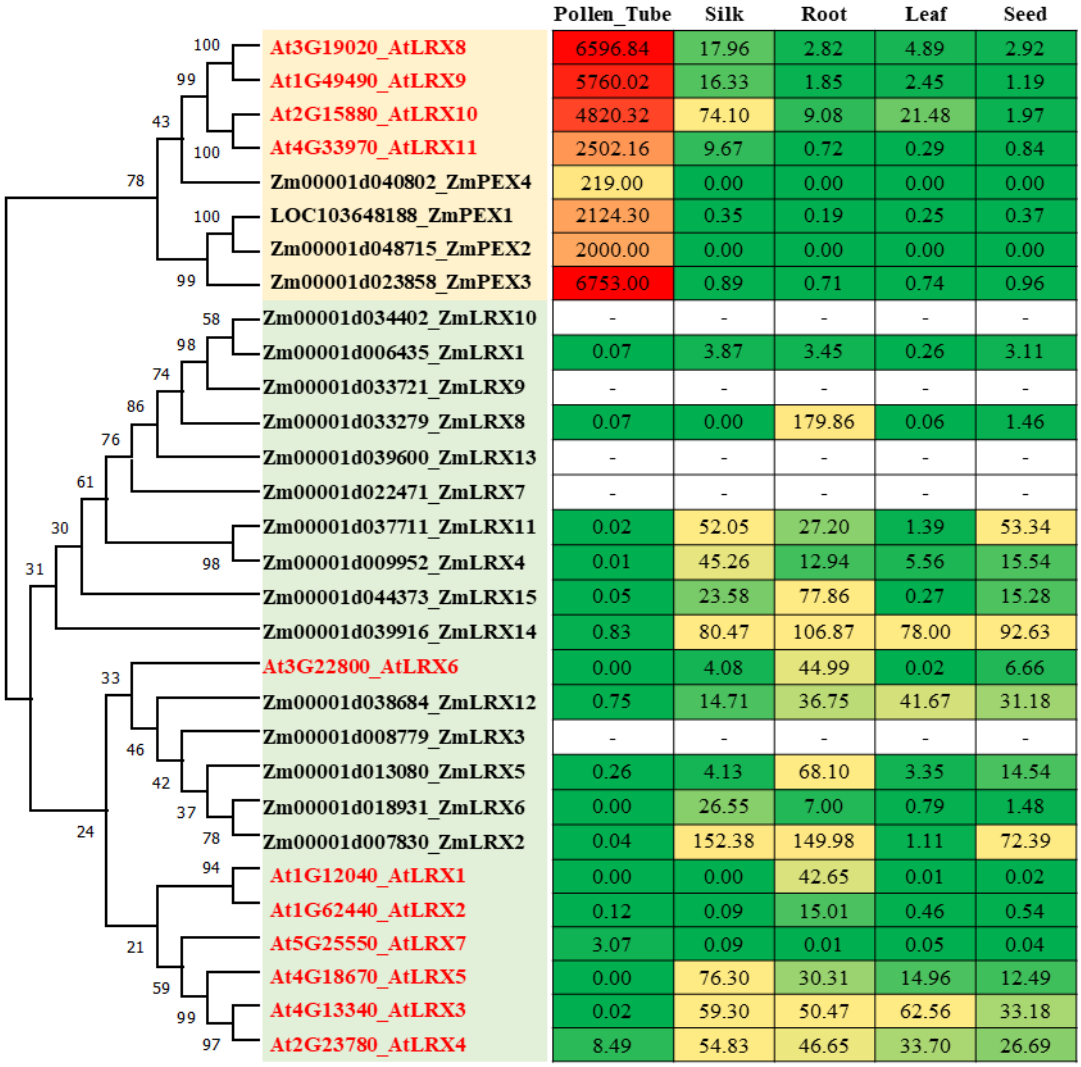

	Pollen_Tube	Silk	Root	Leaf	Seed
At3G19020_AtLRX8	6596.84	17.96	2.82	4.89	2.92
At1G49490_AtLRX9	5760.02	16.33	1.85	2.45	1.19
At2G15880_AtLRX10	4820.32	74.10	9.08	21.48	1.97
At4G33970_AtLRX11	2502.16	9.67	0.72	0.29	0.84
Zm00001d040802_ZmPEX4	219.00	0.00	0.00	0.00	0.00
LOC103648188_ZmPEX1	2124.30	0.35	0.19	0.25	0.37
Zm00001d048715_ZmPEX2	2000.00	0.00	0.00	0.00	0.00
Zm00001d023858_ZmPEX3	6753.00	0.89	0.71	0.74	0.96
Zm00001d034402_ZmLRX10	-	-	-	-	-
Zm00001d006435_ZmLRX1	0.07	3.87	3.45	0.26	3.11
Zm00001d033721_ZmLRX9	-	-	-	-	-
Zm00001d033279_ZmLRX8	0.07	0.00	179.86	0.06	1.46
Zm00001d039600_ZmLRX13	-	-	-	-	-
Zm00001d022471_ZmLRX7	-	-	-	-	-
Zm00001d037711_ZmLRX11	0.02	52.05	27.20	1.39	53.34
Zm00001d009952_ZmLRX4	0.01	45.26	12.94	5.56	15.54
Zm00001d044373_ZmLRX15	0.05	23.58	77.86	0.27	15.28
Zm00001d039916_ZmLRX14	0.83	80.47	106.87	78.00	92.63
At3G22800_AtLRX6	0.00	4.08	44.99	0.02	6.66
Zm00001d038684_ZmLRX12	0.75	14.71	36.75	41.67	31.18
Zm00001d008779_ZmLRX3	-	-	-	-	-
Zm00001d013080_ZmLRX5	0.26	4.13	68.10	3.35	14.54
Zm00001d018931_ZmLRX6	0.00	26.55	7.00	0.79	1.48
Zm00001d007830_ZmLRX2	0.04	152.38	149.98	1.11	72.39
At1G12040_AtLRX1	0.00	0.00	42.65	0.01	0.02
At1G62440_AtLRX2	0.12	0.09	15.01	0.46	0.54
At5G25550_AtLRX7	3.07	0.09	0.01	0.05	0.04
At4G18670_AtLRX5	0.00	76.30	30.31	14.96	12.49
At4G13340_AtLRX3	0.02	59.30	50.47	62.56	33.18
At2G23780_AtLRX4	8.49	54.83	46.65	33.70	26.69

Figure 3.15 Phylogenetic analysis and expression data of *PEX/LRX* from maize and *Arabidopsis*. Phylogenetic analysis of chimeric LRR-extensin-like proteins from maize (19 proteins) and *Arabidopsis* (11 proteins). Whole protein sequences were used to generate the phylogram. Homologous *Arabidopsis* LRX proteins are indicated in red. Pollen-specific genes are colored in light yellow; the vegetatively expressed genes are colored in light green. The table shows expression levels of corresponding maize genes in indicated tissues as mRNA expression values.

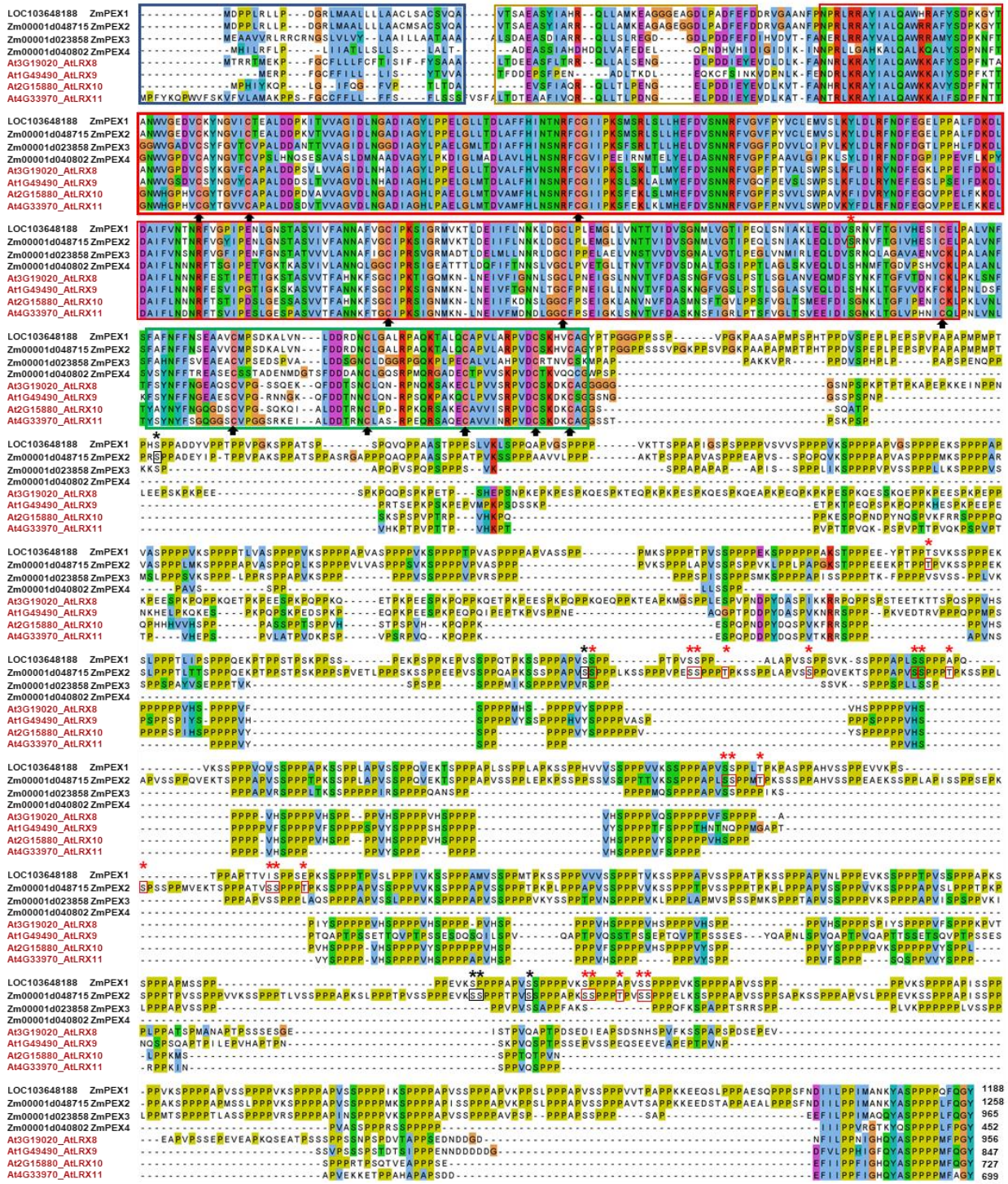

Figure 3.16 Sequence alignment of pollen expressed LRX proteins in maize and *Arabidopsis*. N-terminal signal peptide, N-D domain, LRR domain and cystine-rich motif are boxed in blue, yellow, red and green, respectively. Arrows indicate conserved cysteine residues. The extensin-like domain is especially rich in proline (in yellow-green) and serine/threonine (in green). Phosphorylation sites are highlighted in rectangles and with asterisks (differently phosphorylated sites are marked in red).

3.3.8 RALF-LRX interaction in maize and *Arabidopsis*

To investigate the interaction of RALF peptides and PEX2, pull-down assays were carried out. The N-terminal MBP-tagged ectodomain of PEX2 and PEX4 were expressed and purified from *E.coli*. They were incubated with N-terminal 6xHis-tagged ZmRALF1/2/3/5 mature peptides. The result showed that ZmRALF2/3 mature peptides can interact with PEX2/4, but ZmRALF1/5 cannot (Figure 3.17.A-B).

ZmPEX2 was found to be localized in the callosic sheath of pollen tubes, which directly attached to pollen tube membranes (Rubinstein *et al.*, 1995b). As mentioned, the membrane-localized ZmFERL4/7/9 proteins could interact with ZmRALF2/3 peptides. However, a complex including RALF-LLGs-CrRLK1Ls-PEXs were not found (Moussu *et al.*, 2020), indicating that RALF

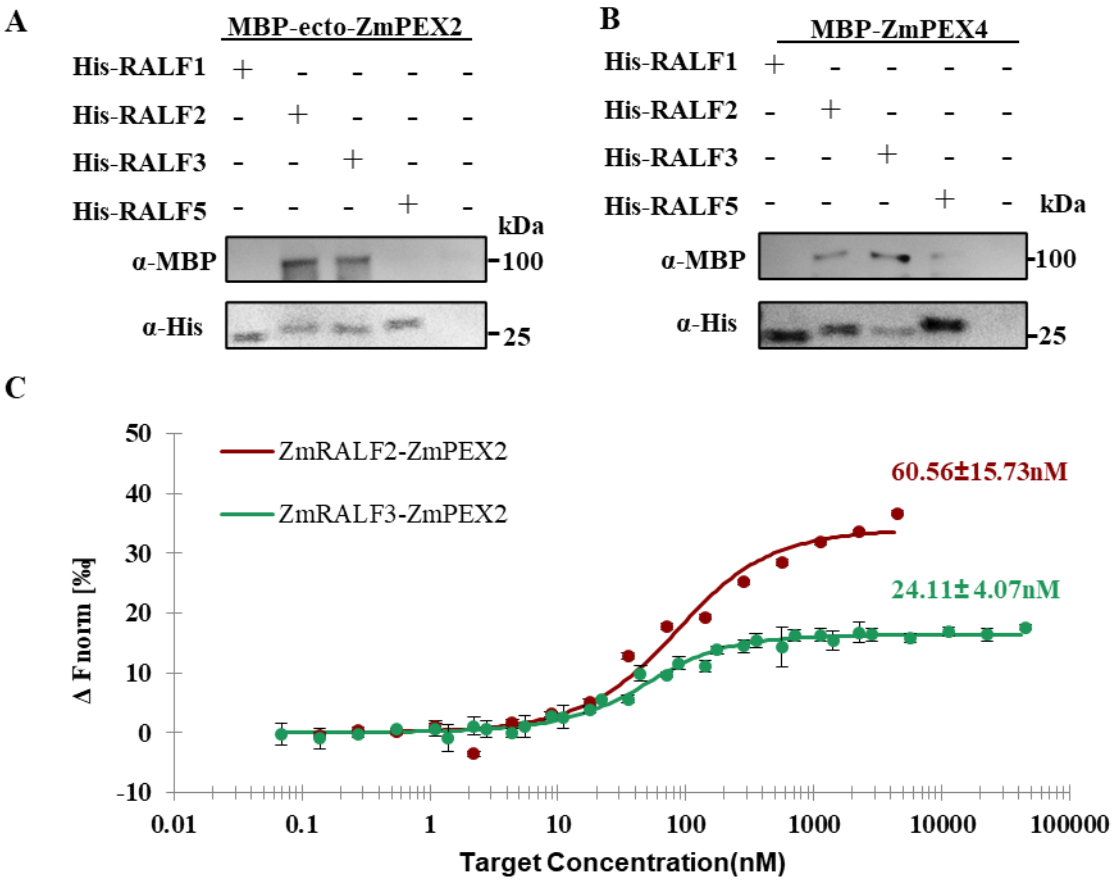

Figure 3.17 ZmRALF2/3 interact with ZmPEX2/4. (A,B) Pull-down assay between MBP-tagged ectodomain of ZmPEX2, MBP-tagged ZmPEX4 proteins and 6xHis-tagged ZmRALF1/2/3/5 mature peptides (C) Binding affinity between ectodomain of ZmPEX2 and ZmRALF2/3 by MST analysis; Kd values are indicated. ΔFNorm, change in fluorescence.

peptide binding to PEX or LLGs-CrRLK1Ls was independent. It is thus of interest to check the binding preference between ZmRALF2/3-ZmFERL4/7/9 and ZmRALF2/3-ZmPEX2. An MST assay was carried out to explore the corresponding binding affinity. From the MST curves (Figure 3.17.C), it is apparent that ZmRALF3 peptide shows the highest binding affinity with ZmPEX2 protein (24 nM), a similar binding affinity was also found for ZmRALF2-PEX2 (60 nM).

To further investigate the conservation of RALF-LRX interaction, the interactions of ZmRALF peptides with AtLRX proteins were tested. *Arabidopsis* LRX proteins AtLRX9/10/11 were purified from *E. coli* individually. The pull-down tests of ZmRALFs-AtLRXs showed similar results as ZmRALFs- ZmPEXs. ZmRALF2/3 mature peptides can interact with AtLRX9/10/11 proteins, but ZmRALF1/5 cannot (Figure 3.18)

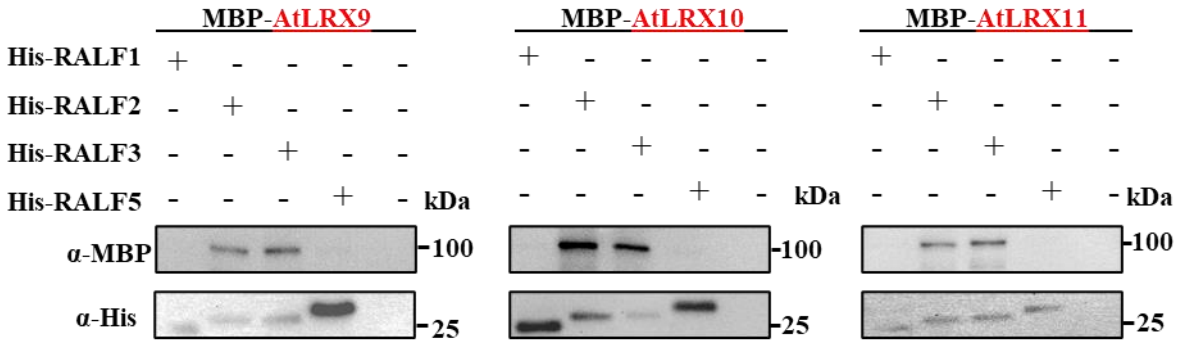

Figure 3.18 ZmRALF2/3 interact with AtLRX9/10/11. Pull-down assay between MBP-tagged AtLRX9/10/11 proteins and 6xHis-tagged ZmRALF1/2/3/5 mature peptides.

3.3.9 *ZmRALFs* downregulation increases the phosphorylation frequency of ZmPEX2

RNAi-*RALFs* mutant lines had a pre-burst pollen tube phenotype, which hints to an unstable pollen tube. To investigate the effect of *ZmRALFs* downregulation on the molecular level, phosphoproteomic analysis was carried out. Pollen from RNAi-*RALFs* mutant lines and the corresponding wild type were collected and germinated in liquid pollen germination medium. 20 minutes later, the intact pollen tubes were collected and used for phosphorylation status checking.

In RNAi-*RALFs* mutant lines, many proteins differed in their phosphorylation status. Among the differently phosphorylated proteins, PEX2 attracted our attention for its dramatic phosphorylation change (Figure 3.19). In the pollen tube of RNAi-*RALFs* mutant lines, PEX2 phosphorylation frequency was significantly increased at 22 out of 27 phosphorylation sites in the proline-rich extensin motif (Figure 3.19.B-C).

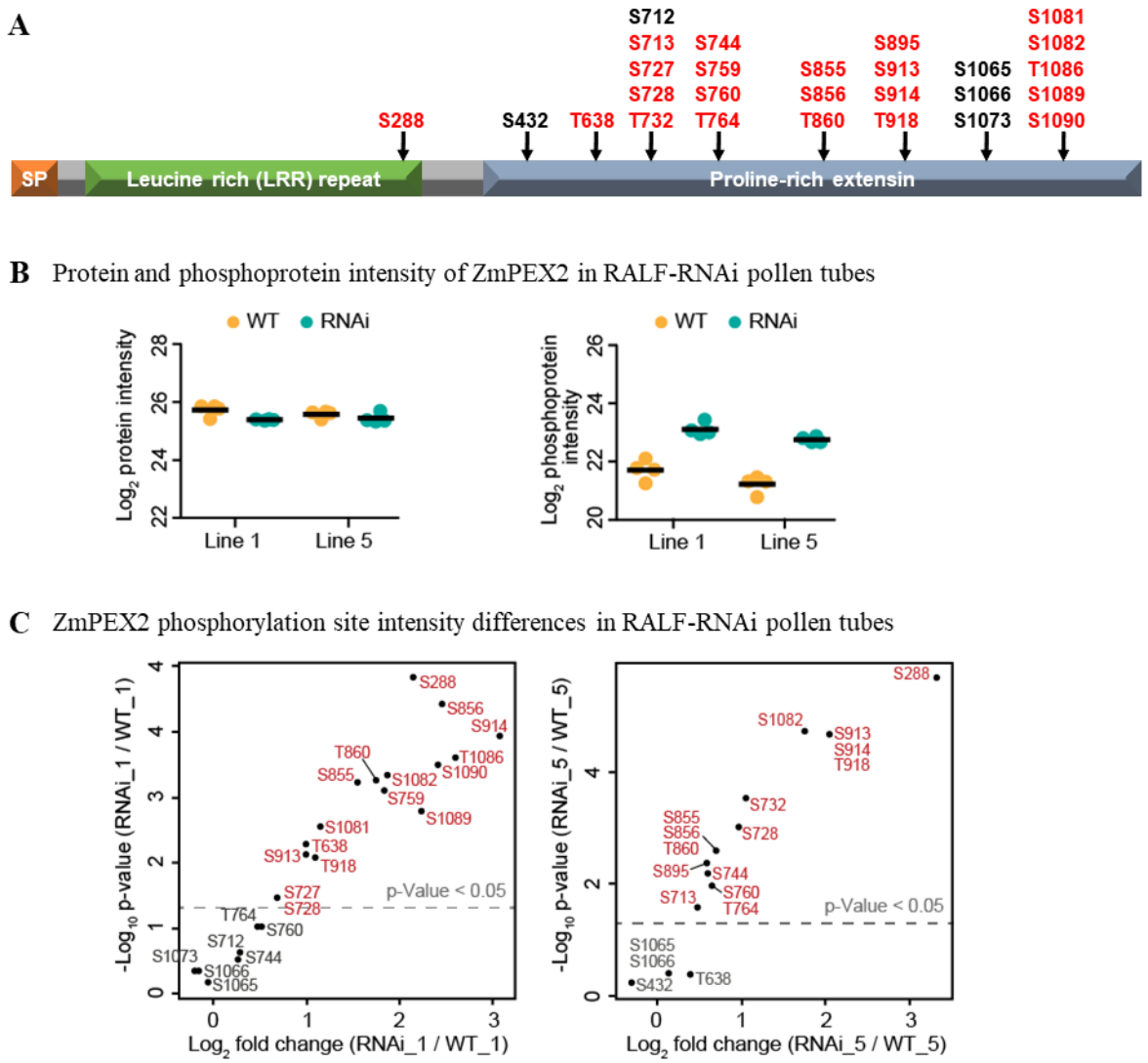

Figure 3.19 Cell wall-localized maize PEX2 protein is stronger phosphorylated in RNAi-*RALFs* lines. (A) Schematic diagram of the chimeric ZmPEX2 protein structure consisting of an N-terminal signal sequence (SP) for secretion, a globular leucine-rich repeat (LRR) and an extensin-like domain. Serine (S) and threonine (T) phosphorylation sites are indicated. (B) ZmPEX2 protein and phosphoprotein intensity in pollen tubes of Wild type (WT) and two RNAi-RALF mutant lines. (C) Scatterplot of ZmPEX2 phosphorylation site intensity fold changes and significance values between RNAi-RALF mutant Line 1 and 5 and the respective WT lines. Phosphorylation sites with significantly different intensities in RNAi-*RALFs* mutant lines compared to the WT are indicated in red (Student's T-test; n=4; p-Value < 0.05).

3.4 Discussion

It is unclear when and how RALF-LLG-CrRLK1L and RALF-PEX signaling pathways have been established during land plant evolution and when family members were further specified to take over roles in reproduction and pollen tube growth. RALFs and CrRLK1Ls were first detected in bryophytes. There exists, for example, a single *CrRLK1L* and three *RALF* genes in *Marchantia polymorpha* (Galindo-Trigo *et al.*, 2016). An amplification of *RALF* genes was reported in angiosperms. While the basal angiosperm *Amborella trichopoda* contains nine genes, >30 genes were reported in various eudicot and monocot families (Campbell and Turner, 2017). So far, research of RALF peptides functions focused on eudicots and were especially conducted in *Arabidopsis*. In monocots, one study reported that in the grass sugarcane SacRALF1 is involved in the regulation of tissue expansion (Mingossi *et al.*, 2010). By comparing RALF peptides from the eudicot model *Arabidopsis* and the grass model maize, we distinguished four clades. Our nomenclature differs from a previous phylogenetic study comparing 795 identified RALF peptides (Campbell and Turner, 2017). Four major clades we reported with Clades I-III containing an RRXL protease cleavage site and the YISY motif for receptor interaction. Clade IV contains all other RALF peptides. In the meantime, we have learned that the YISYxxLRRN domain mediates interaction with the CrRLK1L FER receptor forming a heterotrimeric complex (Xiao *et al.*, 2019). Moreover, four tyrosine residues are involved in LRX-binding including the two Ys of the YISY motif and two additional YYs (Moussu *et al.*, 2020). According to our nomenclature and biochemical studies, Clade I and Clade II RALF peptides are likely capable to interact both with all available CrRLK1L and LRX/PEX-proteins and thus could also be described as Clade IA and Clade IB RALFs. Notably, Clade II RALF peptides that are more conserved after the cleavage site contain ‘reproductive’ RALFs including RALF peptides of basal land plants like mosses, and thus appear to represent the most original clade. Clade I, which is highly variable after the cleavage site and which contains only ‘vegetative’ RALFs in the two species including the well described AtRALF1, may have acquired specific sub-functions during land plant evolution with individual members being able to interact with so far unknown proteins. Clade III RALF peptides that do not occur in maize still contain the YISY-motif, and thus may still be able to interact with CrRLK1Ls, but not with LRX proteins. This hypothesis has to be tested in future studies. Clade IV RALFs lack both motifs. This finding explains the observation that ZmRALF1 and ZmRALF5 did not interact with any of the tested proteins and suggests that they have acquired novel, unknown functions during evolution.

Quantitative biochemical assays revealed that Clade II AtRALF4 from *Arabidopsis* binds LLGs and LRX cell-wall modules with drastically different binding affinities, and with distinct and mutually exclusive binding modes (Moussu *et al.*, 2020). Binding of AtRALF4 with AtLRX8 could be very strong with a Kd of 3.5 nM. For the interaction with ANXs/BUPSs, the strongest binding presented in the AtRALF4-ANX1 complex was reported as 310 nM (Ge *et al.*, 2017). This drastic difference in binding affinity could be partially explained by optimized AtRALF4 folding in the recent report, but points towards the same finding in the present study that ZmRALF2 and ZmRALF3 bind on average about five times stronger to ZmPEXs compared to pollen-specific ZmFERLs, and even much weaker to vegetative ZmFERL1. In conclusion, taking also into consideration that binding of LRX/PEX cell wall proteins and LGG-CrRLK1Ls receptor complexes to the RALF motif YISY motif is mutually exclusive, we propose the following model shown in Figure 3.20: at low RALF concentrations in the cell wall, RALFs bind almost

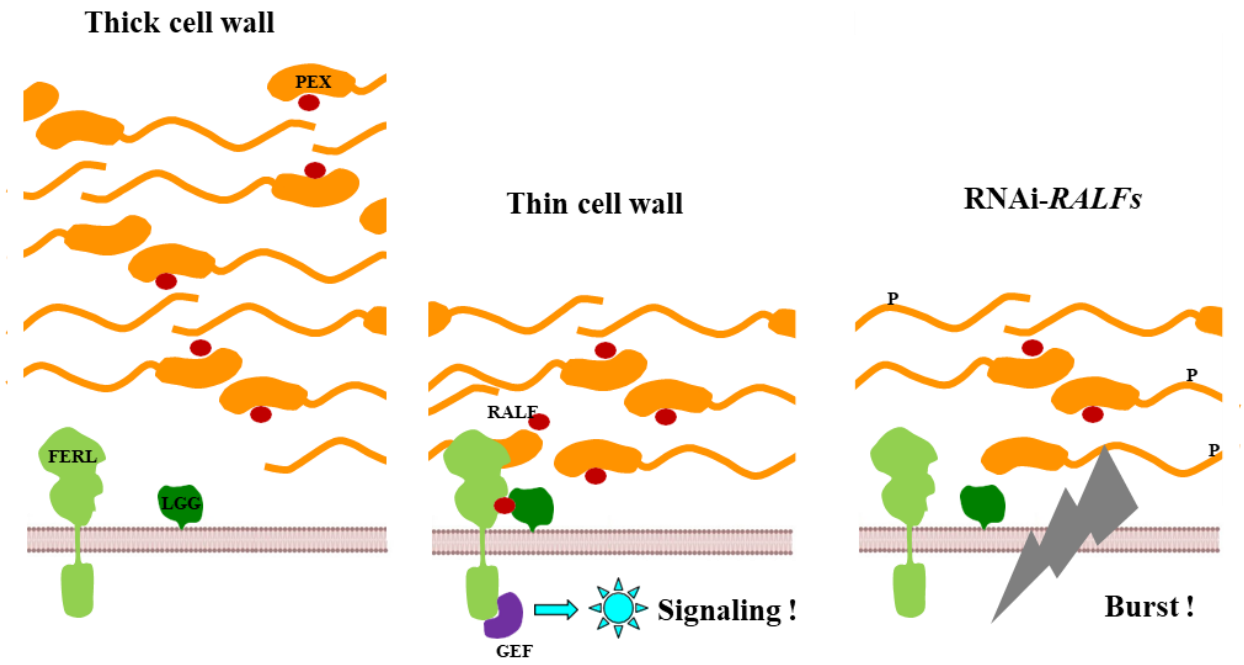

Figure 3.20 Dosage dependent RALF signaling model showing the role of Clade II RALF peptides as sensors of cell wall integrity and thickness during pollen tube growth. Due to higher affinity of RALFs to cell wall PEX proteins, RALFs are predominately located at the cell wall, and the FERL-LGG signaling pathway is inactive in thick walls. In thin walls, all PEXs are saturated and non-bound RALF peptides activates FERL-LGG signaling leading, among others, to deceleration of pollen tube growth providing extra time for cell wall synthesis and modification. The FERL-LGG signaling pathway is inactive in lines with reduced RALF levels. Phosphorylation of PEXs partially compensates for cell wall instability in thin wall areas, but ultimately pollen tubes burst.

exclusively to LRX/PEX proteins and the CrRLK1L signaling pathway is inactive. Similarly, if the cell wall is thick and contains many LRX/PEX proteins, the signaling pathway is silent. However, in the presence of high RALF levels or in thin cell walls, LRX/PEX proteins are saturated and RALF peptides activate CrRLK1L signaling leading for example, to reduction of pollen tube growth speed or at high concentration to complete growth arrest. If RALF levels are artificially reduced, CrRLK1L signaling remains silent even in thin cell walls. Then fine tune control of cell expansion and growth speed, which depends on cell wall sensing, leads to growth defects and in the case of pollen tubes to burst. This simple model did not consider further aspects, as the described RALF interactions are pH-dependent (Moussu *et al.*, 2020) and likely also depend on the redox status of interaction partners as it was shown, for example, that AtRALF4 induced the generation of reactive oxygen species (ROS), which stimulated pollen tube growth and reduced pollen burst rate (Feng *et al.*, 2019).

Compared with above described protein interactions studies, little is known about RALF-induced downstream signaling processes. A phosphoproteome approach has shown that AtRALF-FER interaction caused phosphorylation and thus inhibition of plasma membrane H^+-ATPase2 explaining extracellular alkalinization (Haruta *et al.*, 2014). AtRALF1 also enhanced the interaction of FER with the receptor-like cytoplasmic kinase RIPK, which mutually phosphorylate each other to regulate cell growth in roots (Du *et al.*, 2016). AtRALF1 treatment promotes direct phosphorylation of ERBB3 binding protein 1 (EBP1) by FER leading to its accumulation in the nucleus and inhibition of RALF peptide responses (Li *et al.*, 2018). It was further shown that AtRALF1 promotes FER-mediated phosphorylation of the elongation factor eIF4E1. Phosphorylated eIF4E1 regulates the synthesis of root hair proteins including ROOT HAIR DEFECTIVE 6-LIKE 4 (RSL4), which is required for root hair growth (Zhu *et al.*, 2020). Phosphoproteome measurements usually depend on RALF application and have to our knowledge neither been performed with pollen tubes nor with knock-outs or RNAi lines. The finding that ZmPEXs are hyperphosphorylated in RALF-*RNAi* lines was unexpected. It is unclear whether RALFs interact with LRX/PEX proteins already in the secretory pathway or outside the cell and we do not know where phosphorylation takes place. Notably, the first phosphorylation site that was most often hyperphosphorylated affects a conserved serine in the LRR-domain. This and perhaps other sites might be protected by RALFs bound already in the secretory pathway and thus prevent phosphorylation. Co-expression studies of labelled RALFs and LRX/PEX proteins would

be helpful to investigate whether interaction occurs already during the secretory pathway. It is also possible that an increase of phosphorylated ZmPEXs might counteract reduced RALF signaling and is used to add cross-bridges to pectic acids to partly stabilize the cell wall. The generation of phospho-mimic mutants would help to elucidate the role of LRX/PEX phosphorylation in future studies.

In conclusion, we have reported that the autocrine pollen tube signaling pathway regulating cell wall integrity during pollen tube growth involving Clade II RALF-LLG-CrRLK1Ls and RALF-LRX/PEX interactions are conserved between *Arabidopsis* and maize, and thus likely also in other angiosperms. We further suggest a simple model taking findings of this report into consideration, but also published interaction studies, structural data and RALF application studies. The idea that RALFs serve as cell wall sensors is not new and has been proposed before (Ge *et al.*, 2019a; Gonneau *et al.*, 2018). However, the dosage dependent RALF signaling model presented here taking also different binding affinities into consideration explains part of the complex signaling network and various phenotypes of RALF knockout/knock-down studies described. It will now be important to elucidate the function(s) of RALFs from other clades including pollen tube specific genes encoding, for example, ZmRALF1 and ZmRALF5 that are located during *in vitro* growth to cytoplasmic vesicles or granules but not in the apoplast.

CHAPTER 4. POLLEN OLE E 1 AND DEFENSIN-LIKE

4.1 Introduction

Beside RALF peptides, other small secreted proteins may play important roles in pollen and fertilization. In this chapter, two classes of small secreted proteins, Pollen Ole e1 (ZmPOE) and Defensin-like (ZmDEFL) proteins were investigated. As the work on these two protein groups was limited, they are introduced together.

4.1.1 Zmc13 or maize Pollen Ole e 1

Olive tree (*Olea europaea*, *Ole e*) pollen causes pollen allergy in Mediterranean countries (Lombardero *et al.*, 1994). Among the allergens of olive pollen, the protein Pollen Ole e 1 was described as the most important one. The molecular weight of Pollen Ole e 1 differs glycosylation-status dependent between 17 kDa or 19 kDa.

Pollen Ole e 1-like peptides (POEs) are most probably secreted and consist of around 145 residues (Silverstein *et al.*, 2007). They contain a predicted signal sequence and a Pollen Ole e 1 family domain. POE peptides belong to the group of cystine-rich peptides: six cysteine residues form disulfide bonds and are conserved in the POE family. Within this family, there are two cysteine models: CX{2,3}CX{19,23}CX{31,42}CX{8, 16} CX{32,54}C or CX{2,3}CX{19,22}CX{9, 13}CX{31,32}CX{11,14}C (X denotes any amino acid; numbers in curly braces indicate a range of variable residues). The Pollen Ole e 1 family domain are characterized by the amino acid sequence [EQT]-G-X-V-Y-C-D-[TNP]-C-R (Figure 4.1) (Sigrist *et al.*, 2012).

Figure 4.1 Amino acid sequence of the Pollen Ole e 1 family domain (PS00925**).** The size of the amino acids at the individual sequence positions depends on the degree of conservation amino acids are stacked in order from most to least frequent.

Research on POE peptides showed that it consists of at least 571 sequences encoding Pollen Ole e 1 or Pollen Ole e 1 like proteins (José Carlos Jiménez-López *et al.*, 2011) and distribute across varies of plants. However, the function of POE peptides in plants is poorly understand. Among the known POE peptides, LATE ANTHER TOMATO 52 (LAT52) is comparably well studied. *LAT52* was found as a tomato pollen-specific gene, which plays a role in pollen hydration and germination (Twell *et al.*, 1989). *LAT52* downregulation resulted in a decrease of male gametophyte transmission efficiency and abnormal pollen germination (Muschietti *et al.*, 1994). It was assumed that LAT52 act as an autocrine signaling molecule cooperating with tomato pollen-specific receptor kinases LePRK2 to maintain the pollen integrity (Tang *et al.*, 2002). However, the interaction between LePRK2 and LAT52 only detected before pollen germination. At this development stage, *LAT52* showed strong expression (de Dios Alche *et al.*, 1999; Song *et al.*, 2015). After germination, the interaction cannot be detected anymore. The disassociation could be the result from the competition of LeSTIG1, another small cysteine-rich protein from pistil, with LAT52 for binding to LePRK2 (Tang *et al.*, 2004). Therefore, LAT52 was speculated to function before pollen tube emerge. In a similar way, wheat *POE* gene *F8-1* is only expressed in anthers during the binucleate and trinucleate stages and the expression gradually decreased later (Song *et al.*, 2015). Downregulation of *F8-1* resulted in the pollen abortion.

Intriguingly, expression of *POE* genes was not limited to pollen. In *Arabidopsis thaliana*, 28 *POE* genes are expressed in stem, leave, root, and seedling (Hu *et al.*, 2014). Expression of the *Glycine max POE* gene *GmPOI* was induced by various stresses, which extends the possible function beside pollen (Song *et al.*, 2013).

Zmc13 (*ZmPOE1.2*)was discovered as a pollen-specific gene and the gene product localized in the cytoplasm before germination (Hanson *et al.*, 1989). It is also the first pollen-specific expressed sequence to be characterized (Hanson *et al.*, 1989). Even though the amino acids sequence of Zmc13 is very similar to olive Pollen Ole e 1, it is not likely that ZmC13 function as an allergen (Oldenburg *et al.*, 2011). Zmc13 belongs to the POE protein family in maize, which contains 42 protein entries (José Carlos Jiménez-López *et al.*, 2011). In an attempt to identify maize small secreted peptides, 16 reproductive *POE* genes were discovered (Li *et al.*, 2014). In this chapter, a comprehensive analysis of *POE* genes in maize and the function of Zmc13 will be investigated.

4.1.2 Defensin-like proteins

Defensin proteins are antimicrobial peptides that are widely distributed across plants and mammalian (Parisi *et al.*, 2019). According to the orientation of the most conserved pair of disulfides, they were classified into two groups: *trans*-defensins in mammalian and *cis*-defensins in plants (Shafee *et al.*, 2016).

Plant defensins are cysteine-rich proteins that ubiquitously distributed through the plant kingdom. They are common in seeds, and also expressed in other tissues including root, shoot, and flower (Silverstein *et al.*, 2005). Defensins are normally small proteins (45-54 amino acids) that contain an N-terminal signal sequence (Van der Weerden and Anderson, 2013). The amino acid sequence varies except for eight conserved in the eight cystine residues, which form four disulfide bonds and built a conserved core scaffold containing an α-helix and three antiparallel β-sheet (CSαβ) (Figure 4.2). In accordance with the structure of the precursor proteins, plant defensins are further divided into Class I and Class II. The difference is that Class II defensins contain C-terminal propeptide that target defensins to the vacuole (Parisi *et al.*, 2019).

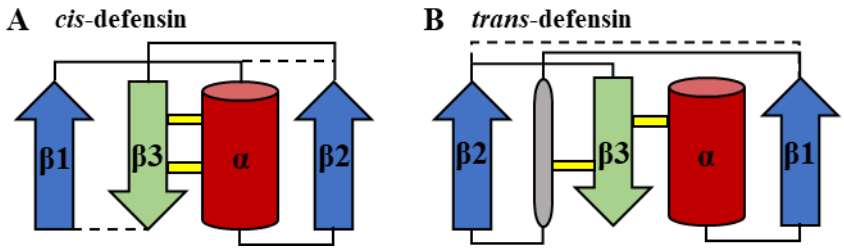

Figure 4.2 Conserved disulfide bridges and structures of defensins. The most conserved disulfide bridges of the cis-defensin superfamily (in yellow) point from the central β-strand to the same α-helix in a 'cis' orientation. (B)The most conserved disulfides of the trans-defensin superfamily (in yellow) point from the central β-strand to two different secondary structure elements in a 'trans' orientation. Non-conserved disulfide bonds are shown as dashed lines Image were drawn based on description in Parisi *et al.*, 2019.

Compared with typical defensins, plant defensin-like proteins are more divergent in cystine residues number, which could be 4, 6, 8, or 10 cysteine residues (Silverstein *et al.*, 2005). The identification of defensin-like proteins greatly enlarges the gene family. In *Arabidopsis thaliana*, there are 15 defensin proteins and more than 300 defensin-like proteins (Graham *et al.*, 2008).

In a most recent study, 57 defensin proteins were found in maize, several of which were investigated in more detail (Odintsova *et al.*, 2020). Beside the antimicrobial activity, defensins also function in reproduction: *Arabidopsis* defensin-like proteins, the so-called LUREs, play an

important role in pollen tube attraction to the ovule (Zhang *et al.*, 2017); the maize defensin protein ZmES4 mediates pollen tube burst via opening of a potassium channel (Amien *et al.*, 2010). However, there is not any investigation in the pollen-specific defensin or defensin-like proteins. In this chapter, the function of a pollen-specific defensin-like protein will be investigated.

4.2 Experimental procedures

The methods used in this chapter are similar with those described in Chapter 2 and Chapter 3.

4.3 Results

4.3.1 Maize *Pollen Ole e 1-like* genes

Pollen Ole e 1 (POE) like proteins were searched in the protein database InterPro (PF01190), which revealed 84 UniProtKB protein accessions. In this database, multiple protein accessions can refer to a single gene. Thus, the extracted 84 protein accessions were mapped to 27 *Pollen ole*

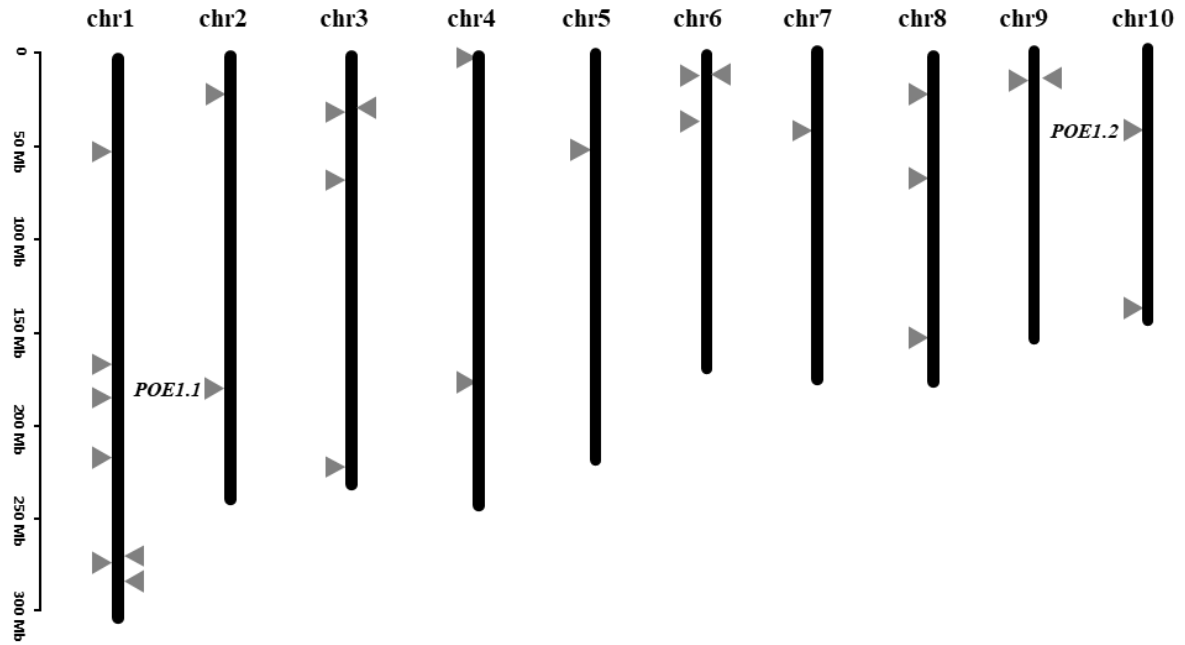

Figure 4.3 Chromosomal distribution of 27 maize *Pollen Ole e 1-like genes*. Chromosome numbers are showed at the top of each chromosome and the approximate size in megabases (MB) is provided at the left side. Gene location are indicated by triangle. *ZmPOE1.1* and *ZmPOE1.2* are marked.

e 1-like (*POE*) genes with Gramene genome IDs (Supplemental Table 1).

A chromosome localization map was drawn to illustrate the genome organization of maize *POE* genes (Figure 4.3). They distribute across all ten chromosomes of maize. Chromosome 1 contains seven *POE-like genes*, which is the highest count among all chromosomes. *POE1.2*, well known by name *Zmc13*, is located on chromosome 10.

To explore the protein sequence conservation, a multiple sequences alignment was carried out (Figure 4.4). The cysteine residues arrangement is relatively fixed. However, the other amino acids are diverse, even inside the Pollen Ole e1 recognition motif.

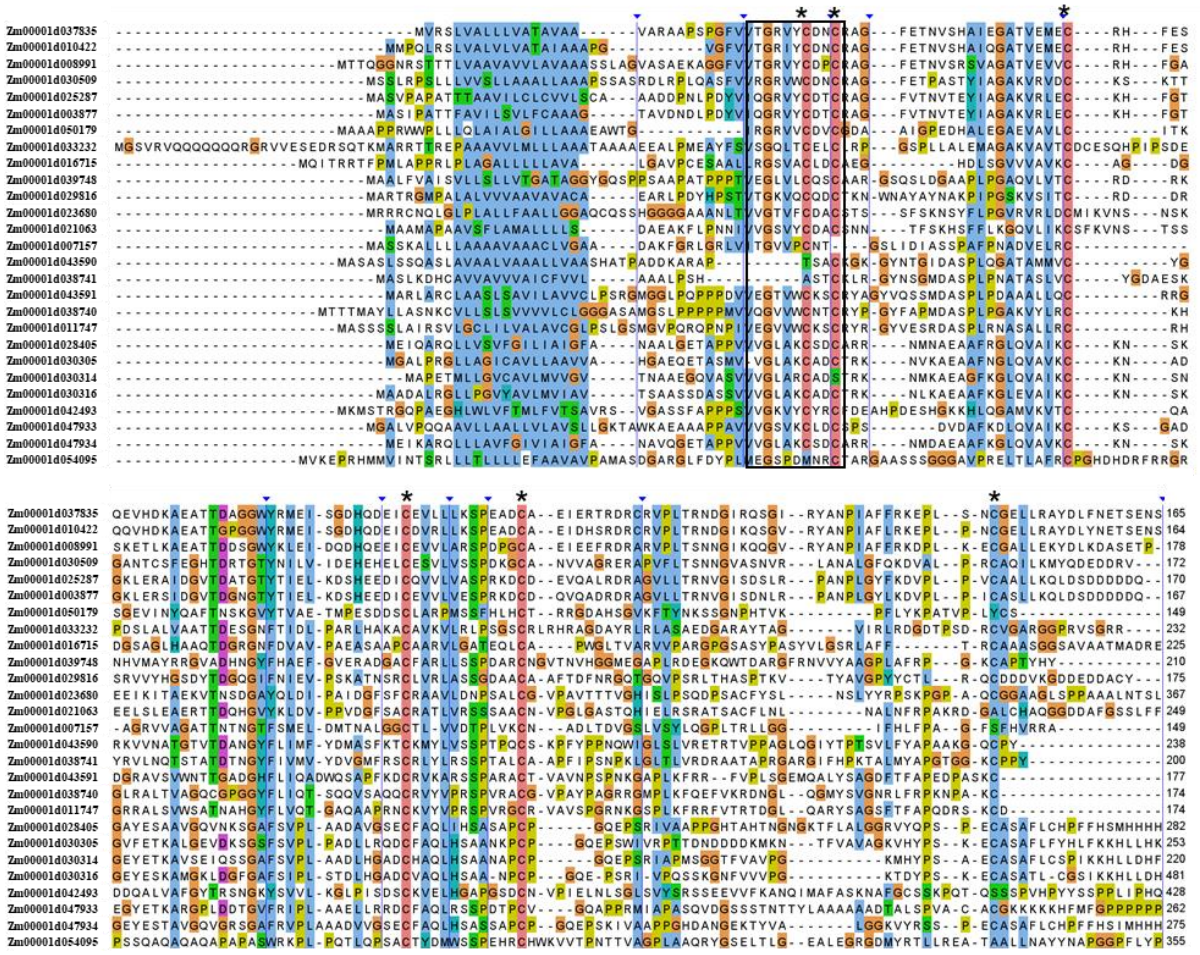

Figure 4.4 Multiple sequence alignment of ZmPOE proteins. Full length of 27 Pollen Ole e1 proteins alignment using MUSCLE method in MEGAX, and visualized with JalView (Waterhouse et al., 2009). Alignment of the sequences displayed in Clustal color code. Highly variable sequence fragments are marked with a triangle on the top. The Pollen Ole e1 protein recognition motif is highlight with a black box, cysteine residues were marked by asterisks.

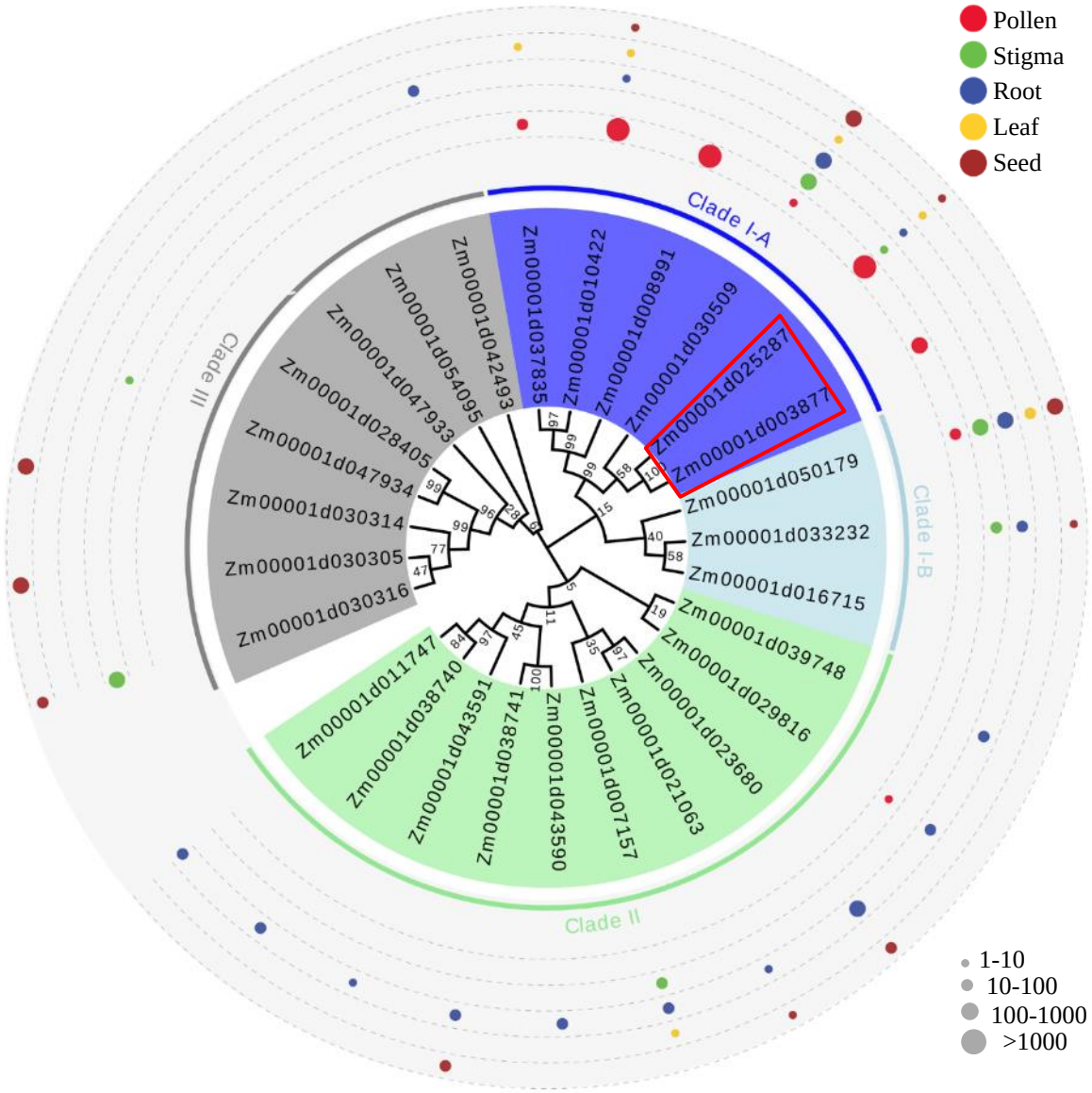

Figure 4.5 Phylogenetic analysis of 27 maize Pollen Ole e 1 (POE) family proteins. The phylogenetic tree was constructed using the NJ method with 500 bootstrap replicates in MEGA X and adjusted by Evolview. The POE proteins fell into three clades. Colored dots indicate the expression level (in TPM) of the correspond *POE* genes in different tissues. The expression data of maize *POEs* were extracted from mRNA-seq test (unpublished data from Dresselhaus group). The size of dots indicates the correspond mRNA expression level, only those expression level higher than 1 were shown. ZmPOE1.1 and ZmPOE1.2 were highlight in rectangle.

To further explore the evolutionary relationship of maize POE peptides, a phylogenetic analysis was carried out (Figure 4.5). 27 maize POE proteins could be separated into three groups. Group I was further divided into Group I-A and Group I-B according to sequence features and expression patterns. Group I-A proteins in Ole e 1 family domain is highly conserved (Figure 4.6.A), while it is more variable in the other POE proteins. Besides, Group I-A *POE* genes are pollen-specific expressed. Group II *POE* genes are mostly expressed in roots. In general, expression of Group III *POE* genes is low and only three out of eight genes are expressed in seeds. Among these three genes, *Zm00001d030316* may also be involved in the reproduction process, as it strongly expressed in silk and mildly expression after pollination (Table 4.1).

Among the 27 *POE* genes, pollen-specific *ZmPOE1.2* has the highest RNA expression level (19215 TPM, Table 4.1). The paralogue *ZmPOE1.1* (83.64% identity) also shows strong expression in pollen. Expression patterns of *ZmPOE1.1* and *ZmPOE1.2* were further validated in reproduction tissues of Hi-II plants by RT-qPCR (Figure 4.7), the expression level of *ZmPOE1.1* was similar with *ZmPOE1.2* in Hi-II pollen.

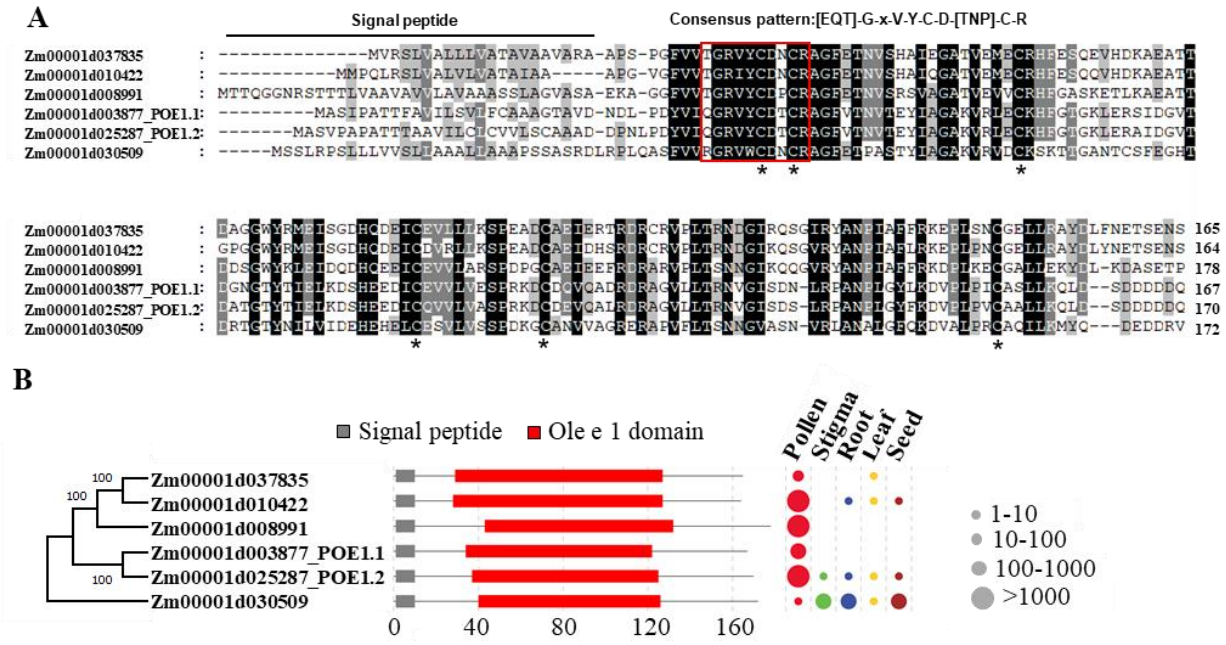

Figure 4.6 Sequence alignment and phylogenetic tree of maize Clade I-A ZmPOE peptides. (A) Amino acid alignment of six ZmPOEs. The signal peptide is marked, the pollen Ole e I family consensus pattern is highlight in a red rectangle, the cysteine residues are marked with asterisks. (B) Phylogenetic analysis of six ZmPOEs, the signal peptide is represented by gray box, the structure feature in the middle and the correspond gene expression in five given tissues.

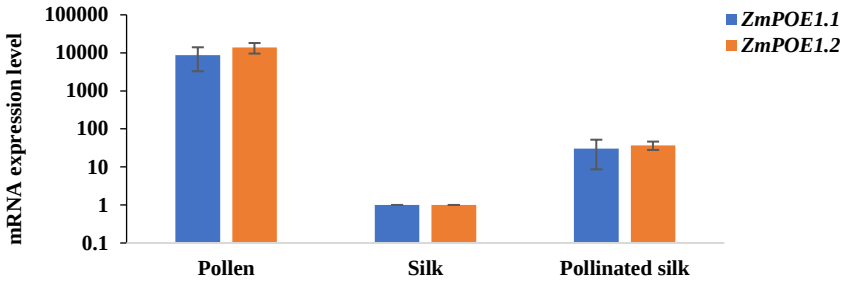

Figure 4.7 Expression level of *ZmPOE1.1/1.2* in pollen and silks of Hi-II plants. The expression levels obtained by RT-qPCR analysis were normalized by two reference genes. *ZmPOEs* expression level in silk were set as baseline, the pollinated silks were taken eight hours after germination.

Table 4.1 Expression level of maize *POE* genes. Genes' mRNA expression levels were extracted from RNA-seq data (Dresselhaus group). Values are in transcripts per million (TPM).

	GeneID	Pollen Tube	Silk	Pollinated Silk	Leaf	Root	Seed
ZmPOE1.1	Zm00001d003877	295	0	25	0	0	0
	Zm00001d007157	0	11	18	7	96	1
	Zm00001d008991	1011	0	100	0	0	0
	Zm00001d010422	1776	0	230	4	2	2
	Zm00001d011747	0	0	0	0	17	0
	Zm00001d016715	0	0	0	0	0	0
	Zm00001d021063	0	0	0	0	3	4
	Zm00001d023680	0	0	0	0	376	19
ZmPOE1.2	Zm00001d025287	19215	3	2097	2	2	3
	Zm00001d028405	0	0	0	0	0	0
	Zm00001d029816	1	0	0	0	11	0
	Zm00001d030305	0	0	0	0	0	450
	Zm00001d030314	0	0	0	0	0	579
	Zm00001d030316	0	809	257	0	0	84
	Zm00001d030509	2	267	151	4	168	385
	Zm00001d033232	0	20	46	1	13	5
	Zm00001d037835	78	0	9	1	0	0
	Zm00001d038740	0	0	0	0	32	0
	Zm00001d038741	0	0	0	0	24	12
	Zm00001d039748	0	0	0	0	24	0
	Zm00001d042493	0	0	0	0	61	0
	Zm00001d043590	0	0	0	0	42	0
	Zm00001d043591	0	0	0	0	9	0
	Zm00001d047933	0	0	0	0	0	0
	Zm00001d047934	0	3	1	0	0	0
	Zm00001d050179	31	222	192	81	178	240
	Zm00001d054095	0	0	0	0	0	0

Low Middle High

4.3.2 Functional exploration of ZmPOEs with RNAi mutant

To explore the function of *ZmPOE* genes, RNA interference (RNAi) was applied to obtain knock-down double mutants of *ZmPOE1.1* and *ZmPOE1.2*. Gene specific regions of *ZmPOE1.1* and *ZmPOE1.2* (*ZmPOE1.1*: 240 bp; *ZmPOE1.2*: 228 bp, Supplemental Table 3) were selected for the RNAi constructs. In total, five independent RNAi-*POEs* mutant lines were identified. Transgenic plants from the T0 generation were self-pollinated or crossed with Hi-II. Subsequently. RNAi-*POEs* plants from the first generation (T1) were used to analysis the phenotype.

Expression levels of *ZmPOEs* were checked in the five T1 mutant lines by RT-qPCR (Figure 4.8). T1 plants, which do not harbor the RNAi-*POEs* construct integration, were used as correspond wild type. The mRNA expression of *ZmPOE1.1* and *ZmPOE1.2* were down-regulated to different levels: in Line4 was no significance difference with correspond wild type; in Line6, Line7, and Line12, the expression levels were reduced by 50% compared to wild type; in Line3 the lowest expression level of *ZmPOEs*, 20% of the wild type expression level, was detected.

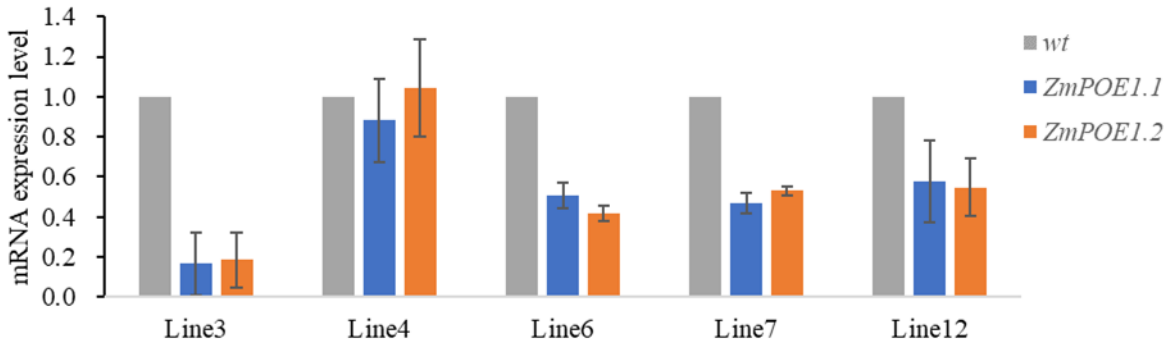

Figure 4.8 Expression level of *ZmPOE1.1/1.2* in *RNAi-POEs* mutant lines and wild type. The expression levels were normalized by two reference genes. Five RNAi-*POEs* mutant lines were tested and compared with wild type.

In RNAi-*POEs*, the pollen activity was analyzed by *in vitro* germination assays. Fresh pollen from RNAi-*POEs* mutant lines and the correspond wild type were collected, germinated under the same conditions and observed. Pollen status was checked 45 minutes after germination (Figure 4.9). In RNAi-*POEs* mutant Line3, pollen germination ratio, un-germinated pollen ratio, and pollen burst ratio was comparable to wild type. There was only slightly difference in the pollen burst ratio between RNAi-*POEs* mutant line and wild type. In the RNAi-*POEs* mutant Line12, the germination ratio was significantly higher than in wild type, which up to 80%. However, it was not considerably higher compared with the pollen status in Line3. As the correspond wild type

was selected form the RNAi-*POEs* T1 plants without RNAi-*POEs* construct integration, the difference may be due to unhealthy condition of wild type.

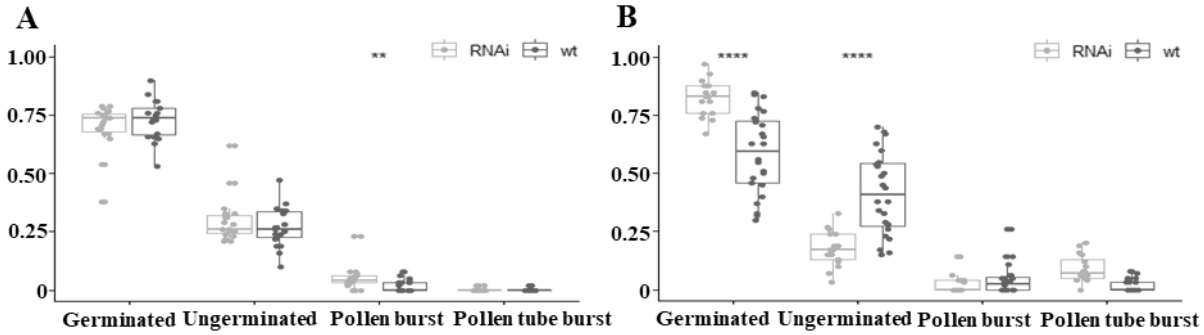

Figure 4.9 RNAi-*POEs* pollen germination. (A) Pollen germination in Line3; (B) Pollen germination in Line12. Pollen was classified as health pollen tube (Germinated), un-germinated pollen grain, burst pollen grain, and burst pollen tube. Significance was compared with the correspond wild type: * $p<0.05$, ** $p<0.01$, *** $p<0.001$,**** $p<0.0001$

4.3.3 Functional exploration of ZmPOEs with CRISPR/Cas9 mutant

To generate knock out mutants of *ZmPOEs*, CRISPR/Cas9 gene editing was applied. As mentioned before, the protein sequence of ZmPOE1.1 and ZmPOE1.2 are highly identical (Figure 4.6.A) and the correspond genes have similar expression. Therefore, knock out of both *ZmPOEs* genes was attempted in a single transformation. Two guide RNAs were selected from the common DNA sequences of *ZmPOE1.1* and *ZmPOE1.2* (Figure 4.10.A). To ensure specificity of guide RNAs, which were designed based on the B71 reference genome, bot *ZmPOEs* genes were sequenced using Hi-II genomic DNA (Supplemental Figure 2). The final construct was integrated into pGW-Cas9 and transformed into maize Hi-II immature embryos. The T0 generation Cas9-*POEs* transgenic plants were self-pollinated.

Cas9 editing on target sequences was checked in the T1 generation. Several plants showed editing on the target sequences, for example, 42 base pairs deletion in both *ZmPOE1.1* and *ZmPOE1.2* was detected in mutant Line3.2. However, it is likely that the exist of Cas9 construct would continuously edit the target genome. Therefore, the identified mutant plants were self-pollinated to out-cross the Cas9 construct.

The present of the Cas9 construct was analyzed in part of the T2 Cas9-*POEs* plants by Cas9 specific PCR (Supplemental Table 2). Mutant plants without the Cas9 construct were sequenced

to analyze *ZmPOEs* gene editing (Figure 4.10.B). In mutant Line1.5, 42 base pair nucleotides were deleted. The deleted region includes the coding sequence for a cysteine residue, which may result in the disruption of disulfide bridge. *ZmPOE1.2* genome editing resulted in a 38 base pair deletion. This deletion produces a frame shift. CRISPR/Cas9 induced mutant were homozygous for both genes.

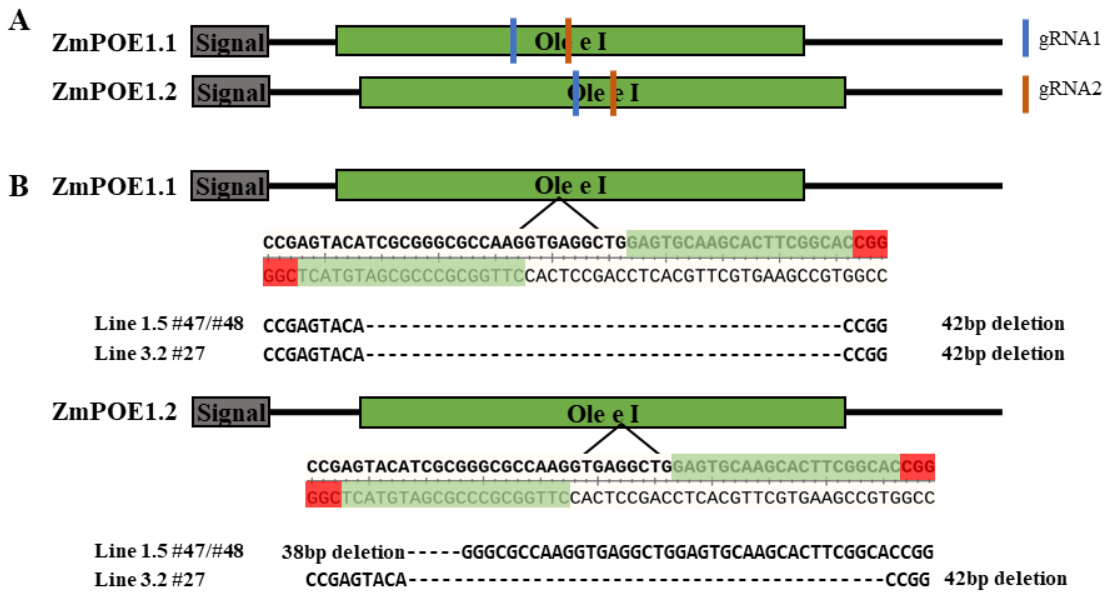

Figure 4.10 Cas9/gRNA-induced mutations in *ZmPOE1.1* and *ZmPOE1.2*. (A) Guide RNA sequences and the localization *in ZmPOEs*. (B) Cas9/gRNA editing on the target genome region. Two mutant lines were present with fragments deletion. The editing resulted in 14 amino acids deletion or fragment shift. The PAM (NGG) motifs were indicated in red letters.

In mutant Line3.2, the editing of *ZmPOE1.1* and *ZmPOE1.2* was similar to the editing in *ZmPOE1.1* of Line1.5, in which 42 base pair nucleotides were deleted. It is likely that the disruption of disulfide bridge occurred on both proteins. It is noticeable that the editing was heterozygotes.

To investigate the effect of Cas9-*POEs* editing, *in vitro* pollen germination was carried out. The Cas9 transgene plants without *ZmPOEs* editing were selected as corresponding wild type (Figure 4.11). Pollen from wild type were germinated together with those from Cas9-*POEs* and the status of pollen was recorded 90 minutes after germination. The observed pollens were separated into four groups: healthy pollen tube, ungerminated pollen, burst pollen, and burst pollen tube. Pollen from wild type performed best, more than 88% of pollen tubes were still growing at 90 minutes after germination and only 2.6% burst pollen tubes were identified. In Cas9-*POEs* mutant Line1.5

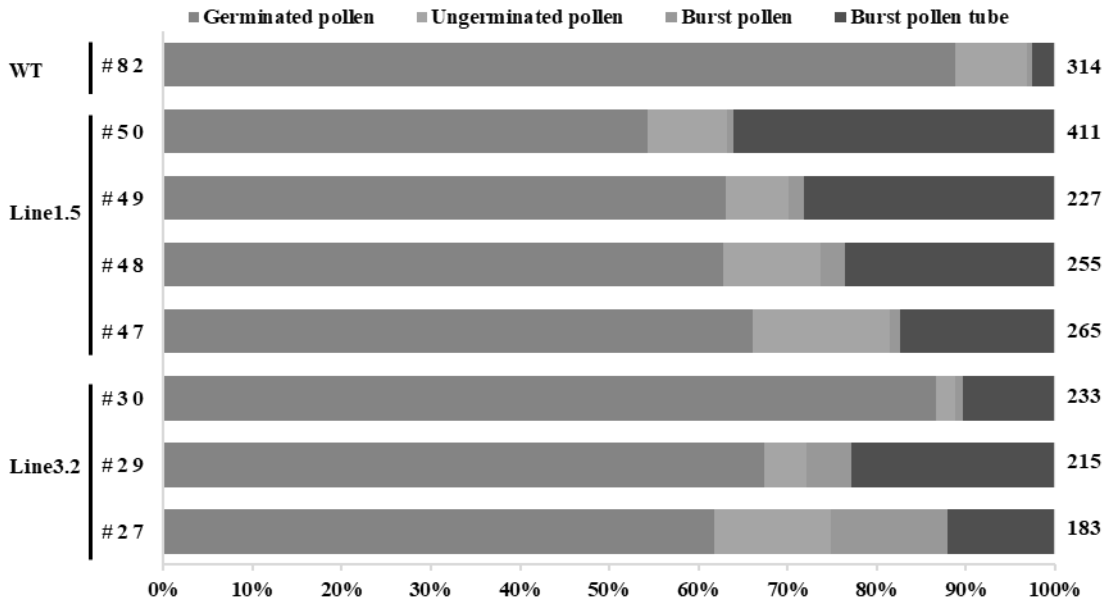

Figure 4.11 Cas9-*POEs* pollen germination status (90 minutes after germination *in vitro*) . Pollen germination status from Cas9-*POEs* mutant Line1.5 and Line3.2 was recorded. The wild type was selected from transformed plants with no editing in target region. Pollen were classified as health pollen tube, un-germinated pollen grain, burst pollen grain, and burst pollen tube. Total number of analyzed pollen grains is listed on in right side.

and Line3.2 the pollen germination status was decreased compared to wild type: around 62% pollen from Cas9-*POEs* mutant Line1.5 showed healthy pollen tubes, in contrast, 26% pollen tubes bursted. Pollen from Cas9-*POEs* mutant Line3.2 was similar, which own 72% healthy pollen tube and 15% burst pollen tube. It seems that pollen tubes from Cas9-*POEs* mutants were less stable than those from wild type.

4.3.4 Maize pollen *Defensin-like* genes

In a search for the small secret proteins, 62 maize *defensin-like* genes (*ZmDEFL*) were identified with low identity (15.37%) (Li *et al.*, 2014). Based on their CSαβ motifs, these *ZmDEFLs* can be divided into three groups (Li *et al.*, 2014). Expression data on maize reproductive tissues revealed that *ZmDEFL1 (Zm00001d017293)* is the only *ZmDEFL* gene highly expressed in pollen (13326 TPM). To identify possible paralogues, the ZmDEFL1 protein sequence was subjected to blast search using the published maize genome B73. Seven similar proteins, which own an identical cysteine residues pattern (CX{10}CX{5}CX{3}CX{9}CX{6,8}CX{1}CX{3}C) were found (Figure 4.12). These eight ZmDEFLs belong to group1-type maize DEFLs (Supplemental Table 1) (Li *et al.*, 2014). *Defensin* genes are well-known for their anti-fungal or anti-bacterial function.

However, the infection of Ustilago or Fusarium on silks did not affect the expression of the eight *ZmDEFL* genes (Figure 4.13), indicating a different function.

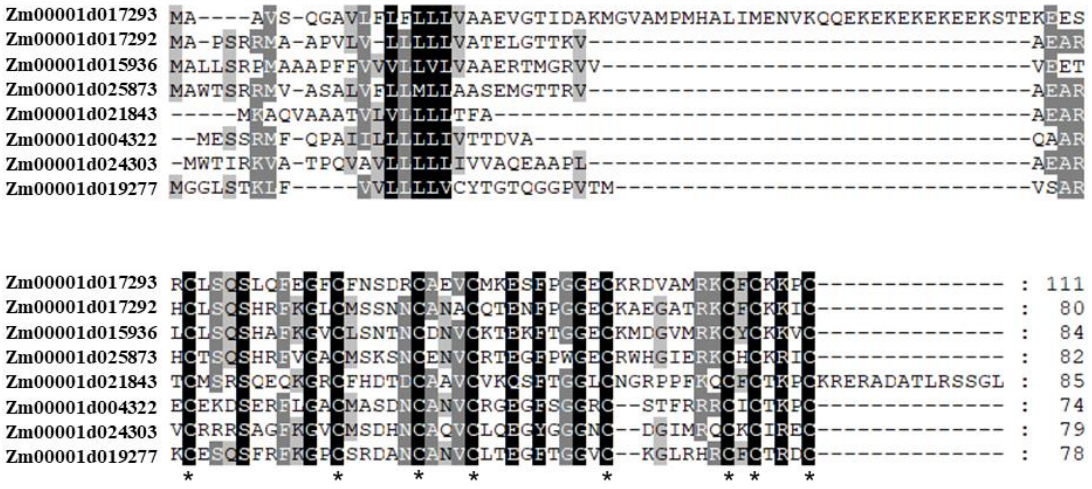

Figure 4.12 Protein alignment of ZmDEFLs. Full length protein sequences of 8 ZmDEFLs were aligned using MUSCLE method in MEGAX, and visualizing with GeneDoc (Nicolas et al., 1997). The cysteine and glycine residues are marked with asterisks.

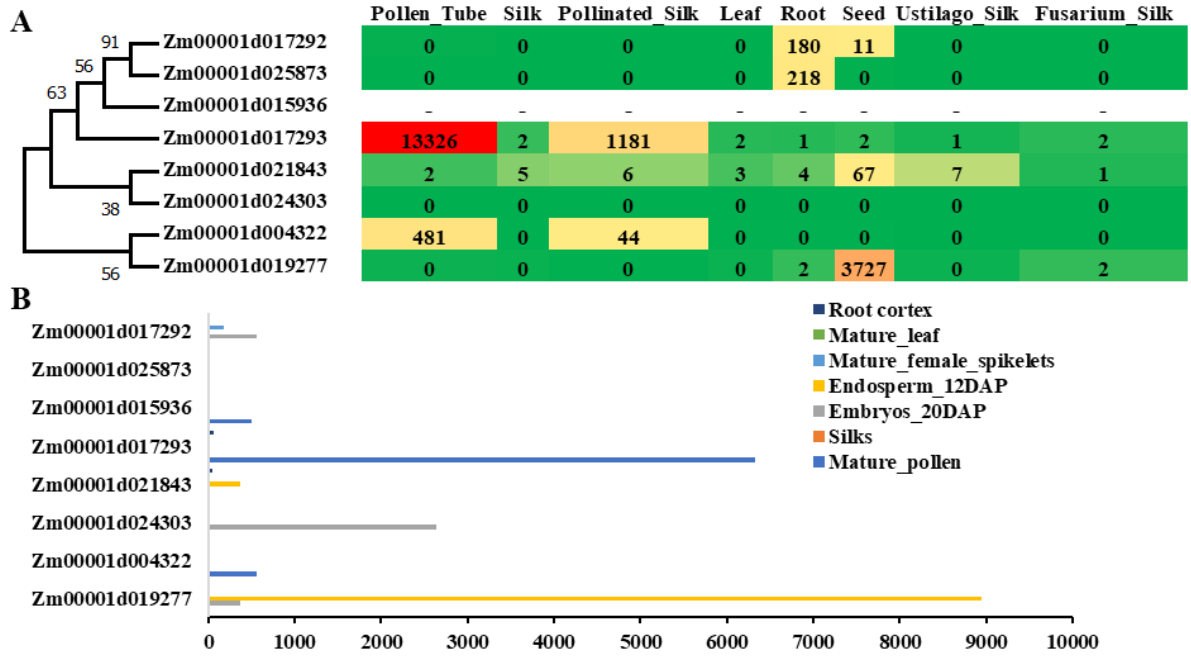

Figure 4.13 Expression levels of *ZmDEFL* genes. (A) Phylogenetic analysis of ZmDEFLs and the mRNA expression (in TPM) expression within five maize tissues and during infection of silks with *Ustilago maydis* or *Fusarium graminearum*. (B) mRNA expression patterns (in FPKM) ZmDEFLs in different maize tissues. Data were obtained from MaizeGDB qTeller.

4.3.5 Functional exploration of ZmDEFL1 with RNAi mutant

To explore the function of *ZmDEFL1*, RNAi-*DEFL* mutant was generated. Therefore, a 382 base pairs nucleotides fragment spanning the 5' UTR to the gamma-thionin region of *ZmDEFL1* was taken for the RNAi construct (Supplemental Table 3). The construct was transformed into maize embryos via *Agrobacterium*. T0 plants were self-pollinated and T1 plants were used to analyze the *ZmDEFL1* expression levels and by that verification of successful introduction of RNAi.

ZmDEFL1 RNA expression was analyzed in nine transgene lines by RT-qPCR (Figure 4.14). T1 transformed plants without the *RNAi-DEFL* construct were selected as corresponding wild type. Expression of *ZmDEFL1* was down-regulated from 40% to 65% in Line3, line5, line7, line13, and Line20; the expression level was 29% compared with the wild type in Line4. The strongest down-regulation occurred in Line1, Line6, and line9, in which the *ZmDEFL1* gene expression lower than 5%.

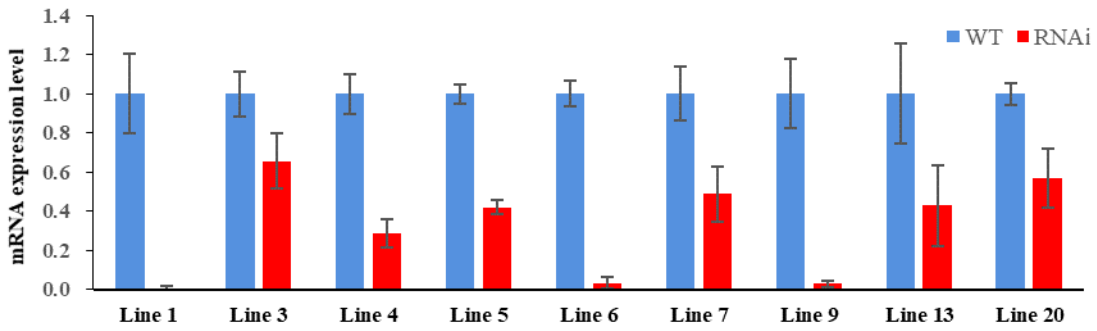

Figure 4.14 Expression level of *ZmDEFL1* in RNAi-*DEFL* mutant lines and wild type. Nine RNAi-*DEFL* mutant lines and the correspond wild type were tested for expression of ZmDEFL1 by RT-qPCR . The expression levels were normalized by two reference genes (PB1A10.07c and Cullin). Error bars represent standard deviation and expression of ZmDEFL1 in wild type plants (WT) was set to 1.

To test the effect of *ZmDEFL* downregulation, pollen from RNAi-*DEFL* mutant plants and the correspond wild type were germinated *in vitro* (Figure 4.15). In RNAi-*DEFL* mutant Line9, the germination ratio was 59.59%, a little bit lower than in the corresponding wild type, whose germination ratio was 66.3%. Except for the Line9, there was no significant difference in germination ratio in RNAi-*DEFL* mutants compared to wild types. A portion of pollen grains burst without germination. However, the burst pollen ratio was no more than 10% in all experiments. The burst pollens were significantly more in RNAi-*DEFL* mutant Line1 (6.54%),

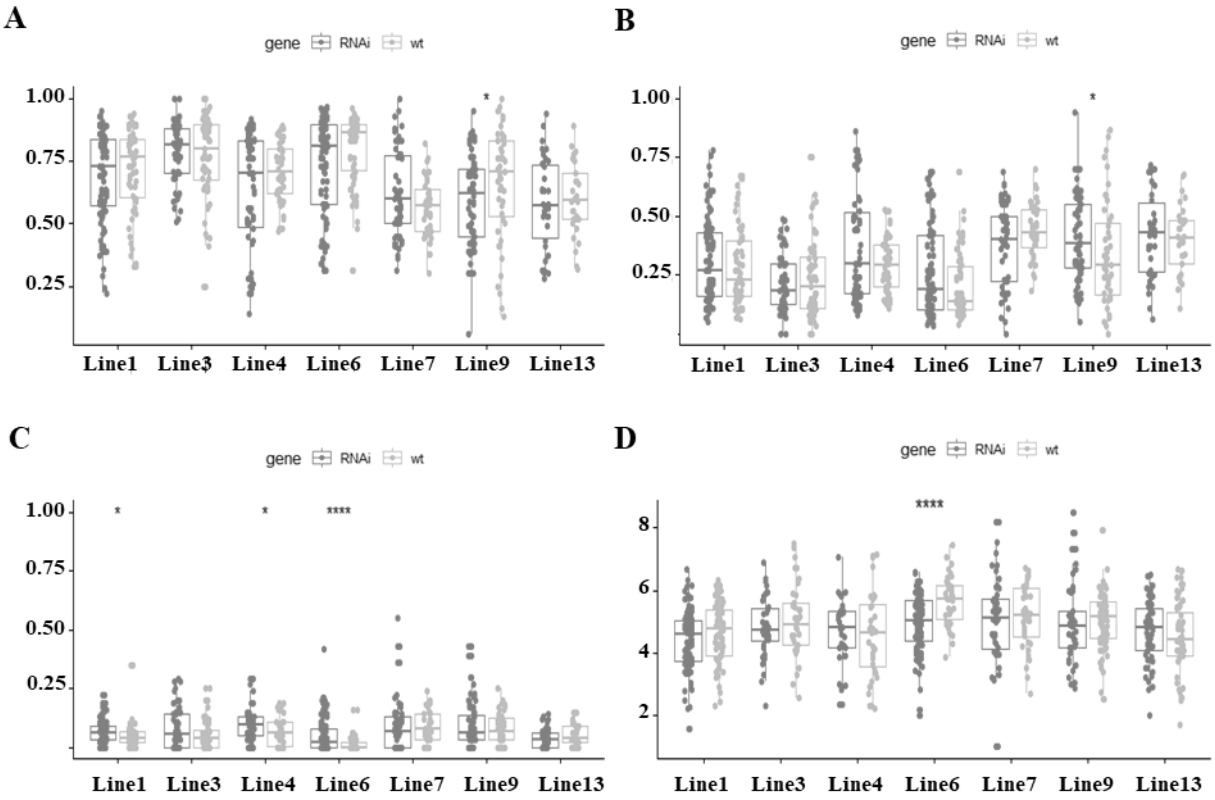

Figure 4.15 RNAi-*DEFL* pollen germination status (45 minutes after germination *in vitro*). Pollen was classified as health pollen tube, un-germinated pollen grain, burst pollen grain, and burst pollen tube. Also, pollen tube growth speed was measured. Seven RNAi-*DEFL* mutant lines and the corresponding wild type were recorded. (A) Germinated pollen ratio (B) Ungerminated pollen ratio. (C) burst pollen ratio. (D) Pollen tube growth speed (μm /minutes). Significance: * p<0.05, ** p<0.01, *** p<0.001,**** p<0.0001.

line4 (9.8%), and Line6 (4.98%). However, a comparably higher pollen burst ratio (8.71%) was observed in Line7 wild type. It is not likely that the *ZmDEFL* downregulation resulted in higher pollen burst ration. In a similar way, the pollen tube growth speed of RNAi-*DEFL* mutant Line6 (4.93 μm/min) was significantly slower than the corresponding wild type (5.66 μm/min). However, it was not slower than those in the wild type of Line1 (4.63 μm/min), line4 (4.55 μm/min), and Line13 (4.53 μm/min). In general, there was no obvious correlation between *ZmDEFL1* mRNA expression and pollen germination status.

To further investigate the effect of *ZmDEFL* downregulation, male gametophyte transmission efficiency tests were carried out. Pollen from RNAi-*DEFL* mutant Line1, Line6, and Line9 was used to crossed with wild type B73 or for self-pollination (Table 4.2). In all performed cross the observed segregation ratio matched the expected ratio.

In summary, the activity of pollen was not affected by the down-regulation of *ZmDEFL1*.

Table 4.2 Gametophyte transmission efficiency analysis of RNAi-*DEFL* mutant maize lines. Mutant lines were crossed with wild type (inbred line B73) plants as indicated. A transmission efficiency of ≥1:1 and ≥3:1, is expected as lines may contain multiple transgene integrations. The transgene is fully transmitted via the male gametophyte.

RNAi-*DEFL* mutant	Female	x	Male	Numbers of plants			Segregation expected	Segregation observed
				RNAi	WT	total		
Line1	RNAi-*DEFL*	×	RNAi-*DEFL*	57	0	57	≥3:1	1:0
	B73	×	RNAi-*DEFL*	60	37	97	≥1:1	1.62:1
Line6	RNAi-*DEFL*	×	RNAi-*DEFL*	32	4	36	≥3:1	8:1
	B73	×	RNAi-*DEFL*	53	28	81	≥1:1	1.89:1
Line9	B73	×	RNAi-*DEFL*	37	45	82	≥1:1	0.82:1

4.4 Discussion

4.4.1 ZmPOE: An antigen that does not cause an allergy

For the first time, the *Pollen Ole e1-like* gene family in maize was investigated. It was reported before that there are quite a number of *POE* genes in maize: 42 protein accessions (José Carlos Jiménez-López *et al.*, 2011) or 16 *genes* (Li *et al.*, 2014) were identified. In this research, 27 *ZmPOE* genes were found. The cysteine residue arrangements are quite conserved across 27 ZmPOE peptides, while the amino acids between cysteine residues varies. A similar situation was found in rice and pear, each of them contain 45 *POE* genes and the corresponding protein sequences are highly diverse (Jiang *et al.*, 2005; Qian *et al.*, 2020).

Phylogenetic analysis indicated that maize has three types of POE proteins. Among these three types, pollen-expressed *POE* genes were clustered in Clade I-A which is conserved in POE protein motif. Zmc13 (ZmPOE1.2) belong to Clade IA and has a paralogue (ZmPOE1.1) that is highly similar in protein sequences and expression pattern, suggesting a functional redundancy. ZmPOE1.1 is likely to be the result of duplication of ZmPOE1.2 (Van Bel *et al.*, 2018). Expression of *ZmPOE* genes also were detected in vegetative tissues, indicating the multiple function of *POE* genes during plant development. It was reported that in *Glycine max*, the root expressed *POE* gene *GmPOI* was involved in response to abiotic stress. Plants overexpressing *GmPOI* showed higher tolerance to drought stress (Song *et al.*, 2013).

Both *ZmPOE1.1* and *ZmPOE1.2* showed strong expression in pollen based on RNA-seq data, while *ZmPOE1.2* were significantly higher than *ZmPOE1.1*. However, according to RT-qPCR

result, these two genes have similar expression levels in pollen. It should be noticed that the gene expression levels were checked on Hi-II maize plants, which was also used for the transgene plant generation. The genetic diversity among different maize inbred lines is remarkable (Yang *et al.*, 2019), the polymorphic structural variants could significantly affect gene expression and trait performance. For example, within two different inbred lines, more than thousand drought tolerance response genes showed differential expression (Zhang *et al.*, 2017). Thus, it is reasonable that the RNA-seq expression data from B73 did not precisely match those in maize line Hi-II. However, in conclusion both of two *ZmPOE* genes showed strong expression in pollen.

In our research, RNA interfering and CRISPR/Cas9 technologies were used to generate mutant lines against *ZmPOE1.1/1.2* genes. In the RNAi-*ZmPOEs*, the expression level of these two genes was down-regulated to 20% compared with wild type. However, *in vitro* pollen germination test revealed that there is no significantly difference between RNAi mutant pollen and the corresponding wild type. A possible reason is that even though these two genes were down-regulated, their remaining expression was still able to fulfill their function. Another possible reason for the observed pollen germination is gene redundancy. For example, in *Arabidopsis* pollen tubes, mutation of just one of the receptors like cytoplasm kinases LIP1 or LIP2 did not exhibit any phenotype, while their double mutant showed male gametophyte transmission decrease (Liu *et al.*, 2013). There are six ZmPOEs from Clade IA, four of which showed expression in pollen. Beside *ZmPOE1.1/1.2*, the other two genes may also contribute to maintain function. It is also possible that the function of *ZmPOEs* rely on the communication with female tissues, which would be not detectable by the used pollen growth assay. The ZmPOEs homologues Ole e 1 for example was detected in pollen germination medium (de Dios Alche *et al.*, 2004). Yet, the Cas9-*ZmPOEs* mutant pollen showed an abnormal pollen burst /pollen tube burst around 90 min after germination. Supported by the transmitting tract enables the pollen tube for long distance growth and response to the attraction signal from female tissues (Higashiyama *et al.*, 1998). Without the support from female tissues, the pollen tube will stop growth after consuming its own energy (Lausser *et al.*, 2010). Compared with wild type pollen, the Cas9-*ZmPOEs* pollen may need more support from female tissue.

The study of *ZmPOEs* just started, there are still many experiments need to be carried out. For example, a gametophyte transmission efficiency test would be a direct prove of their functional importance. Besides, heterologous expressed and purified recombinant ZmPOEs and protein

specific antibodies would benefit to the search for possible interactors.

4.4.2 Unclear function of ZmDEFL

Due to the sequence variability among defensins (Parisi *et al.*, 2019), no identification of all maize defensin-like family members was not carried out. Instead, the closes paralogues of *ZmDEFL1* were identified using NCBI blast. Seven defensin-like proteins were found, two of those showed strong pollen expression. Based on this analysis, RNAi-*DEFL* mutant maize lines were constructed. These mutant lines exhibited no defect in pollen germination or gametophyte transmission efficiency compared to wild type plants.

The unexpected lack of an pollen germination phenotype in RNAi-*DEFL* mutant maize lines can be a result of various factors: (1) Rescue by paralogues, (2) Rescue by remaining transcripts, (3) Protein levels are not directly correlated with transcript levels. The closest paralogues of *ZmDEFL1* is *Zm00001d017292*, which localized next to *ZmDEFL1* on chromosome 5. Except for the conserved cysteine residue arrangements and some conserved amino acids (Figure 4.12), their protein sequences only share 52% overlap and 57% identity, which is comparably low and not likely a result of gene duplication. Based on this rescue of RNAi-*DEFL* mutant lines by redundancy, resulting in wild-type like pollen germination, is unlikely. In the RNAi-*DEFL* mutant lines, the *ZmDEFL1* expression level was downregulated to around 5% compared with wild type. However, the original expression level is extremely high (13326 TPM); RNAi mediated transcript level decrease of 95% still results in a remaining level of more than 500 TPM. It was reported that the gene expression level was not always linked with protein level, there was only weakly positive correlation between them (Walley *et al.*, 2016). So, it is possible that the protein level was not altered in the *ZmDEFL1* mutant lines.

CHAPTER 5. COMPREHENSIVE DISSCUSSION AND OUTLOOK

As discussed already above in Chapters 1-4, CRPs are involved in multiple signaling events especially during reproduction processes. Although signaling peptides ZmEA1, LUREs and XIUQIUs were shown to play vital roles for pollen tube guidance, and RALFs, ES1-4 and PMEI1 regulate pollen tube integrity, our knowledge about additional CRP functions is still scarce despite their high expression during reproduction. In maize and other grasses, almost nothing is known about CRP function(s). In this work, with *RALFs*, *POEs* and *DEFL* three types of *CRP* genes with pollen-specific highly expression levels were studied.

RALF genes and their interactors were identified in this thesis in maize, and the conservation of the RALF signaling pathway regulating cell wall integrity was shown to be conserved between maize and *Arabidopsis*, and thus likely in all other angiosperm species. It was recently hypothesized that AtRALF4 mediated pollen tube growth arrest could be exclusively regulated by LRX proteins (Moussu *et al.*, 2020). ZmRALF2/3 are mainly localized to the cell wall of pollen tubes, where PEX2 is anchored. Downregulation of *ZmRALFs* resulted in the alteration of PEX2 phosphorylation, providing a direct hint on the importance of RALF-LRX complex in maintaining pollen tube wall integrity. A dosage-dependent RALF signaling model was postulated, which nicely combines RALF-LRX and RALF-CrRLK1L-LLG complexes for maintaining of pollen tube cell wall integrity.

However, there are still many questions that need to be answered regarding RALF function(s). For example, the major component affected by RALF in the pollen tube cell wall is unclear. An alkaline band at the base of clear zone was reported in the pollen tubes of lily (Scholz *et al.*, 2020). This alkaline band was eliminated when pollen tube growth inhibitor potassium cyanide (KCN) was applicated but recovered abruptly. Pollen tube growth turned back to normal only when the alkaline band reappeared (Winship *et al.*, 2017). It was further hypothesized that a pH increase in the alkaline band stimulates actin cytoskeleton related proteins, which in turn supports faster growth rates and proton influx (Lovy-Wheeler *et al.*, 2006). As a strong alkalinization factor, RALF peptides might be involved in the pH regulation in the alkaline band by stimulating proton pumps (Haruta *et al.*, 2014). Pollen tube elongation requires a precisely regulated balance between

turgor pressure and cell wall integrity. Esterified pectin is ultimately secreted to the pollen tube clear zone, are de-esterified towards the shank by pectin methylesterases (PMEs) and incorporate with increasing contents of cellulose and callose, thus ensure fast tip growth and cell wall stiffness (for review see Scholz *et al.*, 2020). It was recently reported that the CrRLK1L family member FERONIA, which is not present in pollen tubes, is important in maintaining de-esterified pectin at the filiform apparatus of the egg apparatus (Duan *et al.*, 2020). The function of other CrRLK1L members in pollen tubes was not yet tested. It is thus possible that CrRLK1L family members ANXs and BUPSs are also required to regulate pectin accumulation in the pollen tube cell wall. Moreover, the impact of RALF-LRX on pollen tube cell wall characteristics could be transduced by pollen-specific CrRLK1Ls and function on de-esterified pectin accumulation. To test this hypothesis, pectin as well as cellulose and callose status in RNAi-*RALFs* and CRISPR/Cas9-*RALFs* mutant pollen tubes need to be examined. Furthermore, how RALF function on surrounding tissues need to be investigated as well. As an autocrine signaling peptide, RALF is secreted to the apoplast may also be sensed by receptors of maternal cells, for example, of the transmitting tract. This is not unlikely, as RALF peptides could be detected in germination medium during *in vitro* pollen germination (Flores-Tonero *et al.*, 2020). In conclusion, it is well possible that RALF in maize plays a major role in softening the cell wall in the silk to ensure pollen tube penetration.

Besides, Clade IV RALF genes *ZmRALF1/5* lacking typical RALF features were investigated. Different from Clade II RALFs described above, they localized to vesicles in pollen tube cytoplasm and didn't interact with "conventional" RALF interactors like CrRLK1Ls, although Clade IV RALF proteins were previously described as RALF-related peptides (Campbell and Turner, 2017). This work thus revealed that they were not only different from classical RALF peptides in amino acid sequences, but also in chemical features, subcellular localization and interaction partners. Clade IV RALF genes *AtRALF8/9* are similar and also showed pollen-specific strong expression (Figure 2.5) without any clue about their function. Further investigation on Clade IV RALF genes may uncover a totally new signaling pathway with different and novel functions. In this work, CRISPR/Cas9-*ZmRALF1/5* mutant lines were constructed already. *ZmRALF1/5* editing were only identified in a few Cas9-*RALF1/5* mutant lines so far, thus identification on *ZmRALF1/5* editing needs to be done in the remaining not yet characterized CRISPR/Cas9-*RALF1/5* mutant lines. With different types of gene editing in *ZmRALF1/5*, phenotype test and function exploration could be carried out. Notably, in mature pollen grain,

ZmRALF1/5 genes are mainly expressed in sperm cells (Chen *et al.*, 2017) indicating a fertilization-related function. The effect of *ZmRALF1/5* knockout on sperm cell should be checked with DAPI and FDA staining to study DNA content and viability. After germination, ZmRALF1/5 peptides localized in cytoplasm of transiently transformed cell (Figure 2.21). This should be improved by studying localization using the endogenous promoters. The impact of *ZmRALF1/5* knockout on pollen tube growth should be further investigated during *in vitro* and *in vivo* pollen germination as well as gametophyte transmission efficiency test. More detailed analyses will depend on the outcome of these experiments.

As one of the earliest discovered pollen-specific gene, the function of ZmPOE1.2 or Zmc13 during pollen development or pollen tube growth is still unclear. Its homologue LAT52 in tomato could bind to the receptor LePRK2 before pollen tube germination (Tang *et al.*, 2004), while its function during pollen tube growth is also still unknown. In CRISPR/Cas9-*POEs* mutants, pollen tubes from two types of *ZmPOE1.1/1.2* edited mutants showed impaired integrity *in vitro*, which represents the first step to uncover ZmPOEs/LAT52 function during reproduction. To clearly understand the influence on pollen tube growth, a longer and time-lapse record on pollen germination *in vitro* and better imaging of growth *in vivo* is needed. Besides, a gametophyte transmission efficiency test would provide a direct evidence on the impact of *ZmPOEs* edited mutants during fertilization.

Taken together, function of three so far not studied CRPs during reproductive processes of maize and other grasses were investigated in this thesis. It was found that the signaling network regulated by Clade II RALFs is conserved in maize and *Arabidopsis*. In a step further, we found that reduced *RALF* levels impacted the PEX2 phosphorylation status. This is an exciting finding, but cannot yet be explained. It was speculated that the function of the extensin domain in LRXs is merely anchoring and immobilizing the protein in the cell wall (Herger *et al.*, 2019). However, in this study, PEX2 hyper-phosphorylation induced by reduced levels of *RALFs* revealed a possible function to maintain cell wall stiffness by providing negatively charged LRX/PEX proteins that can be cross-bridged, for example, by calcium ions. The PEX2 extensin domain was previously shown to be localized to the callosic layer (Rubinstein *et al.*, 1995b), which is enriched in callose and localized in the inner cell wall (Mollet *et al.*, 2013). Callose is a permeability barrier, which resists tension and compression stress (Parre and Geitmann, 2005). The alteration of PEX2 phosphorylation status might thus be directly related to the callose status. To test the hypothesis,

the interaction between callose hydrolyzing enzyme and PEX2 could be investigated as well as the stiffness and thickness of *RALF* mutant lines. A new-dosage dependent RALF signaling model integrating interactions of RALFs with CrRLK1Ls, LLGs, and PEXs was established that will help to understand general RALF signaling in plant development and reproduction. In the plant kingdom, the presence of RALF peptides and CrRLK1L proteins appear to be coupled indicating co-evolution (Figure 3.2). With the discovery of interactors like LLGs and PEXs/LRXs, the RALF signaling network appears to be more complicated. The dosage model described here nicely combines RALF-CrRLK1L-LLG and RALF-LRX/PEX complex interaction, which maybe an explanation to the similar defect in cell wall caused by mutants of RALF interactors. Also, we can deduce that the interaction with any RALF interactors might be very similar and thus cause similar phenotypes. For example, RALF peptides secreted from fungi interact with CrRLK1Ls to inhibit the immune response (Thynne *et al.*, 2017). It is possible that before reaching the plasma membrane, they would bind with cell wall LRXs to penetrate the cell.

Finally, *ZmPOE1.1/1.2* CRISPR-Cas9 mutant pollen have shown unstable pollen tube growth *in vitro*, while *ZmDEFL1* gene downregulation did not affect double fertilization. The available CRISPR/Cas9 mutants now provide possibilities to study the function of these genes in future analyses. However, considering the extremely high expression level of *ZmDEFL1,* the generated knockdown might not be sufficient and knock-outs of the whole gene have to be generated to explore its function. In conclusion, the findings of this work extends the knowledge of these three types of CRPs in plant reproduction and may help to improve future plant breeding processes by utilizing the male gametophyte transmission defect feature of mutant pollen, and thus contribute to improve the yield of maize and other grass crops.

REFERENCES

Abarca, A., Franck, C.M., and Zipfel, C. (2020). Family-wide evaluation of RALF peptides in *Arabidopsis thaliana*. *BioRxiv*, 2020.2006.2026.174169.

Alfalah, M., Wetzel, G., Fischer, I., Busche, R., Sterchi, E.E., Zimmer, K.-P., Sallmann, H.-P., and Naim, H.Y. (2005). A novel type of detergent-resistant membranes may contribute to an early protein sorting event in epithelial cells. *Journal of Biological Chemistry* **280**, 42636-42643.

Almagro Armenteros, J.J., Tsirigos, K.D., Sønderby, C.K., Petersen, T.N., Winther, O., Brunak, S., von Heijne, G., and Nielsen, H. (2019). SignalP 5.0 improves signal peptide predictions using deep neural networks. *Nature Biotechnology* **37**, 420-423.

Amien, S., Kliwer, I., Márton, M.L., Debener, T., Geiger, D., Becker, D., and Dresselhaus, T. (2010). Defensin-like ZmES4 mediates pollen tube burst in maize via opening of the potassium channel KZM1. *PLOS Biology* **8**, e1000388.

Atkinson, N.J., Lilley, C.J., and Urwin, P.E. (2013). Identification of genes involved in the response of *Arabidopsis* to simultaneous biotic and abiotic stresses. *Plant Physiology* **162**, 2028-2041.

Bailey, T.L., Boden, M., Buske, F.A., Frith, M., Grant, C.E., Clementi, L., Ren, J., Li, W.W., and Noble, W.S. (2009). MEME SUITE: tools for motif discovery and searching. *Nucleic Acids Research* **37**, W202-W208.

Baumberger, N., Doesseger, B., Guyot, R., Diet, A., Parsons, R.L., Clark, M.A., Simmons, M., Bedinger, P., Goff, S.A., and Ringli, C. (2003a). Whole-genome comparison of leucine-rich repeat extensins in *Arabidopsis* and rice. A conserved family of cell wall proteins form a vegetative and a reproductive clade. *Plant Physiology* **131**, 1313-1326.

Baumberger, N., Steiner, M., Ryser, U., Keller, B., and Ringli, C. (2003b). Synergistic interaction of the two paralogous *Arabidopsis* genes *LRX1* and *LRX2* in cell wall formation during root hair development. *The Plant Journal* **35**, 71-81.

Bedinger, P.A., and Fowler, J.E. (2009). The maize male gametophyte. In Handbook of maize: its biology. (Springer), pp. 57-77.

Begcy, K., and Dresselhaus, T. (2017). Tracking maize pollen development by the leaf collar method. *Plant Reproduction* **30**, 171-178.

Bergonci, T., Ribeiro, B., Ceciliato, P.H.O., Guerrero-Abad, J.C., Silva-Filho, M.C., and Moura, D.S. (2014). *Arabidopsis thaliana* RALF1 opposes brassinosteroid effects on root cell elongation and lateral root formation. *Journal of Experimental Botany* **65**, 2219-2230.

Bircheneder, S., and Dresselhaus, T. (2016). Why cellular communication during plant reproduction is particularly mediated by CRP signalling. *Journal of Experimental Botany* **67**, 4849-4861.

Boisson-Dernier, A., Franck, C.M., Lituiev, D.S., and Grossniklaus, U. (2015). Receptor-like cytoplasmic kinase MARIS functions downstream of CrRLK1L-dependent signaling during tip growth. *Proceedings of the National Academy of Sciences* **112**, 12211-12216.

Boisson-Dernier, A., Kessler, S.A., and Grossniklaus, U. (2011). The walls have ears: the role of plant CrRLK1Ls in sensing and transducing extracellular signals. *Journal of Experimental Botany* **62**, 1581-1591.

Boisson-Dernier, A., Lituiev, D.S., Nestorova, A., Franck, C.M., Thirugnanarajah, S., and Grossniklaus, U. (2013). ANXUR receptor-like kinases coordinate cell wall integrity with growth at the pollen tube tip via NADPH oxidases. *PLOS Biology* **11**, e1001719.

Boisson-Dernier, A., Roy, S., Kritsas, K., Grobei, M.A., Jaciubek, M., Schroeder, J.I., and Grossniklaus, U. (2009). Disruption of the pollen-expressed FERONIA homologs ANXUR1 and ANXUR2 triggers pollen tube discharge. *Development* **136**, 3279-3288.

Campbell, L., and Turner, S.R. (2017). A comprehensive analysis of RALF proteins in green plants suggests there are two distinct functional groups. *Frontiers in Plant Science* **8**.

Campos, W.F., Dressano, K., Ceciliato, P.H., Guerrero-Abad, J.C., Silva, A.L., Fiori, C.S., do Canto, A.M., Bergonci, T., Claus, L.A., and Silva-Filho, M.C. (2018). *Arabidopsis thaliana* rapid alkalinization factor 1–mediated root growth inhibition is dependent on calmodulin-like protein 38. *Journal of Biological Chemistry* **293**, 2159-2171.

Cao, J., and Shi, F. (2012). Evolution of the RALF gene family in plants: gene duplication and selection patterns. *Evolutionary Bioinformatics* **8**, EBO.S9652.

Capron, A., Gourgues, M., Neiva, L.S., Faure, J.-E., Berger, F., Pagnussat, G., Krishnan, A., Alvarez-Mejia, C., Vielle-Calzada, J.-P., and Lee, Y.-R. (2008). Maternal control of male-gamete delivery in *Arabidopsis* involves a putative GPI-anchored protein encoded by the LORELEI gene. *The Plant Cell* **20**, 3038-3049.

Char, S.N., Neelakandan, A.K., Nahampun, H., Frame, B., Main, M., Spalding, M.H., Becraft, P.W., Meyers, B.C., Walbot, V., and Wang, K. (2017). An Agrobacterium-delivered CRISPR/Cas9 system for high-frequency targeted mutagenesis in maize. *Plant Biotechnology Journal* **15**, 257-268.

Chen, J., Strieder, N., Krohn, N.G., Cyprys, P., Sprunck, S., Engelmann, J.C., and Dresselhaus, T. (2017). Zygotic genome activation occurs shortly after fertilization in maize. *The Plant Cell* **29**, 2106-2125.

Chen, J., Yu, F., Liu, Y., Du, C., Li, X., Zhu, S., Wang, X., Lan, W., Rodriguez, P.L., and Liu, X. (2016). FERONIA interacts with ABI2-type phosphatases to facilitate signaling cross-talk between abscisic acid and RALF peptide in Arabidopsis. *Proceedings of the National Academy of Sciences* **113**, E5519-E5527.

Clough, S.J., and Bent, A.F. (1998). Floral dip: a simplified method for Agrobacterium-mediated transformation of *Arabidopsis thaliana*. *The plant journal* **16**, 735-743.

Combier, J.-P., Küster, H., Journet, E.-P., Hohnjec, N., Gamas, P., and Niebel, A. (2008). Evidence for the involvement in nodulation of the two small putative regulatory peptide-encoding genes MtRALFL1 and MtDVL1. *Molecular Plant-Microbe Interactions* **21**, 1118-1127.

Consortium, U. (2019). UniProt: a worldwide hub of protein knowledge. *Nucleic Acids Research* **47**, D506-D515.

Cosgrove, D.J., Bedinger, P., and Durachko, D.M. (1997). Group I allergens of grass pollen as cell wall-loosening agents. *Proceedings of the National Academy of Sciences* **94**, 6559-6564.

Covey, P.A., Subbaiah, C.C., Parsons, R.L., Pearce, G., Lay, F.T., Anderson, M.A., Ryan, C.A., and Bedinger, P.A. (2010). A pollen-specific RALF from tomato that regulates pollen tube elongation. *Plant Physiology* **153**, 703-715.

Cox, J., and Mann, M. (2008). MaxQuant enables high peptide identification rates, individualized ppb-range mass accuracies and proteome-wide protein quantification. *Nature Biotechnology* **26**, 1367-1372.

Crooks, G.E., Hon, G., Chandonia, J.M., and Brenner, S.E. (2004). WebLogo: A sequence logo generator. *Genome Research* **14**, 1188-1190.

Dayhoff, M., Schwartz, R., and Orcutt, B. (1979). Matrices for detecting distant relationships. *Atlas of Protein Sequences*, 353-358.

de Dios Alche, J., Castro, A.J., Olmedilla, A., Fernandez, M.C., Rodriguez, R., Villalba, M., and Rodriguez-Garcia, M.I. (1999). The major olive pollen allergen (Ole e I) shows both gametophytic and sporophytic expression during anther development, and its synthesis and storage takes place in the RER. *Journal of Cell Science* **112**, 2501-2509.

de Dios Alche, J., M'rani-Alaoui, M., Castro, A., and Rodriguez-Garcia, M. (2004). Ole e 1, the major allergen from olive (*Olea europaea L.*) pollen, increases its expression and is released to the culture medium during in vitro germination. *Plant and Cell Physiology* **45**, 1149-1157.

do Canto, A.M., Ceciliato, P.H., Ribeiro, B., Morea, F.A.O., Garcia, A.A.F., Silva-Filho, M.C., and Moura, D.S. (2014). Biological activity of nine recombinant AtRALF peptides: implications for their perception and function in *Arabidopsis*. *Plant Physiology and Biochemistry* **75**, 45-54.

Dressano, K., Ceciliato, P.H.O., Silva, A.L., Guerrero-Abad, J.C., Bergonci, T., Ortiz-Morea, F.A., Bürger, M., Silva-Filho, M.C., and Moura, D.S. (2017). BAK1 is involved in AtRALF1-induced inhibition of root cell expansion. *PLOS Genetics* **13**, e1007053.

Du, C., Li, X., Chen, J., Chen, W., Li, B., Li, C., Wang, L., Li, J., Zhao, X., and Lin, J. (2016). Receptor kinase complex transmits RALF peptide signal to inhibit root growth in *Arabidopsis*. *Proceedings of the National Academy of Sciences* **113**, E8326-E8334.

Duan, Q., Kita, D., Johnson, E.A., Aggarwal, M., Gates, L., Wu, H., and Cheung, A.Y. (2014). Reactive oxygen species mediate pollen tube rupture to release sperm for fertilization in *Arabidopsis*. *Nature Communications* **5**, 1-10.

Duan, Q., Liu, M.-C.J., Kita, D., Jordan, S.S., Yeh, F.-L.J., Yvon, R., Carpenter, H., Federico, A.N., Garcia-Valencia, L.E., and Eyles, S.J. (2020). FERONIA controls pectin-and nitric oxide-mediated male–female interaction. *Nature* **579**, 561-566.

Edgar, R.C. (2004). MUSCLE: a multiple sequence alignment method with reduced time and space complexity. *BMC Bioinformatics* **5**, 113.

El-Gebali, S., Mistry, J., Bateman, A., Eddy, S.R., Luciani, A., Potter, S.C., Qureshi, M., Richardson, L.J., Salazar, G.A., and Smart, A. (2019). The Pfam protein families database in 2019. *Nucleic Acids Research* **47**, D427-D432.

Escobar-Restrepo, J.-M., Huck, N., Kessler, S., Gagliardini, V., Gheyselinck, J., Yang, W., and Grossniklaus, U. (2007). The FERONIA receptor-like kinase mediates male-female interactions during pollen tube reception. *Science* **317**, 656-660.

Escobar, N.M., Haupt, S., Thow, G., Boevink, P., Chapman, S., and Oparka, K. (2003). High-throughput viral expression of cDNA–green fluorescent protein fusions reveals novel subcellular addresses and identifies unique proteins that interact with plasmodesmata. *The Plant Cell* **15**, 1507-1523.

Fabrice, T.N., Vogler, H., Draeger, C., Munglani, G., Gupta, S., Herger, A.G., Knox, P., Grossniklaus, U., and Ringli, C. (2018). LRX proteins play a crucial role in pollen grain and pollen tube cell wall development. *Plant Physiology* **176**, 1981-1992.

Felsenstein, J. (1985). Confidence limits on phylogenies: an approach using the bootstrap. *Evolution* **39**, 783-791.

Feng, H., Liu, C., Fu, R., Zhang, M., Li, H., Shen, L., Wei, Q., Sun, X., Xu, L., and Ni, B. (2019). LORELEI-LIKE GPI-ANCHORED proteins 2/3 regulate pollen tube growth as chaperones and coreceptors for ANXUR/BUPS receptor kinases in *Arabidopsis*. *Molecular Plant* **12**, 1612-1623.

Franck, C.M., Westermann, J., Bürssner, S., Lentz, R., Lituiev, D.S., and Boisson-Dernier, A. (2018). The protein phosphatases ATUNIS1 and ATUNIS2 regulate cell wall integrity in tip-growing cells. *The Plant Cell* **30**, 1906-1923.

Galindo-Trigo, S., Gray, J.E., and Smith, L.M. (2016). Conserved roles of CrRLK1L receptor-like kinases in cell expansion and reproduction from algae to angiosperms. *Frontiers in Plant Science* **7**.

Galindo-Trigo, S., Blanco-Touriñán, N., DeFalco, T.A., Wells, E.S., Gray, J.E., Zipfel, C., and Smith, L.M. (2020). CrRLK1L receptor-like kinases HERK 1 and ANJEA are female determinants of pollen tube reception. *EMBO Reports* **21**, e48466.

Ge, Z., Bergonci, T., Zhao, Y., Zou, Y., Du, S., Liu, M.-C., Luo, X., Ruan, H., García-Valencia, L.E., and Zhong, S. (2017). *Arabidopsis* pollen tube integrity and sperm release are regulated by RALF-mediated signaling. *Science* **358**, 1596-1600.

Ge, Z., Dresselhaus, T., and Qu, L. (2019a). How CrRLK1L receptor complexes perceive RALF signals. *Trends in Plant Science* **24**, 978-981.

Ge, Z., Zhao, Y., Liu, M., Zhou, L., Wang, L., Zhong, S., Hou, S., Jiang, J., Liu, T., Huang, Q., Xiao, J., Gu, H., Wu, H., Dong, J., Dresselhaus, T., Cheung, A.Y., and Qu, L. (2019b). LLG2/3 are co-receptors in BUPS/ANX-RALF signaling to regulate *Arabidopsis* pollen tube integrity. *Current Biology* **29**, 3256-3265. e3255.

Germain, H., Chevalier, E., Caron, S., and Matton, D.P. (2005). Characterization of five RALF-like genes from *Solanum chacoense* provides support for a developmental role in plants. *Planta* **220**, 447-454.

Gjetting, S.K., Mahmood, K., Shabala, L., Kristensen, A., Shabala, S., Palmgren, M., and Fuglsang, A.T. (2020). Evidence for multiple receptors mediating RALF-triggered Ca2+ signaling and proton pump inhibition. *The Plant Journal* **104**, 433-446.

Gong, F., Wu, X., and Wang, W. (2015). Diversity and function of maize pollen coat proteins: from biochemistry to proteomics. *Frontiers in Plant Science* **6**.

Gonneau, M., Desprez, T., Martin, M., Doblas, V.G., Bacete, L., Miart, F., Sormani, R., Hématy, K., Renou, J., and Landrein, B. (2018). Receptor kinase THESEUS1 is a rapid alkalinization factor 34 receptor in *Arabidopsis*. *Current Biology* **28**, 2452-2458. e2454.

Goto, H., Okuda, S., Mizukami, A., Mori, H., Sasaki, N., Kurihara, D., and Higashiyama, T. (2011). Chemical visualization of an attractant peptide, LURE. *Plant and cell physiology* **52**, 49-58.

Graham, M.A., Silverstein, K.A., and VandenBosch, K.A. (2008). Defensin-like genes: genomic perspectives on a diverse superfamily in plants. *Crop Science* **48**, S-3-S-11.

Hanson, D.D., Hamilton, D.A., Travis, J.L., Bashe, D.M., and Mascarenhas, J.P. (1989). Characterization of a pollen-specific cDNA clone from *Zea mays* and its expression. *The Plant Cell* **1**, 173-179.

Haruta, M., and Constabel, C.P. (2003). Rapid alkalinization factors in poplar cell cultures. peptide isolation, cDNA cloning, and differential expression in leaves and methyl jasmonate-treated cells. *Plant Physiology* **131**, 814-823.

Haruta, M., Monshausen, G., Gilroy, S., and Sussman, M.R. (2008). A cytoplasmic Ca2+ functional assay for identifying and purifying endogenous cell signaling peptides in *Arabidopsis* seedlings: identification of AtRALF1 peptide. *Biochemistry* **47**, 6311-6321.

Haruta, M., Sabat, G., Stecker, K., Minkoff, B.B., and Sussman, M.R. (2014). A peptide hormone and its receptor protein kinase regulate plant cell expansion. *Science* **343**, 408-411.

Hater, F., Nakel, T., and Groß-Hardt, R. (2020). Reproductive multitasking: the female gametophyte. *Annual Review of Plant Biology* **71**, 517-546.

He, F. (2011). Bradford protein assay. *Bio-Protocol* **1**, e45.

Herger, A., Dünser, K., Kleine-Vehn, J., and Ringli, C. (2019). Leucine-rich repeat extensin proteins and their role in cell wall sensing. *Current Biology* **29**, R851-R858.

Herger, A., Gupta, S., Kadler, G., Franck, C.M., Boisson-Dernier, A., and Ringli, C. (2020). Overlapping functions and protein-protein interactions of LRR-extensins in *Arabidopsis*. *PLOS Genetics* **16**, e1008847.

Higashiyama, T., Kuroiwa, H., Kawano, S., and Kuroiwa, T. (1998). Guidance in vitro of the pollen tube to the naked embryo sac of *Torenia fournieri*. *The Plant Cell* **10**, 2019-2031.

Hirano, N., Marukawa, Y., Abe, J., Hashiba, S., Ichikawa, M., Tanabe, Y., Ito, M., Nishii, I., Tsuchikane, Y., and Sekimoto, H. (2015). A receptor-like kinase, related to cell wall sensor of higher plants, is required for sexual reproduction in the unicellular charophycean alga, *Closterium peracerosum–strigosum–littorale* complex. *Plant and Cell Physiology* **56**, 1456-1462.

Holzinger, A., Phillips, K.S., and Weaver, T.E. (1996). Single-step purification/solubilization of recombinant proteins: application to surfactant protein B. *BioTechniques* **20**, 804-808.

Hou, Y., Guo, X., Cyprys, P., Zhang, Y., Bleckmann, A., Cai, L., Huang, Q., Luo, Y., Gu, H., Dresselhaus, T., Dong, J., and Qu, L.-J. (2016). Maternal ENODLs Are Required for Pollen Tube Reception in *Arabidopsis*. *Current Biology* **26**, 2343-2350.

Hu, B., Liu, B., Liu, L., Liu, C., Xu, L., and Ruan, Y. (2014). Epigenetic control of Pollen Ole e 1 allergen and extensin family gene expression in *Arabidopsis thaliana*. *Acta Physiologiae Plantarum* **36**, 2203-2209.

Huang, W., Liu, H., McCormick, S., and Tang, W. (2014). Tomato pistil factor STIG1 promotes in vivo pollen tube growth by binding to phosphatidylinositol 3-phosphate and the extracellular domain of the pollen receptor kinase LePRK2. *The Plant Cell* **26**, 2505-2523.

Huang, Y.-Y., Liu, X.-X., Xie, Y., Lin, X.-Y., Hu, Z.-J., Wang, H., Wang, L.-F., Dang, W.-Q., Zhang, L.-L., Zhu, Y., Feng, H., Pu, M., Zhao, J.-Q., Zhang, J.-W., Li, Y., Fan, J., and Wang, W.-M. (2020). Identification of FERONIA-like receptor genes involved in rice-Magnaporthe oryzae interaction. *Phytopathology Research* **2**, 14.

Huck, N., Moore, J.M., Federer, M., and Grossniklaus, U. (2003). The *Arabidopsis* mutant feronia disrupts the female gametophytic control of pollen tube reception. *Development* **130**, 2149-2159.

Jiang, S., Jasmin, P.X.H., Ting, Y.Y., and Ramachandran, S. (2005). Genome-wide identification and molecular characterization of Ole_e_I, Allerg_1 and Allerg_2 domain-containing pollen-allergen-like genes in *Oryza sativa*. *DNA Research* **12**, 167-179.

Jiao, Y., Peluso, P., Shi, J., Liang, T., Stitzer, M.C., Wang, B., Campbell, M.S., Stein, J.C., Wei, X., Chin, C.-S., Guill, K., Regulski, M., Kumari, S., Olson, A., Gent, J., Schneider, K.L., Wolfgruber, T.K., May, M.R., Springer, N.M., Antoniou, E., McCombie, W.R., Presting, G.G., McMullen, M., Ross-Ibarra, J., Dawe, R.K., Hastie, A., Rank, D.R., and Ware, D. (2017). Improved maize reference genome with single-molecule technologies. *Nature* **546**, 524-527.

Johnson, M. (2013). Detergents: Triton X-100, Tween-20, and more. *Mater Methods* **3**.

Jones, R., Ougham, H., Thomas, H., and Waaland, S. (2012). Flowering and sexual reproduction. In Molecular life of plants. (Wiley-Blackwell), pp. 605-610.

José Carlos Jiménez-López, María Isabel Rodríguez-García, and Alche, J.d.D. (2011). Systematic and phylogenetic analysis of the Ole e 1 pollen protein family members in plants. In Systems and Computational Biology, N. Yang, ed., pp. 245-260.

Kapust, R.B., and Waugh, D.S. (1999). *Escherichia coli* maltose-binding protein is uncommonly effective at promoting the solubility of polypeptides to which it is fused. *Protein Science* **8**, 1668-1674.

Kessler, S.A., Shimosato-Asano, H., Keinath, N.F., Wuest, S.E., Ingram, G., Panstruga, R., and Grossniklaus, U. (2010). Conserved molecular components for pollen tube reception and fungal invasion. *Science* **330**, 968-971.

Kim, Y., Zhang, D., and Jung, K. (2019). Molecular basis of pollen germination in cereals. *Trends in Plant Science* **24**, 1126-1136.

Kou, X., Qi, K., Qiao, X., Yin, H., Liu, X., Zhang, S., and Wu, J. (2017). Evolution, expression analysis, and functional verification of Catharanthus roseus RLK1-like kinase (CrRLK1L) family proteins in pear (Pyrus bretchneideri). *Genomics* **109**, 290-301.

Kumar, S., Stecher, G., Li, M., Knyaz, C., and Tamura, K. (2018). MEGA X: molecular evolutionary genetics analysis across computing platforms. *Molecular Biology and Evolution* **35**, 1547-1549.

Laemmli, U.K. (1970). Cleavage of structural proteins during the assembly of the head of bacteriophage T4. *Nature* **227**, 680-685.

Lausser, A., and Dresselhaus, T. (2010). Sporophytic control of pollen tube growth and guidance in grasses. *Biochemical Society Transactions* **38**, 631-634.

Lausser, A., Kliwer, I., Srilunchang, K.-o., and Dresselhaus, T. (2010). Sporophytic control of pollen tube growth and guidance in maize. *Journal of Experimental Botany* **61**, 673-682.

LaVallie, E.R., DiBlasio, E.A., Kovacic, S., Grant, K.L., Schendel, P.F., and McCoy, J.M. (1993). A thioredoxin gene fusion expression system that circumvents inclusion body formation in the *E. coli* Cytoplasm. *Bio/Technology* **11**, 187-193.

Lei, Y., Lu, L., Liu, H., Li, S., Xing, F., and Chen, L. (2014). CRISPR-P: a web tool for synthetic single-guide RNA design of CRISPR-system in plants. *Molecular Plant* **7**, 1494-1496.

Li, B., Yan, J., and Jia, W. (2017). FERONIA/FER-like receptor kinases integrate and modulate multiple signaling pathways in fruit development and ripening. *Plant Signaling & Behavior* **12**, 8-1099.

Li, C., Liu, X., Qiang, X., Li, X., Li, X., Zhu, S., Wang, L., Wang, Y., Liao, H., and Luan, S. (2018). EBP1 nuclear accumulation negatively feeds back on FERONIA-mediated RALF1 signaling. *PLOS Biology* **16**, e2006340.

Li, C., Wu, H., and Cheung, A.Y. (2016). FERONIA and her pals: functions and mechanisms. *Plant Physiology* **171**, 2379-2392.

Li, C., Yeh, F., Cheung, A.Y., Duan, Q., Kita, D., Liu, M., Maman, J., Luu, E.J., Wu, B.W., Gates, L., Jalal, M., Kwong, A., Carpenter, H., and Wu, H. (2015). Glycosylphosphatidylinositol-anchored proteins as chaperones and co-receptors for FERONIA receptor kinase signaling in *Arabidopsis*. *eLife* **4**, e06587.

Li, X., Sang, Y., Zhao, X., and Zhang, X. (2013). High-throughput sequencing of small RNAs from pollen and silk and characterization of miRNAs as candidate factors involved in pollen-silk interactions in maize. *PLOS ONE* **8**, e72852.

Li, Y., Dai, X., Yue, X., Gao, X., and Zhang, X. (2014). Identification of small secreted peptides (SSPs) in maize and expression analysis of partial SSP genes in reproductive tissues. *Planta* **240**, 713-728.

Liang, Y., Tan, Z., Zhu, L., Niu, Q., Zhou, J., Li, M., Chen, L., Zhang, X., and Ye, D. (2013). MYB97, MYB101 and MYB120 Function as male factors that control pollen tube-synergid interaction in *Arabidopsis thaliana* fertilization. *PLOS Genetics* **9**, e1003933.

Lindner, H., Kessler, S.A., Müller, L.M., Shimosato-Asano, H., Boisson-Dernier, A., and Grossniklaus, U. (2015). TURAN and EVAN mediate pollen tube reception in *Arabidopsis* synergids through protein glycosylation. *PLOS Biology* **13**, e1002139.

Liu, J., Zhong, S., Guo, X., Hao, L., Wei, X., Huang, Q., Hou, Y., Shi, J., Wang, C., and Gu, H. (2013). Membrane-bound RLCKs LIP1 and LIP2 are essential male factors controlling male-female attraction in *Arabidopsis*. *Current Biology* **23**, 993-998.

Liu, J.X., Srivastava, R., Che, P., and Howell, S.H. (2007). Salt stress responses in *Arabidopsis* utilize a signal transduction pathway related to endoplasmic reticulum stress signaling. *The Plant Journal* **51**, 897-909.

Liu, L., Zheng, C., Kuang, B., Wei, L., Yan, L., and Wang, T. (2016a). Receptor-like kinase RUPO interacts with potassium tansporters to regulate pollen tube growth and integrity in Rice. *PLOS Genetics* **12**, e1006085.

Liu, X., Castro, C., Wang, Y., Noble, J., Ponvert, N., Bundy, M., Hoel, C., Shpak, E., and Palanivelu, R. (2016b). The role of LORELEI in pollen tube reception at the interface of the synergid cell and pollen tube requires the modified eight-cysteine motif and the receptor-like kinase FERONIA. *The Plant Cell* **28**, 1035-1052.

Liu, X., Wolfe, R., Welch, L.R., Domozych, D.S., Popper, Z.A., and Showalter, A.M. (2016c). Bioinformatic identification and analysis of extensins in the plant kingdom. *PLOS ONE* **11**, e0150177.

Livak, K.J., and Schmittgen, T.D. (2001). Analysis of relative gene expression data using real-time quantitative PCR and the $2^{-\Delta\Delta CT}$ method. *Methods* **25**, 402-408.

Lombardero, M., Barbas, J.A., Delprado, J.M., and Carreira, J. (1994). cDNA sequence analysis of the main olive allergen, Ole e I. *Clinical and Experimental Allergy* **24**, 765-770.

Loraine, A.E., McCormick, S., Estrada, A., Patel, K., and Qin, P. (2013). RNA-seq of *Arabidopsis* pollen uncovers novel transcription and alternative splicing. *Plant Physiology* **162**, 1092-1109.

Loubert-Hudon, A., Mazin, B.D., Chevalier, É., and Matton, D.P. (2020). The ScRALF3 secreted peptide is involved in sporophyte to gametophyte signalling and affects pollen mitosis I. *Plant Biology* **22**, 13-20.

Lovy-Wheeler, A., Kunkel, J.G., Allwood, E.G., Hussey, P.J., and Hepler, P.K. (2006). Oscillatory increases in alkalinity anticipate growth and may regulate actin dynamics in pollen tubes of lily. *The Plant Cell* **18**, 2182-2193.

Manoli, A., Sturaro, A., Trevisan, S., Quaggiotti, S., and Nonis, A. (2012). Evaluation of candidate reference genes for qPCR in maize. *Journal of Plant Physiology* **169**, 807-815.

Márton, M.L., Cordts, S., Broadhvest, J., and Dresselhaus, T. (2005). Micropylar pollen tube guidance by egg apparatus 1 of maize. *Science* **307**, 573-576.

Masachis, S., Segorbe, D., Turrà, D., Leon-Ruiz, M., Fürst, U., El Ghalid, M., Leonard, G., López-Berges, M.S., Richards, T.A., and Felix, G. (2016). A fungal pathogen secretes plant alkalinizing peptides to increase infection. *Nature Microbiology* **1**, 1-9.

Matos, J.L., Fiori, C.S., Silva-Filho, M.C., and Moura, D.S. (2008). A conserved dibasic site is essential for correct processing of the peptide hormone AtRALF1 in *Arabidopsis thaliana*. *FEBS Letters* **582**, 3343-3347.

Mecchia, M.A., Santos-Fernandez, G., Duss, N.N., Somoza, S.C., Boisson-Dernier, A., Gagliardini, V., Martínez-Bernardini, A., Fabrice, T.N., Ringli, C., and Muschietti, J.P. (2017). RALF4/19 peptides interact with LRX proteins to control pollen tube growth in *Arabidopsis*. *Science* **358**, 1600-1603.

Mingossi, F.B., Matos, J.L., Rizzato, A.P., Medeiros, A.H., Falco, M.C., Silva-Filho, M.C., and Moura, D.S. (2010). SacRALF1, a peptide signal from the grass sugarcane (*Saccharum spp.*), is potentially involved in the regulation of tissue expansion. *Plant Molecular Biology* **73**, 271-281.

Miyazaki, S., Murata, T., Sakurai-Ozato, N., Kubo, M., Demura, T., Fukuda, H., and Hasebe, M. (2009). ANXUR1 and 2, sister genes to FERONIA/SIRENE, are male factors for coordinated fertilization. *Current Biology* **19**, 1327-1331.

Mizukami, Akane G., Inatsugi, R., Jiao, J., Kotake, T., Kuwata, K., Ootani, K., Okuda, S., Sankaranarayanan, S., Sato, Y., Maruyama, D., Iwai, H., Garénaux, E., Sato, C., Kitajima, K., Tsumuraya, Y., Mori, H., Yamaguchi, J., Itami, K., Sasaki, N., and Higashiyama, T. (2016). The AMOR Arabinogalactan sugar chain Induces pollen-tube competency to respond to ovular guidance. *Current Biology* **26**, 1091-1097.

Mollet, J.-C., Leroux, C., Dardelle, F., and Lehner, A. (2013). Cell wall composition, biosynthesis and remodeling during pollen tube growth. *Plants* **2**, 107-147.

Moussu, S., Broyart, C., Santos-Fernandez, G., Augustin, S., Wehrle, S., Grossniklaus, U., and Santiago, J. (2020). Structural basis for recognition of RALF peptides by LRX proteins during pollen tube growth. *Proceedings of the National Academy of Sciences* **117**, 7494-7503.

Mueller, A.M., Breitsprecher, D., Duhr, S., Baaske, P., Schubert, T., and Längst, G. (2017). Microscale thermophoresis: a rapid and precise method to quantify protein–nucleic acid interactions in solution. In Functional Genomics. (Springer), pp. 151-164.

Murphy, E., Vu, L.D., Van den Broeck, L., Lin, Z., Ramakrishna, P., van de Cotte, B., Gaudinier, A., Goh, T., Slane, D., Beeckman, T., Inzé, D., Brady, S.M., Fukaki, H., and De Smet, I. (2016). RALFL34 regulates formative cell divisions in *Arabidopsis* pericycle during lateral root initiation. *Journal of Experimental Botany* **67**, 4863-4875.

Muschietti, J., Dircks, L., Vancanneyt, G., and McCormick, S. (1994). LAT52 protein is essential for tomato pollen development: pollen expressing antisense LAT52 RNA hydrates and germinates abnormally and cannot achieve fertilization. *The Plant Journal* **6**, 321-338.

Nasrallah, J.B. (2019). Chapter Sixteen - Self-incompatibility in the Brassicaceae: Regulation and mechanism of self-recognition. In Current Topics in Developmental Biology, **Volume 131**, U. Grossniklaus, ed. (Academic Press), pp. 435-452.

Ngo, Q.A., Vogler, H., Lituiev, D.S., Nestorova, A., and Grossniklaus, U. (2014). A calcium dialog mediated by the FERONIA signal transduction pathway controls plant sperm delivery. *Developmental Cell* **29**, 491-500.

Nguyen, Q.-N., Lee, Y.-S., Cho, L.-H., Jeong, H.-J., An, G., and Jung, K.-H. (2015). Genome-wide identification and analysis of *Catharanthus roseus* RLK1-like kinases in rice. *Planta* **241**, 603-613.

Nicholas, K.B., and Nicholas, J.H.B. (1997). GeneDoc: a tool for editing and annotating multiple sequence alignments. . *Embnew News* **4,14**.

Odintsova, T.I., Slezina, M.P., and Istomina, E.A. (2020). Defensins of grasses: a systematic review. *Biomolecules* **10**, 1029.

Okuda, S., Tsutsui, H., Shiina, K., Sprunck, S., Takeuchi, H., Yui, R., Kasahara, R.D., Hamamura, Y., Mizukami, A., Susaki, D., Kawano, N., Sakakibara, T., Namiki, S., Itoh, K., Otsuka, K., Matsuzaki, M., Nozaki, H., Kuroiwa, T., Nakano, A., Kanaoka, M.M., Dresselhaus, T., Sasaki, N., and Higashiyama, T. (2009). Defensin-like polypeptide LUREs are pollen tube attractants secreted from synergid cells. *Nature* **458**, 357-361.

Oldenburg, M., Petersen, A., and Baur, X. (2011). Maize pollen is an important allergen in occupationally exposed workers. *Journal of Occupational Medicine and Toxicology* **6**, 32.

Oliveros, J.C., Franch, M., Tabas-Madrid, D., San-León, D., Montoliu, L., Cubas, P., and Pazos, F. (2016). Breaking-Cas—interactive design of guide RNAs for CRISPR-Cas experiments for ENSEMBL genomes. *Nucleic Acids Research* **44**, W267-W271.

Olsen, A.N., Mundy, J., and Skriver, K. (2002). Peptomics, identification of novel cationic *Arabidopsis* peptides with conserved sequence motifs. *In Silico Biology* **2**, 441-451.

Parisi, K., Shafee, T.M., Quimbar, P., van der Weerden, N.L., Bleackley, M.R., and Anderson, M.A. (2019). The evolution, function and mechanisms of action for plant defensins. In Seminars in Cell & Developmental Biology, Volume **88**. (Elsevier), pp. 107-118.

Parre, E., and Geitmann, A. (2005). More than a leak sealant. The mechanical properties of callose in pollen tubes. *Plant Physiology* **137**, 274-286.

Pearce, G., Moura, D.S., Stratmann, J., and Ryan, C.A. (2001a). Production of multiple plant hormones from a single polyprotein precursor. *Nature* **411**, 817-820.

Pearce, G., Moura, D.S., Stratmann, J., and Ryan, C.A. (2001b). RALF, a 5-kDa ubiquitous polypeptide in plants, arrests root growth and development. *Proceedings of the National Academy of Sciences* **98**, 12843-12847.

Pearce, G., Yamaguchi, Y., Munske, G., and Ryan, C.A. (2010). Structure–activity studies of RALF, Rapid Alkalinization Factor, reveal an essential–YISY–motif. *Peptides* **31**, 1973-1977.

Pereira, A.M., Lopes, A.L., and Coimbra, S. (2016a). Arabinogalactan Proteins as Interactors along the Crosstalk between the Pollen Tube and the Female Tissues. *Front Plant Sci* **7**, 1895.

Pereira, A.M., Lopes, A.L., and Coimbra, S. (2016b). Arabinogalactan proteins as interactors along the crosstalk between the pollen tube and the female tissues. *Frontiers in Plant Science* **7**.

Pu, C., Han, Y., Zhu, S., Song, F., Zhao, Y., Wang, C., Zhang, Y., Yang, Q., Wang, J., and Bu, S. (2017). The rice receptor-like kinases DWARF AND RUNTISH SPIKELET1 and 2 repress cell death and affect sugar utilization during reproductive development. *The Plant Cell* **29**, 70-89.

Qian, M., Xu, L., Tang, C., Zhang, H., Gao, H., Cao, P., Yin, H., Wu, L., Wu, J., and Gu, C. (2020). PbrPOE21 inhibits pear pollen tube growth in vitro by altering apical reactive oxygen species content. *Planta* **252**, 1-14.

Ringli, C. (2005). The role of extracellular LRR-extensin (LRX) proteins in cell wall formation. *Plant Biosystems* **139**, 32-35.

Rosano, G.L., and Ceccarelli, E.A. (2014). Recombinant protein expression in *Escherichia coli*: advances and challenges. *Frontiers in Microbiology* **5**.

Rotman, N., Rozier, F., Boavida, L., Dumas, C., Berger, F., and Faure, J.-E. (2003). Female control of male gamete delivery during fertilization in *Arabidopsis thaliana*. *Current Biology* **13**, 432-436.

Rubinstein, A.L., Broadwater, A.H., Lowrey, K.B., and Bedinger, P.A. (1995a). Pex1, a pollen-specific gene with an extensin-like domain. *Proceedings of the National Academy of Sciences* **92**, 3086-3090.

Rubinstein, A.L., Marquez, J., Suarez-Cervera, M., and Bedinger, P.A. (1995b). Extensin-like glycoproteins in the maize pollen tube wall. *The Plant Cell* **7**, 2211-2225.

Rudolph, R., and Lilie, H. (1996). In vitro folding of inclusion body proteins. *The FASEB Journal* **10**, 49-56.

Saitou, N., and Nei, M. (1987). The neighbor-joining method: a new method for reconstructing phylogenetic trees. *Molecular Biology and Evolution* **4**, 406-425.

Schäfer, F., Seip, N., Maertens, B., Block, H., and Kubicek, J. (2015). Purification of GST-tagged proteins. In Methods in Enzymology, **Volume 559**. (Elsevier), pp. 127-139.

Schägger, H., and Von Jagow, G. (1987). Tricine-sodium dodecyl sulfate-polyacrylamide gel electrophoresis for the separation of proteins in the range from 1 to 100 kDa. *Analytical Biochemistry* **166**, 368-379.

Scheer, J.M., Pearce, G., and Ryan, C.A. (2005). LeRALF, a plant peptide that regulates root growth and development, specifically binds to 25 and 120 kDa cell surface membrane proteins of *Lycopersicon peruvianum*. *Planta* **221**, 667-674.

Schmid, M.W., Schmidt, A., and Grossniklaus, U. (2015). The female gametophyte: an emerging model for cell type-specific systems biology in plant development. *Frontiers in Plant Science* **6**, 907.

Schneider, C.A., Rasband, W.S., and Eliceiri, K.W. (2012). NIH Image to ImageJ: 25 years of image analysis. *Nature Methods* **9**, 671-675.

Scholz, P., Anstatt, J., Krawczyk, H.E., and Ischebeck, T. (2020). Signalling pinpointed to the tip: the complex regulatory network that allows pollen tube growth. *Plants* **9**, 1098.

Schreiber, D.N., and Dresselhaus, T. (2003). In vitro pollen germination and transient transformation of *Zea mays* and other plant species. *Plant Molecular Biology Reporter* **21**, 31-41.

Sede, A.R., Borassi, C., Wengier, D.L., Mecchia, M.A., Estevez, J.M., and Muschietti, J.P. (2018). *Arabidopsis* pollen extensins LRX are required for cell wall integrity during pollen tube growth. *FEBS Letters* **592**, 233-243.

Shafee, T.M., Lay, F.T., Hulett, M.D., and Anderson, M.A. (2016). The defensins consist of two independent, convergent protein superfamilies. *Molecular Biology and Evolution* **33**, 2345-2356.

Sharma, A., Hussain, A., Mun, B.-G., Imran, Q.M., Falak, N., Lee, S.-U., Kim, J.Y., Hong, J.K., Loake, G.J., and Ali, A. (2016). Comprehensive analysis of plant rapid alkalization factor (RALF) genes. *Plant Physiology and Biochemistry* **106**, 82-90.

Sher Khan, R., Iqbal, A., Malak, R., Shehryar, K., Attia, S., Ahmed, T., Ali Khan, M., Arif, M., and Mii, M. (2019). Plant defensins: types, mechanism of action and prospects of genetic engineering for enhanced disease resistance in plants. *3 Biotech* **9**, 192.

Shi, F., Zhou, X., Liu, Z., and Feng, H. (2017). Rapid alkalinization factor (RALF) genes are related to genic male sterility in Chinese cabbage (*Brassica rapa L.* ssp. *pekinensis*). *Scientia Horticulturae* **225**, 480-489.

Showalter, A.M. (2001). Arabinogalactan-proteins: structure, expression and function. *Cellular and Molecular Life Sciences CMLS* **58**, 1399-1417.

Sigrist, C.J., De Castro, E., Cerutti, L., Cuche, B.A., Hulo, N., Bridge, A., Bougueleret, L., and Xenarios, I. (2012). New and continuing developments at PROSITE. *Nucleic Acids Research* **41**, D344-D347.

Silverstein, K.A., Graham, M.A., Paape, T.D., and VandenBosch, K.A. (2005). Genome organization of more than 300 defensin-like genes in *Arabidopsis*. *Plant Physiology* **138**, 600-610.

Silverstein, K.A., Moskal Jr, W.A., Wu, H.C., Underwood, B.A., Graham, M.A., Town, C.D., and VandenBosch, K.A. (2007). Small cysteine-rich peptides resembling antimicrobial peptides have been under-predicted in plants. *The Plant Journal* **51**, 262-280.

Song, W., Duan, F., Li, W., Lin, Q., Zhou, H., Han, X., and Wang, J. (2013). GmPOI gene encoding a Pollen_Ole_e_I conserved domain is involved in response of soybean to various stresses. *Biologia Plantarum* **57**, 85-90.

Song, Y., Wang, J., Zhang, G., Zhao, X., Zhang, P., Niu, N., and Ma, S. (2015). Isolation and characterization of a wheat F8-1 homolog required for physiological male sterility induced by a chemical hybridizing agent (CHA) SQ-1. *Euphytica* **205**, 707-720.

Srivastava, R., Liu, J., Guo, H., Yin, Y., and Howell, S.H. (2009). Regulation and processing of a plant peptide hormone, AtRALF23, in *Arabidopsis*. *The Plant Journal* **59**, 930-939.

Stegmann, M., Monaghan, J., Smakowska-Luzan, E., Rovenich, H., Lehner, A., Holton, N., Belkhadir, Y., and Zipfel, C. (2017). The receptor kinase FER is a RALF-regulated scaffold controlling plant immune signaling. *Science* **355**, 287-289.

Subramanian, B., Gao, S., Lercher, M.J., Hu, S., and Chen, W. (2019). Evolview v3: a webserver for visualization, annotation, and management of phylogenetic trees. *Nucleic Acids Research* **47**, W270-W275.

Suen, D., Wu, S., Chang, H., Dhugga, K.S., and Huang, A.H. (2003). Cell wall reactive proteins in the coat and wall of maize pollen potential role in pollen tube growth on the stigma and through the style. *Journal of Biological Chemistry* **278**, 43672-43681.

Suen, D.F., and Huang, A.H. (2007). Maize pollen coat xylanase facilitates pollen tube penetration into silk during sexual reproduction. *Journal of Biological Chemistry* **282**, 625-636.

Takeuchi, H., and Higashiyama, T. (2012). A species-specific cluster of Defensin-like genes encodes diffusible pollen tube attractants in *Arabidopsis*. *PLOS Biology* **10**, e1001449.

Takeuchi, H., and Higashiyama, T. (2016). Tip-localized receptors control pollen tube growth and LURE sensing in *Arabidopsis*. *Nature* **531**, 245-248.

Tang, W., Ezcurra, I., Muschietti, J., and McCormick, S. (2002). A cysteine-rich extracellular protein, LAT52, interacts with the extracellular domain of the pollen receptor kinase LePRK2. *The Plant Cell* **14**, 2277-2287.

Tang, W., Kelley, D., Ezcurra, I., Cotter, R., and McCormick, S. (2004). LeSTIG1, an extracellular binding partner for the pollen receptor kinases LePRK1 and LePRK2, promotes pollen tube growth in vitro. *The Plant Journal* **39**, 343-353.

Thynne, E., Saur, I.M., Simbaqueba, J., Ogilvie, H.A., Gonzalez-Cendales, Y., Mead, O., Taranto, A., Catanzariti, A.M., McDonald, M.C., and Schwessinger, B. (2017). Fungal phytopathogens encode functional homologues of plant rapid alkalinization factor (RALF) peptides. *Molecular Plant Pathology* **18**, 811-824.

Tsou, C.-H., Cheng, P.-C., Tseng, C.-M., Yen, H.-J., Fu, Y.-L., You, T.-R., and Walden, D.B. (2015). Anther development of maize (*Zea mays*) and longstamen rice (*Oryzalongistaminata*) revealed by cryo-SEM, with foci on locular dehydration and pollen arrangement. *Plant Reproduction* **28**, 47-60.

Twell, D., Wing, R., Yamaguchi, J., and McCormick, S. (1989). Isolation and expression of an anther-specific gene from tomato. *Molecular and General Genetics MGG* **217**, 240-245.

Uebler, S., Márton, M.L., and Dresselhaus, T. (2015). Classification of EA1-box proteins and new insights into their role during reproduction in grasses. *Plant Reproduction* **28**, 183-197.

Van Bel, M., Diels, T., Vancaester, E., Kreft, L., Botzki, A., Van de Peer, Y., Coppens, F., and Vandepoele, K. (2018). PLAZA 4.0: an integrative resource for functional, evolutionary and comparative plant genomics. *Nucleic Acids Research* **46**, D1190-D1196.

van der Linde, K., and Walbot, V. (2019). Chapter Ten - Pre-meiotic anther development. In Current Topics in Developmental Biology, **Volume 131**. (Elsevier), pp. 239-256.

Van der Weerden, N.L., and Anderson, M.A. (2013). Plant defensins: common fold, multiple functions. *Fungal Biology Reviews* **26**, 121-131.

Walley, J.W., Sartor, R.C., Shen, Z., Schmitz, R.J., Wu, K.J., Urich, M.A., Nery, J.R., Smith, L.G., Schnable, J.C., and Ecker, J.R. (2016). Integration of omic networks in a developmental atlas of maize. *Science* **353**, 814-818.

Wang, J., Feng, C., Liu, H., Feng, Q., Li, S., and Zhang, Y. (2017). AP1G mediates vacuolar acidification during synergid-controlled pollen tube reception. *Proceedings of the National Academy of Sciences* **114**, E4877-E4883.

Wang, L., Yang, T., Wang, B., Lin, Q., Zhu, S., Li, C., Ma, Y., Tang, J., Xing, J., and Li, X. (2020). RALF1-FERONIA complex affects splicing dynamics to modulate stress responses and growth in plants. *Science Advances* **6**, eaaz1622.

Wang, M., Chen, Z., Zhang, H., Chen, H., and Gao, X. (2018a). Transcriptome analysis provides insight into the molecular mechanisms underlying gametophyte factor 2-mediated cross-incompatibility in maize. *International journal of molecular sciences* **19**, 1757.

Wang, T., Liang, L., Xue, Y., Jia, P.-F., Chen, W., Zhang, M., Wang, Y., Li, H., and Yang, W. (2016). A receptor heteromer mediates the male perception of female attractants in plants. *Nature* **531**, 241-244.

Wang, X., Wang, K., Yin, G., Liu, X., Liu, M., Cao, N., Duan, Y., Gao, H., Wang, W., and Ge, W. (2018b). Pollen-expressed leucine-rich repeat extensins are essential for pollen germination and growth. *Plant Physiology* **176**, 1993-2006.

Waterhouse, A.M., Procter, J.B., Martin, D.M., Clamp, M., and Barton, G.J. (2009). Jalview Version 2—a multiple sequence alignment editor and analysis workbench. *Bioinformatics* **25**, 1189-1191.

Wieghaus, A., Prüfer, D., and Schulze Gronover, C. (2019). Loss of function mutation of the Rapid Alkalinization Factor (RALF1)-like peptide in the dandelion *Taraxacum koksaghyz* entails a high-biomass taproot phenotype. *PLOS ONE* **14**, e0217454.

Wingfield, P.T. (1995). Preparation of Soluble Proteins from Escherichia coli. *Current Protocols in Protein Science* **00**, 6.2.1-6.2.15.

Winship, L.J., Rounds, C., and Hepler, P.K. (2017). Perturbation analysis of calcium, alkalinity and secretion during growth of lily pollen tubes. *Plants* **6**, 3.

Woriedh, M., Wolf, S., Márton, M.L., Hinze, A., Gahrtz, M., Becker, D., and Dresselhaus, T. (2013). External application of gametophyte-specific ZmPMEI1 induces pollen tube burst in maize. *Plant Reproduction* **26**, 255-266.

Wu, H., De Graaf, B., Mariani, C., and Cheung, A. (2001). Hydroxyproline-rich glycoproteins in plant reproductive tissues: structure, functions and regulation. *Cellular and Molecular Life Sciences CMLS* **58**, 1418-1429.

Wu, J., Kurten, E.L., Monshausen, G., Hummel, G.M., Gilroy, S., and Baldwin, I.T. (2007). NaRALF, a peptide signal essential for the regulation of root hair tip apoplastic pH in *Nicotiana attenuata*, is required for root hair development and plant growth in native soils. *The Plant Journal* **52**, 877-890.

Xiao, Y., Stegmann, M., Han, Z., DeFalco, T.A., Parys, K., Xu, L., Belkhadir, Y., Zipfel, C., and Chai, J. (2019). Mechanisms of RALF peptide perception by a heterotypic receptor complex. *Nature* **572**, 270-274.

Xu, X., Chen, H., Sang, Y., Wang, F., Ma, J., Gao, X., and Zhang, X. (2012). Identification of genes specifically or preferentially expressed in maize silk reveals similarity and diversity in transcript abundance of different dry stigmas. *BMC Genomics* **13**, 294.

Xu, X.H., Wang, F., Chen, H., Sun, W., and Zhang, X.S. (2013). Transcript profile analyses of maize silks reveal effective activation of genes involved in microtubule-based movement, ubiquitin-dependent protein degradation, and transport in the pollination process. *PLOS ONE* **8**, e53545.

Yang, N., Liu, J., Gao, Q., Gui, S., Chen, L., Yang, L., Huang, J., Deng, T., Luo, J., and He, L. (2019). Genome assembly of a tropical maize inbred line provides insights into structural variation and crop improvement. *Nature Genetics* **51**, 1052-1059.

Yu, Y., and Assmann, S.M. (2018). Inter-relationships between the heterotrimeric Gβ subunit AGB1, the receptor-like kinase FERONIA, and RALF1 in salinity response. *Plant, Cell & Environment* **41**, 2475-2489.

Yu, Y., Chakravorty, D., and Assmann, S.M. (2018). The G protein β-subunit, AGB1, interacts with FERONIA in RALF1-regulated stomatal movement. *Plant Physiology* **176**, 2426-2440.

Zhang, X., Liu, X., Zhang, D., Tang, H., Sun, B., Li, C., Hao, L., Liu, C., Li, Y., Shi, Y., Xie, X., Song, Y., Wang, T., and Li, Y. (2017). Genome-wide identification of gene expression in contrasting maize inbred lines under field drought conditions reveals the significance of transcription factors in drought tolerance. *PLOS ONE* **12**, e0179477.

Zhao, C., Jiang, W., Zayed, O., Liu, X., Tang, K., Nie, W., Li, Y., Xie, S., Li, Y., Long, T., Liu, L., Zhu, Y., Zhao, Y., and Zhu, J. (2020). The LRXs-RALFs-FER module controls plant growth and salt stress responses by modulating multiple plant hormones. *National Science Review*.

Zhao, C., Zayed, O., Yu, Z., Jiang, W., Zhu, P., Hsu, C.-C., Zhang, L., Tao, W.A., Lozano-Durán, R., and Zhu, J.-K. (2018). Leucine-rich repeat extensin proteins regulate plant salt tolerance in *Arabidopsis*. *Proceedings of the National Academy of Sciences* **115**, 13123-13128.

Zhong, S., Liu, M., Wang, Z., Huang, Q., Hou, S., Xu, Y., Ge, Z., Song, Z., Huang, J., Qiu, X., Shi, Y., Xiao, J., Liu, P., Guo, Y., Dong, J., Dresselhaus, T., Gu, H., and Qu, L. (2019). Cysteine-rich peptides promote interspecific genetic isolation in *Arabidopsis*. *Science* **364**, eaau9564.

Zhou, L., and Dresselhaus, T. (2019). Friend or foe: signaling mechanisms during double fertilization in flowering seed plants. In Current Topics in Developmental Biology, **Volume 131**, U. Grossniklaus, ed. (Academic Press), pp. 453-496.

Zhou, L., Juranić, M., and Dresselhaus, T. (2017). Germline development and fertilization mechanisms in maize. *Molecular Plant* **10**, 389-401.

Zhu, S., Estévez, J.M., Liao, H., Zhu, Y., Yang, T., Li, C., Wang, Y., Li, L., Liu, X., Pacheco, J.M., Guo, H., and Yu, F. (2020). The RALF1–FERONIA complex phosphorylates eIF4E1 to promote protein synthesis and polar root hair growth. *Molecular Plant* **13**, 698-716.

Zuo, C., Zhang, W., Ma, Z., Chu, M., Mao, J., An, Z., and Chen, B. (2018). Genome-wide identification and expression analysis of the CrRLK1L gene family in apple (*Malus domestica*). *Plant Molecular Biology Reporter* **36**, 844-857.

SUPPLEMENTARY MATERIAL

Supplemental figures

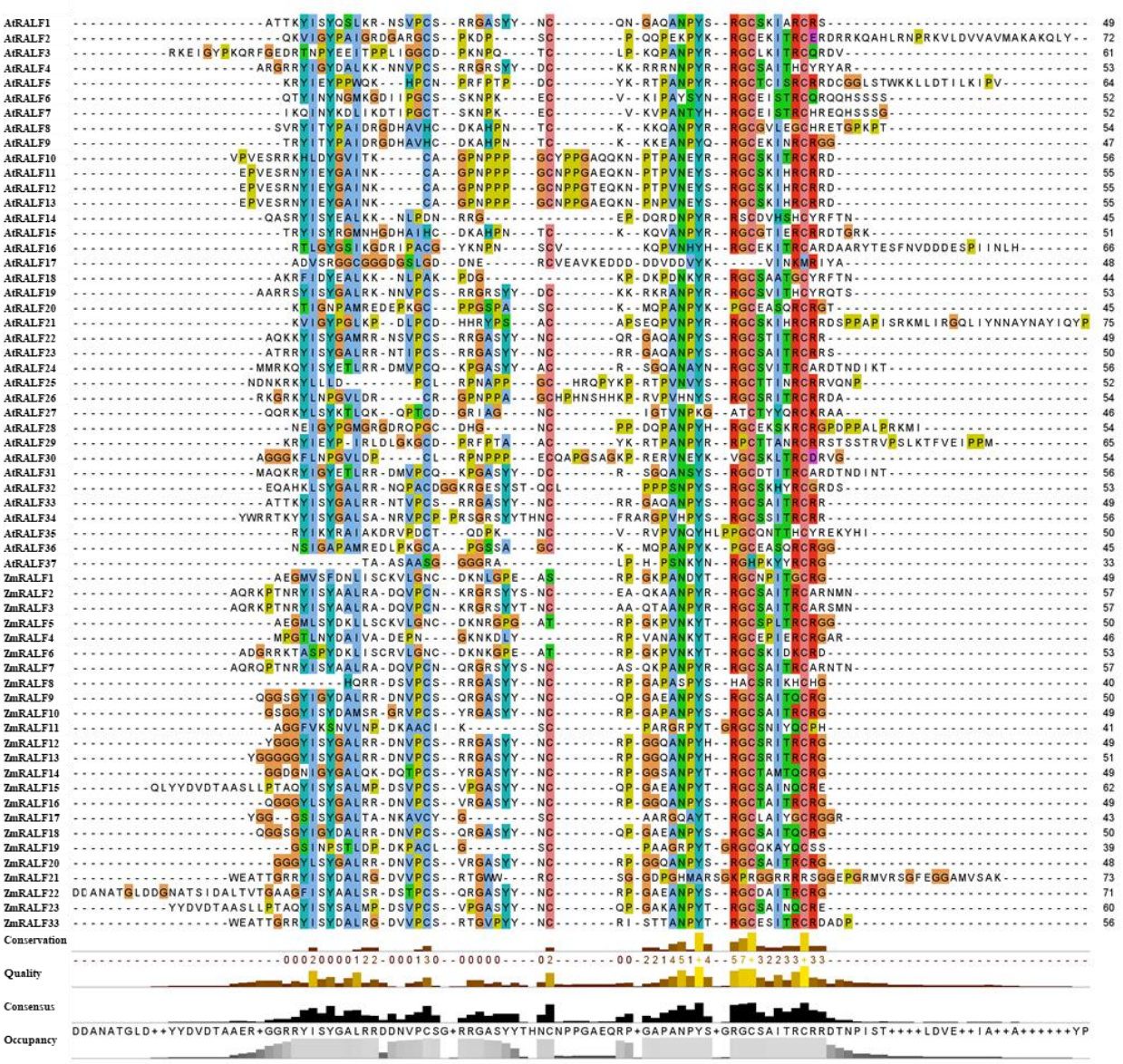

Supplemental Figure 1 Multiple sequence alignment of mature RALFs in maize and *Arabidopsis*. The alignment included 24 maize RALFs and 37 *Arabidopsis* RALFs. The signal peptide and propeptide recognized by RXLX/RXXL were deleted (if exist), mature RALF sequences were taken. The method MUSCLE was used for multiple alignment. The sequence was shown in Jalview with colored in ClustalX form.

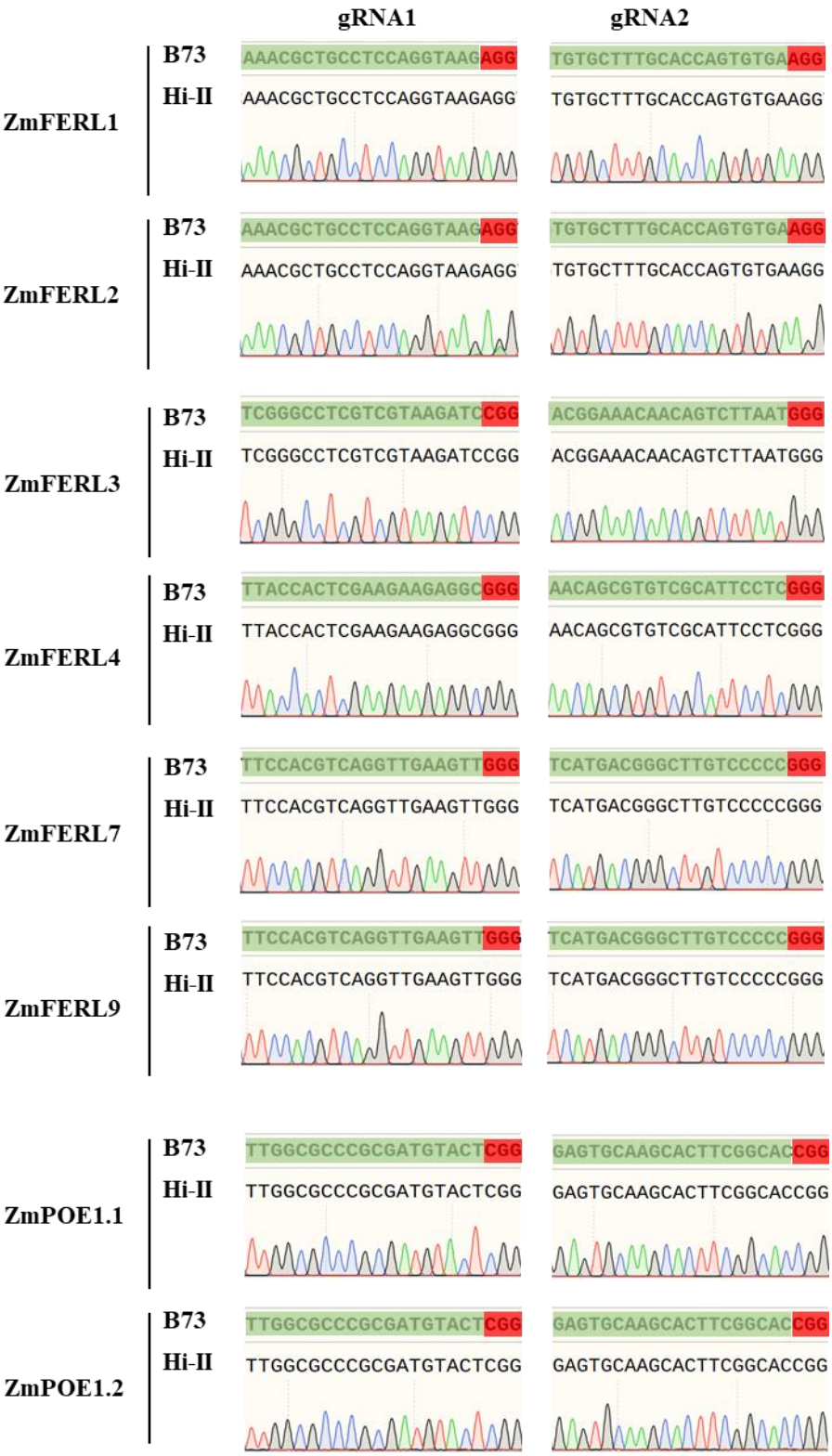

Supplemental Figure 2 Sequences alignment of guide RNAs between B73 and Hi-II.

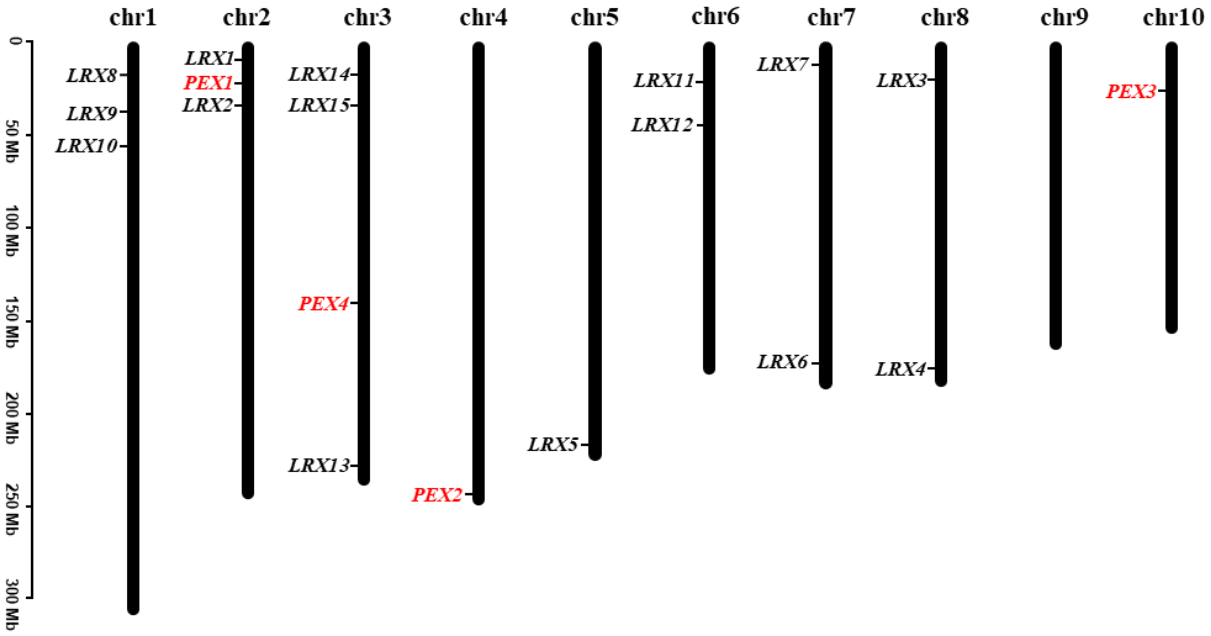

Supplemental Figure 3 Chromosomal distribution of maize *LRXs* (*leucine-rich repeat extensin genes)*. Chromosome numbers are shown at the top of each chromosome and the approximate size in megabases (MB) is provided at the left side. The name of each *LRX* gene is shown on the sides of each chromosome. *ZmPEX* genes are highlight in red.

Supplemental tables

Supplemental Table 1 Gene information.

Gene	Gene ID	Location	Length/ bp	UniProt_ID	Protein/ aa
		ZmRALF			
ZmRALF1	Zm00001d039766	3:14260432-14260656 (-)	225	A0A1D6ML12	74
ZmRALF2	Zm00001d008881	8:23662010-23662438 (-)	429	B6UE55	142
ZmRALF3	Zm00001d039429	3:4033017-4033454 (-)	438	B6TUL0	145
ZmRALF4	LOC100276036	3: 14234146-14234497 (-)	352	B6T3L0	78
ZmRALF5	Zm00001d019239	7:23574858-23575082 (-)	225	A0A1D6HWB9	74
ZmRALF6	Zm00001d008650	8:15918882-15919151 (+)	270	K7VAJ2	89
ZmRALF7	Zm00001d037738	6:135959877-135960266 (+)	390	B6TDV1	129
ZmRALF8	Zm00001d048716	4:4145643-4146017 (-)	375	K7TUG2	124
ZmRALF9	Zm00001d040297	3:36319753-36320169 (-)	417	B6U664	138
ZmRALF10	Zm00001d011921	8:164602381-164602755 (+)	375	B6U7M7	124
ZmRALF11	Zm00001d004232	2: 94071612-94071953 (-)	342	B6TP23	113
ZmRALF12	Zm00001d023856	10:25214019-25214375 (+)	357	B6SJC1	118
ZmRALF13	Zm00001d041685	3:133286614-133286988 (-)	375	A0A1D6MXM3	124
ZmRALF14	Zm00001d011922	8:164677723-164678097 (+)	375	A0A1D6G4W6	124
ZmRALF15	Zm00001d029122	1:59021967-59022404 (-)	438	A0A317YCN2	145
ZmRALF16	Zm00001d040803	3:66922907-66923248 (-)	342	B4FV46	113
ZmRALF17	Zm00001d044677	3:234649677-234649991 (+)	315	B6SMV8	104
ZmRALF18	LOC100284473	8:5024428-5025355 (+)	787	B6TU33	131
ZmRALF19	Zm00001d004242	2: 95395775-95396095 (+)	321	A0A1D6EEN0	106
ZmRALF20	Zm00001d009247	8:47084311-47084637 (-)	327	B6TEE3	108
ZmRALF21	Zm00001d036706	6:98210806-98211135 (+)	330	A0A317Y5Z2	125
ZmRALF22	Zm00001d022472	7:178318703-178319089 (-)	387	A0A096TNN4	128
ZmRALF23	LOC103634741	1:59028108-59029521 (-)	1305	XP_008655554.1	146
ZmRALF33	Zm00001d049233	4:21990923-21991252 (+)	330	B6T8G2	109
		ZmFERL			
ZmFERL1	Zm00001d029047	1:56040100-56042760 (+)	2661	A0A1D6K1Z7	886
ZmFERL2	Zm00001d047533	9:134025005-134027671 (-)	2667	K7VM35	888
ZmFERL3	Zm00001d002175	2:7264838-7267531 (-)	2694	A0A1D6DXI0	897
ZmFERL4	Zm00001d037839	6:139311841-139314453 (+)	2613	A0A1D6M101	870
ZmFERL5	Zm00001d008347	8:6080858-6083509 (+)	2652	K7VP31	883
ZmFERL6	Zm00001d040269	3:35197326-35199956 (-)	2631	A0A1D6MPL6	876
ZmFERL7	Zm00001d035992	6:65101474-65106753 (-)	2362	A0A1D6LK58	766
ZmFERL8	Zm00001d002282	2:9498177-9500738 (+)	2562	A0A1D6DZ77	853
ZmFERL9	Zm00001d045515	9:25084738-25087293 (+)	2556	K7VBM7	851
ZmFERL10	Zm00001d046838	9:108226063-108230008 (+)	3283	K7VJK4	842
ZmFERL11	Zm00001d028686	1:43080647-43083202 (+)	2556	A0A1D6JYK4	851
ZmFERL12	Zm00001d037544	6:128804148-128806658 (-)	2511	A0A1D6LYS3	836
ZmFERL13	Zm00001d034089	1:283693163-283695688 (-)	2526	A0A1D6L5G6	841
ZmFERL14	Zm00001d027436	1:5328311-5330875 (+)	2406	A0A1D6JM48	801
ZmFERL15	Zm00001d018789	7:5224217-5226970 (-)	2754	A0A1D6HS51	917
ZmFERL16	Zm00001d027439	1:5412144-5413568 (+)	1425	B6TWY5	474
ZmFERL17	Zm00001d039911	3:19172631-19188173 (+)	2799	B7ZX34	634

ZmLRX					
ZmLRX15	Zm00001d044373	3:226336497-226338425 (+)	1929	A0A1D6NL97	642
ZmLRX8	Zm00001d033279	1:257310330-257311502 (+)	1173	A0A1D6KXF5	390
ZmLRX11	Zm00001d037711	6:134677233-134678471 (-)	1239	B8A1C9	412
ZmPEX4	Zm00001d040802	3:66808174-66809532 (-)	1359	A0A1D6MT10	452
ZmLRX10	Zm00001d034402	1:292031928-292032921 (+)	903	A0A1D6L7B9	300
ZmLRX3	Zm00001d008779	8:19717269-19718855 (-)	1587	A0A1D6FFF3	528
ZmLRX13	Zm00001d039600	3:8723887-8725695 (+)	1809	A0A1D6MJB2	602
ZmLRX9	Zm00001d033721	1:272218064-272219057 (+)	933	A0A1D6L1R2	310
ZmLRX6	Zm00001d018931	7:9625026-9631617 (-)	966	A0A1D6HTF9	321
ZmLRX1	Zm00001d006435	2:207995752-207998297 (-)	1287	A0A1D6EW97	428
ZmLRX4	Zm00001d009952	8:92079626-92080870 (+)	1245	B4FCT4	414
ZmLRX7	Zm00001d022471	7:178316200-178317623 (-)	480	A0A1D6IN50	159
ZmLRX14	Zm00001d039916	3:19335810-19341690 (+)	1980	A0A096SVP6	659
ZmLRX12	Zm00001d038684	6:162562559-162568746 (+)	1116	A0A1D6M9S2	371
ZmPEX2	Zm00001d048715	4:4114481-4118893 (+)	3051	Q9SPM0	1016
ZmPEX1	LOC103648188	2:237391789-237395738 (-)	3567	Q41805	1188
ZmLRX5	Zm00001d013080	5:4432208-4433838 (+)	1140	B4F7Z3	379
ZmLRX2	Zm00001d007830	2:240482786-240483928 (+)	1143	B4FR31	380
ZmPEX3	Zm00001d023858	10:25245123-25248808 (-)	2898	A0A1D6IWD7	965
ZmLLG					
ZmLLG1	Zm00001d003139	2: 33,432,820-33,434,209 (-)	1169	C4IYA0	149
ZmLLG2	Zm00001d020876	7: 135,223,556-135,224,745 (+)	994	A0A1D6I6Q2	172
ZmLLG3	Zm00001d051672	4: 166,285,927-166,296,530 (-)	974	B6T982	169
ZmLLG4	Zm00001d017874	5: 209,352,390-209,357,003 (-)	1307	A0A1D6HIN9	172
ZmPOE					
ZmPOE1.1	Zm00001d003877	2:64525595-64526098 (+)	504	B4FKQ2	167
	Zm00001d007157	2:223447284-223448572 (+)	1200	B4FF58	149
	Zm00001d008991	8:29058300-29058836 (-)	537	B6T2Z8	178
	Zm00001d010422	8:114407024-114407967 (-)	819	B4FCC1	164
	Zm00001d011747	8:160680862-160681664 (-)	703	K7V513	174
	Zm00001d016715	5:173614753-173615752 (+)	906	B4FQB6	225
	Zm00001d021063	7:141944251-141946568 (-)	750	A0A1D6I861	249
	Zm00001d023680	10:15095362-15098284 (+)	1492	K7UCP0	367
ZmPOE1.2	Zm00001d025287	10:112727580-112728092 (-)	513	P33050	170
	Zm00001d028405	1:33744708-33745907 (-)	1100	B4FQ36	282
	Zm00001d029816	1:88322356-88323479 (+)	981	A0A1D6K7W8	175
	Zm00001d030305	1:121211811-121213196 (+)	1283	C4JAB8	253
	Zm00001d030314	1:121820597-121821836 (-)	916	B6TBY5	220
	Zm00001d030316	1:122018879-122020803 (+)	1769	Q9SBX4	481
	Zm00001d030509	1:140364656-140376186 (+)	902	B6SJ40	172
	Zm00001d033232	1:255276609-255280338 (-)	1094	A0A1D6KX43	232
	Zm00001d037835	6:139204219-139205281 (+)	932	A0A1D6M0X0	165
	Zm00001d038740	6:163596670-163597706 (-)	928	A0A1D6MA71	174
	Zm00001d038741	6:163651425-163652698 (-)	1109	A0A1D6MA73	200
	Zm00001d039748	3:13694033-13694665 (+)	633	A0A1D6MKY8	210
	Zm00001d042493	3:169439385-169441492 (+)	1709	A0A1D6N4F4	428
	Zm00001d043590	3:204497738-204498996 (+)	1142	A0A1D6NDG8	238
	Zm00001d043591	3:204507554-204508408 (+)	772	A0A1D6NDG9	177
	Zm00001d047933	9:145669272-145670568 (+)	1100	K7VK24	262

	Zm00001d047934	9:145672848-145674204 (+)	1246	B6T564	275
	Zm00001d050179	4:71069808-71072994 (-)	819	K7TZ39	149
	Zm00001d054095	4:246377520-246379135 (-)	1418	K7V8A0	355
		ZmDEFL			
ZmDEFL1	Zm00001d017293	5:192005969-192006112 (+)	897	AFW72426	111
	Zm00001d017292	5:192003788-192003928 (+)	711	A0A0A1P1P4	80
	Zm00001d025873	10:132238817-132238957 (+)	680	B6TC15	82
	Zm00001d015936	5:132744348-132744488 (-)	613	B6TP10	84
	Zm00001d021843	7:164343551-164343691 (+)	442	B6SMX5	85
	Zm00001d024303	10:62903652-62903774 (+)	821	B6SL97	79
	Zm00001d004322	2:103035195-103035290 (+)	591	A0A1D6EET4	74
	Zm00001d019277	7:25229043-25229144 (+)	620	B6SJS8	78

Supplemental Table 2 Primers used in this study.

Purpose	Primer name	Sequence (5'-3')
RNAi genome PCR	RNAi-F	GGCATATGCAGCAGCTATATG
	RNAi-R	TAAGCAGATCTATCGTGAGCG
Reference gene	Zm00001d018359-F	TGTACTCGGCAATGCTCTTG
	Zm00001d018359-R	TTTGATGCTCCAGGCTTACC
	Zm00001d024855-F	GAAGAGCCGCAAAGTTATGG
	Zm00001d024855-R	ATGGTAGAAGTGGACGCACC
RT-qPCR	ZmRALF1_qPCR_1-F	GCAACTGCGACAAGAACCTG
	ZmRALF1_qPCR_1-R	CGCACATCGACCAGAGAGAT
	ZmRALF1_qPCR_2-F	GCTTGCTCCTCGATCCATCA
	ZmRALF1_qPCR_2-R	CGCTAACAGGAGGCACAGAA
	ZmRALF2_qPCR_1-F	GCCGGTCCTACTACAGCAAC
	ZmRALF2_qPCR_1-R	CGACGACGACGTCAATGTAT
	ZmRALF2_qPCR_2-F	AACCGGTACATCAGCTACGC
	ZmRALF2_qPCR_2-R	AGACCAGACCAGACCAGACC
	ZmRALF3_qPCR_1-F	AACCGGTACATCAGCTACGC
	ZmRALF3_qPCR_1-R	CCTTGGCGCTCAGTTCAT
	ZmRALF3_qPCR_2-F	CGGTCTGATCTGCCTGCT
	ZmRALF3_qPCR_2-R	TGGTTGGTCATTGGTGTTTG
	POE1.1_qPCR1 -F	TGCTCAAACAGTTGGACTCG
	POE1.1_qPCR1 -R	GGTACAGCCACGCAGTTACA
	POE1.1_qPCR2-F	GACATCTGCGAGGTGGTCTT
	POE1.1_qPCR2-R	CGAGTCCAACTGTTTGAGCA
	POE1.2_qPCR1 -F	CTATGCCTATGCGTCGTCCT
	POE1.2_qPCR1 -R	TGAGCTCGATCGTGTAGGTG
	POE1.2_qPCR2 -F	CAACCCGCTAGGCTACTTCA
	POE1.2_qPCR2 -R	AGCAGCAAGTGAATCAAGCA
	DEFL_qPCR1 -F	TGCTTATCGCAGAGTCTCCA
	DEFL_qPCR1 -R	TCATGCCCTGCATTTTATCA
	DEFL_qPCR2 -F	ATGCAGGGCATGAAAAGCGT
	DEFL_qPCR2 -R	GCAAACCCCTCCATGCAGTT
Subcellular localization	ZmRALF1_whole-F	CACCATGGCGAGGCTGGCCT
	ZmRALF1_whole-R	GCCGCGACAGCCGG
	ZmRALF2_whole-F	CACCATGGCCCGCCTCGG
	ZmRALF2_whole-R	GTTCATGTTGCGGGCGC
	ZmRALF3_whole-F	CACCATGGCCCGCCTCGGA
	ZmRALF3_whole-R	GTTCATGCTGCGGGCG
	ZmRALF5_whole-F	CACCATGGGCGAAGCTAAGCTCAA
	ZmRALF5_whole-R	GCGCGCGCCCCT
	pAtRALF4-F	AAGGAAGCTTTGCGACGATAAGTACGAG
	pAtRALF4-R	AAGGGAGCTCTGCGACGATAAGTACGAG
Protein expression	pET32b -F	CCGGATATAGTTCCTCCTTTCA
	pET32b -R	CTGCTGTTCAAAAACGGTGA
	pMAL sequence-F	GTCGTCAGACTGTCGATG
	pMAL sequence-R	TGTGCTGCAAGGCGATTA

pGEX sequence-F	GGGCTGGCAAGCCACGTTTGGTG
pGEX sequence-R	CCGGGAGCTGCATGTGTCAGAGG
ZmRALF1_topo-F	CACCGCCGAGGGGATGGTGTC
ZmRALF1_topo-R	TCAGCCGCGACAGCC
ZmRALF2_topo-F	CACCAAGTCCGGGGAGCTGAGC
ZmRALF2_topo-R	TCAGTTCATGTTGCGGGC
ZmRALF3_topo-F	CACCAAGGTCGGGGACCTGAGC
ZmRALF3_topo-R	TCAGTTCATGCTGCGGGC
ZmRALF5_topo-F	CACCATGCCAGGCACG
ZmRALF5_topo-R	TCAGCGCGCGCC
pET32b-ZmRALF1-F	AAGGGAATTCTCAGCCGCGACAGCC
pET32b-ZmRALF1-R	AAGGGGATCCTGCCGAGGGGATGGTGT
pET32b-ZmRALF2-F	AAGGGAATTCTCAGTTCATGTTGCGGGC
pET32b-ZmRALF2-R	AAGGGGATCCAGCGCAGCGGAAGCC
pET32b-ZmRALF3-F	AAGGGAATTCTCAGTTCATGCTGCGGG
pET32b-ZmRALF3-R	AAGGGGATCCTGCGCAGCGCAAGC
pET32b-ZmRALF5-F	AAGGGAATTCTCAGCGCGCGCC
pET32b-ZmRALF5-R	AAGGGGATCCTATGCCAGGCACGTTGAAC
pGEX-6P1_ecto-ZmFERL1-F	AAGGGAATTCCAAGGGGCCAACTCCA
pGEX-6P1_ecto-ZmFERL1-R	AAGGCTCGAGTCAAGGCCCAACACTTGACT
pGEX-6P1_ecto-ZmFERL4-F	AAGGGGATTCGACAAGTACAAGCCGACGG
pGEX-6P1_ecto-ZmFERL4-R	AAGGGAATTCTTACTGGAGGTTGCTTTGCTTG
pGEX-6P1_ecto-ZmFERL7-F	AAGGGGATTCCAGGGCCGACCCG
pGEX-6P1_ecto-ZmFERL7-R	AAGGGAATTCTCACTTGCGCCCGCC
pGEX-6P1_ecto-ZmFERL9-F	AAGGGGATTCCAAGGCCGGCCCGT
pGEX-6P1_ecto-ZmFERL9-R	AAGGGAATTCTCACTTGCGCCCACCGC
pMAL-p2p_ecto-ZmFERL1-F	AAGGGAATTCCAAGGGGCCAACTCCA
pMAL-p2p_ecto-ZmFERL1-R	AAGGCTCGAGTCAAGGCCCAACACTTGACT
pMAL-p2p_ecto-ZmFERL4-F	AAGGGGATCCGACAAGTACAAGCCGACGG
pMAL-p2p_ecto-ZmFERL4-R	AAGGGAATTCTTACTGGAGGTTGCTTTGCTTG
pMAL-p2p_ecto-ZmFERL7-F	AAGGGGATCCCAGGGCCGACCCG
pMAL-p2p_ecto-ZmFERL7-R	AAGGGAATTCTCACTTGCGCCCGCC
pMAL-p2p_ecto-ZmFERL9-F	AAGGGGATCCCAAGGCCGGCCCGT
pMAL-p2p_ecto-ZmFERL9-R	AAGGGAATTCTCACTTGCGCCCACCGC
pMAL-p2p_ZmLLG1-F	AAGGGGATCCGCCCCGGGGGAAACCC
pMAL-p2p_ZmLLG1-R	AAGGCTCGAGTCAGCACTGGAGGCCCAG
pMAL-p2p_ZmLLG2-F	AAGGGGATCCGCCGGGTTCATCTCAAACGACG
pMAL-p2p_ZmLLG2-R	AAGGGAATTCTCAGCAAGACATGAGCAGCA
pMAL-p2p_ecto-ZmPEX2-F	AAGGGGATCCGACCCTCCTCTCCGGCT
pMAL-p2p_ecto-ZmPEX2-R	AAGGGAATTCTTAGCAGTTGTCCCTGTCGTCGA
pMAL-p2p_ZmPEX4-F	AAGGGGATCCGCAGATGAGGCGTCATCCAT
pMAL-p2p_ZmPEX4-R	AAGGGAATTCTTAGTAGCCTGGAAAAAGCGGT
pMAL-p2p_AtLRX9-F	AAGGGGATCCTATACCGTCGTTGCCACCTTTGA
pMAL-p2p_AtLRX9-R	AAGGCTCGAGTTATTTAGCCGGCTTTTGGCTCG
pMAL-p2p_AtLRX10-F	AAGGGGATCCGAAGTTTCATTTATTGCACAGCGA
pMAL-p2p_AtLRX10-R	AAGGCTCGAGTTAACTACAATCAACTGGACGGCTA

	pMAL-p2p_AtLRX11-F	AAGGGGATCCTTTGTCTCATTTGCCCTAACCGA
	pMAL-p2p_AtLRX11-R	AAGGCTCGAGTTAGCTACAATCAACCGGGCGG
CRISPR-Cas9 gRNA	gRNA test-F	TAGTACCACCTCGCCTACCG
	gRNA test-R	AGGGACCTGGTTGGAAATCT
	RALF1-gRNA1-F	TGTTGCCTGCGGCCCTGTCGCTAAC
	RALF1-gRNA1-R	AAACGTTAGCGACAGGGCCGCAGGC
	RALF1-gRNA2-F	GTGTGTCAAACGACACCATCCCCT
	RALF1-gRNA2-R	AAACAGGGGATGGTGTCGTTTGAC
	RALF2-gRNA1-F	TGTTGTCCGGGGAGCTGAGCGCGAT
	RALF2-gRNA1-R	AAACATCGCGCTCAGCTCCCCGGAC
	RALF2-gRNA2-F	GTGTGCGGGCCCGCAGAAGTGCTC
	RALF2-gRNA2-R	AAACGAGCACTTCTGCGGGCCCGC
	RALF3-gRNA1-F	TGTTGCAGCAAGTGCTCGGGCGCCG
	RALF3-gRNA1-R	AAACCGGCGCCCGAGCACTTGCTGC
	RALF3-gRNA2-F	GTGTGAGCCAGCAGGAGCGTCAACA
	RALF3-gRNA2-R	AAACTGTTGACGCTCCTGCTGGCTC
	RALF5-gRNA1-F	TGTTGACGCCAATAAATACACCCGC
	RALF5-gRNA1-R	AAACGCGGGTGTATTTATTGGCGTC
	RALF5-gRNA2-F	GTGTGAGCCCATAGAACGCTGCAG
	RALF5-gRNA2-R	AAACCTGCAGCGTTCTATGGGCTC
	FERL1/2-gRNA1-F	TGTTGAAACGCTGCCTCCAGGTAAG
	FERL1/2-gRNA1-R	AAACCTTACCTGGAGGCAGCGTTTC
	FERL1/2-gRNA2-F	GTGTGTGTGCTTTGCACCAGTGTGA
	FERL1/2-gRNA2-R	AAACTCACACTGGTGCAAAGCACAC
	FERL3-gRNA1-F	TGTTGTCGGGCCTCGTCGTAAGATC
	FERL3-gRNA1-R	AAACGATCTTACGACGAGGCCCGAC
	FERL3-gRNA2-F	GTGTGACGGAAACAACAGTCTTAAT
	FERL3-gRNA2-R	AAACATTAAGACTGTTGTTTCCGTC
	FERL4-gRNA1-F	TGTTGTTACCACTCGAAGAAGAGGC
	FERL4-gRNA1-R	AAACGCCTCTTCTTCGAGTGGTAA
	FERL4-gRNA2-F	GTGTGAACAGCGTGTCGCATTCCTC
	FERL4-gRNA2-R	AAACGAGGAATGCGACACGCTGTT
	FERL7/9-gRNA1-F	TGTTGTACTTCTTCCCGCTCAAGGG
	FERL7/9-gRNA1-R	AAACCCCTTGAGCGGGAAGAAGTA
	FERL7/9-gRNA2-F	GTGTGTCATGACGGGCTTGTCCCCC
	FERL7/9-gRNA2-R	AAACGGGGGACAAGCCCGTCATGA

Supplemental Table 3 siRNA target sequences.

Gene	RNAi fragments
RALF1	CGGCTGCAACCCGATCACCGGCTGTCGCGGCTGATCATATCTCTCTGGTCGATGTGCGCGCAATGTCAATGTCG CACGCGCGTGCAGGTACCAGGCCTCAGCGTGTGGTGCCGCGTGTGTGTATATATTACACACATGCATTATACAT TGGTCGTCGATCGTTACTGTATGCATGGCAACTGATGTTTCT
RALF2	GCCCAGCGCTAGCTGCTGCCGGGGCGCGCCGTCGTCGCCGAGCCGGTCGGTCTGGTCTGGTCTGGTCTGCCTGC CTGCCAGGTCACGCAGCCTGGCTCCACCGATCGCACACCATACATTGACGTCGTCGTCGCGGCCGTACGTGCCG TTGGACGGTGGAGGAGGCGGTGGCGCTACGACAGTATATATATACACAATTACACATACACACC
RALF3	AGGAGGAGGCGGCGGCGCGACGATAGTATATACAAACACCAATGACCAACCATACTACCAGTTCTATTGTCGC TGTGGCGTAGCTTCTCTATAAATAATATCTAACTCCAACAAGATATGTTTGATTATGGATCGCGATCTATCATAT GTATGCCATTCATTCGTTAATTTGAAAAAATGATGCTGAAAAAGAGAAGCTACA
POE1.1	CGATCAGTAATAGCACATCGACGACGACGATCGATATGTAATAGCACGTCGTCGACGACCGACCGCAGTCGTC GCAGACTGGCTGGCACTAAACCACAAATCCTCTTCACCTGGATTACAAATATGTAACTGAGAAAGGAAAGGAA AACAAAAATGTAACTGCGTGGCTGTACCAAATTCTGAGTGCTGGATTCTTGCTATTGTCACCCATTGTTCGTTTT ATCATACAAGTTGCAGCGC
POE1.2	CTATACCACGGCGGCGTCGCGGACATGCTGCACAAAACTACAACGATACAGAGCGAACGCATGGCATGGATAG CAGTATCTACGGAAAGAAAAGGAAGAAAAGGAAAATAAAAAATGTATCAGAGTGCTTGATTCACTTGCTGCTG TCACCCATTCCCCGTTCTTAACATAACATGTGGGCCGGCTTGGCCCAGGCACAAGCCTATCTACGCATGGCCTA CGGTCCGC
DEFL	ACACCTTGCGACCTGCGTTGTCACCCACCCATCAAGGTTGGGGCCGCCAGCAGGTTCAGCCGTTCCTGTTCTTG ATAAAACGAGAGAAGGATGGCGGCAGTGTCTCAGGGAGCTGTCCTATTCTTGTTTCTCCTCCTCGTCGCAGCAG AGGTGGGAACCATCGATGCCAAAATGGGAGTAGCCATGCCCATGCATGCCTTGATAATGGAGAACGTGAAACA GCAGGAGAAGGAGAAGGAGAAGGAGAAGGAGGAGAAAAGCACGGAGAAGGAAGAGAGTCGATGCTTATCGC AGAGTCTCCAGTTCGAGGGCTTCTGCTTCAACAGCGACAGATGCGCCGAGGTGTGCATGAAGGAGAGCTTTCC CGGTGGCGAGTGCAA

Vector maps

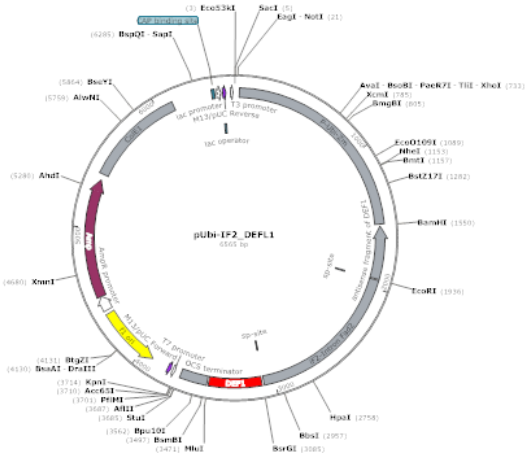
pUbi-IF2_DEFL1

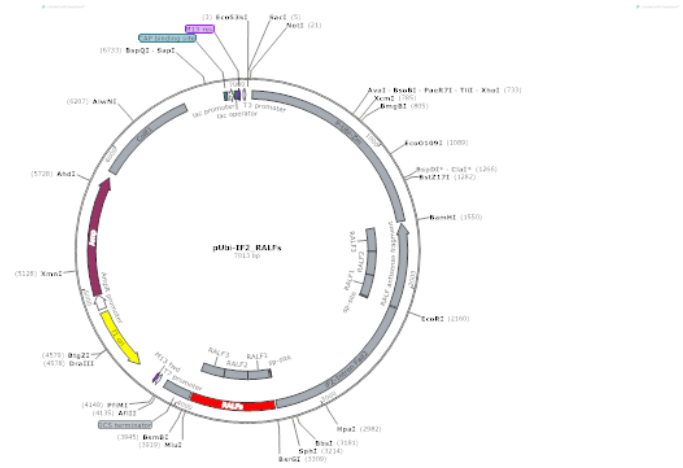
pUbi-IF2_RALFs

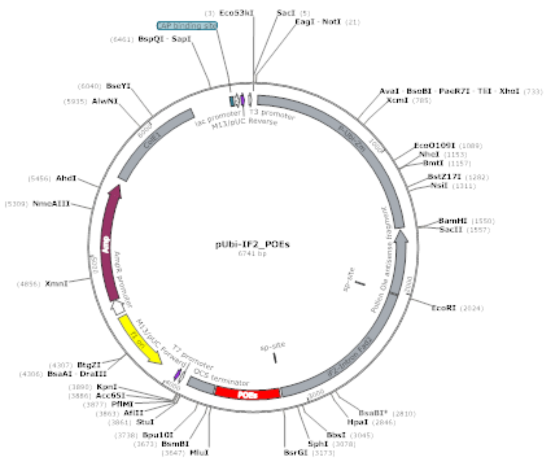
pUbi-IF2_PDEs

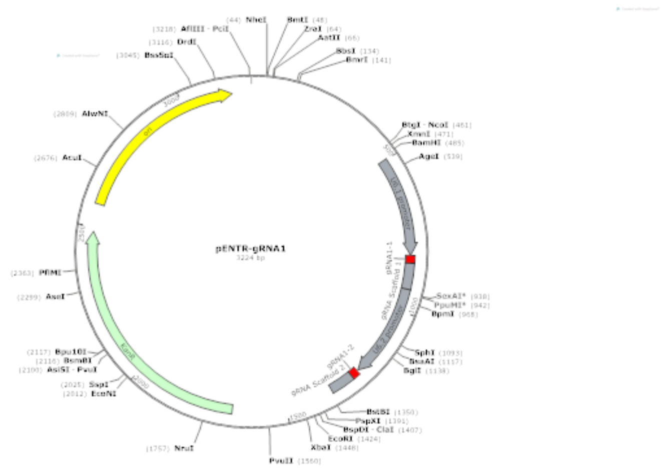
pENTR-gRNA1

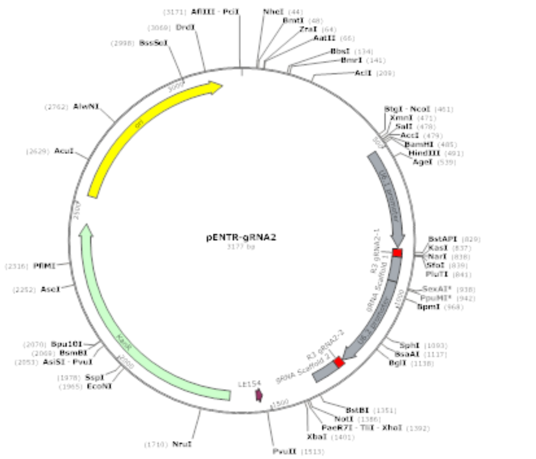
pENTR-gRNA2

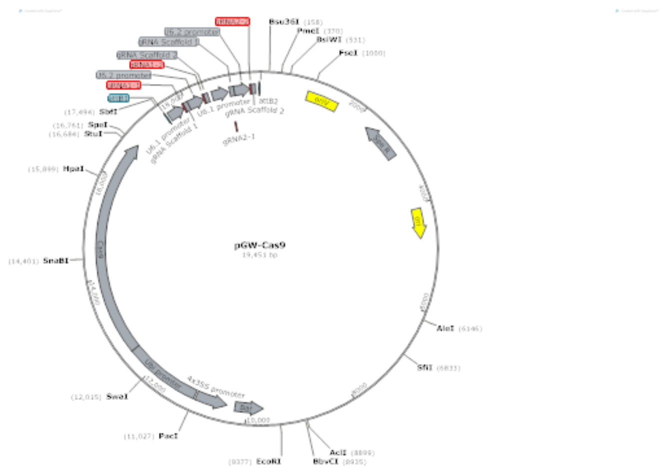
pGW-Cas9

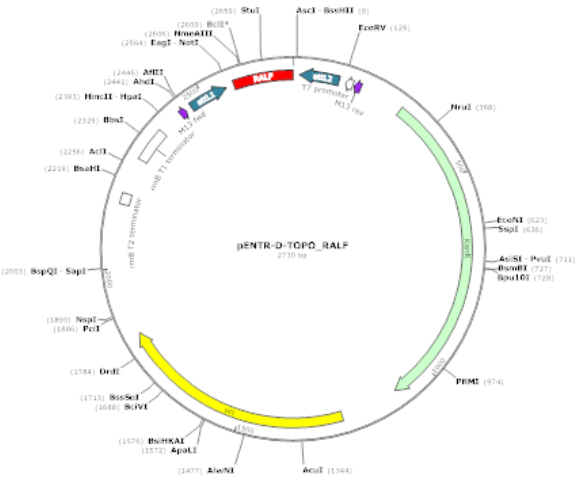
pENTR-D-TOPO_RALF
2730 bp

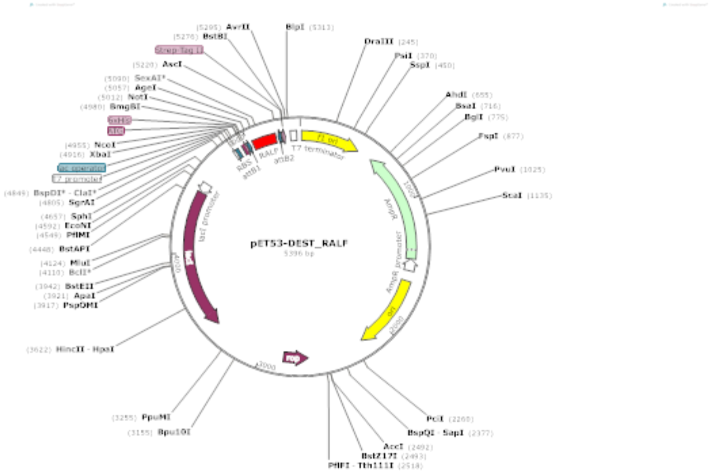
pET53-DEST_RALF
5396 bp

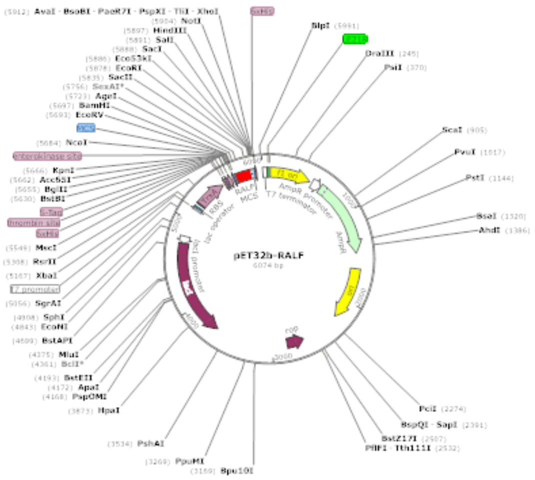
pET32b-RALF
6074 bp

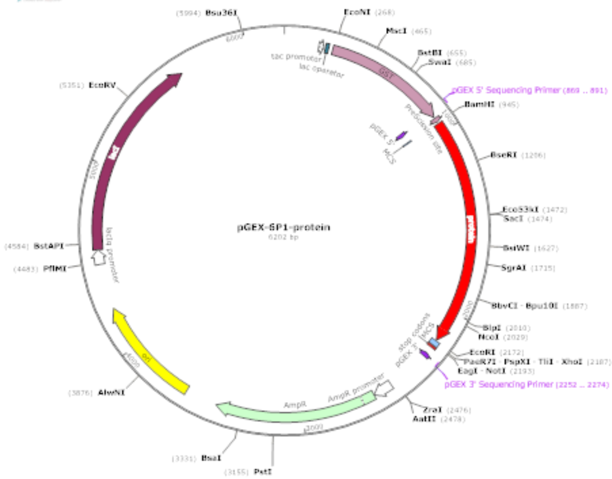
pGEX-6P1-protein
6202 bp


pMAL-p2p_protein
7963 bp


pB7FWG2.0_ZmRALFs
11,456 bp

ABBREVIATIONS

ANX	ANXURE
bp	base pair
BUPS	Buddha's Paper Seal
cDNA	complementary DNA
CRISPR	clustered regularly interspaced short palindromic repeats
CRPs	cysteine-rich peptides
CrRLK1L	*Catharanthus roseus* 1 like
DEFL	defensin-like
DNA	deoxyribonucleic acid
eGFP	enhanced green fluorescent protein
ER	endoplasmic reticulum
FERL	FERONIA-like
FPKM	Fragments Per Kilobase Million
GST	glutathione S-transferases
kDa	kilodalton
LLG	LORRELEI-like GPI-anchored
LRX	leucine-rich repeat extensin
MAP	minutes after germination
MBP	maltose binding protein
mRNA	messenger RNA
MS	mass spectrometry
MST	microscale thermophoresis
MW	molecular weight
ORF	open reading frame
PCR	polymerase chain reaction
PEX	pollen extensin-like
PGM	pollen germination medium
POE	Pollen Ole e
PT	pollen tube
RALF	rapid alkalinization factor
RNA	ribonucleic acid
RNAi	RNA interference
RNA-seq	RNA sequencing
ROS	reactive oxygen species
RT	room temperature
RT-PCR	reverse transcriptase PCR
RT-qPCR	real-time quantitative PCR
S1P	Sphinogosine-1-Phosphate

SDS-PAGE	sodium dodecyl sulfate polyacrylamide gel electrophoresis
TPM	transcripts per kilobase million
TrxA	thioredoxin 1
UTR	untranslated region
WT	wild type

FIGURES AND TABLES

Figures

Tables

Supplemental Figures

Supplemental Tables

ACKNOWLEDGEMENTS

First of all, I want to thank Prof. Dr. Thomas Dresselhaus for giving me this great chance to explore the scientific world. I did my master in plant genetics and breeding and at that time started to be interested in the complex processes of plant reproduction. I very much appreciated that I could get the fortunate to study in this nice maize group. His ability to encourage people is magic: I always got inspired from his words. I learn a lot in these five years, epically the serious attitude to what you are donging and open mind to cooperate with colleagues. This quality will be my lifelong fortune.

Special thanks need to be given to my direct lab supervisor Dr. Liangzi Zhou. She is always generous to share her knowledge with me and try to solve the problems I met. In the field of science, if Prof. Dresselhaus is the one telling me where to go, she is the one teaching me how to go. Furthermore, I would like to thank Prof. Dr. Gernot Längst and PD Dr. Joachim Griesenbeck for being part of the examination committee and my external mentor Prof. Dr. Benedikt Kost (University of Erlangen-Nuremberg) for advice and support during my PhD student time.

I gratefully acknowledge Prof. Dr. Klaus Grasser and Dr. Marion Grasser for helping me with protein experiments and Dr. Karina van der Linde and Dr. Stefanie Dukowic-Schulze for correcting parts of my thesis. I appreciate PD. Dr. Stefanie Sprunck, Dr. Andrea Bleckmann, Dr. Maria Flores Tornero, and Dr. Kevin Begcy for advices and help on experimental questions. I also want to appreciate the kind support of Veronika Mrosek and Sabine Kolb in all administrative questions, which are very useful for efficient work. I also would like to thank our collaborators Dr. Julia Mergner (Technische Universität München) for phosphoproteome analysis, Dr. Zengxiang Ge (Peking University) for providing samples for protein interaction test and Prof. Dr. Gernot Längst for the support with MST assays.

I want to thank all members of the maize lab: our technicians Annemarie Taffner for always being helpful and my PhD colleagues Sandra Bertrand, Xingli Li, Isabell-Christin Fiedler, Regina Stöckl, Leon Kutzner, and Finn Hartmann for interesting chats and a joyful time. Special thanks go to Armin Hildebrand, Susanne Bauer and Noureddine Djella for taking care of all my plants. Furthermore, I want to thank all other members of the department, Philipp Cyprys, Philipp Michl-Holzinger and Raphael Malka for help on protein purification, Amelie Rödel for MST assay...The

great time I had made up of working together with you.

Finally, I want to thank my parents, who always respect my decision. Without their support, I can't go so far and do what I want. Also, my cute nephew and niece, although they don't understand so many things, their laugh is already so much sweet and fun. Last but not latest, I want to appreciate my love, Liuting. Her support and accompany helped me a lot to go through the hard times of my research work and she is always so positive and patient. Even there is a distance of 8000 km, our hearts are always together.

Eidesstattliche Erklärung

Ich erkläre hiermit an Eides statt, dass ich die vorliegende Arbeit ohne unzulässige Hilfe Dritter und ohne Benutzung anderer als der angegebenen Hilfsmittel angefertigt habe. Die aus anderen Quellen direkt oder indirekt übernommenen Daten und Konzepte sind unter Angabe des Literaturzitats gekennzeichnet.

Lele Wang

Regensburg, den 12 November 2020